Modern Approaches in Solid Earth Sciences

Andrew Y. Glikson
Colin Groves

Climate, Fire and Human Evolution

The Deep Time Dimensions of the Anthropocene

Springer

Modern Approaches in Solid Earth Sciences

Volume 10

More information about this series at http://www.springer.com/series/7377

Andrew Y. Glikson • Colin Groves

Climate, Fire and Human Evolution

The Deep Time Dimensions of the Anthropocene

Springer

Andrew Y. Glikson
School of Archaeology and Anthropology
Australian National University
Canberra, ACT, Australia

Colin Groves
School of Archaeology and Anthropology
Australian National University
Canberra, ACT, Australia

Responsible Series Editor: F. Pirajno

This book represents an expansion of the book by Andrew Y. Glikson, *Evolution of the Atmosphere, Fire and the Anthropocene Climate Event Horizon* (Springer, 2014).

ISSN 1876-1682 ISSN 1876-1690 (electronic)
Modern Approaches in Solid Earth Sciences
ISBN 978-3-319-22511-1 ISBN 978-3-319-22512-8 (eBook)
DOI 10.1007/978-3-319-22512-8

Library of Congress Control Number: 2015951975

Springer Cham Heidelberg New York Dordrecht London

Printed on acid-free paper

Springer International Publishing AG Switzerland is part of Springer Science+Business Media (www.springer.com)

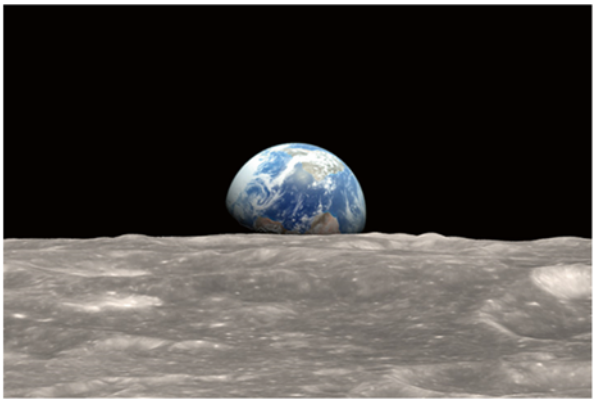

Earthrise (NASA) (http://svs.gsfc.nasa.gov/cgi-bin/details.cgi?aid=4129)

Bushfire smoke covering the sun in Tasmania's Southern Midlands, looking west towards Lake Repulse, Friday, Jan. 4, 2013 (Kim Foale; AAP Image, by permission)

In honor of Sir David Attenborough

Foreword

Andrew Y. Glikson and Colin Groves' new book *Climate, Fire, and Human Evolution* traces the fascinating and complex history of the Earth over the past 4 billion years. It explores the fundamental context of the Earth's climate system; the cycles of carbon, oxygen and nitrogen and the crucial role of fire, to provide the critical baseline for our understanding of how a single species, *Homo sapiens*, has changed the atmosphere, oceans and biosphere.

The fate of our species, and all the others with which we share this planet, is now in peril from the unintended consequences of our development, and especially our use of energy. I commend this scholarly yet readable work as a vital reference for understanding our past and present, and hopefully for saving our future.

North Ryde, Sydney, NSW, Australia — Lesley Hughes

Prologue

On Earth – a unique habitable planet in the solar system and possibly beyond – the evolution of the atmosphere, oceans and life are intimately intertwined, where life depends critically on the presence of liquid water allowed by the Earth's unique orbital position around the sun and evolving atmosphere–ocean processes which regulate surface temperatures in the range of ~ −90° to +58 °C (Fig. 1). The carbon

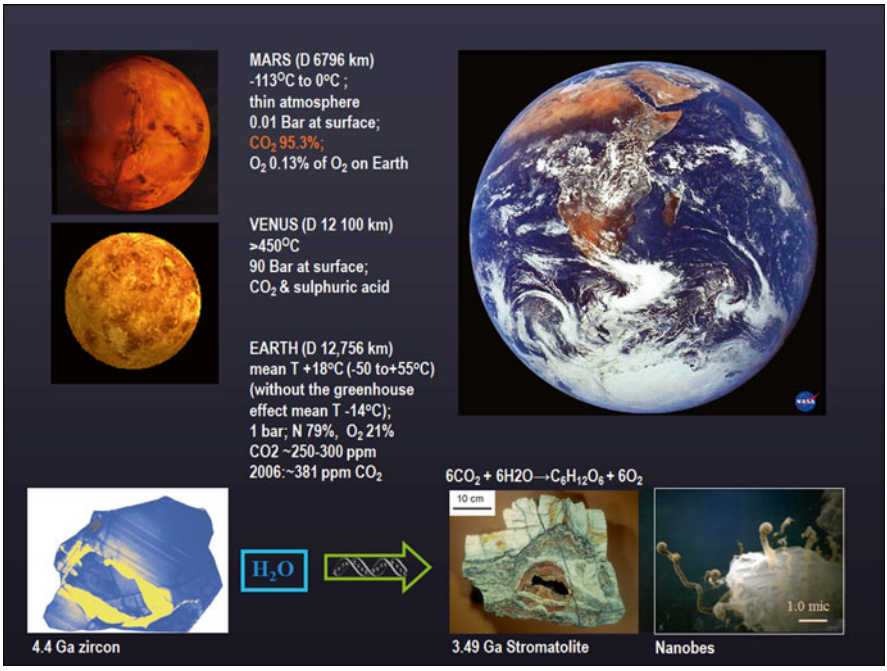

Fig. 1 Earth, Mars and Venus comparison and the terrestrial evolutionary chain, showing a ~4.4 Ga zircon crystal (Peck et al. 2001; Elsevier, by permission); water, DNA-RNA chains; Pilbara stromatolite (courtesy J.W. Schopf) and Nanobe organisms (Uwins et al. 1998) (courtesy P. Uwins)

cycle is intrinsically linked to Earth's mantle and tectonic activity, releasing carbon through volcanic eruptions and returning it to the mantle via tectonic subduction. The atmosphere, mediating the carbon, oxygen and nitrogen cycles, acts as lungs of the biosphere, allowing the existence of an aqueous medium where metabolic microbiological processes are performed in aqueous, land, air and extreme environments, including by chemo-bacteria around volcanic fumaroles, microbes and algae within and below ice and nanobes in deep crustal fractures and near-surface phototrophs. In this book, we trace milestones in the evolution of the atmosphere, oceans and biosphere through natural evolution and cataclysms from about ~3.8 billion years ago [Ga] all the way to the Anthropocene – an era triggered by a genus which uniquely mastered fire, a source of energy allowing it to release energy orders of magnitude higher than its own physiological capacity, facilitating its domination over the composition of the terrestrial atmosphere and large part of the biosphere.

Based on evidence from 4.4 billion–year-old zircons, hydrous activity has already been in existence at the earliest stages of the development of the Earth crust, in spite of solar luminosity being some 28 % lower than at present (Sagan and Mullen 1972), consistent with concepts regarding homeostasis in the Earth's atmosphere–ocean–biosphere system (Lovelock and Margulis 1974). According to this hypothesis, life acquired a homeostatic influence over the planetary environment where the physical and chemical conditions of most of the planetary surface adjusted to conditions mostly favourable for life through maintenance of liquid water with pH not far from neutral, despite major changes including increase in insolation, escape of hydrogen to space and enrichment of the atmosphere in oxygen. Maintenance of liquid water occurred through variations in the greenhouse gas levels of the atmosphere and distribution of infrared-absorbing oceans. From an initial Venus-like atmosphere dominated by CO, CH_4, CO_2, SO_2, N_2O, H_2 and H_2S, the sequestration of CO_2 and build-up of nitrogen – a stable non-reactive gas – has led to intermittent ice ages from at least as early as ~3.0 Ga, succeeded by multi-stage variations in the level of atmospheric photosynthetic oxygen produced by phytoplankton and from the Silurian ~420 Ma ago by land plants. The advent of land plants under an oxygen-rich atmosphere resulted in a flammable carbon-rich biosphere. Shifts in state of the climate caused by re-arrangement of continent–ocean patterns through plate tectonics and changes in atmospheric composition associated with erosion and weathering processes led to changes in the carbon cycle. Abrupt events such as volcanism, asteroid impacts, possible supernovae and episodic release of methane and hydrogen sulphide were superposed on longer-term trends, triggering amplifying feedback processes. Changes in atmospheric chemistry resulted in variations in alkalinity, acidity (pH) and oxidation/reduction state (Eh) of the hydrosphere and thereby of the marine food chain.

Born on a combustible Earth surface under increasingly unstable climates shifting from the relatively warm Pliocene (5.2–2.6 Ma) to the deep ice ages of the Pleistocene, the arrival of humans depended on both biological adaptations and cultural evolution. The mastering of fire as a necessity allowed the genus *Homo* to increase entropy in nature by orders of magnitude. Gathered around campfires during long nights for hundreds of thousands of years, captivated by the flickering life-

like dance of the flames, humans developed insights, imagination, cravings, hope, premonitions of death and aspiration for immortality, omniscience, omnipotence and concepts of spirits and gods. Inherent in pantheism is the reverence of Earth, its rocks and its living creatures, contrasted by the subsequent rise of monotheistic sky-god creeds, many of which regard Earth as but a corridor to heaven. Once the climate stabilized in the early Holocene, from about 7000 years ago production of excess grain and animal husbandry by Neolithic civilizations, in particular along the great river valleys, allowed human imagination and dreams to express themselves through the construction of monuments to immortality and through genocidal tribal and national wars in the name of gods and of ideologies. Further to burning large parts of the forests, the discovery of combustion and exhumation of carbon deposits derived from the Earth's ~420 million–year-old fossil biospheres set the stage for an anthropogenic oxidation event, leading to an abrupt shift in state of the atmosphere–ocean–cryosphere system. The consequent progressive mass extinction of species is tracking towards levels commensurate with those of the past five great mass extinctions of species, constituting a geological event horizon in the history of planet Earth.

Acknowledgements

This book represents an expansion of *Evolution of the Atmosphere, Fire and the Anthropocene Climate Event Horizon* (Glikson 2014), in connection with which we wish to thank the following people: Brenda McAvoy kindly helped with proof corrections. Helpful comments were obtained from Wallace Ambrose, Barrie Pittock, Hugh Davies, Leona Ellis, Miryam Glikson-Simpson, Victor Gostin, Clive Hamilton, Edward Linacre, Tony McMichael, Reg Morrison, Bruce Radke and Colin Soskolne. I thank Petra Van Steenbergen and Corina Van der Giessen for editorial help. I am grateful to Reg Morrison for contributing special figures and photographs, Jim Gehler for Ediacara photos, Mary White and John Laurie for fossil plant photos and Gerta Keller for reproduction of figures. The following people gave permission to reproduce figures in the book: John Adamek, Anita Andrew, Annemarie Abbondanzo, Robert Berner, Tom Boden, David Bowman, Karl Braganza, Pep Canadell, Randall Carlson, Giuseppe Cortese, Peter deMenocal, Gifty Dzah, Alexey Fedorov, Jim Gehling, Kath Grey, Jeanette Hammann, James Hansen, Paul Hoffman, John Johnson, Jean Jouzel, Barry Lomax, Petra Löw, Cesca McInerney, Michele McLeod, Yvonne Mondragon, Jennifer Phillips, Miha Razinger, Dana Royer, Elizabeth Sandler, Bill Schopf, Appy Sluijs, Phillipa Uwins, John Valley, Simon Wilde and James Zachos.

Contents

1 Early Earth Systems 1
1.1 Archaean and Proterozoic Atmospheres 2
1.2 Early Biospheres 12
1.3 Greenhouse States and Glaciations 22

2 Phanerozoic Life and Mass Extinctions of Species 45
2.1 Acraman Impact and Acritarchs Radiation 61
2.2 Cambrian and Late Ordovician Mass Extinction 61
2.3 Late and End-Devonian Mass Extinctions 62
2.4 Late Permian and Permian-Triassic Mass Extinctions 62
2.5 End-Triassic Mass Extinction 63
2.6 Jurassic-Cretaceous Extinction 64
2.7 K-T (Cretaceous-Tertiary Boundary) Mass Extinction 64
2.8 Paleocene-Eocene Extinction 67
2.9 The End-Eocene Freeze 67

3 Cenozoic Biological Evolution (by Colin Groves) 69
3.1 The Evolution of Mammals 69
3.2 From Primates to Humans 75
3.3 From Genetic Evolution to Cultural Evolution 81

4 Fire and the Biosphere 85
4.1 An Incendiary Biosphere 86
4.2 The Deep-Time History of Fire 88
4.3 Fire and Pre-historic Human Evolution 94
4.4 Neolithic Burning and Early Civilizations 111

5 The Anthropocene 123
5.1 The Modern Atmosphere 124
5.2 Neolithic Burning and Early Global Warming 133
5.3 The Great Carbon Oxidation Event 137

5.4 The Sixth Mass Extinction of Species 154
5.5 The Faustian Bargain 158
5.6 The Post-Anthropocene World 172

6 Rare Earth 177

7 Prometheus: An Epilogue 189

References 197

About the Book and the Authors 219

Index 221

Chapter 1
Early Earth Systems

Ancient Water

No one
Was there to hear
The muffled roar of an earthquake
Nor anyone who froze with fear
Of rising cliffs, eclipsed deep lakes
And sparkling comet-lit horizons
Brighter than one thousand suns
That blinded no one's vision
No one
Stood there in awe
Of an angry black coned volcano
Nor any pair of eyes that saw
Red streams eject from inferno
Plumes spewing out of Earth
And yellow sulphur clouds
Choking no one's breath
No one
Was numbed by thunder
As jet black storms gathered
Nor anyone was struck asunder
By lightning, when rocks shuttered
Engulfed by gushing torrents
That drowned the smouldering ashes
Which no one was to lament
In time
Once again an orange star rose
Above a sleeping archipelago
Sun rays breaking into blue depth ooze
Waves rippling sand's ebb and flow
Receding to submerged twilight worlds
Where budding algal mats
Declare life
On the young Earth

(By Andrew Glikson)

A.Y. Glikson, C. Groves, *Climate, Fire and Human Evolution*, Modern Approaches in Solid Earth Sciences 10, DOI 10.1007/978-3-319-22512-8_1

Abstract The development of isotopic age determination methods and stable isotopic tracers to paleo-climate investigations, including oxygen ($\delta^{18}O$), sulphur ($\delta^{33}S$) and carbon ($\delta^{13}C$), integrated with Sedimentological records and organic and biological proxies studies, allows vital insights into the composition of early atmosphere–ocean-biosphere system, suggesting low atmospheric oxygen, high levels of greenhouse gases (CO_2, CO, CH_4 and likely H_2S), oceanic anoxia and high acidity, limiting habitats to single-cell methanogenic and photosynthesizing autotrophs. Increases in atmospheric oxygen have been related to proliferation of phytoplankton in the oceans, likely about ~2.4 Ga (billion years-ago) and 0.7–0.6 Ga. The oldest recorded indirect traces of biogenic activity are provided by dolomite and banded iron formation (BIF) from ~3.85 Ga-old Akilia and 3.71–3.70 Ga Isua greenstone belt, southwest Greenland, where metamorphosed banded ironstones and dolomite seawater-like REE and Y signatures (Bolhar et al. Earth Planet Sci Lett 222:43–60, 2004; Friend et al. Contrib Miner Petrol 183(4):725–737, 2007) were shown to be consistent with those of sea water (Nutman et al. Precamb Res 183:725–737, 2010). Oldest possible micro-fossils occur in ~3.49 Ga black chert in the central Pilbara Craton (Glikson. Aust J of Earth Sci 55:125–139, 2008; Glikson. Icarus 207:39–44, 2010; Duck et al. Geochim Cosmochim Acta 70:1457–1470, 2008; Golding et al. Earliest seafloor hydrothermal systems on earth: comparison with modern analogues. In: Golding S, Glikson MV (eds) Earliest life on earth: habitats, environments and methods of detection. Springer, Dordrecht, pp 1–15, 2010) and in 3.465 Ga brecciated chert (Schopf et al. Precamb Res 158:141–155, 2007). Possible stromatolites occur in ~3.49 and ~3.42 carbonates. The evidence suggests life may have developed around fumaroles in the ancient oceans as soon as they formed. The evidence indicates extended atmospheric greenhouse periods interrupted by glacial periods which led to an increase in oxygen solubility in water, with implications for enhanced life. Intermittent volcanic eruptions and asteroid and comet impacts, representing continuation of the Late Heavy Bombardment as recorded on the Moon, resulted in major crises in biological evolution.

1.1 Archaean and Proterozoic Atmospheres

Terrestrial climates are driven through the exposure of the Earth surface to solar insolation cycles (Solanki 2002; Bard and Frank 2006), variations in the gaseous and aerosol composition of the atmosphere, the effects of photosynthesis on CO_2 and O_2 cycles, microbial effects on methane levels, volcanic eruptions, asteroid and comet impacts and other factors. By contrast to the thick CO_2 and SO_2 blankets on Venus, which exert an extreme pressure of 93 bar at the surface, and unlike the thin 0.006 bar atmosphere of Mars, the presence in the Earth's atmosphere of trace concentrations of well-mixed greenhouse gases (GHG) (CO_2, CH_4, N_2O, O_3) modulates surface temperatures, allowing the presence of liquid water (Fig. 1.1) and thereby

Fig. 1.1 Natural mortar and pestle – Komati River, Barberton Mountain Land, Swaziland (Photograph by Andrew Glikson)

life. During the Holocene surface temperatures ranged between −89 °C and +58 °C, with a mean of about +14 °C.

During early stages of terrestrial evolution low solar luminosity *(The Faint Young Sun)* lower luminosity than at present representing early stages in the fusion of hydrogen to helium (Sagan and Mullen 1972), is thought to have been compensated by high greenhouse gas (GHG) levels (Fig. 1.2), allowing surface temperature to remain above freezing (Kasting 1993). This author suggested that to warm the oceans above freezing point the atmosphere would have needed CO_2 levels some 100–1000 times the present atmospheric level. Alternative hypotheses were proposed by Longdoz and Francois (1997) in terms of albedo and seasonal variations on the early Earth. Rosing et al. (2010) pointed out a high ocean to continent surface area ratio in the Archaean would have led to a lower albedo and due to absorption of infrared radiation by open water. Temporal fluctuations in atmospheric GHG levels constituted a major driver of alternating glacial and greenhouse states (Kasting and Ono 2006). Rosing et al. 2010 suggested the Archaean atmosphere was less clouded and more transparent than later atmospheres due to a paucity of condensation nuclei such as occur above land, including dust particles, soot and sulphuric acid released by plant photosynthesis (Kreidenweis and Seinfeld 1988). The relations between GHG, clouds and surface albedo during the Archaean remains a subject of continuing debate (Goldblatt and Zahnle 2011).

Planetary evolution transpires through gradual changes as well as major upheavals. The former include plate tectonics, crustal accretion, crustal subduction, rise and erosion of mountain belts. The latter include abrupt magmatic and tectonic events and extra-terrestrial impact-triggered cratering. Geochronological age sequences, geochemistry and isotopic indices point to secular evolution from a

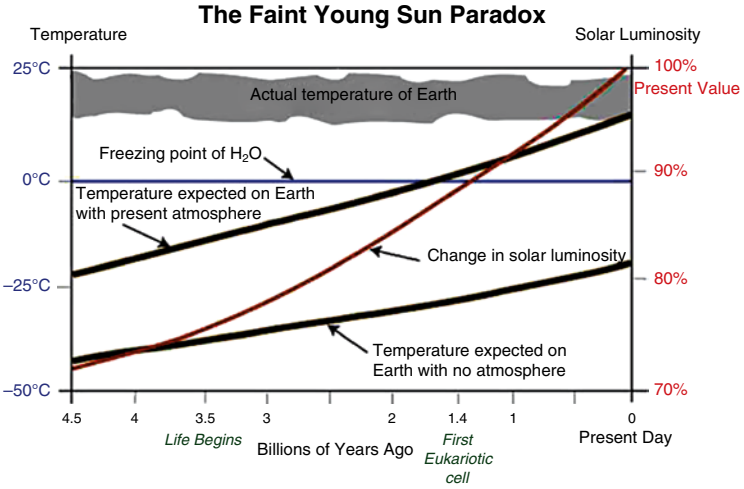

Fig. 1.2 The faint young sun paradox according to Sagan and Mullen (1972), suggesting compensation of the lower solar luminosity by high atmospheric greenhouse gas levels at early stages of terrestrial evolution. (From the *Habitable Planet*: A system approach to environmental science, produced by the Harvard-Smithsonian Center for Astrophysics, Science Media Group and used with permission by the Annenberg Learner (Courtesy Michele McLeod) www.learner.org; http://www.learner.org/courses/envsci/unit/text.php?unit=1&secNum=4)

mainly basaltic crust (SIMA: Silica-Magnesium-iron-dominated crust) to granite-dominated crustal nuclei (SIAL: Silica-Alumina-dominated crust) (Glikson 1972, 1980, 1984; McCulloch and Bennett 1994).

Atmospheric CO_2 levels are buffered by the oceans (at present ~37,000 GtC) which contain about 48 times the atmospheric CO_2 inventory (currently ~800 GtC). The solubility of CO_2 in water decreases with higher temperature and salinity and the transformation of the $CO_3^{[-2]}$ ion to carbonic acid ($HCO_3^{[-1]}$) retards the growth of calcifying organisms, including corals and plankton. Plants and animals work in opposite directions of the entropy scale, where plants synthesize complex organic compounds from CO_2 and water, producing oxygen, whereas animals burn oxygen and expel CO_2. Disturbances in the carbon and oxygen balance occur when changes occur in the extent of photosynthetic processes, CO_2 solubility in the oceans, burial of carbon in carbonate and from remains of plants and oxidation of carbon through fire and combustion.

Forming a thin breathable veneer only slightly more than one thousandth the Earth's diameter, evolving both gradually as well as through major perturbations, the atmosphere acts as lungs of the biosphere, facilitating an exchange of carbon and oxygen with plants and animals (Royer et al. 2004, 2007; Siegenthaler et al. 2005; Berner 2006; Berner et al. 2007; Beerling and Royer 2011). In turn biological activity continuously modifies the atmosphere, for example through production of methane in anoxic environments, release of photosynthetic oxygen from plants and

of dimethyl sulphide from marine phytoplankton. Long term chemical changes in the air-ocean system are affected by changes in plate tectonic-driven geomorphic changes including subduction of oceanic and continental plates (Ruddiman 1997, 2003, 2008), weathering, volcanic and methane eruptions, and variations in marine and terrestrial photosynthetic activity (Broecker 2000; Zachos et al. 2001; Hansen et al. 2007; Glikson 2008). The range of paleo-climate proxies used in these studies are reviewed in detail by Royer et al. (2001).

Early terrestrial beginnings are interpreted in terms of a cosmic collision ~4.5 billion years-ago between an embryonic semi-molten Earth and a Mars-scale body – *Theia* – determined from Pb isotopes (Stevenson 1987). The consequent formation of a metallic core, inducing a magnetic field which protects the Earth from cosmic radiation, and a strong gravity field which to a large extent prevents atmospheric gases from escaping into space, resulted in a haven for life at the Earth surface (Gould 1990). Relict ~4.4 Ga and younger zircons, representing the *Hadean* era, a term coined by Preston Cloud in 1972, signify vestiges of granitic and felsic volcanic crustal nuclei, implying the presence of a water component in the melt and low-temperature surface conditions (Wilde et al. 2001; Mojzsis et al. 2001; Knauth 2005, Valley et al. 2002) (Figs. 1.3 and 1.4). However, Pidgeon et al. (2013) and Pidgeon (2014) attributed the $\delta^{18}O$ values of zircon to secondary radiation damage and associated with hydrous alteration. Precambrian terrains contain relict ~4.1–3.8 Ga-old rocks, including volcanic and sedimentary components, exposed in Greenland, Labrador, Slave Province, Minnesota, Siberia, northeast China, southern Africa, India, Western Australia and Antarctica (Van Kranendonk 2007). These formations, formed parallel to the Late Heavy Bombardment (LHB) on the Moon (~3.95–3.85 Ga) (Ryder 1991), are metamorphosed to an extent complicating recognition of primary impact shock features, which to date precluded an identification of signatures of the LHB on Earth.

Knauth and Lowe (2003) and Knauth (2005) measured low $\delta^{18}O$ values in ~3.5–3.2 Ga cherts of the Onverwacht Group, Barberton Greenstone Belt (BGB), Kaapvaal Craton, suggesting extremely high ocean temperatures in the range of 55–85 °C (Figs. 1.3, and 1.4). The maximum $\delta^{18}O$ value in Barberton chert (+22‰) is lower than the minimum values (+23‰) in Phanerozoic sedimentary cherts, precluding late diagenesis as the explanation of the overall low $\delta^{18}O$ values. Regional metamorphic, hydrothermal, or long-term resetting of original $\delta^{18}O$ values is also precluded by preservation of $\delta^{18}O$ across different metamorphic grades. According to Knauth (2005) high-temperature conditions extended beyond submarine fumaroles and the Archaean oceans were characterized by high salinities 1.5–2.0 times the modern level. In this interpretation ensuing evaporite deposits were removed by subduction, allowing lower salinities. However, well preserved Archaean sedimentary sequences contain little evidence of evaporite deposits. The low-oxygen levels of the Archaean atmosphere and hydrosphere limited marine life to extremophile cyanobacteria. Microbial methanogenesis involves reactions of CO_2 with H_2 or acetate (CH_3CO_2—) produced from fermenta-

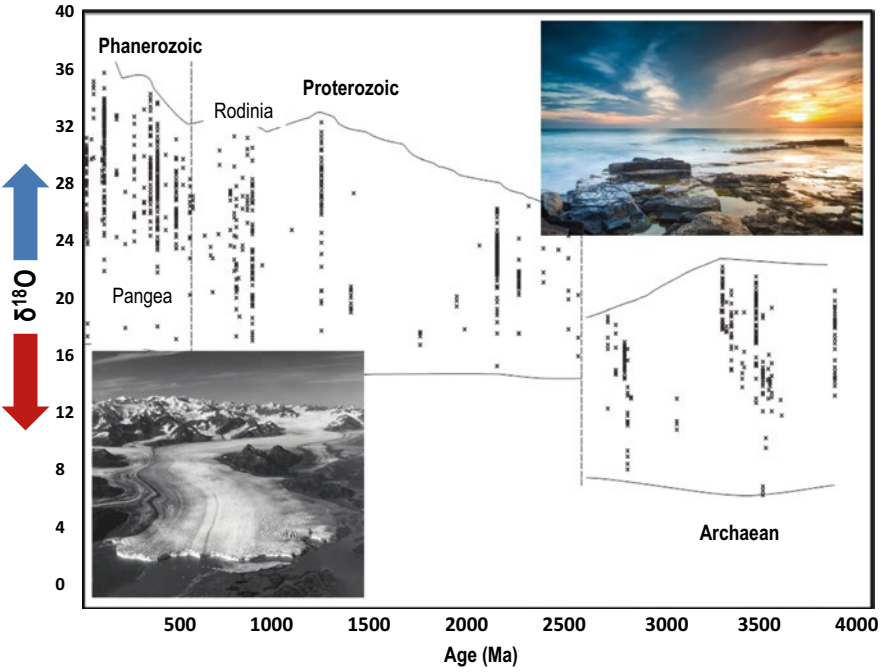

Fig. 1.3 A compilation of oxygen isotope data for cherts. The overall increase in $\delta^{18}O$ with time is interpreted as global cooling over the past 3500 Ma. The variation in $\delta^{18}O$ for cherts at any given time is caused by the presence of low $\delta^{18}O$ meteoric waters during burial at elevated temperatures (Knauth 2005; Elsevier, by permission). Insets: (1) Columbia Glacier (NASA). (http://www.google.com.au/search?q=nasa+glacier&hl=en&tbm=isch&tbo=u&source=univ&sa=X&ei=hkmEUbCDBonGkgXDg4C4CQ&sqi=2&ved=0CEYQsAQ&biw=1360&bih=878); (2) http://www.flickr.com/photos/anieto2k/8636213185/sizes/l/in/photostream/ (anieto2k's photo stream)

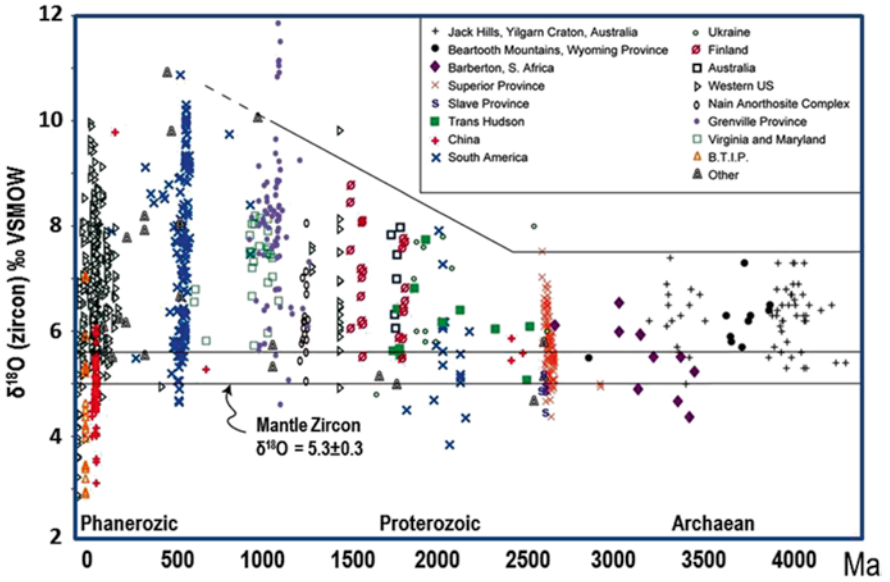

Fig. 1.4 $\delta^{18}O$ ratio of igneous zircons from 4.4 Ga to recent, displaying an increase in abundance of low-temperature effects with time from approximately ~2.3 Ga (Courtesy J.W. Valley)

tion of photo-synthetically produced organic matter. Photolysis of methane may have created a thin atmospheric organic haze.

By contrast to the high temperature estimates by Knauth and Lowe (2003) and Knauth (2005), combined relationship of $\delta^{18}O$ and δD (deuterium) suggests chert precipitated from ocean water at temperatures no warmer than 40 °C (Hren et al. 2009). A subsequent study of the $\delta^{18}O$ of Barberton phosphates (Blake et al. 2010) placed Archaean ocean temperatures at 26–35 °C. High temperature low pH water can be expected to have resulted in extensive corrosion and syngenetic dissolution of Archaean cherts and quartz grains in arenites, for which there is little evidence.

Studies of oxygen isotopes of Hadean zircons indicate little difference between the maximum $\delta^{18}O$ values of ~4.4–4.2 Ga zircons and those of younger ~3.6–3.4 Ga zircons (Fig. 1.4), which suggests presence of relatively low temperature water near or at the surface (Valley et al. 2002). However, secondary penetration of meteoric OH^{-1} molecules associated with radiation damage zircons must be borne in mind (Pidgeon et al. 2013; Pidgeon 2014).

An overall increase with time in $\delta^{18}O$ shown by terrestrial sediments (Valley 2008) (Fig. 1.4) reflects a long term cooling of the hydrosphere, consistent with an overall but intermittent temporal decline in atmospheric CO_2 shown by plant leaf pore (stomata) studies (Berner 2004, 2006; Beerling and Berner 2005; Royer et al. 2001, 2004, 2007). This long-term decline may have been associated with increased rates of weathering-sequestration of CO_2 related to erosion of rising orogenic belts, including the Caledonian, Hercynian, Alpine, Himalayan and Andean mountain chains (Ruddiman 1997, 2003). Such a trend is consistent with suggested increase in the role of plate tectonics through time (Glikson 1980), which led to an increase in sequestration of CO_2 by weathering of orogenic belts and subduction of CO_2-rich carbonate and carbonaceous shale.

Studies of the nature of the early terrestrial atmosphere–biosphere system hinge on the sulphur, carbon and oxygen stable isotopes (Kasting 1993; Pavlov and Kasting 2002; Holland 2006; Kasting and Ono 2006). The geochemical behaviour of multiple sulphur isotopes is a key proxy for long-term changes in atmospheric chemistry (Mojzsis 2007; Thiemens 1999). The identification of mass-independent fractionation of sulphur isotopes (MIF-S) in pre-2.45 Ga sediments has been correlated with ultraviolet radiation effects on the $\delta^{33}S$ values, with implications for an ozone and oxygen-poor Archaean atmosphere (Fig. 1.5) (Farquhar et al. 2000, 2007), whereas other authors suggested heterogeneous Archaean oxygen levels (Ohmoto et al. 2006). Development of photosynthesis, and thereby limited release of oxygen as early as about 3.4 Ga, is suggested by identification of heliotropic stromatolite reefs in the Pilbara Craton (Allwood et al. 2007). The abrupt disappearance of positive MIF-S anomalies at ~2.45 Ga poses a problem, as atmospheric enrichment in oxygen due to progressive photosynthesis could, perhaps, be expected to result in a gradual rather than an abrupt decline in MIF-S signatures. MIF-S ($\delta^{33}S$) anomalies (Fig. 1.5) overlap mid-Archaean impact periods (~3.26–3.24 Ga) and Late Archaean impact periods (~2.63, ~2.56, ~2.48 Ga) (Lowe et al. 1989, 2003; Simonson and Hassler 1997; Simonson et al. 2000; Simonson and Glass 2004; Glikson 2001, 2004, 2005, 2006; Glikson et al. 2004; Glikson and Vickers

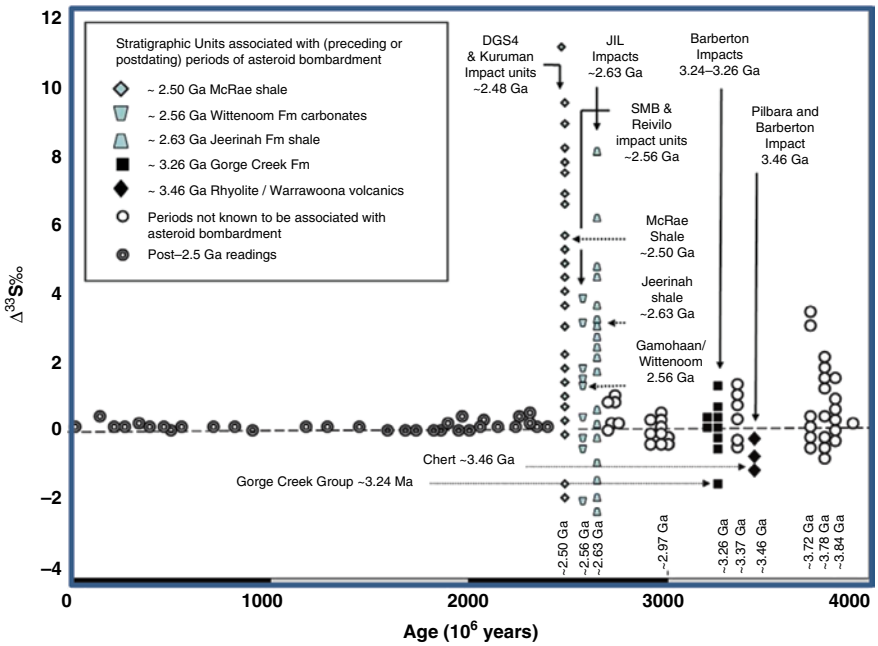

Fig. 1.5 Plots of mass independent fractionation values for Sulphur isotopes ($\Delta^{33}S$ – MIF-S) vs. Age. The high $\Delta^{33}S$ values for pre-2.45 Ga sulphur up to about $\Delta^{33}S = 11$ is interpreted in terms UV-induced isotopic fractionation, allowed by a lack of an ozone layer. Periods of major asteroid impacts during which ozone may have been destroyed are indicated (From Glikson 2010; Elsevier, by permission)

2006, 2007), though no specific age correlations are observed. Estimates of projectile diameters derived from mass balance calculations of iridium levels, $^{53}Cr/^{52}Cr$ anomalies and size-frequency distribution of fallout impact spherules (microkrystites) (Melosh and Vickery 1991), suggest projectiles of the ~3.26–3.24, ~2.63, ~2.56 and ~2.48 Ga impact events reached several tens of kilometre in diameter (Byerly and Lowe 1994; Shukolyukov et al. 2000; Kyte et al. 2003; Glikson et al. 2004; Glikson 2005, 2013). Impacts on this scale would have led to major atmospheric effects, including large scale ejection of carbon and sulphur-bearing materials, effects on the ozone layer and isotopic fractionation of sulphur. Archaean impact ejecta units in the Pilbara and Kaapvaal Cratons are almost invariably overlain by ferruginous shale and banded iron formations (BIF) (Glikson 2006; Glikson and Vickers 2007). The origin of BIFs is interpreted, alternatively, in terms of oxidation of ferrous to ferric iron under oxygen-poor atmospheric and hydrospheric conditions (Cloud 1968, 1973; Morris 1993), direct chemo-lithotropic or photo-ferrotropic oxidation of ferrous iron, and UV-triggered photo-chemical reactions (Cairns-Smith 1978). The relations between sulphur, oxygen and carbon isotopes, atmospheric oxygen levels, photosynthesis, banded iron formations and glaciations

with implications for evolution of the early atmosphere remain the subject of current investigations.

During much of its early history Earth was dominated by an oxygen-poor, CO_2, CO and methane-rich atmosphere of several thousand to tens of thousands ppm CO_2, resulting in low-pH acid oceans. High temperatures of ocean waters (Knauth and Lowe 2003; Knauth 2005) allowed little sequestration of the CO_2 accumulated in the atmosphere from episodic volcanism, impact cratering, metamorphic release of CO_2, dissociation of methane from sediments and microbial activity and, following the advent of plants on land in the Silurian (~420 Ma), from decomposed vegetation (Berner 2004; Berner 2006; Beerling and Berner 2005; Royer et al. 2004, 2007; Royer 2006; Glikson 2008). The low solubility of CO_2 in the warm water of the early hydrosphere and little weathering-capture of CO_2, due to a low continent/ocean crust ratio and limited exposure of land surface, ensured long term at ~2.9 Ga, 2.4–2.2 Ga, 575–543 Ma, the late Ordovician (~446–443 Ma), Carboniferous-Permian (~326–267 Ma), Jurassic (187–163 Ma) and post-Eocene, signifies episodic large-scale CO_2 sequestration events (Ruddiman 2003).

The presence of siderite as crusts on river cobbles in 3.2 Ga conglomerates in the Archaean Barberton greenstone belt and of nahcolite within 3.4 Ga marine sedimentary rocks (Lowe and Tice 2004) requires CO_2 levels 7–10 times the present atmospheric CO_2 concentrations under temperatures of ~25 °C (Eugster 1966; Hessler et al. 2004). The presence of siderite ($FeCO_3$) and nahcolite ($NaHCO_3$) provides a constraint on the amount of CO_2 available for the reactions (Hessler 2012):

$$3FeCO_3 + 2SiO_2 + 2H_2O <—> Fe_3Si_2O_5(OH)_4 + 3CO_2$$

$$2NaHCO_3 <—> Na_2CO_3 + H_2O + CO_2$$

Rosing et al. 2010 suggest an upper limit for Archaean CO_2 within 10 times the present atmospheric level based on the presence of magnetite (Fe_3O_4) in equilibrium with siderite in Archaean shallow-marine sediments, as higher CO_2 concentrations would result in higher FeO levels in the water. According to Hessler (2012) such CO_2 level would not be enough to prevent the oceans from freezing under the faint early sun conditions. That liquid water existed in the early Archaean would have resulted from high levels of atmospheric methane released by methanogenic microbial activity (Kharecha et al. 2005), consistent with views regarding biogenic environments in the Barberton greenstone belt (Tice and Lowe 2006; Noffke et al. 2006; Heubeck 2009) and in the Pilbara (Lowe 1983; Hoffman et al. 1999, Allwood et al. 2007). In a low-oxygen Archaean atmosphere methane would have had a longer residence time (Zahnle 1986; Pavlov and Kasting 2002) reaching higher concentration than during later periods under oxygen-rich atmospheric conditions. High CH_4 would lead to atmospheric hydrocarbon haze as on Saturn's moon Titan (Trainer et al. 2006; Hessler 2012), higher albedo and a possible degree of cooling. According to Goldblatt et al. (2009) a high level of Nitrogen would have been associated with enhancement of a CO_2– CH_4 greenhouse atmosphere as N_2 increases atmospheric

pressure and the rate at which the greenhouse gases can absorb infrared radiation. Estimates of atmospheric CO_2 and CH_4 at 2.5 Ga suggest that doubling of the present atmospheric N_2 concentration would have caused warming by 4.4 °C. The source of nitrogen has been attributed to volcanic degassing (Mather et al. 2004). The presence of fixed nitrogen is considered essential for biological synthesis. Following the development of photosynthesis nitrogen would have been removed from the atmosphere and sequestered through reactions such as $N_2 + 3\ H_2O \rightarrow 2\ NH_3 + 1.5\ O_2$, releasing oxygen to the oceans.

Central to studies of early atmospheres is the level of oxygen and its relation to photosynthesis. Sulphur isotopic analyses record mass-independent fractionation of sulphur isotopes ($\delta^{33}S$) (MIF-S) in sediments older than ~2.45 Ga, widely interpreted in terms of UV-triggered reactions under oxygen-poor ozone-depleted atmosphere and stratosphere (Farquhar et al. 2000, 2007) (Fig. 1.5). From about ~2.45–2.32 Ga – a period dominated by deposition of banded iron formations (BIF) (Figs. 1.6, and 1.7), high $\delta^{33}S$ values signify development of an ozone layer shielding the surface from UV radiation (Farquhar et al. 2000; Kump 2009) (Fig. 1.5). According to Kopp et al. (2005) photosynthetic oxygen release from cyanobacteria

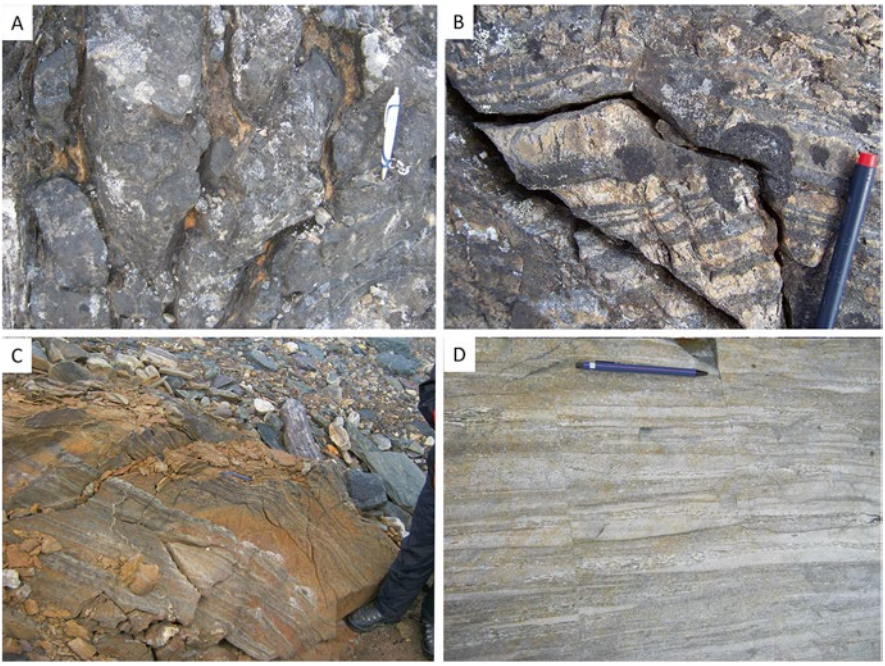

Fig. 1.6 Isua supracrustal belt: (**a**) Relict pillows in amphibolite facies ~3.8 Ga meta-basalts of arc-tholeiite to picrite compositions from the southern flank of the Isua Belt; (**b**) Low strain zone in ~3760 Ma Isua banded iron formations. Note the grading of the layering and the layering on a cm-scale; (**c**) Agglomerate clasts in a ~3.7 Ga Ma felsic intermediate unit from the eastern end of the Isua belt; (**d**) Original layering preserved in quartz + dolomite + biotite ± hyalophane (Na-Ba feldspar) metasediments, likely derived from marl and evaporite (Courtesy Allen Nutman)

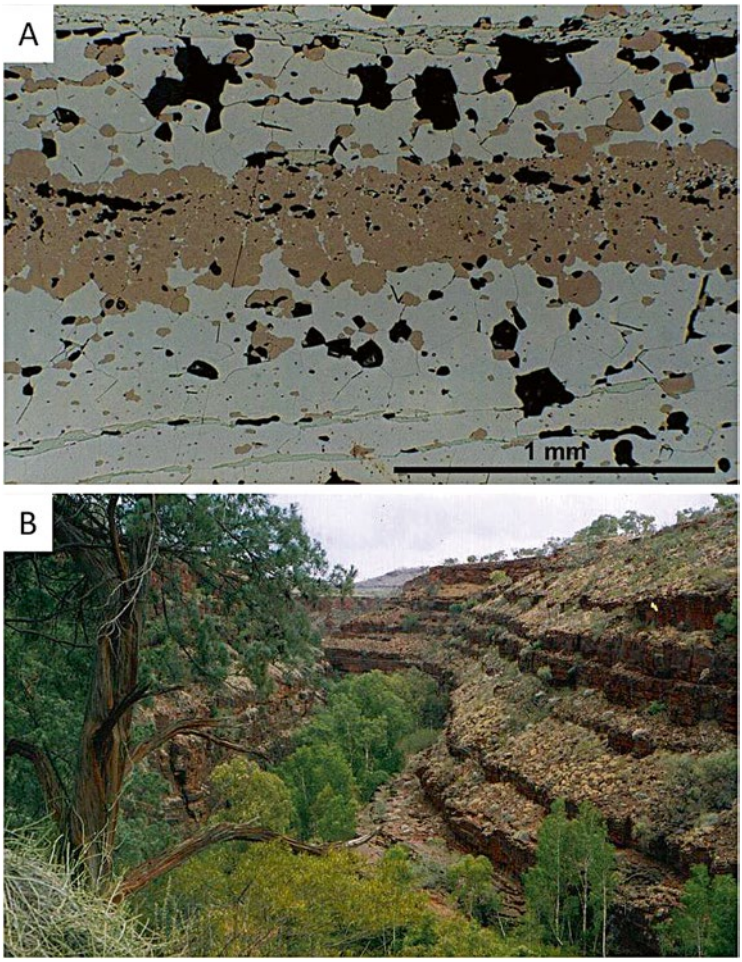

Fig. 1.7 Banded iron formations (BIF). (**a**) Magnetite-quartz banded iron formation, Isua Supracrustal belt, Southwest Greenland. Reflected light in thin section; (**b**) Outcrops of ~2.48 Ga BIF of Hamersley Group, Pilbara Craton, Western Australia, at Dales Gorge near Fortescue Fall (Photographs by A.Y. Glikson)

and aerobic eukaryotes affected oxidation of atmospheric methane, triggering planetary-scale glaciation at least as early as 2.78 Ga and perhaps as long ago as 3.7 Ga (Kopp et al. 2005; Bekker and Kaufman 2007). Examples of reaction of CO_2 with silicates and of formation of carbonates are given below:

$$CaSiO_3 + CO_2 + H_2O \rightarrow Ca^{2+} + HCO_3^- + H_4SiO_4, \text{ and}$$

$$Ca^{2+} + HCO_3^- \rightarrow CaCO_3 + H^+$$

Major glaciations in the early and late Proterozoic are thus thought to have resulted in intermittent transformation of the Earth's climate due to oxygen-producing cyanobacteria and phytoplankton, oxidation of aqueous and atmospheric methane and precipitation of carbonates (Canfield et al. 2007). According to Ohmoto et al. (2006) MIF-S values and oxygen levels fluctuated through time and place, possibly representing local volcanic activity. The role of asteroid impacts in affecting the ozone layer, UV radiation and thus regional MIF-S values has been discussed by Glikson (2010).

1.2 Early Biospheres

Inherent in the search for biological signatures in the Archaean geological record are fundamental questions associated with the origin of life (Darwin 1859; Cloud 1968; Davies 1998; Schopf and Packer 1987; Schopf et al. 2007), conceived according to the Miller–Urey and other experiments to have arisen by racemic abiogenic synthesis of inorganic precursors to organic amino acids, the building blocks of life, triggered by lightning and radiation affecting a "primordial soup" rich in organic matter. Oparin (1924) regarded atmospheric oxygen as a constraint on synthesis of biomolecules, restricting original synthesis of biomolecules to the pre-oxygenation era. In some theories life developed from inanimate matter through complex reactions on the surfaces of silicate minerals (Cairns-Smith (1990). A principal question is whether metabolism occurred prior to replication, or the other way around, leading to a view of life as an extreme expression of kinetic control and the emergence of metabolic pathways manifesting replicative chemistry (Pross 2004).

According to Davies (1998) the probability of the primordial DNA/RNA biomolecules forming by accident is about 1 to 10^{22}, rendering it equally or more likely the natural intelligence underlying the characteristics of these molecules and their more complicated successors resides in undecoded laws of complexity. According to Russell and Hall (2006) viruses, forming parasitic entities on life forms, acted as mobile RNA worlds injecting genetic elements into proto-cells capable of replicating themselves around submarine alkaline hydrothermal vents. There chemical reactions created biosynthetic pathways leading to emergence of sparse metabolic network and the assembly of pre-genetic information by primordial cells. In this concept, life and evolution of prokaryotes constituted a deterministic process governed by bio-energetic principles likely to apply on planets throughout the universe, which means life is everywhere. However, exobiogenic theories which invoke introduction of biomolecules from other planets merely relegate the question of the origin of life further in time and space. Thus, theories suggesting seeding of life on Earth by comets are to date lacking in evidence, since while comets and meteorites may contain amino acids, the difference between amino acids and RNA or DNA is as vast as the difference between atoms of iron and supercomputers.

According to Russell and Hall (2006) chemical reactions involving dissolved H_2, $HCOO^-$ and CH_3S- and CO_2 associated with oxidation of ferrous iron in the early

oceans constituted triggers for development of inorganic membranes and subsequently chemosynthetic life in hydrothermal environments. In this model these reactions produce metallo-enzymes such as greigite (Fe5NiS8) which catalyzes synthesis of acetate (H3C.COO─), leading to synthesis of more complex organic molecules such as Glycine (+H3N.CH2.COO─) and other amino acids and to RNA, generated within cavities of FeS. The process includes polymerizing glycine and other amino acids into short peptides on phosphorylated mineral surface where the peptides are protected. RNA acts as a polymerizing agent for amino acids, regulating metabolism and providing genetic information.

Considerations of original life forms commonly refer to extremophile microbial communities, such as around submarine hydrothermal vents ("black chimneys") (Martin et al. 2008). These authors compare the chemistry of the H2─CO2 redox couple in hydrothermal systems and core energy metabolic biochemical reactions of modern prokaryotic autotrophs. The high greenhouse gas levels (CO_2, CO, CH_4) of the early atmosphere allowing the presence of water at the Earth surface despite low solar luminosity (Fig. 1.2) implies high partial CO_2 pressure and low pH of the Archaean oceans. Dissociation of H_2O associated with microbial Fe^{+2} to Fe^{+3} under these conditions would have released hydrogen (Russell and Hall 2006). According to these authors life emerged around hydrothermal vents in connection with reaction involving H_2, HCOO─, CH_3S─ and CO_2 catalyzed by sulphide, analogous to the synthesis of acetate ($H_3C.COO$─). In this model Glycine (+H3N. CH2.COO─) and other amino acids, as well as tiny quantities of RNA, were trapped within tiny iron sulphide cavities. The released energy from these reactions resulted in polymerizing glycine and other amino acids into short peptides upon the phosphorylated mineral surface. RNA acted as a polymerizing agent for amino acids as a process regulating metabolism and transferring genetic information. Such biosynthetic pathways probably evolved before 3.7 Ga when reduction prevented a buildup of free atmospheric oxygen (Russell and Hall 2006).

Theories regarding the origin of banded iron formations (BIF) (Figs. 1.6, and 1.7) hinge on oxidation by microbial photoautotrophs or, alternatively, abiotic photo-oxidation of ferrous to ferric iron under the unoxidizing conditions of the early atmosphere/hydrosphere (Cloud 1973; Konhausser et al. 2002). A biogenic origin of BIF is supported by evidence for fractionation of the Fe isotopes relative to Fe in igneous rocks (Dauphas et al. 2004). The significance of dolomite hinges on experimental studies indicating precipitation of low-temperature dolomite in sedimentary systems and interstices of pillow lava under unoxidizing conditions requires microbial mediation (Vasconcelos et al. 1995; Roberts et al. 2004). Alternative views regard the dolomite as the product of metasomatism (Rose et al. 1996). Previously low ^{13}C in graphite clouding in Akilia apatite were interpreted in terms of early biogenic activity (Schidlowski et al. 1979; Mojzsis et al. 1996; Rosing 1999). Questions raised in this regard concern the sedimentary origin of host rocks and inorganic de-carbonation processes (Perry and Ahmed 1977; van Zuilen et al. 2002). Further, the significance of low $^{12}C/^{13}C$ indices as discriminants between biogenic and non-biogenic processes has been questioned (McCollom and Seewald 2006).

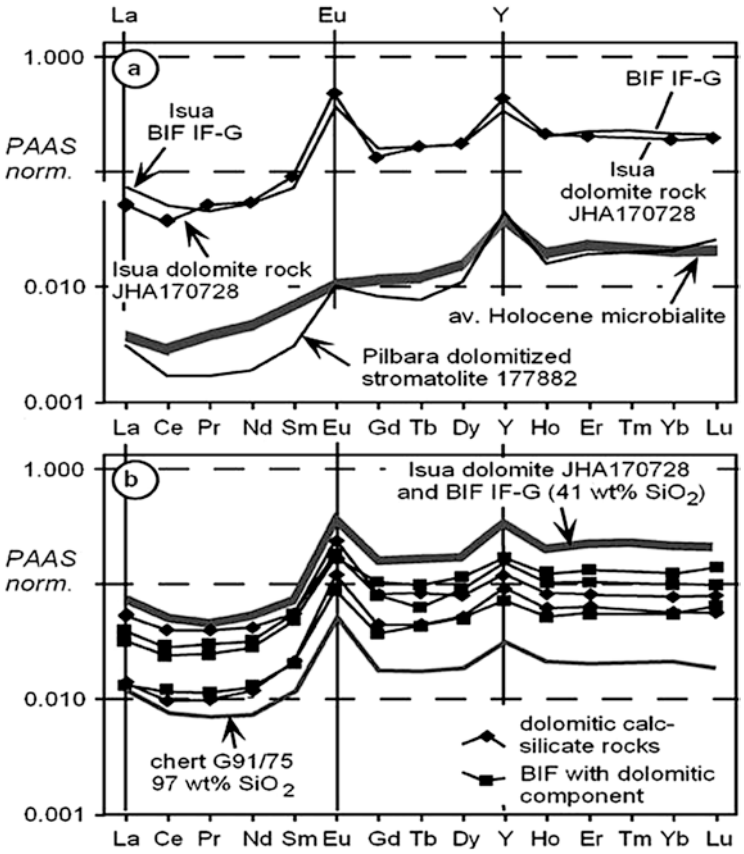

Fig. 1.8 REE+Y patterns normalized to Post-Archaean-Australian-Shale (PAAS). (**a**) IF-G Isua Banded iron formation and metamorphosed dolomite (JHA170728), modern Mg-calcite microbialite from Heron Island, Great Barrier Reef and a Warrawoona 3.45 Ga low-temperature dolomitized stromatolite; (**b**) Isua dolomitic calc-silicate rocks and BIF with a dolomitic component (From Nutman et al. 2010; Elsevier, by permission)

During a LHB (3.95–3.85 Ga) exposure of the Earth surface to cosmic and UV radiation from solar flares, incineration effected by large asteroid impacts, and acid rain, are likely to have retarded or precluded photosynthesizing bacterial activity (Zahnle and Sleep 1997; Chyba 1993; Chyba and Sagan 1996). However, extremophile chemotrophic bacteria of the *deep hot biosphere* (Gold 1999) are likely to have resided in deep faults and fracture following formation of original crustal vestiges. Oldest chemical manifestations of life discovered to date are in the form of dolomite and banded iron formation (BIF) from 3.85 Ga-old Akilia banded ironstones and dolomite, southwest Greenland, where these high-grade meta-sediments have seawater-like Rare Earth element and Y (REE+YSN) signatures (Bolhar et al. 2004; Friend et al. 2007) (Fig. 1.8) consistent with those of sea water (Nutman et al.

2010), similar to metasediments in the 3.71–3.70 Ga-old Isua greenstone belt, southwest Greenland. The suggestion that low $\delta^{13}C$ graphite within apatite in ~3.85 Ga-old banded iron formation in southwestern Greenland provide clues for such a habitat (Mojzsis and Harrison 2000) has not been confirmed as these were shown to arise from secondary contamination (Nutman and Friend 2006).

Some of the earliest manifestations of biological activity may be represented by banded iron formations (BIF) from the ~3.8 Ga Isua supracrustal belt (southwest Greenland) (Figs. 1.6, and 1.7). Banded iron formations are commonly intercalated with volcanic tuff and carbonaceous shale whose low $\delta^{13}C$ indices are indicative of biological activity. The carbon isotopic compositions of Archaean black shale, chert and BIF provide vital clues to the proliferation of autotrophs in the shallow and deep marine environment. Peak biogenic productive periods about 2.7–2.6 Ga are represented by low $\delta^{13}C$ of chert and black shale intercalated with banded iron formations in the Superior Province, Canada (Goodwin et al. 1976), and in the Hamersley Basin, Western Australia (Eigenbrode and Freeman 2006) (Fig. 1.9). This peak, which coincides with intense volcanic activity in greenstone belts world-wide, suggests enhanced biological activity related to volcanic emanations and enriched nutrient supply. Biological processes include oxygen capture by iron-oxidizing microbes, microbial methanogenesis producing atmospheric CH_4, microbial sulphur metabolism producing H_2S, ammonia-releasing microbes, oxygen-releasing photosynthesizing colonial prokaryotes (stromatolites) and algae, culminating in production of O_2-rich atmosphere and the O_3 ozone layer. Earliest manifestations of biological forcing may be represented by banded iron formations, widely held to represent ferrous to ferric iron oxidation by microbial reactions (Cloud 1968, 1973; Morris 1993; Konhausser et al. 2002; Glikson 2006).

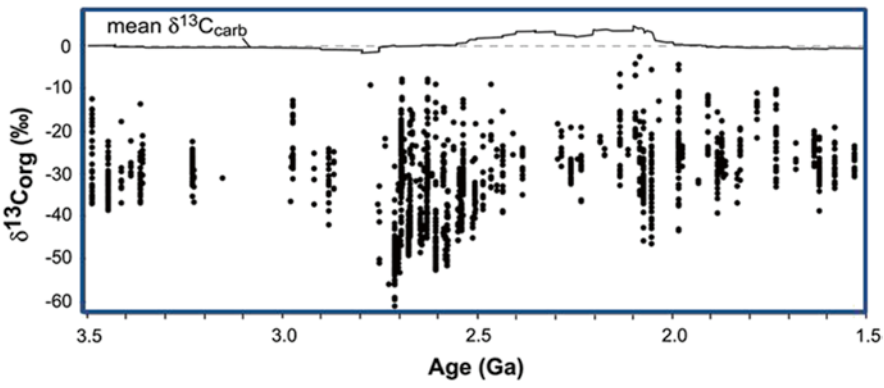

Fig. 1.9 A compilation of published kerogen and total organic carbon $\delta^{13}C$ values (δorg) for all sedimentary rock types (Eigenbrode and Freeman 2006; PNAS by permission). Note high accumulations of organic carbon in the late Archaean at ~2.7–2.6 Ga

The origin of BIFs has been interpreted in terms of transportation of ferrous iron in ocean water under oxygen-poor atmospheric and hydrospheric conditions of the Archaean (Cloud 1968; Garrells et al. 1973; Morris 1993). Oxidation of ferrous to ferric iron could occur through chemotrophic or phototrophic bacterial processes (Konhausser et al. 2002) and/or by UV-triggered photo-chemical reactions. The near-disappearance of banded iron formations (BIF) about ~2.4 Ga, with transient re-appearance about 1.85 Ga and in the Vendian (650–543 Ma), likely reflect increase in oxidation, where ferrous iron became unstable in water and the deposition of BIF was replaced by that of detrital hematite and goethite. Archaean impact ejecta units in the Pilbara and Kaapvaal Cratons are commonly overlain by ferruginous shale and BIF (Glikson 2006; Glikson and Vickers 2007), hinting at potential relations between Archaean impact clusters, impact-injected sulphate, consequent ozone depletion, enhanced UV radiation and formation of BIFs (Glikson 2010), possibly by photolysis through the reaction: $2H_2O <> 2H+ + 2e- + O_2$ followed by $2FeO + O <> Fe_2O_3$.

A study of 3.47 to 3.30 Ga carbonaceous chert layers and veins in the Onverwacht Group of the Barberton Greenstone Belt suggests an origin of the bulk of the carbonaceous matter in the chert by biogenic processes, accompanied by modification through hydrothermal alteration (Walsh and Lowe 1985; Walsh 1992). These studies identified textural evidence in cherts for microbial activity represented by carbonaceous laminations in intercalations within the Hoogenoeg and Kromberg Formations, with affinity to modern mat-dwelling cyanobacteria or bacteria. These include a range of spheroidal and ellipsoidal structures analogous to modern coccoidal bacteria and bacterial structures, including spores. The Pilbara Craton, Western Australia, contains evidence of >3.0 Ga microfossils, trace fossils, stromatolites, biofilms, microbial and microscopic sulfide minerals with distinctive biogenic sulphur isotope signatures (Wacey 2012). Schopf and Packer (1987) identified 11 taxa, including eight new species of cellularly preserved filamentous Prokaryote microbes in a shallow chert sheet of the ~3.459 Ga Apex Basalt. This assemblage indicates morphologically diverse extant trichomic cyanobacterium-like microorganisms, suggesting presence of oxygen-producing photoautotrophs. However, a possibility remains these microbes represent contamination by ground water.

Studies of microbial remains from the ~3.49 Ga Dresser Formation, North Pole Dome, central Pilbara Craton (Glikson et al. 2008) and of filamentous microbial remains and carbonaceous matter (CM) from Archaean black cherts (Duck et al. 2008) (Figs. 1.10, and 1.11) have used the following methods: (1) organic petrology; (2) Transmission Electron Microscopy (TEM); (3) Electron Dispersive Spectral Analysis (EDS); (4) high resolution TEM (HRTEM); (5) elemental and carbon isotope geochemistry studies (6) reflectance measurements determining thermal stress. The analyses resolve images of microbial relics and cell walls analogous to the modern hyperthermophilic *Methano-caldococcus jannaschii* residing in hydrothermal sea floor environments. Analogies include the wall structure and thermal degradation mode about 100 °C considered as the upper limit of life, whereas complete disintegration takes place at 132 °C. The $\delta^{13}C$ values of CM from the ~3.49 Ga Dresser Formation (−36.5 to −32.1‰) show negative correlation with total organic carbon (TOC = 0.13–0.75 %) and positive correlation with Carbon/Nitrogen ratios

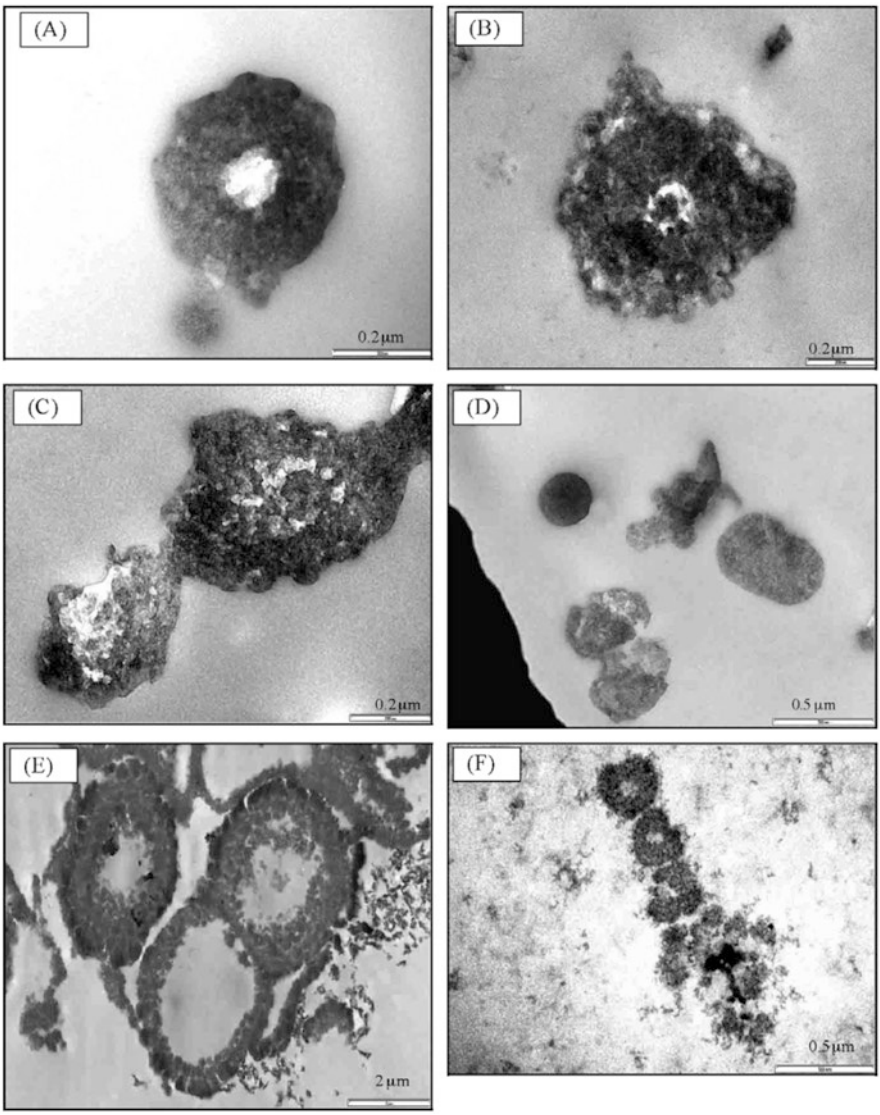

Fig. 1.10 Microbial remains from the ~3.49 Ga Dresser Formation. TEM micrographs of thermally degraded Carbonaceous Matter (*CM*) concentrate after demineralization of rock. (*A and B*) Single granular-textured bodies showing porosity and central cavity following dissolution of mineral matter (samples DF-17 (**a**); DF-10 (**b**). (**c**) Micro-porous bodies connected by extensions of same CM (sample DF-10). (**d**) Cell-like bodies 'caught' at possible early stages of dividing or splitting (sample DF-17). (**e**) Part of an aggregate of cell-like bodies showing central cavities as characteristic of CM concentrate after demineralization (sample H-1). (**f**) *M. jannaschii* harvested after being autoclaved at 132C, showing nano-porosity following breakdown and ejection of cellular material. Shrinkage, deformity of cells and amorphous material formation following thermal stress is evident as is contraction of cell cavity into a tiny central hollow (From Glikson et al. 2008; Elsevier, by permission)

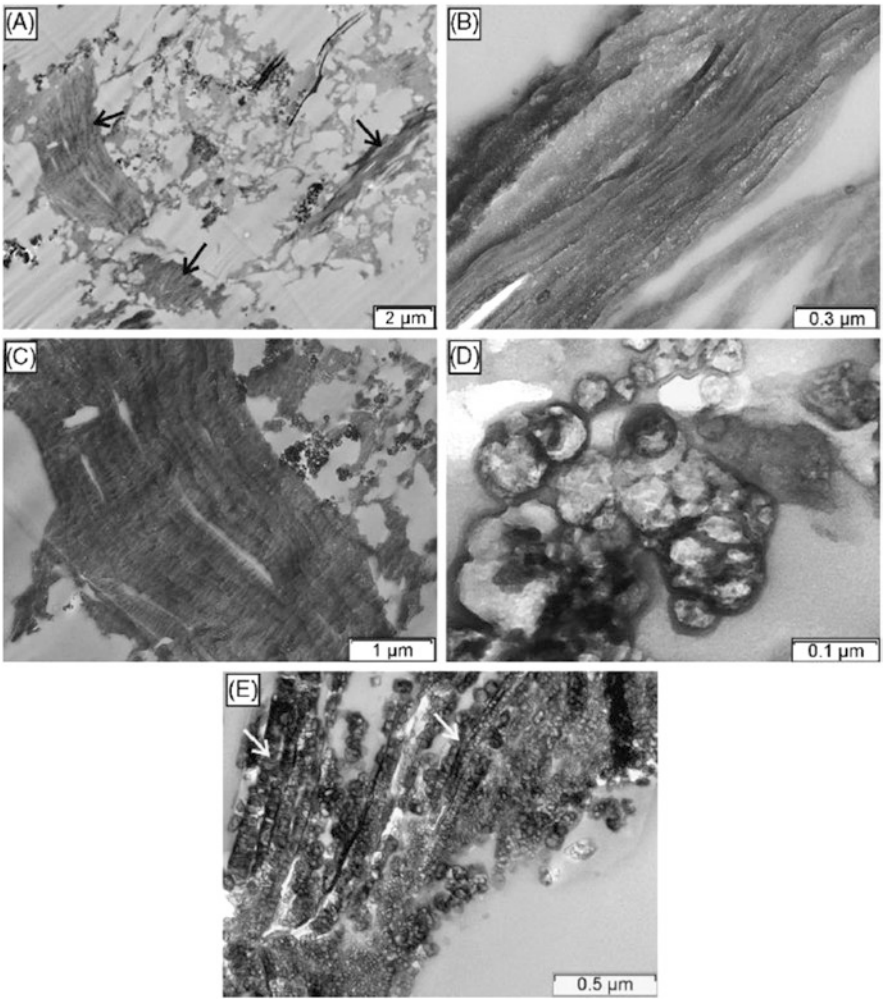

Fig. 1.11 Microbial remains from the 3.24 Ga Sulphur Springs black smoker deposit (**a**) TEM image illustrating the filamentous structure of the striated OM (*arrowed*). This material is comprised of compressed fi laments and bundles of tubular structures, ranging from 1–5 m in width and up to 100 m in length; (**b**) Higher magnification TEM image of compressed fi laments illustrated in (a). (**c**) TEM surface view of bundles of tubular microbial remains; (**d**) TEM cross section of a tubular bundle; (**e**) TEM image of silicified microbial tubes (From Duck et al. 2008; Elsevier, by permission)

(C/N = 134–569). These values are interpreted in terms of oxidation and recycling of the CM and loss of light ^{12}C and N during thermal maturation. The TEM and carbon isotopic compositions are consistent with activity of chemosynthetic microbes in a seafloor hydrothermal system accompanied by rapid silicification at relatively low temperature.

Transmission Electron Microscopy (TEM) studies of filamentous and tubular structured isotopically light ($\delta^{13}C$ −26.8 to −34.0‰ V-PDB) carbonaceous material associated with ~3.24 Ga epiclastic and silicified sediments overlying sulphide indicate close analogies with sea floor hydrothermal environments (Duck et al. 2008). The total organic carbon (<1.0 to 2.3 %) and thermal maturity obtained by reflectance (%Ro) indicates maximum temperatures around 90–100 °C. The association of sulphide with the organic matter suggests a sediment-hosted microbial community and seafloor hydrothermal activity.

Isotopic sulphur $\delta^{33}S$ values from the ~3.49 Ga Dresser Formation and ~3.24 Ga Panorama Zn–Cu deposit indicate presence of seawater sulphate and elemental sulphur of UV-photolysis origin (Golding et al. 2011), representing mixing between mass independently fractionated sulphur reservoirs with positive and negative $\delta^{33}S$ in the Dresser Formation. Pyrite associated with barite is depleted in $\delta^{34}S$ relative to the host barite, interpreted as evidence for microbial sulphate reduction. Alternatively the pyrite may have formed by thermochemical reaction inferred for the chert-barite assemblage units in excess of 100 °C. For the ~3.24 Ga deposit the data absence of significant negative $\delta^{33}S$ anomalies in sulphide suggests volcanic sulphur rather than seawater sulphate.

The observation of stromatolite-like forms in chert-carbonate-barite sequence of the ~3.49 Ga Dresser Formation, North Pole dome (Figs. 1.12), central Pilbara Craton (Dunlop et al. 1978; Dunlop and Buick 1981) gave rise to a major controversy regarding the biogenic origin of these structures. Noffke et al. (2013) documented microbially induced sedimentary structures from the Dresser Formation and interpreted the relations between microbial mats and the physical sedimentary environment. Detailed mapping on the scale of meter to millimeter indicates five subenvironments typical of coastal sabkha which contain distinct macroscopic and microscopic associations of microbially induced sedimentary structures. Outcrop-scale microbial mats include polygonal oscillation cracks and gas domes, erosional remnants and pockets, and mat chips. Microscopic microbial lamina comprises tufts, sinoidal structures, and lamina fabrics and consist of primary carbonaceous matter, pyrite, and hematite, plus trapped grains.

Greater confidence exists regarding the nature of ~3.43 Ga Strelley Pool Chert (Lowe 1980) (Fig. 1.12). Despite reservations (Brasier et al. 2002) the heliotropic reef-forming structure of the microbialites supports a biological origin (Hoffman et al. 1999; Van Kranendonk et al. 2003). Allwood et al. (2007) documented evidence for palaeoenvironmental extensive stromatolite-like reefs, including seven stromatolite morphotypes in different parts of a peritidal carbonate platform. The diversity, complexity and environmental associations of the stromatolites display marked analogies to similar stromatolite reef settings in younger geological systems.

Late Archaean ~2.73 Ga stromatolites, containing inter-bioherm interstitial debris are widespread in the Fortescue Basin, Pilbara Craton, reaching dimensions of tens of meters (Fig. 1.12) and yet younger ~2. 63 Ga stromatolites have flourished in the central and East Fortescue Basin (Fig. 1.12), displaying similarities with modern Shark Bay stromatolites (Fig. 1.12).

Some of the oldest possible micro-fossils occur in black chert of the Dresser Formation, (Duck et al. 2008; Golding and Glikson 2010; Golding et al. 2011) and in brecciated chert of the ~3465 Ma Apex Basalt, Warrawoona Group, Pilbara Craton (Schopf et al. 2007). The paleo-environment, carbonaceous composition, mode of preservation, and morphology of these microbe-like filaments, backed by new evidence of their cellular structure provided by two- and three-dimensional

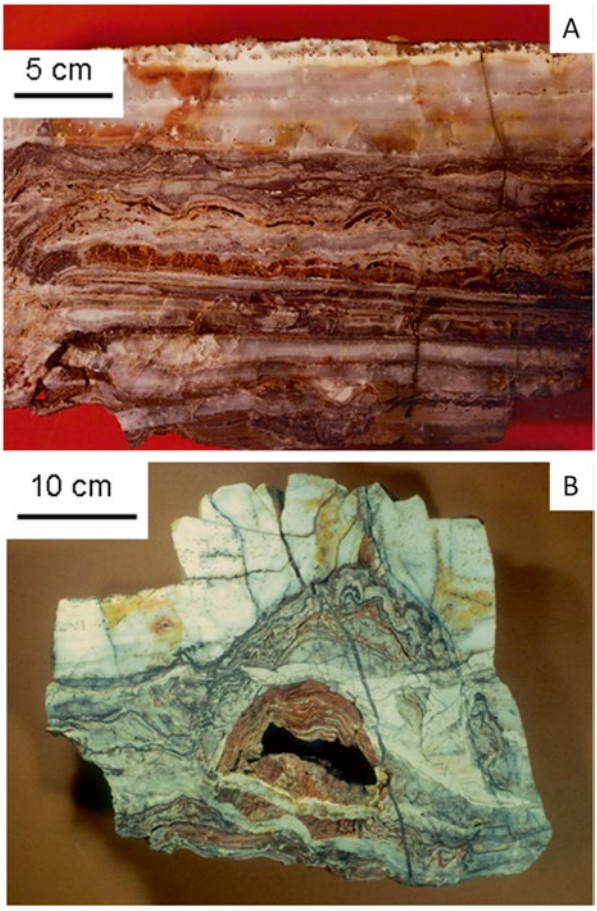

Fig. 1.12 Stromatolites – early contributors to atmospheric oxygen: (**a**) ~3.49 Ga Stromatolites colony, Dresser Formation, North Pole dome, central Pilbara, Western Australia (Courtesy JW Schopf); (**b**) individual ~3.49 Ga stromatolite (location as for A); (**c**) 3.43 Ga stromatolites, Pilbara Craton, Western Australia (courtesy Reg Morrison); (**d**) ~3.43 Ga stromatolites, Pilbara Craton, Western Australia; (**e**) ~2.76 Ga stromatolite, Meentheena Formation, Nullagine River, Western Australia; (**f**) ~2.63 Ga mega-stromatolite, Carawine Pool, Oakover River, Eastern Pilbara, Western Australia (*arrow* points to the *upper left* rim of the stromatolite dome). (Photos **e**, **d**, **f** by A. Glikson); (**g**) Living stromatolites, Shark Bay, Western Australia (Courtesy Reg Morrison)

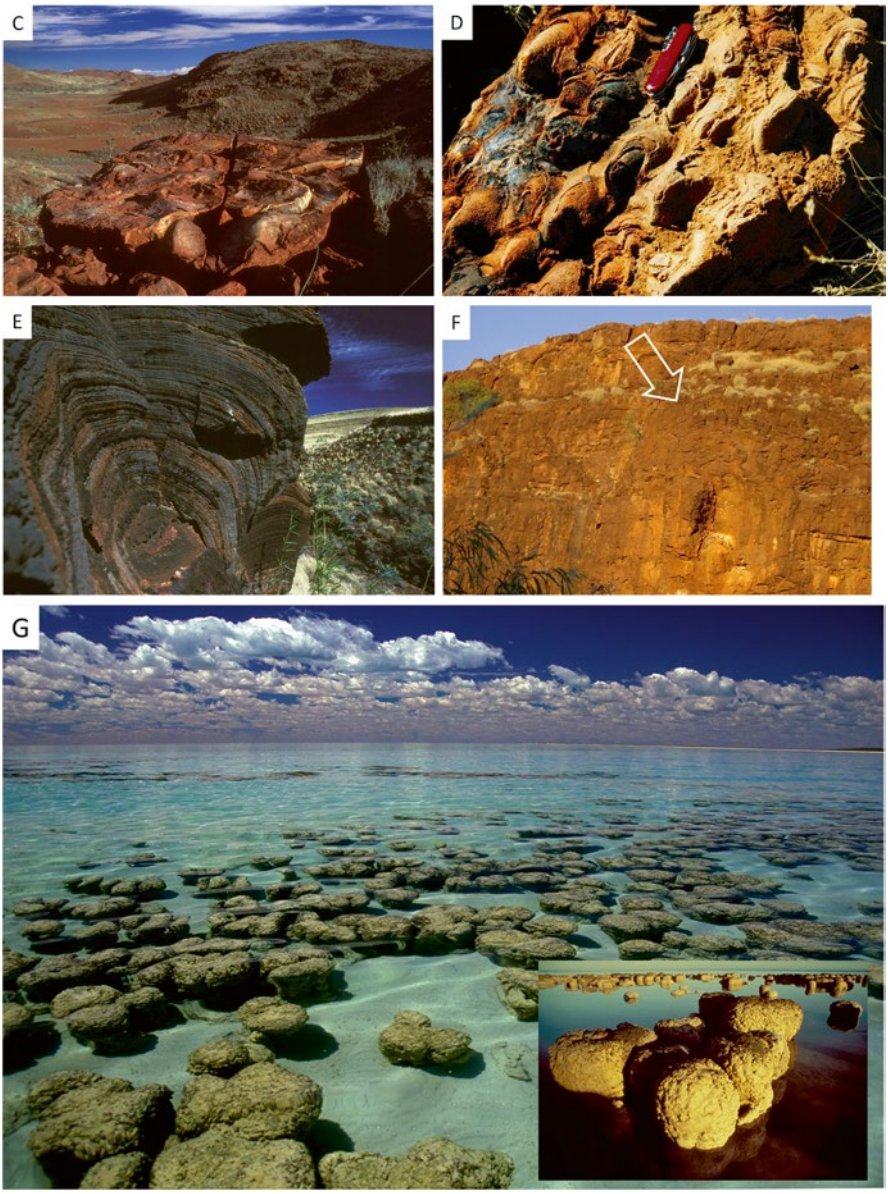

Fig. 1.12 (continued)

Raman imagery, support a biogenic interpretation. Evidence for hydrothermal and methanogenic microbial activity (Schopf and Packer 1987; Schopf et al. 2007; Hoffman et al. 1999; Duck et al. 2008; Golding and Glikson 2010) and intermittent

appearance of shallow water stromatolites in ~3.49 Ga (Fig. 1.12); Dunlop and Buick (1981) and ~3.42 Ga (Allwood et al. 2007) (Fig. 1.12) testify to a diverse microbial habitat. This included heliotropic and by implication photosynthesizing stromatolites affecting release of oxygen. Problems in identifying early Archaean stromatolites were expressed by Lowe (1994) and by Brasier et al. (2002). Whereas the early stromatolites may represent Prokaryotes, Eukaryotes possibly appeared about ~2.1–1.6 Ga (Knoll et al. 2006), or earlier (Sugitania et al. 2009) and exist at present at Shark Bay, Western Australia (Fig. 1.12).

1.3 Greenhouse States and Glaciations

Several Precambrian (pre-0.54 Ga) and Phanerozoic glaciation events, interrupting atmospheric greenhouse states, are recorded by sedimentological, paleontological and stable isotope evidence, including:

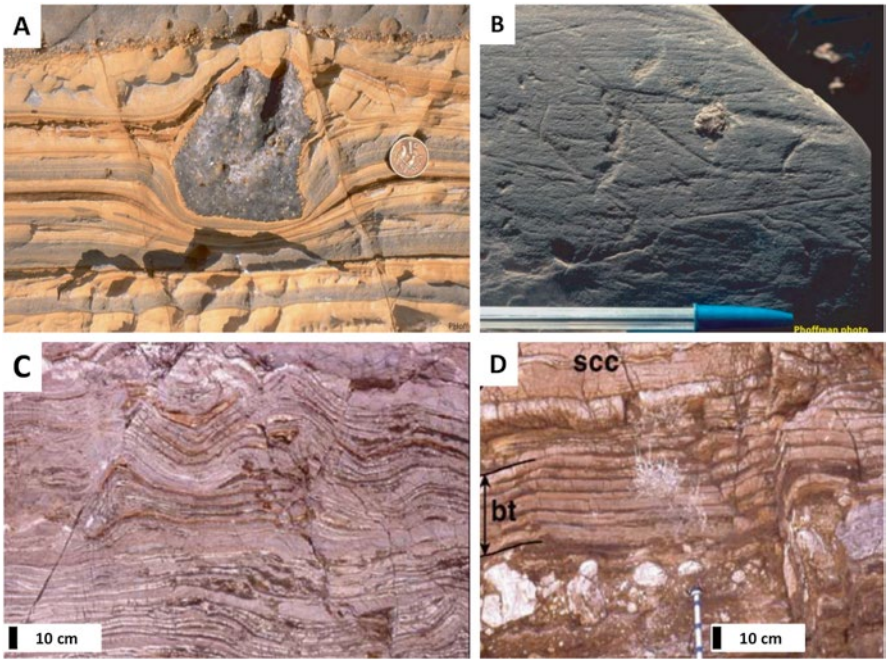

Fig. 1.13 Evidence of the Cryogenian "snow-ball' Earth (850–635 Ma). (**a**) example of ice-rafted dropstone in pro-glacial marine strata, Ghaub Formation, Otavi Group, Namibia (Courtesy Paul Hoffman); (**b**) Scratched pebble from Jbeliat tillite, Mauritania (Courtesy Paul Hoffman); (**c**) Cap carbonates, Namibia – mechanically-laminated peloidal dolostone (Hoffman et al. 2007, Elsevier, with permission); (**d**) Cap carbonates, Namibia – peloidal dolostone (Hoffman et al. 2007; Elsevier, with permission).

A. An upper Archaean glaciation represented by the 5000 meter-thick Mozaan Group of the 2837 ± 5 Ma Pongola Supergroup (Strik et al. 2007), which includes a sequence of diamictite containing striated and faceted clasts and ice-rafted debris (Young et al. 1998), representing the oldest glaciation recorded to date.
B. An early Proterozoic Huronian glaciation (~2.4–2.2 Ga) recorded by outcrops in the North American Great Lakes district, Pilbara Western Australia and the Transvaal (Kopp et al. 2005).
C. The late Proterozoic Cryogenian glaciations (*snowball Earth*), including the Sturtian (~750–700 Ma) and Marinoan (~650–635 Ma) (Fig. 1.13), affected an extensive ocean-wide ice cover, preventing sequestration of volcanic-emitted CO_2 and leading to an atmospheric build-up of the gas to extreme levels, some 350 times the modern concentration (Hoffman et al. 1998). The ice prevented CO_2 sequestration, resulting in a powerful greenhouse effect which culminated in glacial collapse represented by an extensive *cap carbonate* unit which overlies fragmented glacial deposits (Hoffman et al. 1998; Hoffman and Schrag 2000, 2002; Halverson et al. 2005).

Glaciation, cooling of the oceans and thereby enrichment of oxygen due to its higher solubility in cold water led to enhanced photosynthesis by phytoplankton and thereby further enrichment of oxygen. Conversely, Kasting and Ono (2006) invoke biological activity as a driver of the ~2.4 Ga glaciation, including a photosynthetic rise in O_2 and thereby oxidation and concomitant decrease in CH_4.

Glacial deposits of the Cryogenian Snowball Earth (750–635 Ma) observed in Namibia, in South Australia, Oman and Svalbard, correspond to the period of fragmentation of the long-lived Rodinia supercontinent (~1.1–0.75 Ga) (Hoffman et al. 1998) (Fig. 1.13). The onset of glaciation is marked by a large negative $\delta^{13}C$ anomaly and glacial termination is marked by carbonates – the so-called *cap carbonate* (Halverson et al. 2005). Paleomagnetic evidence suggests that the ice sheets reached sea level close to the equator during at least two glacial episodes. Some glacial units include sedimentary iron formations, underpinning potential relations between BIF and glaciations. According to Kirschvink (1992) the runaway albedo feedback exerted by the ice sheets resulted in a near-global ocean ice cover whereas continental ice covers were thin due to retardation of the hydrological cycle. In this model the appearance of banded iron formations may represent sub-glacial anoxia and thereby enrichment of sea water in ferrous iron. Hoffman et al. (1998) report negative carbon isotope anomalies in carbonate rocks bracketing Neoproterozoic glacial deposits in Namibia, indicating collapse of oceanic biological years, accounted for by a global glaciation. Glaciation ended abruptly in connection with volcanic outgassing, raising atmospheric CO_2 to some ×350 times the modern level.

The late Proterozoic thus represents a transition from oxygen-poor composition of early atmospheres which were dominated by reduced carbon species in the air and the oceans, producing methane through inorganic, organic and microbial processes by chemo-bacteria. Following the Cryogenian ice age ~750–635 Ma (Hoffman et al. 1998, 2007; Hoffman and Schrag 2000) the rise in oxygen during

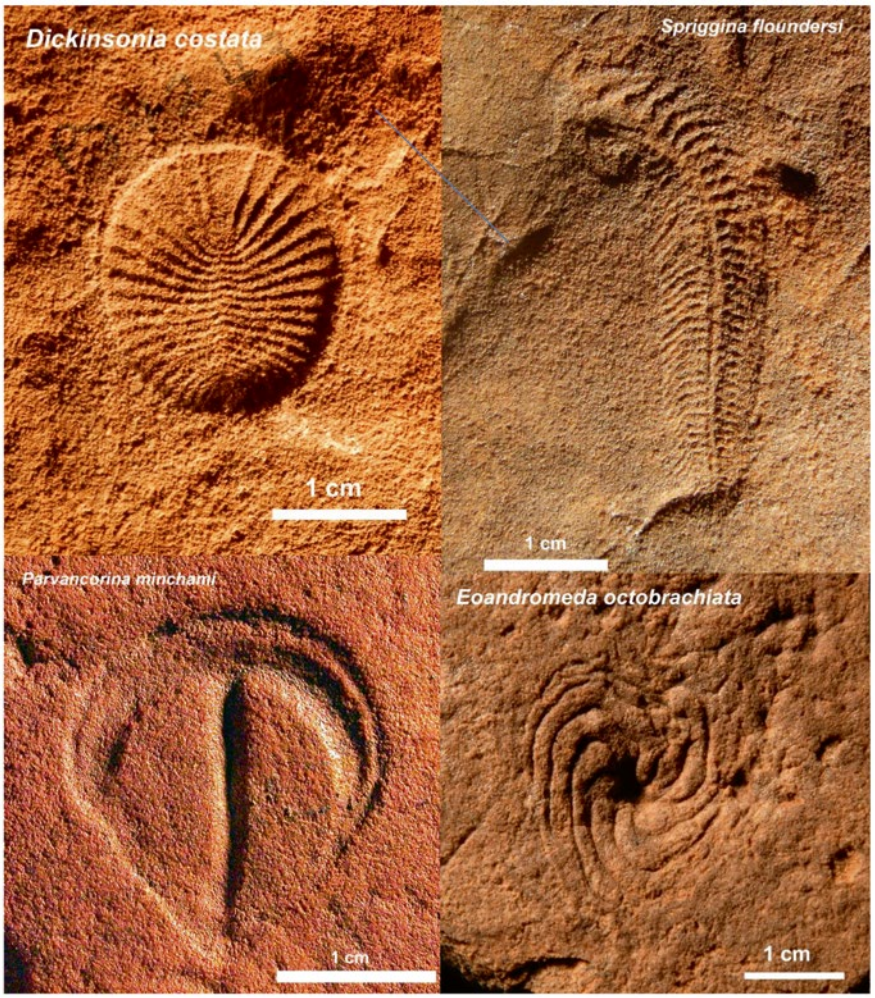

Fig. 1.14 Ediacara fossils, Flinders Ranges, South Australia: *(1) Dickinsonia costata; (2) Spriggina floundersi; (3) Parvancorina minchami;(4) Eoandromeda octobrachiata* (Courtesy Jim Gehling, South Australia Museum)

~635–542 Ma and particularly following ~580 Ma allowed oxygen-binding proteins and emergence of the multicellular Ediacara fauna (Fig. 1.14) in an oxygenated "*Canfield Ocean*". According to Canfield et al. (2007) oxygen levels constituted the critical factor allowing multicellular animals to emerge in the late-Neoproterozoic, as evidenced from the oxidation state of iron before and after the Cryogenian glaciation. A prolonged stable oxygenated environment may have permitted the emergence of bilateral motile animals some 25 million years following glacial termination,

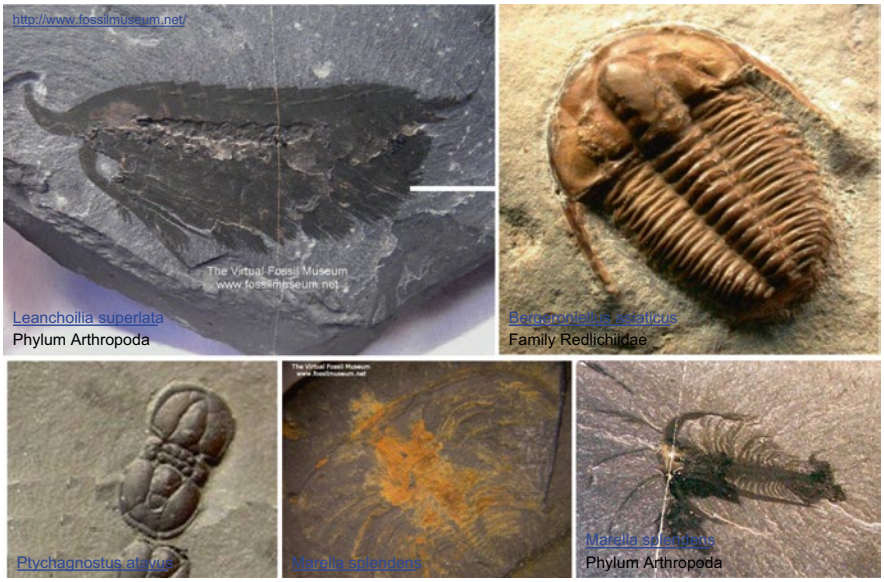

Fig. 1.15 Cambrian arthropods: (1) *Leanchoilia superlata*; (2) *Bergeroniellus asiaticus*, family *Redlichiidae*; (3) *Ptychagnostus atavus*; (4) *Marella splendens*; (5) *Marella splendens* (Courtesy of John P Adamek, Fossilmuseum; http://www.fossilmuseum.net/)

later followed by the onset of the *Cambrian explosion* of life (Gould 1990) from ~542 Ma and development of a rich variety of organisms (Fig. 1.15).

Phanerozoic geochemical models of the carbon, oxygen and sulphur cycles by Berner et al. (2007) underpin the production of O_2 through weathering and burial of organic carbon and pyrite, while biological productivity is indicated by $^{13}C/^{12}C$ and $^{34}S/^{32}S$ indices. These studies reveal well pronounced trends consistent with geological and paleontological observations (Beerling et al. 2001; Berner 2004, 2005, 2006, 2009; Berner et al. 2007; Beerling and Royer 2011) (Figs. 1.16, 1.17, 1.18, and 1.19). Investigations of the carbon isotope composition of Paleozoic organic matter, including plant fossils, coal, bulk terrestrial organic matter and carbonates ($\delta^{13}C_{\text{Total Organic Matter}}$, $\delta^{13}C_{\text{carbonate}}$, $\delta^{13}C_{CO2}$) confirm the dependence of both organic and inorganic carbon composition on the atmospheric O_2/CO_2 ratios (Strauss and Peters-Kottig 2003). The data underpin the intertwined nature of the carbon cycle, oxygen cycle and biological productivity, where the fractionation of atmospheric CO_2 through photosynthesis represents the excess of global photosynthesis (CO_2 capture, O_2 production) over global respiration (O_2 capture; CO_2 release and burial).

Throughout the Phanerozoic, periods of low atmospheric CO_2 coincided with periods of high atmospheric O_2 and high biological productivity, examples being the Carboniferous-Permian interval (326–267 Ma) and upper Cenozoic post-32 Ma glaciations (Figs. 1.16, 1.17, 1.18, 1.20, 1.21, and 1.22). During glacial periods, a large fraction of CO_2 is sequestered by cold ocean waters and fractionation of atmospheric CO_2 occurs via photosynthesis, where the carbon-rich residues of land plants and

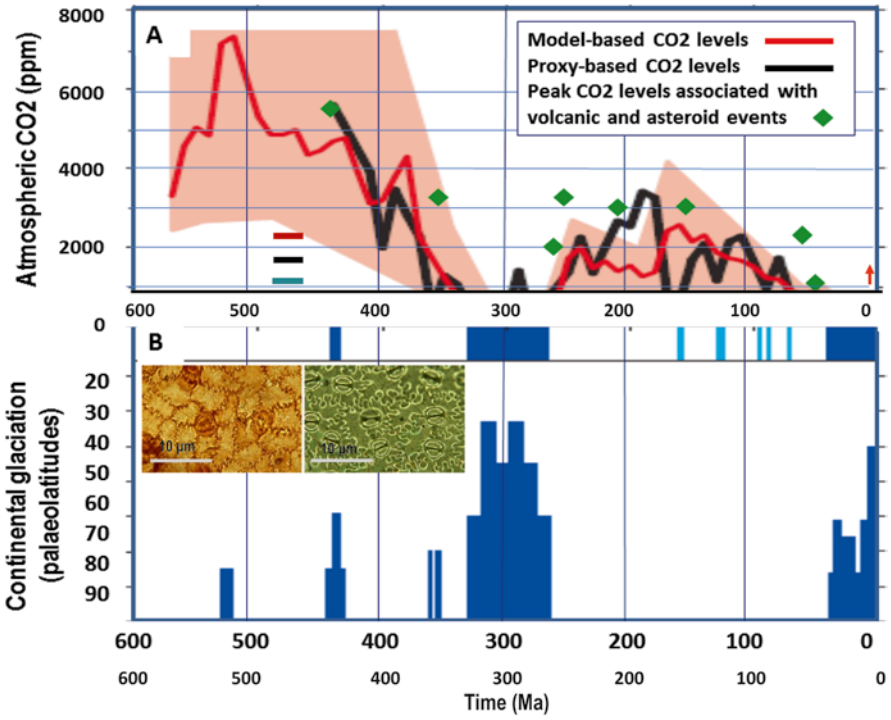

Fig. 1.16 (**a**) Evolution of CO_2 and occurrence of ice ages and cold phases from the Cambrian (542 Ma) to the present. Ice ages from proxy-based temperatures and sedimentological data. after Royer et al. 2004 (Geological Society of America, by permission); (**b**) photomicrographs of stomata pores: *left* – fossil leaf cuticle of the fern affinity *Stenochlaena* from just after the Cretaceous/Tertiary (K/T) boundary. *Right* – the fern's nearest living relative, *Stenochlaena palustris*. The stomatal index of the fossil cuticle is considerably lower than the extant cuticle, indicating that CO_2 was higher directly after the K/T boundary than today (Royer 2008; Geological Society of America, by permission). CO_2 levels corresponding to asteroid impacts, volcanic and mass extinction events, by the author

phytoplankton are buried and removed from the atmosphere-biosphere system, whereas oxygen is released back to the atmosphere. During high-CO_2 periods the warmer ocean waters sequester less CO_2 and dissolve less oxygen. CO_2 saturation of warm water leads to acidification, retarding phytoplankton oxygen production, while on land droughts and fires reduce the carbon/oxygen fractionation effects of plant photosynthesis.

A schematic illustration of the carbon cycle is presented in Fig. 1.19. The evolution of life through the Phanerozoic era can be described in three parts: Palaeozoic (early life ~542–251), Mesozoic (Middle life ~251–65 Ma) and Cenozoic (new life 65–0 Ma), separated by abrupt extinctions at ~251 Ma and 65 Ma (Tables 2.1, 2.2), including the following major mass extinctions of genera (after Keller 2005).

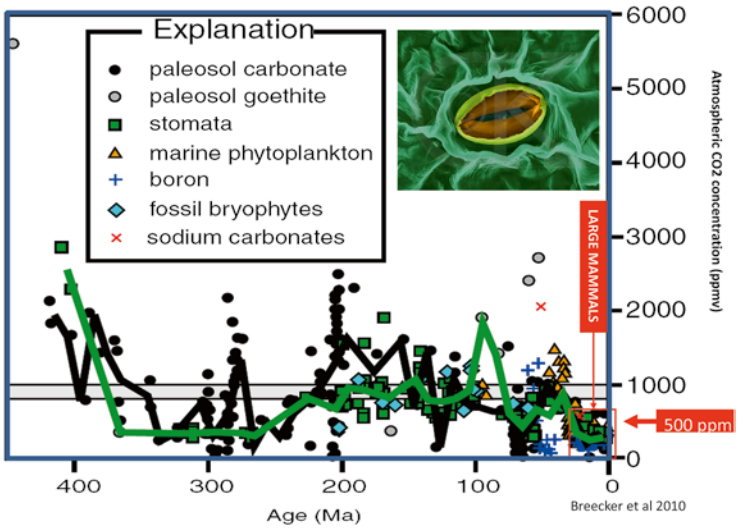

Fig. 1.17 A compilation of Phanerozoic atmospheric CO_2 based on different proxies (Breecker et al. 2009). Oxygen variations through the Phanerozoic. The *upper* and *lower* boundaries are estimates of error in modeling atmospheric O_2 concentration. The numbered intervals denote important evolutionary events that may be linked to changes in O_2 concentration (Berner et al. 2007; Courtesy R.A. Berner; American Association for Advancement of Science and Elsevier, by permission)

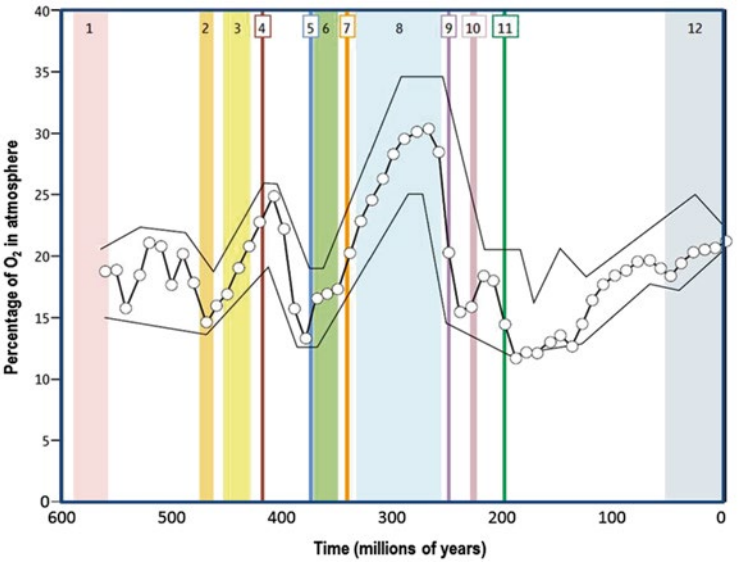

Fig. 1.18 Oxygen variations through the Phanerozoic. The upper and lower boundaries are estimates of error in modeling atmospheric O_2 concentration. The numbered intervals denote important evolutionary events that may be linked to changes in O_2 concentration (Berner et al. 2007; Courtesy R.A. Berner; American Association for Advancement of Science and Elsevier, by permission)

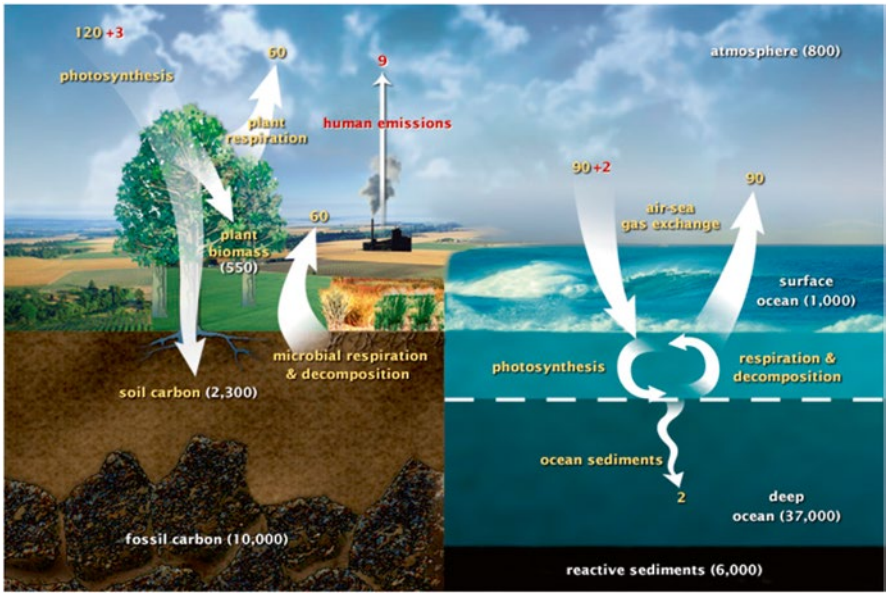

Fig. 1.19 The Carbon cycle. http://earthobservatory.nasa.gov/Features/CarbonCycle/. Values in GtC (billion tons carbon)

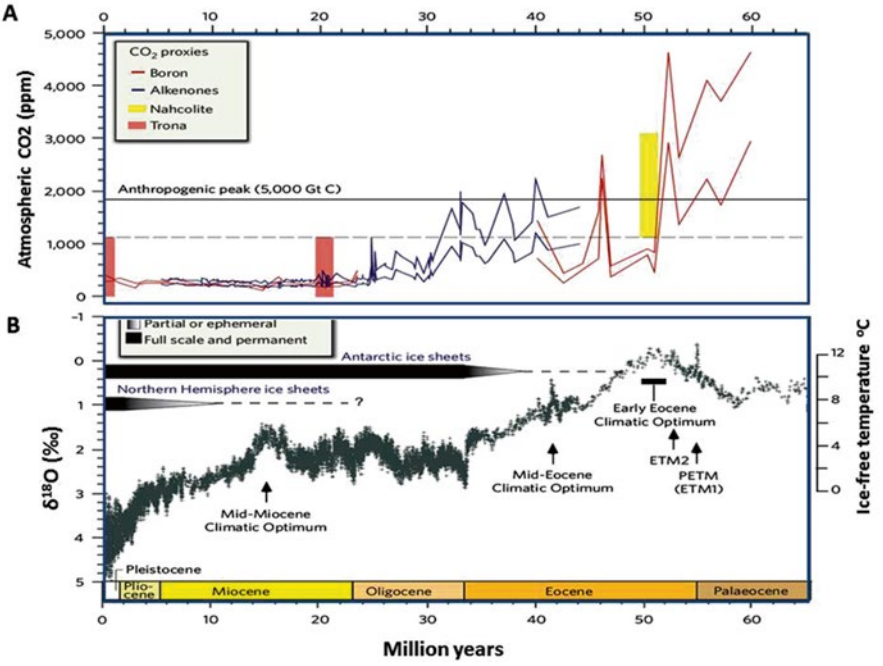

Fig. 1.20 Cainozoic CO_2 and temperature trends showing (**a**) CO_2 levels based on Boron, alkenones, nahcolite and trona proxies; (**b**) development of the Antarctic ice sheet and northern hemisphere glaciations, and (**c**) ice-free water temperatures and $\delta^{18}O$ temperature proxies (Zachos et al. 2008; Nature, by permission. Note the PETM event and the end-Eocene freeze event)

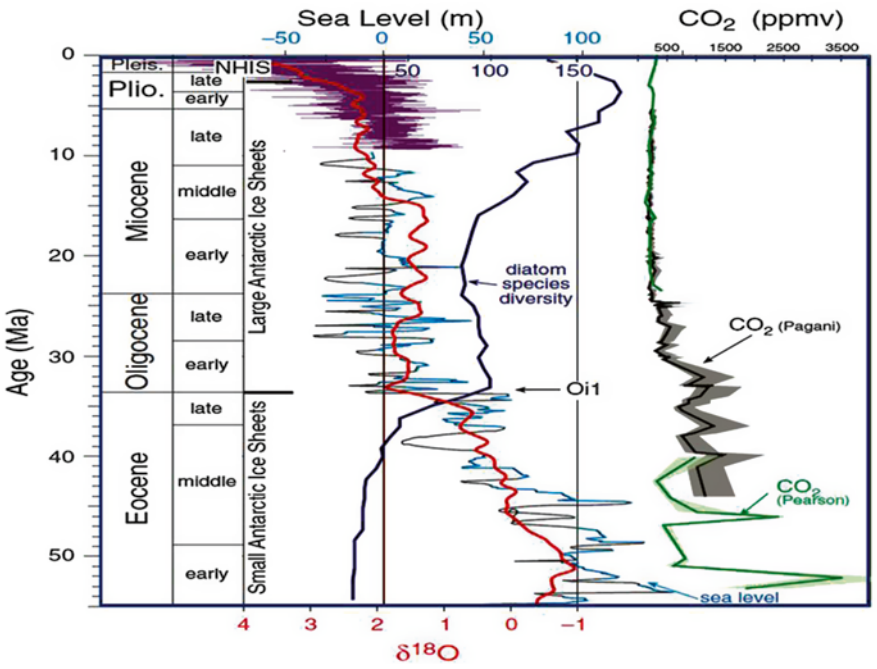

Fig. 1.21 Comparison of the global sea level (blue indicates intervals constrained by data; black indicates estimated low-stands, benthic foraminiferal $\delta^{18}O$ values (reported to *Cibicidoides* and smoothed to remove periods shorter than 1 m.y.), diatom diversity curve and atmospheric CO_2 estimates derived from alkenones and boron isotopes. NHIS – Northern Hemisphere ice sheets. The benthic foraminiferal curve is the Atlantic synthesis which is smoothed to remove periods shorter than 1 m.y. (Miller et al. 2009; The Geological Society of America, by permission)

A. End-Early Cambrian – 513 ± 2 Ma ~42 % extinction of genera;
B. End-Ordovician – 443 ± 7 Ma – ~57 % extinction of genera;
C. Late and end Devonian – 371–349 Ma ~58 and 30 % extinction of genera;
D. Permian-Triassic boundary – 251 ± 0.4 Ma ~80 % extinction of genera:
E. Late Triassic (Norian) – 216 Ma ~34 % extinction of genera;
F. K-T boundary – 65.5 ± 0.3 Ma ~46 % extinction of genera.

During the Cambrian to the late Devonian (~542–370) the dominance of high atmospheric CO_2 levels was interrupted by relatively brief cold periods and ice ages, including the late Ordovician glaciation (~446–443 Ma), Late and end Devonian to early Carboniferous glaciations (371–349 Ma – ~58 and 30 % extinction of genera) and Carboniferous-Permian glaciation (326–267 Ma) (Fig. 1.16). Intermittent rises in ocean temperatures with consequent depletion in oxygen led to anoxia events, a Mesozoic example being a ~94 Ma anoxia event represented by increase in burial of organic carbon (Barclay et al. 2010). These authors report a rise in CO_2 from 370 to 500 ppm consequent on volcanic eruptions, followed by a decrease of ~26 % associated with sequestration of marine organic carbon.

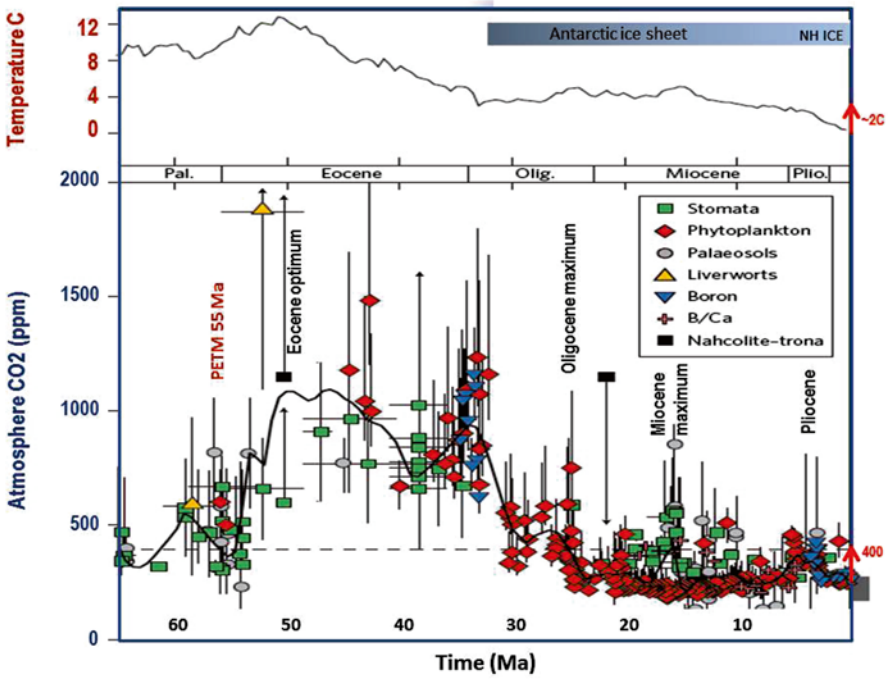

Fig. 1.22 Cainozoic CO_2 multi-proxy-based trends, including data based on stomata, phytoplankton, paleosols, Liverworts, Boron, B/Ca and Nahcolite-trona (Beerling and Royer 2011; Nature Geoscience, by permission)

Based on proxy and model estimates of Phanerozoic carbon and oxygen levels (Beerling et al. 2001; Berner 1999, 2004, 2005, 2006, 2009; Berner et al. 2007; Berner et al. 2003; Beerling and Royer 2011), mean CO_2 levels during the early Paleozoic (~542–370 Ma) ranged up to ~6000 ppm (Figs. 1.16, and 1.17). The models are based on fractionation of carbon isotopes between carbonate and organic matter in sediments, and different rates of weathering of basalts and granitic rocks, using a GEOCARBSULF model. Berner et al. (2007) point to several stages in the evolution of oxygen related to biological evolution (Fig. 1.18):

A. Proliferation of marine animals associated with rise of oxygen to ~15–20 % O_2;
B. The rise of land plants at the end-Silurian (~420 Ma) when O_2 reached ~25 %;
C. Major increase in O_2 to levels of ~25–35 % through the Carboniferous – Permian (~340–220 Ma), when gigantism developed among arthropods and reptiles thanks to the increase in oxygen;
D. A rise in O_2 from ~15 to ~20%f from the end-Triassic ~201 Ma through to the Cenozoic, when the size of dinosaurs and subsequently mammals was linked to oxygen levels.

E. Climate models based on mid-Cenozoic conditions suggest a glaciation threshold of ~500–600 ppm CO_2 according to Zachos et al. (2001) and 560–1120 ppm according to Pollard and DeConto (2005). Based on the study of temperature and biogenic proxies and on carbon cycle models, Cambrian CO_2 levels were as high as ~5000 ppm and Silurian levels to ~3000 ppm (Figs. 1.16, and 1.17). According to Royer (2006) main stages in the Phanerozoic atmospheric history include:

Late Ordovician Glaciation (445.6–443.7 Ma) Widespread glaciations at the Ordovician–Silurian boundary (Frakes et al. 1992) persisted into the early Silurian. CO_2 data are sparse and one point suggests ~5600 ppm, whereas Berner's GEOCARB III model (Berner 2006) suggests ~4200 ppm. However the time span of these CO_2 levels is not clear. According to Kump et al. (1999) CO_2 levels declined during this transition from 5000 to 3000 ppm. Analysis of radiative forcing indicates that, if the CO_2-ice threshold for the present-day Earth is 500 ppm, in the Late Ordovician insolation of about 4 % below the present renders a CO_2 glaciation threshold as high as 2240–3920 ppm (Royer 2006; Kump et al. 1999). These estimates remain to be confirmed by the multiple proxy studies.

Late Devonian-Early Carboniferous Glaciations (371–349 Ma) Two brief but widespread glaciations analogous to the Permo-Carboniferous glaciation and associated with the position of Gondwana at high latitudes have been identified (Royer 2006). There is evidence for ice near the Frasnian–Fammenian boundary (374.5 Ma) when CO_2 levels dropped sharply from 3300 to 350 ppm, but the main glaciation occurred in the Fammenian (361.4–360.6 Ma). Early Carboniferous glaciation appears to span the 353–349 Ma period. CO_2 level of ~1000 ppm was measured for 3.10^6 years before the Late Devonian glaciation and 1300 ppm for 7.10^6 years following the early Carboniferous glaciation (Royer 2006).

Carboniferous-Permian Glaciation (326–267 Ma) This glaciation constitutes the longest and most extensive Phanerozoic glaciation, during which O_2 levels declined to near or less than 500 ppm. Calibrated CO_2 values are based on arborescent lycopsids from equatorial Carboniferous and Permian swamp communities, obtaining concentrations of 344 ppm and 313 ppm for the late Carboniferous and early Permian, respectively. The position of Australia and Antarctica near the South Pole (Frakes et al. 1992; Beerling 2002b) resulted in extensive glaciation over a period of near 60 million years (Crowley 1999; Crowley and Berner 2001; Royer et al. 2004). The low CO_2 levels are in agreement with glaciological evidence for the presence of continental ice and coupled models of climate and ice-sheet growth on Pangaea. A period of 1500 ppm CO_2 occurs at 300 Ma, defining two glacial periods separated by an ice-free phase at 311.7–302 Ma (Isbell et al. 2003). CO_2 levels are consistently low during the first glacial phase (326.4–311.7 Ma), with most data <500 ppm, rising to ~1500 ppm at ~300 Ma, then dropping sharply to below 500 ppm. After 267 Ma levels CO_2 levels rise to ~1000 ppm.

Early Jurassic to Cretaceous Cool Phases (184–66.5 Ma) Marked climate fluctuations occurred during 184–183 Ma. Tropical conditions dominated much of the Mesozoic and little evidence exists for permanent ice during this period (Frakes et al. 1992; Eyles 1993; Price 1999; Zachos et al. 2001), consistent with CO_2 levels in the order of up to ~3000 ppm (Fig. 1.16). However, these conditions were interrupted by cooler climates, such as in the mid-Jurassic to early Cretaceous (171.6–106 Ma) (Frakes et al. 1992) and multiple short cooling events between 184 and 66.5 (Royer 2006).

The onset of the Cenozoic, marked by the ~65 Ma K-T asteroid impact event (Alvarez et al. 1980) which occurred at a time of low to moderate global atmospheric CO_2 concentrations (Figs. 1.16, 1.17, and 1.22) resulted in an increase in atmospheric CO_2 from ~400 ppm to ~2400 ppm (Beerling et al. 2002), subsequently decreasing to ~300 ppm within ~500 kyr. A succeeding warming trend culminated in the Paleocene-Eocene thermal maximum (PETM) at ~55.9 Ma, which involved a release of some ~2000–3000 billion ton carbon (GtC) as methane, elevating atmospheric CO_2 to near-2000 ppm at a rate of approximately ~0.13 ppm/year and mean temperatures rise of several degrees Celsius (Zachos et al. 2008; Cui et al. 2011) (Figs. 1.22, and 1.23). Elevated atmospheric carbon led to ocean acidification from ~8.2 to ~7.5 pH and to an extinction of 35–50 % of benthic foraminifera over the course of ~1000 years (Zachos et al. 2008). Other consequences included a global expansion of subtropical dinoflagellate plankton, appearance of modern orders of mammals (including primates), a transient dwarfing of mammalian species, and migration of large mammals from Asia to North America.

In the wake of the PETM event atmospheric greenhouse levels progressively cooled to about ~34 Ma (Frakes et al. 1992; Eyles 1993; Zachos et al. 1992, 2001; Ruddiman 1997, 2008; Royer et al. 2004; Royer 2006). The cooling is consistent with the CO_2 record, indicating a decline from high CO_2 levels of 1200 ppm at 44 Ma to <500 ppm before the onset of the first cool event at 42 Ma (Royer 2006). Evidence from sea level, temperature, and calcite compensation depth suggests brief glaciations during the upper Eocene at about ~42–41 Ma, ~39–38 Ma, and ~36.5–36 Ma (Browning et al. 1996). The gradual decline in mean global CO_2 and temperatures ended at ~34 Ma with a sharp drop of atmospheric CO_2 to below 500 ppm, a decline of mean global temperature of ~5 °C and the onset of the Antarctic ice sheet (Zachos et al. 2001, 2008) (Figs. 1.20, 1.21, and 1.22). Following ~34 Ma CO_2 levels have been mainly below ~500 ppm, an exception being a late Oligocene (~25 Ma) warming (Zachos et al. 2001) when CO_2 levels higher than 500 ppm are recorded. The upper Eocene temperature decline is interpreted in terms of CO_2 capture associated with erosion of the rising Himalaya and Alpine mountain chains (Ruddiman 1997). The sharp freeze 34 Ma (Figs. 1.22, 1.23, 1.24, and 1.25) is likely related to the opening of the Drake Passage between South America and west Antarctica and onset of the circum-Antarctic current, isolating Antarctica from the influence of warmer currents.

The sharp decline in temperature at ~34 Ma was preceded by a large cluster of ~35.5–35.7 Ma asteroids (Popigai, 100 km, 35.7 ± 0.2 Ma; Chesapeake Bay, 85 km, 35.5 ± 0.3 Ma; Mount Ashmore, >50 km, E-O Boundary) (Glikson et al. 2010),

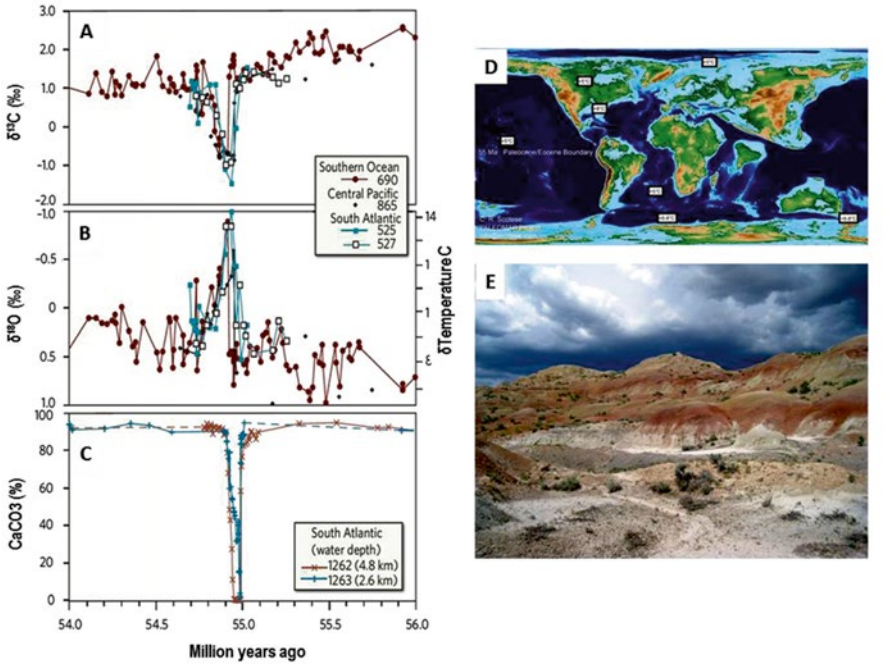

Fig. 1.23 **(a)** The Paleocene-Eocene Thermal Maximum (PETM) represented by sediments in the Southern Ocean, central Pacific and South Atlantic oceans. The data indicate (**a**) deposition of an organic matter-rich layer consequent on extinction of marine organisms; (**b**) lowering of $\delta^{18}O$ values representing an increase in sea water temperature, and (**c**) a sharp decline in carbonate contents of sediments representing a decrease in pH and increase in acidity (Zachos et al. 2008; Nature, by permission. (**d**) PETM map – courtesy Appy Sluijs. (**e**) photograph showing the Willwood Formation, Bighorn Basin, Wyoming, showing the final stages and recovery phase of the Paleocene-Eocene Thermal Maximum (PETM), courtesy Cesca McInerney)

which may have been a factor in enhancing the tectonic breakdown of the previous Antarctic-South America land link.

Formation of the Antarctic ice sheet between 34–33.5 Ma was associated with a sharp decline of atmospheric CO_2 to about 700 ppm (Fig. 1.24) (Miller et al. 2009; Pearson et al. 2009; Liu et al. 2009). Studies of carbonate microfossils using the $\delta^{11}B$ proxy allow tracing of CO_2 levels through the Eocene-Oligocene transition in Tanzania (Pearson et al. 2009), indicating the decline in CO_2 commenced before inception of the Antarctic ice sheet, followed by recovery between 33.5–33.3 Ma to levels as high as ~1100 ppm, succeeded by a decline of CO_2 levels to about or below ~500 ppm about 30 Ma (Fig. 1.24). Once the Antarctic ice sheet formed, hysteresis allowed its persistence despite transient rise in the GHG. However, little $\delta^{18}O$ evidence for a rise in temperatures is observed during the CO_2 rebound period (Fig. 1.25). This is in part explained by major reduction in sea surface area and thereby reduced CO_2 sequestration rates. Other possible factors were release of organic carbon from geological reservoirs, changes in ocean productivity and circulation patterns, and variations in rock weathering rates (Pearson et al. 2009).

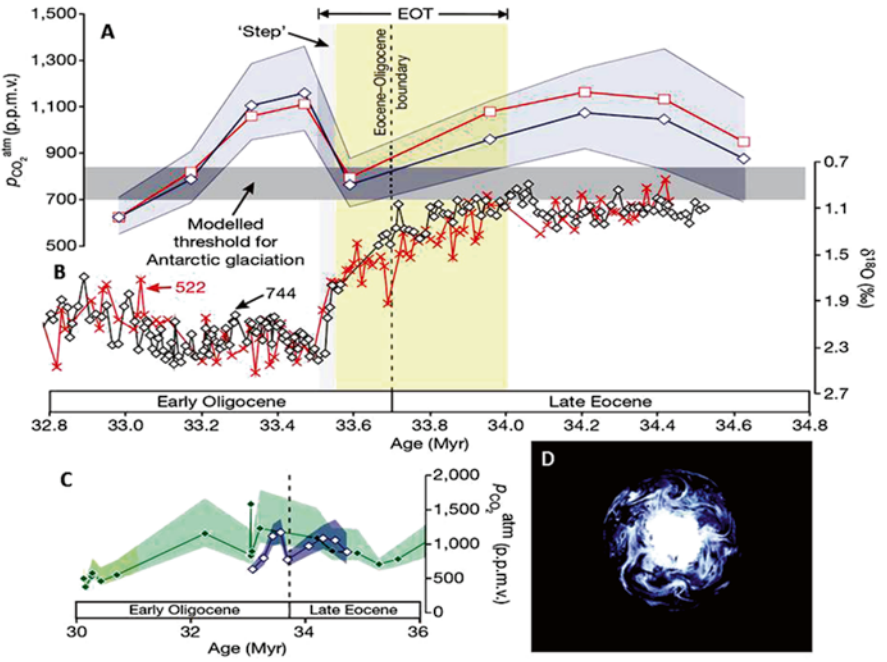

Fig. 1.24 The end-Eocene freeze: (**a**) Reconstructed atmospheric CO_2 levels from Boron isotopes (^{11}B); (**b**) deep-sea oxygen isotopes ($\delta^{18}O$) are from DSDP site 522 (*red crosses*) and ODP site 744 (*black diamonds*); (**c**) Alkenones proxy CO_2 estimates. The grey band is the threshold for Antarctic glaciation; (Pearson et al. 2009; Nature, by permission); (**d**) Satellite image of Antarctica (NASA). Note the sharp drop in CO2 from ~1100 to ~700 ppm and of temperatures (expressed by rising $\delta^{18}O$) to ~33.6, followed by a transient rise in CO_2 (see text and discussion by Pearson et al. 2009)

Following the isolation of the Antarctic ice sheet the global climate was affected by major feedback processes, including

A. Albedo enhancement by continental ice sheets, sea ice and mountain glaciers (Hansen et al. 2007, 2008; Overpeck et al. 2006);
B. Cold currents and weather fronts emanating from the Antarctic vortex and the circum-Antarctic current;
C. Enhanced sequestration of CO_2 by cold water.

As atmospheric CO_2 levels declined the surface became increasingly exposed to orbital forcing of the Milankovic cycles (Roe 2006) (Fig. 1.26), including weak solar cycles such as the 11-years sun spot cycle (Solanki 2002; Bard and Frank 2006).

Once the thermal blanketing effect of high concentrations of greenhouse gases is removed, the terrestrial climate becomes increasingly sensitive to minor variations in insolation. The molecular resonance of GHG (water vapor, carbon dioxide, methane, nitric oxides, ozone), transforming, absorbing and emitting thermal radiation, can act as a driver of global temperatures, as for example during the Paleocene-

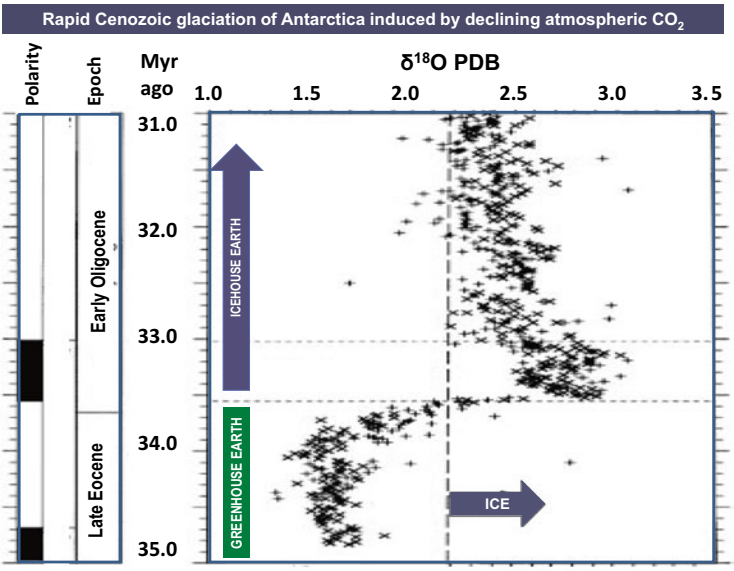

Fig. 1.25 Rapid Cenozoic glaciation of Antarctica induced by declining atmospheric CO_2 (Pollard and DeConto 2005; Nature, by permission)

Eocene Thermal Maximum (PETM) (Figs. 1.22, and 1.23). During the Pleistocene glacial-interglacial era controlled by Milankovic cycles (Fig. 1.26) GHG acts as a feedback mechanism, namely as increasing insolation warms the oceans inducing a release of CO_2 which in turn enhances temperatures

Eocene cooling and the following ice ages saw the flourishing of land mammals, which in the Mesozoic were mostly limited to small burrowing species. The overall cooling was interrupted by a number of warming events which triggered sea level rises, including the late Oligocene (~25 Ma), early and mid-Miocene (22 Ma, 17–14 Ma), mid-Pliocene (3.1–2.9 Ma) and Pleistocene (2.6 Ma–10 kyr) interglacial peaks (Figs. 1.20, 1.21, 1.22, 1.27, 1.28, 1.31, 1.32 and 1.33). These oscillations, generated by Milankovic orbital cycles, included periodic changes in the eccentricity, axial obliquity and precession of the Earth relative to the sun (Fig. 1.26), display increasingly sharper amplitudes with time (Fig. 1.27). Peak Pliocene conditions, reached when CO_2 levels were about <400 ppm, saw temperatures about 2–3 °C higher and sea level 25 ± 12 meters above late Holocene pre-industrial levels (Chandler et al. 2008). Sea levels continued to fluctuate through the Pleistocene in direct relation to temperatures.

About 4.0 Ma, following a rise of the Panama cordillera and closing of the Panama straits, separation of the Pacific and Atlantic Ocean basins augmented longitudinal ocean circulation, enhancing the Pacific Gyre, the El Nino Southern Oscillation (ENSO) cycle (Fig. 1.27) and the North Atlantic Thermohaline Current (Fig. 1.32). The consequent intensification of cross-latitude circulation patterns

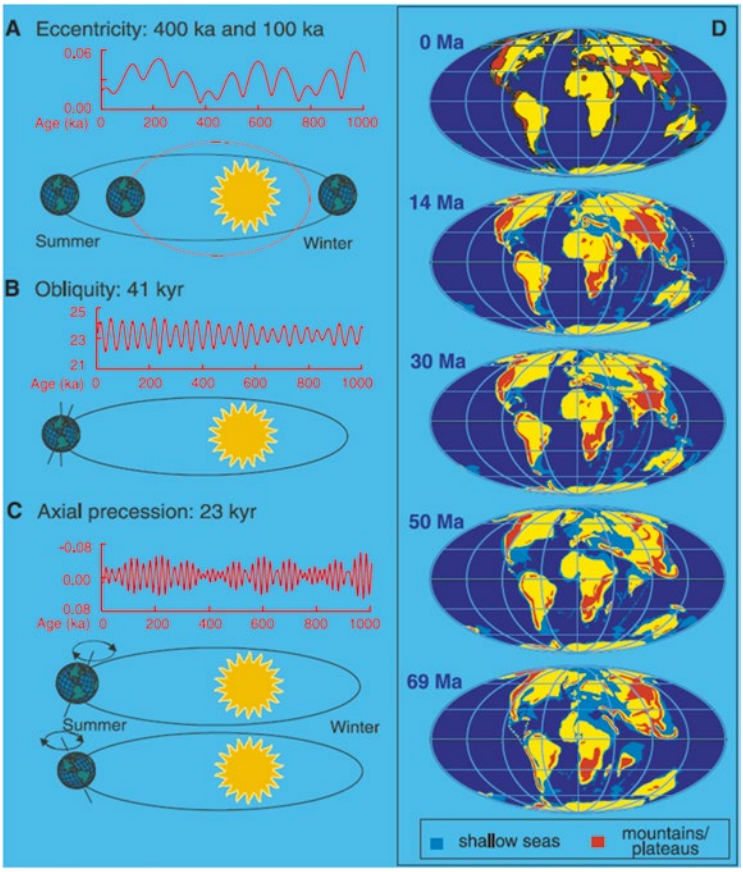

Fig. 1.26 Orbital components of Milankovic cycles and Cenozoic paleogeography. Orbital components include eccentricity (400 and 100 kyr), obliquity (41 kyr), and precession (23 and 19 kyr). (**a**) Eccentricity refers to the shape of Earth's orbit around the sun. Obliquity refers to the tilt of Earth's axis relative to the plane of the ecliptic varying between 22.1° and 24.5°. A high angle of tilt increases the seasonal contrast, most effectively at high latitudes, where winters will be colder and summers hotter as obliquity increases. Precession is the wobble of the axis of rotation describing a circle in space with a period of 26 kyr. The periods of the precession are modulated by eccentricity of 23 and 19 kyr are observed in geological records (Zachos et al. 2001; Courtesy J.C. Zachos; American Association for the Advancement of Science, by permission)

enhanced the cold Humboldt Current along the South America west coast, reaching low latitudes, and associated development of the La Nina phase of the ENSO in the central Pacific Ocean (Fig. 1.27) (Fedorov et al. 2006). Pliocene orbital forcing cycles, mostly modulated by the 19–23 kyr-long precession-controlled cycles are represented by organic-rich sapropel layers (Fig. 1.29). From about ~2.8 Ma orbital forcing was dominated by 41 kyr-long obliquity-modulated cycles associated with increased generation of dust related to drying and glacial erosion and winds. From about ~1.8 Ma increased amplitude of ~41 kyr-long cycles was associated with a

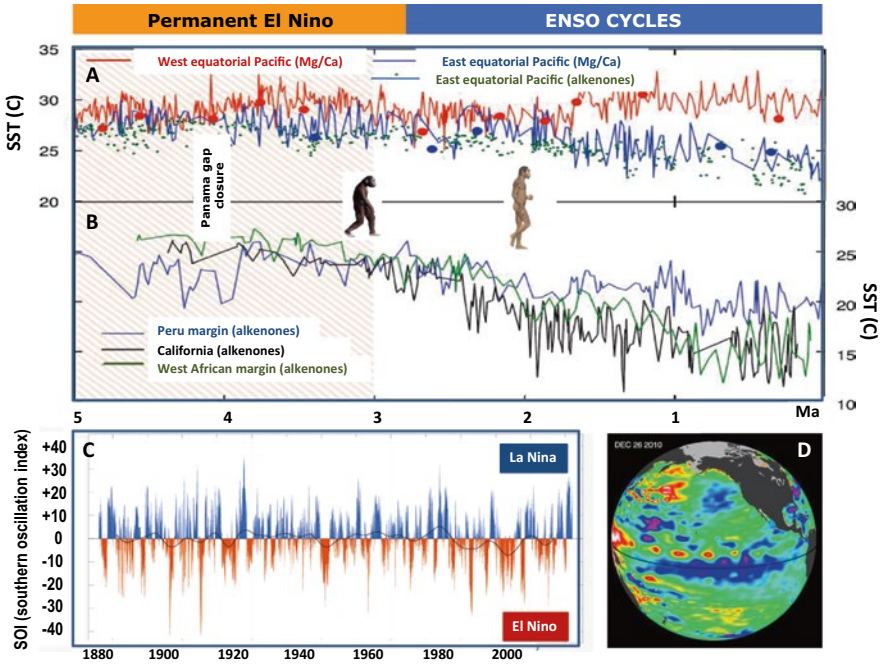

Fig. 1.27 Intermittent overall cooling and evolution of the ENSO since 5 Ma; (**a**) Based on Mg/Ca and alkenones paleo-temperature proxies the plot displays near coincidence between East Pacific and West Pacific sea surface temperatures before about 4 Ma, some divergence between cooler East Pacific and warmer West Pacific temperatures between about 3 and 2 Ma and increasingly marked divergence in temperatures from about 2 Ma when a strong ENSO polarity ensued; (**b**) Alkenones proxy evidence for cooling of the Humboldt Current (Peru margin), California Current and West African (Namibia) Current parallel to the development of ENSO polarity (**b** and **c** from Fedorov et al. 2006; Courtesy A. Fedorov; American Association for Advancement of Science, by permission); (**c**) ENSO oscillations during 1880–2012, displaying intensification of El Nino events about 1900 and between 1980–2000; (**d**) A La Nina event in 2010 (**c** – NASA http://sealevel.jpl.nasa.gov/images/ostm/20101226P-br.jpg; **d** – NASA)

marked increase in the ENSO polarity (Fig. 1.27) and the frequency of the La Nina phase. From about ~0.9 Ma ~100 kyr-long eccentricity-dominated cycles became dominant, displaying glacial-interglacial temperature variations of up to 6 °C and glacial dust levels in marine sediments of up to 40 % (Petit et al. 1999; EPICA 2004). The increased polarity of glacial-interglacial cycles and the abrupt nature of the glacial terminations (Fig. 1.31) may be attributed to a combination of strong insolation pulsations and the decrease in atmospheric CO_2 levels which allowed the solar pulsations to reach the surface, amplified by feedbacks from the ice/melt albedo flip, CO_2 release from warming seas, ocean currents and drying/burning vegetation (Hansen et al. 2007, 2008).

The evolution of hominins in the rift valley region of Eastern Africa (Figs. 1.33 and 1.34) has been intimately related to climatic variability controlled by a combination of tectonic changes and insolation cycles (Maslin and Christensen 2007;

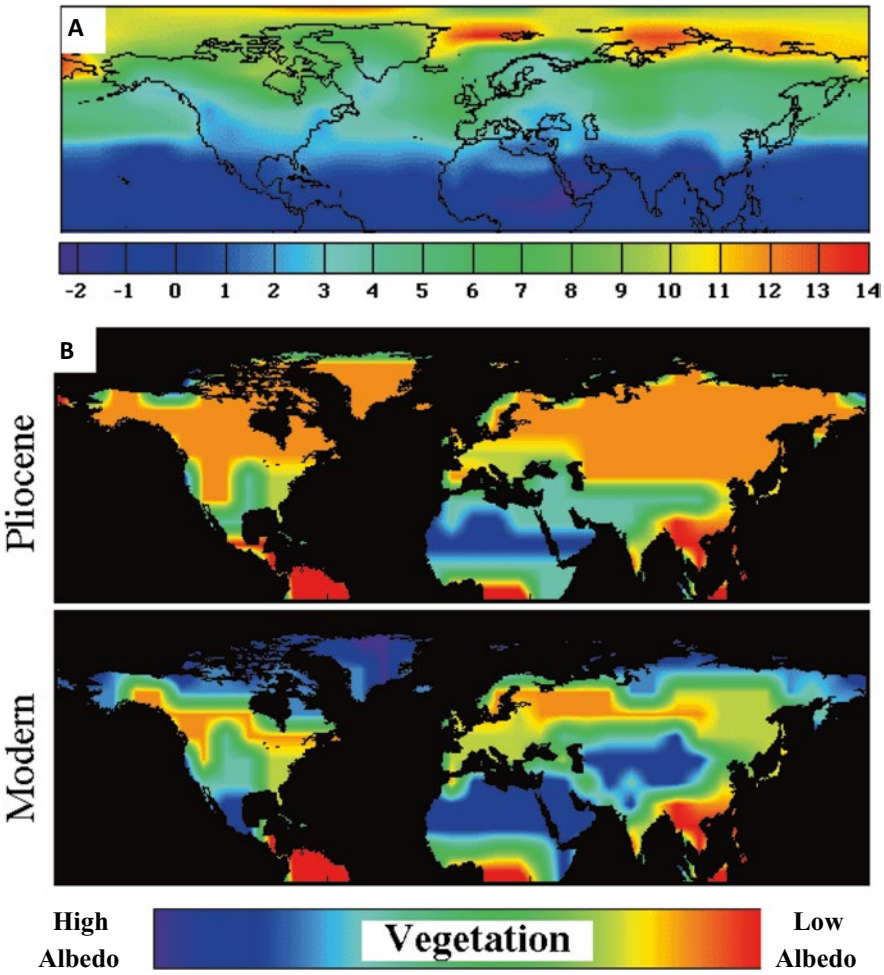

Fig. 1.28 Model and paleo-data based comparisons between Pliocene and late Holocene climates. (**a**) Pliocene Northern Hemisphere surface air temperatures relative to modern temperatures. Model and data indicate significantly warmer temperatures at high latitudes and diminished warming nearer to the equator; (**b**) Pliocene and modern vegetation albedo distribution (NASA – National Aeronautics and Space Administration/Goddard Institute for Space Studies http://www.giss.nasa.gov/research/features/199704_pliocene/page2.html)

Maslin and Trauth 2006, 2009; Trauth et al. 2007, 2010). Down-faulting of rift valleys during 5.5–3.7 Ma resulted in formation of lakes and sheltered environments for the evolution of hominins during the retreat of rainforests and opening of savannah, with further rifting about 1.2 Ma. Deep lakes developed during ~3.20–2.95, ~3.4–3.3, 4.0–3.9, ~4.7–4.3 Ma, 2.7–2.5 Ma, 1.9–1.7 Ma and 1.1–0.9 Ma, periods, which correspond to low-dust relatively humid periods in North Africa represented by sapropel (Fig. 1.29). The 2.7–2.5 Ma Lake phase corresponds to intensification of the Northern Hemisphere Glaciation, the 1.9–1.7 Ma Lake phase to development

Fig. 1.29 An outcrop of late Miocene (9.3–8.4 Ma) sediments displaying dark organic matter (sapropel)-rich cycles representing humid periods, Gibliscemi, Sicily (from deMenocal 2004). The sapropel units represent 19–23 kyr-long precession-induced monsoonal periods affecting increased organic matter production transported through the River Nile to the Mediterranean Sea. Precession cycles are grouped in sets of four, representing ~100 kyr-long eccentricity cycles (deMenocal 2004; Elsevier, by permission)

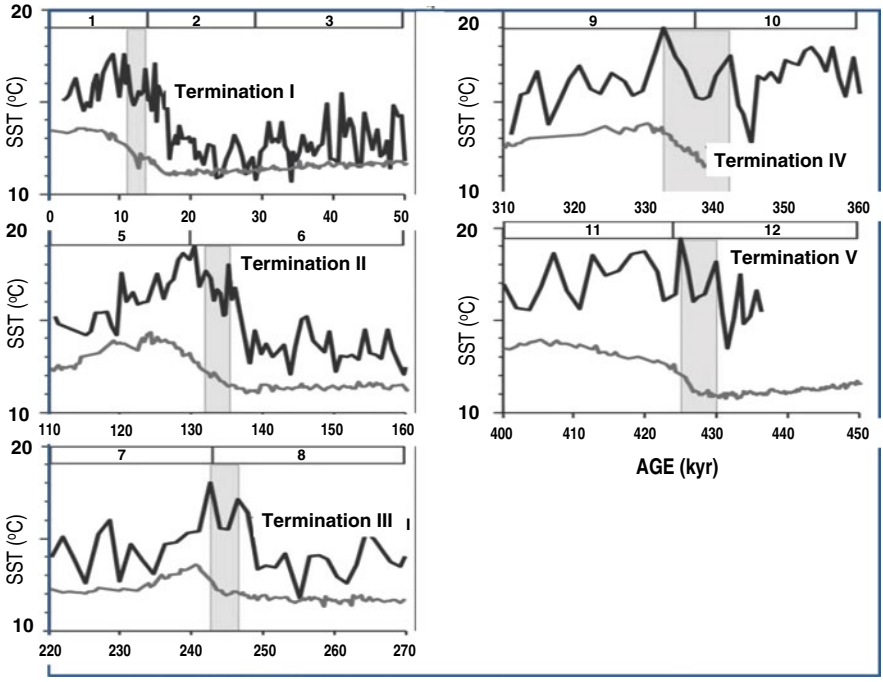

Fig. 1.30 Evolution of sea surface temperatures in 5 glacial-interglacial transitions recorded in ODP 1089 at the sub-Antarctic Atlantic Ocean. Grey lines – $\delta^{18}O$ measured on Cibicidoides plankton; *Black lines* – sea surface temperature. Marine isotope stage numbers are indicated on top of diagrams. Note the stadial following interglacial peak temperatures, analogous to the Younger Dryas preceding the onset of the Holocene (Cortese et al. 2007; John Wiley and Sons, by permission)

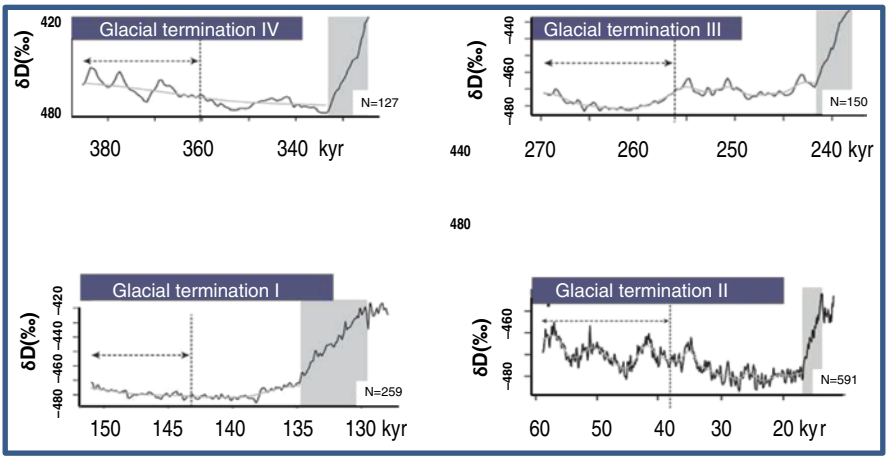

Fig. 1.31 Reconstructions of abrupt climate shifts: in the past. (**a**) glacial termination IV; (**b**) Glacial termination III; (**c**) glacial termination II; (**d**) glacial termination I. Note the slowdown in the dynamics of the system prior to the transition (Data from the GISP-2 ice core, ODP Hole 658C and Antarctica Vostok ice core. Dakos et al. 2008; Proceeding National Academy of Science, by permission)

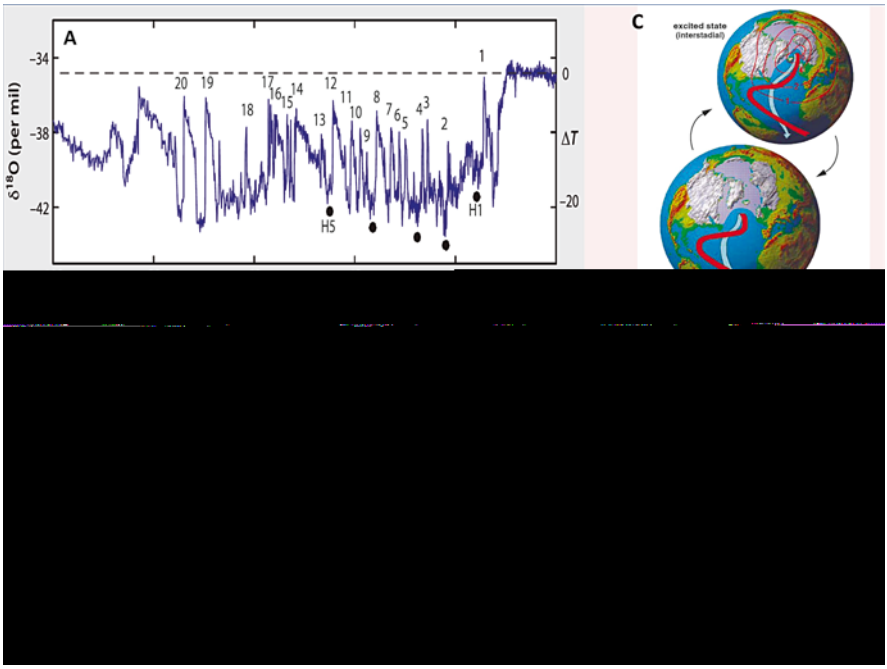

Fig. 1.32 Intra-glacial Dansgaard-Oeschger cycles. (**a**) Temperature variations during the Last Glacial Period since 100 Kyr, displaying 21 Dansgaard-Oeschger cycles recorded by $\delta^{18}O$ values from the GRIP ice core of the Greenland Ice Sheet; (**b**) A single Dansgaard-Oeschger cycle. The black line shows a model simulated D/O event (Rahmstorf and Stocker 2004; Springer, by permission); (**c**) phases of the North Atlantic Thermal current during the warm excited state (interstadial, *upper globe*) and the cold basic state (stadial, *lower globe*) state of the D-O cycle (Ganopolski and Rahmstorf 2002; Springer, by permission); (**d**) Changes in surface air temperature caused by a stadial state shutdown of North Atlantic Deep Water (NADW) formation in a current ocean–atmosphere circulation model (Ganopolski and Rahmstorf 2002; Nature, by permission. Note the extreme rate of temperature rise during the D-O cycles)

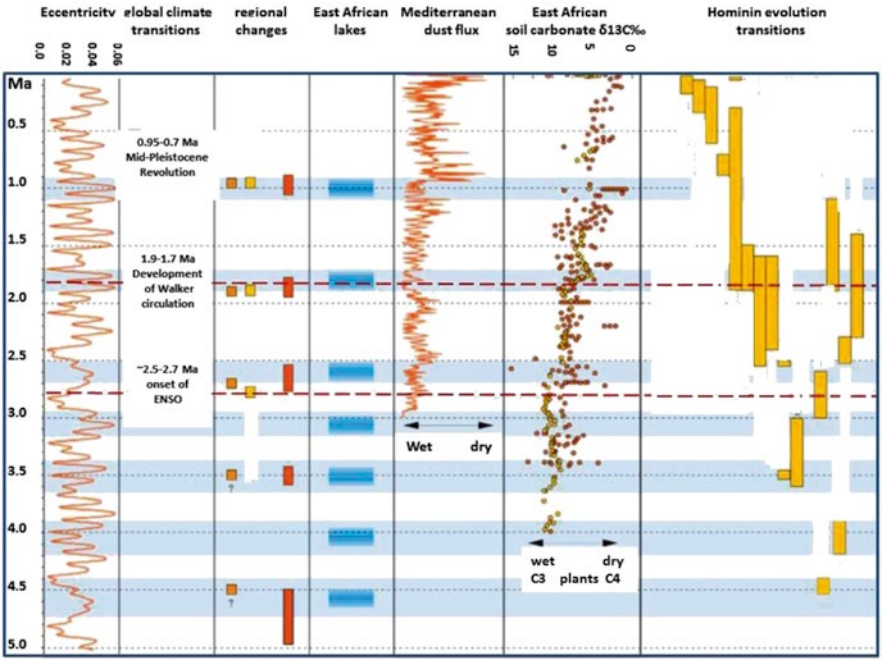

Fig. 1.33 A tabulated summary of climate and hominin evolution from 5.0 Ma-ago, including comparisons of eccentricity variations, high-latitude climate transitions, Mediterranean dust flux, soil carbonate carbon isotopes, East African lake occurrences, hominins species appearances and durations (Maslin and Trauth 2006; Springer, by permission)

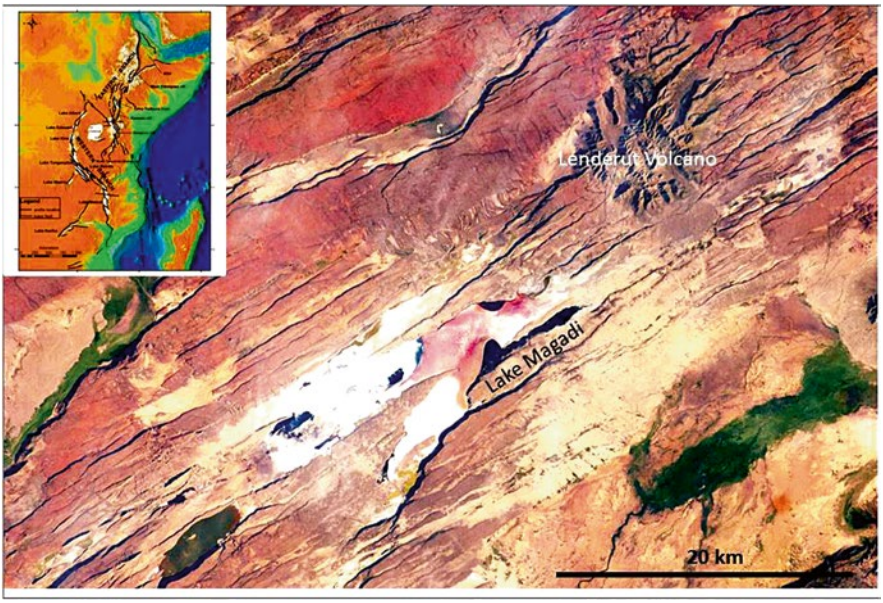

Fig. 1.34 East African rift valleys (http://earthobservatory.nasa.gov/IOTD/view.php?id=77566), including Lake Magadi – the southernmost lake in the Kenyan Rift Valley in a catchment of faulted volcanic rocks The area is rich in fossils of the hominin ancestors of modern humans, including the famous 3.2-million-year-old "Lucy" skeleton, the earliest known adult hominin. Location map from: http://www.sciencedirect.com/science/article/pii/S1464343X05001251 (Elsevier, with permission)

of the Walker Circulation, and the 1.1–0.9 Ma Lake phase to initiation of the Mid-Pleistocene transition from 41 kyr cycles to 100 kyr cycles (Berger and Jansen 1994). Moisture levels and the filling of the lakes were sensitively related to movements of the Intertropical Convergence Zone (ITCZ) and the Indian Ocean monsoon (Maslin and Trauth 2009). Major lacustrine episodes during 2.7–2.55 Ma consist of five paleo-lake phases which correspond to the precession cycle of 23 kyr and extreme climate variability (Deino et al. 2006). Carbon isotopes from both soil carbonates and biomarkers from deep-sea sediments indicate progressive vegetation shift from C3 (trees and shrubs) to C4 (tropical grasses) plants during the Plio-Pleistocene (Feakins et al. 2005) and thus increased aridity. Extreme climate variability is supported by paleo-diet reconstructions of mammals and hominins (Teaford and Ungar 2000).

The close relations between orbital forcing, climate variability and vegetation in East Africa resulted in the rapid appearance and disappearance of ephemeral lakes over periods of hundreds to thousands of years, with implications for the speciation and dispersal of mammals (Deino et al. 2006). Lake formation peaks during periods of high eccentricity appear to have near-coincided with the appearance of Olduvan stone culture about ~2.6 Ma and Acheulean stone culture about 1.9–1.8 Ma (Fig. 1.33). 12 out of the 15 hominin species first appeared during alternating wet-dry periods (Maslin and Trauth 2009), including *Homo habilis, H. rudolfensis, and H. ergaster*. Transitions between different climate states may have been gradual, abrupt or extreme, the latter supporting variability selection in human evolution (Potts 1998). Extreme variability is documented at Lake Baringo where diatomite units and fish-bearing units grade into high-energy terrestrial facies (Maslin and Trauth 2009). Variability selection invokes key hominin adaptations during periods of rapid change, including development of bipedal locomotion, high brain/body mass relations and complex human social behaviour.

Fastest rates of temperature rise are recorded over ~1500 years-long cycles (Dansgaard-Oeschger [D-O] cycles) (Fig. 1.32) during the last glacial period of ~75–20 kyr, superposed on longer-term cooling trends and culminating in Heinrich events (Yokoyama and Esat 2011). The cycles were related to melting of the Greenland and Laurentian ice sheets, with effects extending to the North Atlantic Thermohaline Current (NATH) (Fig. 1.32) (Broecker 2000). Temperature rises recorded in Greenland ice cores at the outset of D-O cycles reach ~6–8 °C (Ganopolski and Rahmstorf 2002) within several decades, suggestive of ~3–4 °C mean global changes. Approximate mean global temperature rise rates are estimated in the range of ~0.01–0.2 °C/year, commensurate with, or higher than, twenty to twenty-first centuries temperature rise rates (Table 2.2). CO_2 increases associated with D-O cycles are estimated as ~20 ppm, with CO_2 rise rates of ~0.2 ppm/year, which is an order of magnitude less than modern rates (Table 2.2).

Abrupt climate shifts including stadial cooling during the interglacials (Fig. 1.30) are exemplified by (1) the onset and termination of the 12.9–11.7 kyr *Younger Dryas* cold phase over periods as short as 1–3 years (Steffensen et al. 2008), and (2) a sharp temperature decline by several degrees Celsius at ~8.2 kyr in the North

Atlantic, associated with discharge of cold water from the Laurentian ice sheet through Lake Agassiz (Wagner et al. 2002; Lewis et al. 2012).

The transitions through the Pliocene and Pleistocene from tropical to savannah environments in Africa, accompanied by faunal diversification from tropical species toward arid-zone type species, including Antelopes (Bovids) about 2.8 Ma, 1.8–1.7 Ma and 0.8–0.7 Ma, signify an increase in climate variability and enhanced pace of evolution. Glacial termination events, preceded by low-variability lulls (Dakos et al. 2008) (Fig. 1.31), involved high rates of greenhouse gas rise and of temperature rise in the order of 0.0004 °C/year and 0.009 ppm CO_2/year, faster than Miocene and Pliocene rates but lower by orders of magnitude compared to modern rates (Table 2.2).

Human evolution associated with these climate transitions was expressed by diversification and appearance of Olduvan stone tools from about ~2.7 Ma and Acheulean stone tools from about ~1.7 Ma (deMenocal 2004; Klein 2009) (Fig. 1.33). Survival stresses associated with extreme glacial-interglacial climates from about 0.9 Ma saw near-trippling of the *Homo* cranial cavity from ~450 cc to ~1200–1500 cc, mastering of fire about or later than 2 Ma and, from about ~160 kyr, cultural developments including burial, ornamentation and rock painting by *Homo sapiens*.

Chapter 2
Phanerozoic Life and Mass Extinctions of Species

Falling Star

For an infinitely long second, nascent
Your tail plots a crescent, a fiery arc
From a star-spangled sky incandescent
To the fast sleeping Earth, in the dark
Your grave for all time.

Who are you, friend or foe, stranger
Fragment fallen by a space highway
Of the asteroid belt, posing danger
Or some orbit-decayed fancy hardware
Of fatal star wars fleets?

Are you a harbinger of good news
Or signal dire distress
For this embattled Earth, in its blues
Will your fleeting torch impress
A new truth?

Will you plunge way beyond yonder
Or fall here, close by my side
On this red desert dune, I wonder
Stranded tonight, wide eyed
In awe, without faith?

(By Andrew Glikson)

Abstract Early conflicts between uniformitarian and gradual theories of evolution (James Hutton 1726–1797; Charles Lyell 1797–1875) and catastrophic theory (Georges Cuvier 1769–1832) have been progressively resolved by advanced paleontological, sedimentary, volcanic and asteroid impact studies and by paleo-climate studies coupled with precise isotopic age determinations, indicating periods of gradual evolution were interrupted by abrupt events which have transformed the habitat of plants and organisms and resulted in mass extinction of species. Detailed investigations of the carbon, oxygen and sulphur cycles using a range of proxies, including leaf pore stomata, $\delta^{13}C$, $\delta^{34}S$ and $^{87/86}Sr$ isotopes, as well as geochemical mass balance modeling, provide detailed evidence of major trends as well as distinct events in the atmosphere–ocean-land system during the Paleozoic and Mesozoic eras (542–65 Ma), including greenhouse Earth periods ($CO_2 \sim 2{,}000$–$5{,}000$ ppm)

A.Y. Glikson, C. Groves, *Climate, Fire and Human Evolution*, Modern Approaches in Solid Earth Sciences 10, DOI 10.1007/978-3-319-22512-8_2

and glacial phases ($CO_2 < 500$ ppm), with implications for biological evolution. The Cenozoic era includes four components (A) post K-T impact warming culminating with the Paleocene-Eocene hyperthermal at ~55 Ma; (B) long term cooling ending with a sharp temperature plunge toward formation of the Antarctic ice sheet from 32 Ma; (C) a post-32 Ma era dominated by the Antarctic ice sheet, including limited thermal rises in the end-Oligocene, mid-Miocene and end-Pliocene, and (D) Pleistocene glacial-interglacial cycles. Hominin evolution in Africa occurred during a transition from tropical to dry climates punctuated by alternating periods of extreme orbital forcing-induced glacial-interglacial cycles, suggesting variability selection of Hominins.

The geological record betrays a close correspondence between paleontological, sedimentary, volcanic, asteroid impact and paleo-CO_2 and paleo-temperature trends, allowing identification of environmental factors which underlie the evolution and extinction of species (McElwain et al. 1999; McElwaine and Punyasena 2007; Beerling 2002a, b; Beerling et al. 2002; Keller 2005; Glikson 2005). Five major mass extinction events and several moderate extinction events have affected the evolution of marine invertebrates (Fig. 2.1). High-resolution regional palaeoecological studies indicate extensive ecological upheaval, high species-level turnover and recovery intervals lasting millions of years, with close correlations to upheavals affecting terrestrial vegetation (McElwain and Punyasena 2007).

When a large (>200 meters) asteroid hits a solid surface at a high angle it penetrates to a depth of approximately ×1.5 times its diameter, depending on the rheology of the impacted rocks, where its kinetic energy is translated into heat, triggering an explosion, fragmentation, cratering, melting and vaporization of the immediately surrounding rocks. In craters larger than about 4 km the Earth's crust rebounds to form a central uplift (French 1998; Glikson 2013). Depending on the size of the impact, seismic waves propagate, leading to earthquakes, faulting and tsunami waves over large regions. Environmental effects of asteroid impacts include the initial fireball flash, mega-tsunami waves, release of aerosols (dust, sulphur dioxide, carbon soot), acid rain and release of greenhouse gases (water, CO_2, methane, Nitrous oxide) from cratered regions, leading to ocean acidification. This leads to an asteroid winter phenomenon, with some 10–20 % of solar radiation blocked for 8–13 years (Pope et al. 1997), followed by a greenhouse-gas induced warm period lasting centuries to millennia. Species which have escaped the immediate regional and transient effects of large impacts were affected by the long-lasting consequences of the well-mixed greenhouse gases, mainly CO_2, Nitrous oxide and methane. CO_2 stays in the atmosphere for thousands to tens of thousands years, leading to extended periods of high global temperatures, compounding the effects on the biosphere. Effects on the oceans include acidification, anoxia (oxygen solubility decreasing with higher temperatures) and consequent anoxic conditions and toxic H_2S forming emanations (Ward 2007).

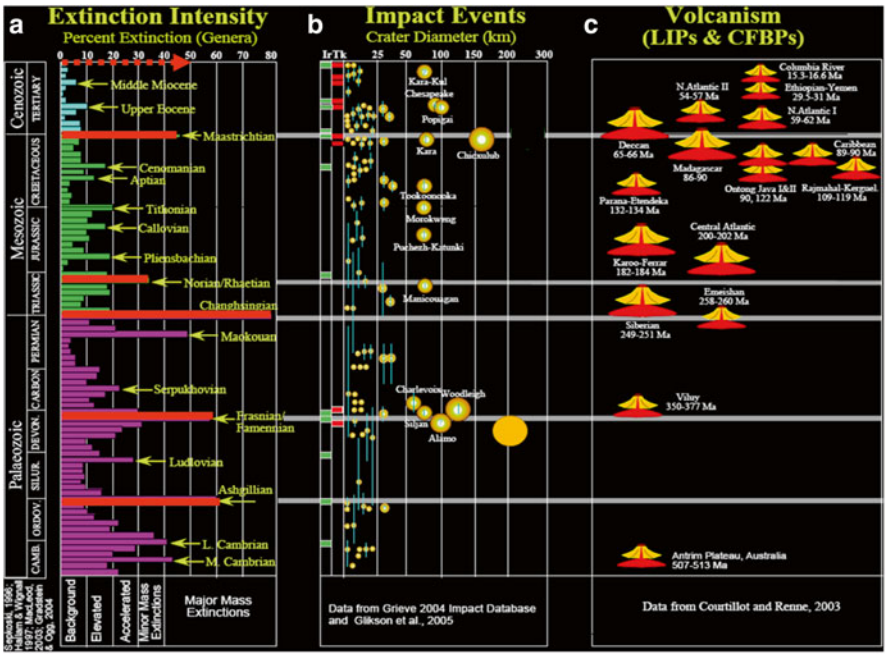

Fig. 2.1 Phanerozoic mass extinctions, asteroid impacts, and large igneous provinces. (**a**) Extinction intensity; (**b**) Impact events; (**c**) Volcanism. Stratigraphic subdivisions and numerical ages are after Gradstein and Ogg (2004). The extinction record is based on genus-level data by Sepkoski (1996). The number of impact events, size and age of craters follows largely the Earth Impact Database (2005), with modification by AG (Courtesy G. Keller)

Phanerozoic mass extinctions marked by carbon and oxygen isotopic anomalies include the End-Ordovician (Marshall 1992; Marshall et al. 1997; Brenchley et al. 2003), Late Devonian (Stephens and Sumner 2002), Permian-Triassic boundary, Late Triassic and K-T boundary (Maruoka et al. 2007). Changes in the carbon cycle recorded by total organic carbon (TOC) and stable carbon isotope ratios (δ^{13}Ccarb and δ^{13}Corg) constitute sensitive fingerprints of mass burial of organic matter derived from marine organisms, fallout from forest fires, or increased biological productivity. Variations in oxygen isotope ratios (δ^{18}O) reflect changes in ice volumes and salinity. Marked changes in these parameters accompany major volcanic eruptions, asteroid impacts (Maruoka et al. 2007) and methane release (Zachos et al. 2008) (Fig. 1.23).

Positive excursions in both δ^{18}O and δ^{13}Ccarb at the end-Ordovician signify parallel decrease in temperature and in biological productivity at the onset of 443.4 ± 1.5 Ma Ashgill/Hirnatian glaciation and extinction event (Marshall 1992; Marshall et al. 1997; Brenchley et al. 2003). A global nature of the glaciation is indicated from the widespread positive carbon isotope, including δ^{13}Ccarb and δ^{13}Corg,

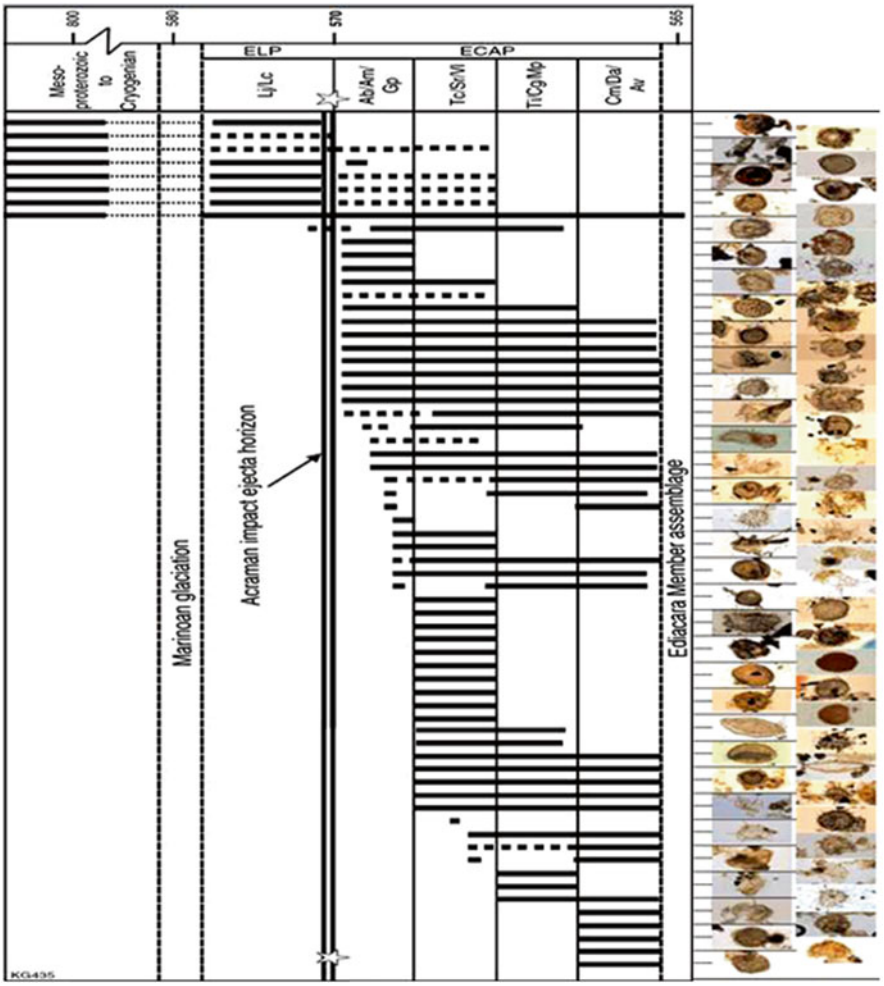

Fig. 2.2 Stratigraphic distribution of Acritarchs following the Marinoan glaciation at ~580 Ma, displaying a major discontinuity at ~570 Ma coinciding with ejecta from the Acraman impact event, followed by major radiation (Grey 2005; Courtesy K. Grey. Image courtesy of the Geological Survey of Western Australia, Department of Mines and Petroleum, State of Western Australia 2013. ELP – Ediacaran Leiosphere Palynoflora; ECAP – Ediacaran Complex Acanthomorph Palynoflora)

and oxygen isotope shifts measured from Brachiopod shells over a wide range of paleo-latitudes. Upper Ordovician cores from Estonia and Latvia record a δ^{13}Ccarb shift of up to 6‰ and similar profiles were measured in Nevada, suggesting a global chronostratigraphic signal (Brenchley et al. 2003). Positive correlation between δ^{13}C and δ^{18}O militates for genetic relations between biological activity and temperature (Figs. 2.3, and 2.4).

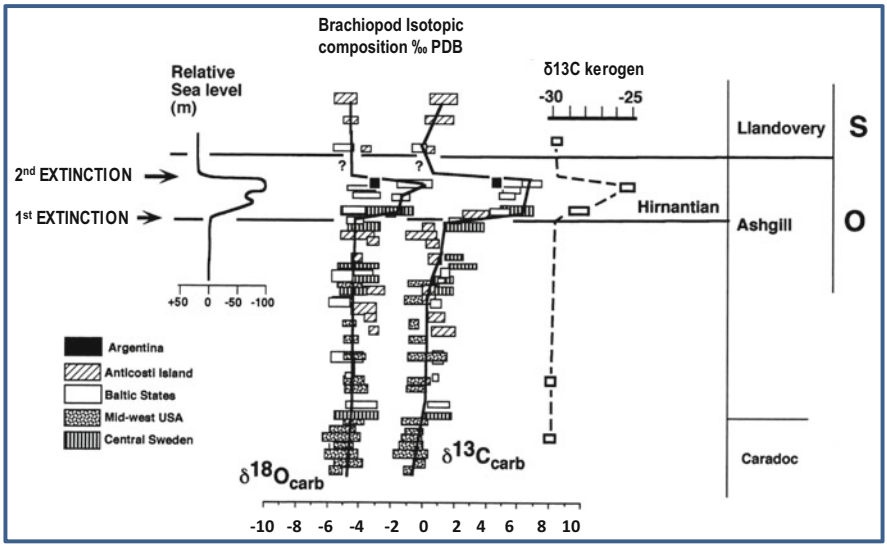

Fig. 2.3 Summary diagram showing the relationships between biological, bathymetric and stable isotopic changes in the late Ordovician. The marked positive carbonate isotopic excursion in the early Hirnantian is paralleled by a shift in the isotopic composition of organic carbon. Data from Argentina demonstrate elevated $\delta^{13}C$ in brachiopods from high palaeolatitudes but the oxygen values should be regarded as a minimum because even the least-altered sample showed signs of diagenetic alteration (Marshall et al. 1997; Elsevier, by permission)

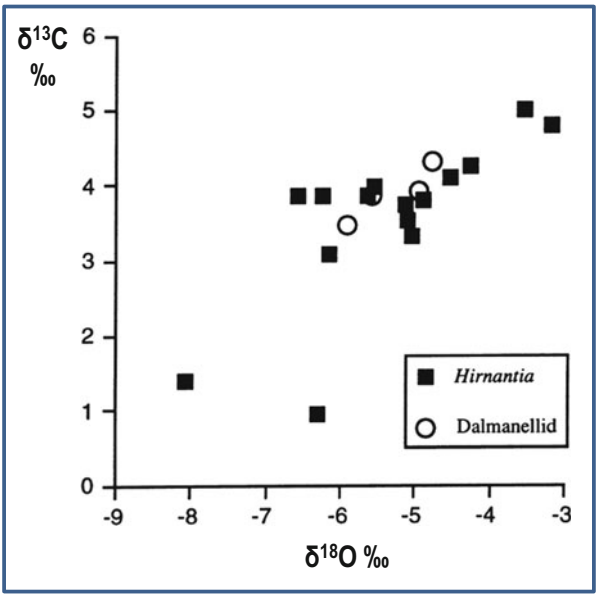

Fig. 2.4 The relations between organic matter-related $\delta^{13}C$ and temperature related $\delta^{18}O$ stable isotope proxies in Ordovician brachiopod samples from the La Pola and Don Braulio sections (Marshall et al. 1997; Elsevier, by permission)

Upper Devonian isotopic excursions were studied at the Fitzroy reef complex of the Canning Basin, Western Australia, where well-exposed continuous Frasnian-Fammenian sequences record interactions between sea level changes, sediment supply, ocean chemistry, and paleoecology (Stephens and Sumner 2002). The Frasnian-Fammenian transition correlates with positive $\delta^{13}C$ shifts, consistent with similar intervals of the Kellwasser horizons in Europe (Figs. 2.5 and 2.6). By analogy to the end-Ordovician, an overall positive correlation pertains between $\delta^{13}C$ and $\delta^{18}O$ relations (Fig. 2.7), suggesting a decline in biological productivity with lower temperatures (Stephens and Sumner 2002). Likely connections between the Frasnian-Fammenian (~374 Ma) and End-Devonian (~359 Ma) mass extinctions (Fig. 2.1, and 2.6) and asteroid impacts (Woodleigh, Western Australia ~359 ± 4 Ma; Siljan, Sweden, 376.8 ± 1.7 Ma; Charlevoix, Quebec, 342 ± 15; Alamo, New Mexico, ~360 Ma) (Glikson 2005; Keller 2005) remain to be established once the relations between the stratigraphic context of fallout/ejecta units of these impact is studied.

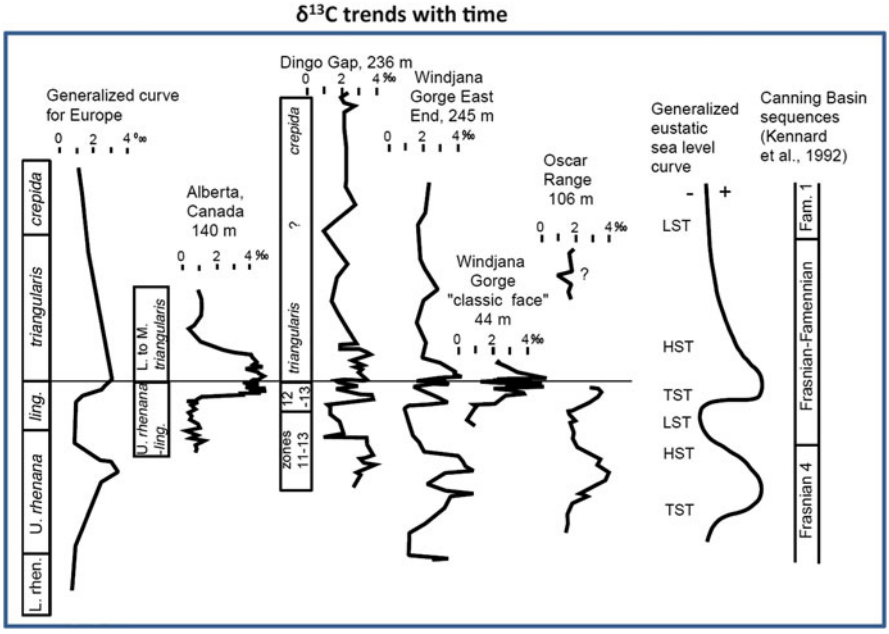

Fig. 2.5 $\delta^{13}C$ rises representing decline in biological activity following the Frasnian-Fammenian mass extinction. The trends from Canning Basin compared to generalized carbon isotope curve from Europe and carbon isotope curve from Canada. The $\delta^{13}C$ curve from Europe is plotted against time. The $\delta^{13}C$ curves from Australia and Canada are plotted against thickness and adjusted so conodont dates correlate with the European section. Gap in Oscar Range curve is due to unconformity. The generalized eustatic sea level curve is interpreted from Canning Basin and European sections and agrees with Hallam and Wignall's (1997) interpretation (Stephens and Sumner 2002; Elsevier, by permission)

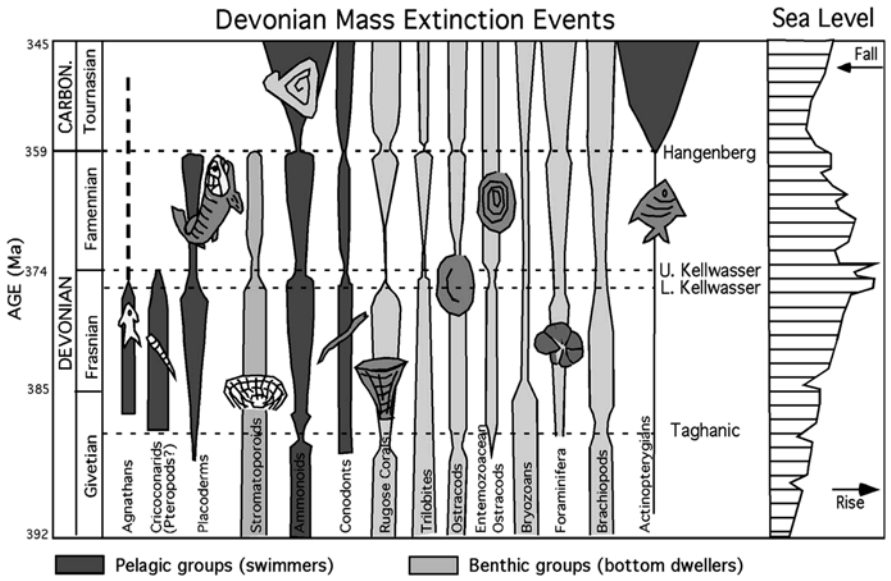

Fig. 2.6 Biotic effects of Devonian mass extinction events (Hallam and Wignall 1997). Major mass extinctions are in the lower and upper Kellwasser at the end of the Frasnian, decimating reef system, shallow benthic fauna and pelagic swimmers. The crises were associated with sea-level rises, warm climate and widespread ocean anoxia. The Hangenberg extinction affected mainly pelagic groups including ammonoids and fish. The mid-Devonian Taghanic extinction was part of a long-term diversity decline (after Keller 2005; Australian Journal of Earth Science, by permission)

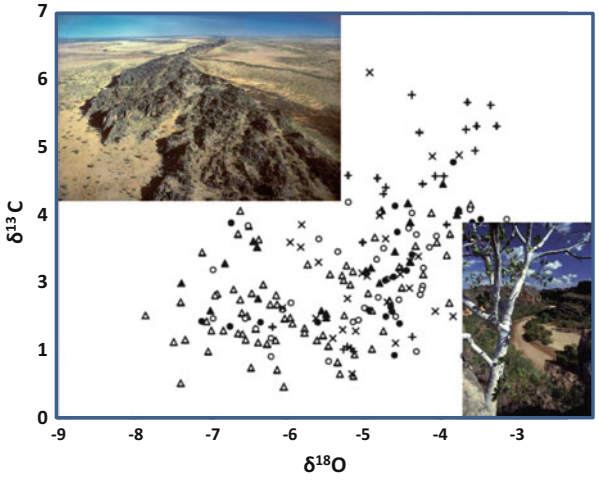

Fig. 2.7 Carbon and oxygen isotopic values of samples used for $\delta^{13}C$ correlations (Stephens and Sumner 2002; Elsevier, by permission). Photographs: *top left* – Napier Range, Kimberley (courtesy Reg Morrison; bottom right – Windgina Gorge, Kimberley (Courtesy Reg Morrison)

A marked decline of between 4‰ and 7‰ $\delta^{13}C$ values straddling the Permian-Triassic boundary (251 Ma), associated with sharp fluctuation of CO_2 (Fig. 2.8), represents world-wide deposition of extinct biota high in ^{12}C (Ward 2007; Korte and Kozur 2010) (Figs. 2.9 and 2.10). Low $\delta^{13}C$ values lasted over about 0.5 million years, beginning in the Changhsingian (253.8 ± 0.7 Ma) and reaching a first minimum at the P-T boundary (251 ± 0.4 Ma). The trend is interrupted by two short-term positive excursions following which a decline in $\delta^{13}C$ values continues. Korte and Kozir (2010) interpret these variations in terms of (1) direct and indirect effects of volcanism of the Siberian Traps; (2) anoxic deep waters occasionally reaching very shallow sea levels. The authors question an abrupt release of isotopically light methane from sediments or permafrost soils as a source for the negative carbon-isotope trend. With near to 80 % mass extinction of genera (Keller 2005), a prolonged recovery of the biosphere followed over a period of near to 5 million years (Erwin 1994, 2006; Korte and Kozur 2010).

Oxygen isotope ratios measured on phosphate-bound oxygen in conodont apatite from South China decrease by 2‰ in the latest Permian, translating into low-latitude surface water warming of 8 °C (Joachimski et al. 2012). The oxygen excursion coincides with a negative $\delta^{13}C$carb shift, suggesting CO_2 emission by Siberian Trap volcanism constituted a factor driving warming. Temperature rise commenced immediately prior to the main extinction phase, with maximum temperatures documented in the latest Permian at Meishan (bed 27), coinciding with the main pulse of extinction and the collapse of marine and terrestrial ecosystems. Prolonged warming through the Early Triassic may have played a major role in the delayed recovery in the aftermath of the Permian-Triassic crisis.

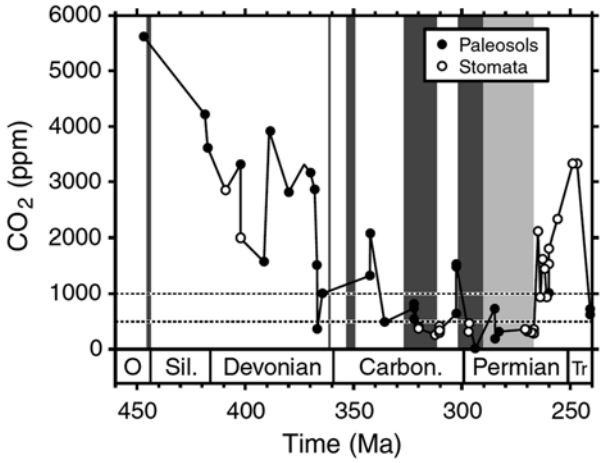

Fig. 2.8 CO_2 and temperature records for the Late Ordovician to early Triassic (460–240 Ma) (Royer 2006; Elsevier, by permission). Note the upper to late Devonian and Permian-Triassic boundary peaks of ~3000 ppm CO_2, corresponding to a major mass extinction of species

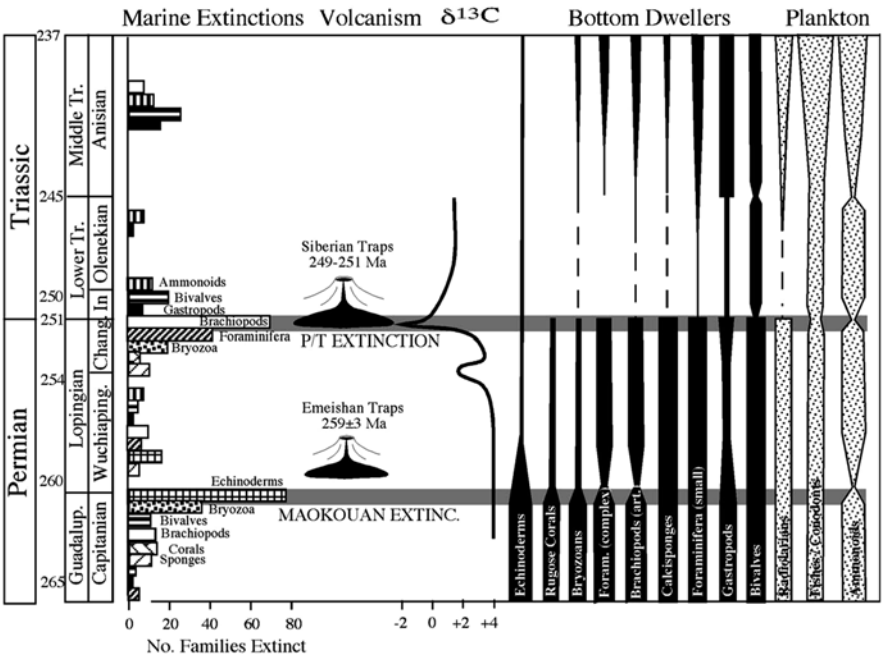

Fig. 2.9 Faunal turnover, impacts and volcanism across the Permian – Triassic transition. Faunal data modified after Hallam and Wignall (1997); volcanism after Courtillot and Renne (2003). (Keller 2005; Australian Journal of Earth Science, by permission)

The end-Triassic extinction at 201.4 Ma, associated with opening of the Central Atlantic Magmatic Province (CAMP), is marked by large negative carbon isotope excursion, including a transient increase in CO_2 (Fig. 2.11) Carbon isotopic anomalies of leaf wax derived lipids (n-alkanes), wood, and total organic carbon from lacustrine sediments intercalated with CAMP volcanics in eastern North America are similar to anomalies in sections across the Atlantic, suggesting synchronous onset of the extinction (Whiteside et al. 2010). The onset of the anomalies precedes the oldest basalts in eastern North America but is simultaneous with the eruption of the oldest flows in Morocco, signifying a CO_2 super greenhouse and marine acidification crisis. Bachan et al. (2012) report $\delta^{13}C$ anomalies from six newly sampled sections in Italy displaying sharp negative $\delta^{13}C$carb excursions coincident with the disappearance of the Triassic fauna and two overlying positive excursions (Fig. 2.12). No negative $\delta^{13}C$org were recorded, suggesting diagenetic alteration of organic matter. The data suggest perturbation of the global carbon cycle persisting for substantial lengths of geologic time following the mass extinction (Fig. 2.13).

The most extensively studied asteroid impact boundary of the 65 Ma K-T event has yielded definitive carbon, oxygen and sulphur isotopic values diagnostic of the geological, geochemical and biological effects of large-scale impact. Detailed studies

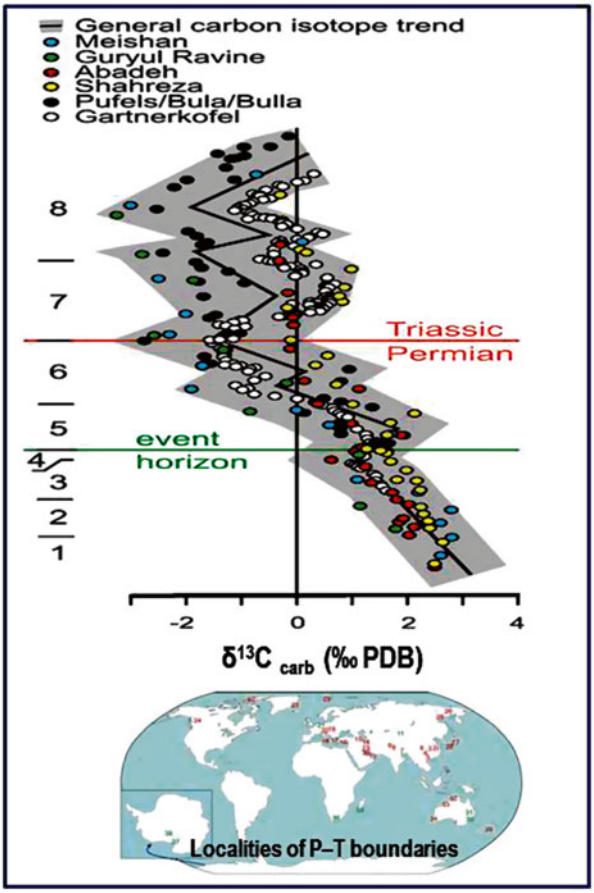

Fig. 2.10 General carbon-isotope trend across the P–T boundary constructed from the stratigraphically well-defined $\delta^{13}C$ data from Meishan, Guryul Ravine, Abadeh, Shahreza, Pufels/Bula/Bulla and the Gartnerkofel core. 1: *C. changxingensis–C. deflecta Zone*, 2: *C. zhangi Zone*, 3: *C. iranica Zone*, 4: *C. hauschkei Zone*, 5: *C. meishanensis–H. praeparvus Zone* (5 + 6: *H. praeparvus Zone* for shallow-water without Clarkina such as the Southern Alps), 6: *M. ultima–S.* 7: *H. parvus Zone* = Triassic part of *C. zhejiangensis* (for South Chinese intraplatform basins), 8 = *I. isarcica Zone* (Korte and Kozur 2010; Elsevier, by permission)

of TOC and $\delta^{13}C$ anomalies across the K-T boundary in freshwater floodplains and swamp environments of Montana and Wyoming by Maruoka et al. (2007) reveal a marked decrease of $\delta^{13}C$ values by 2.6‰ (from −26.15‰ to −28.78‰) at Brownie Butte (Fig. 2.14), similar to the trend in carbonate at marine K–T sites. The $\delta^{13}Corg$ values are thought to reflect variations in carbon isotopes in atmospheric CO_2 in equilibrium with the ocean surface water. Other factors include enhanced contribution of organic matter derived from algae in a high-productivity environment due to

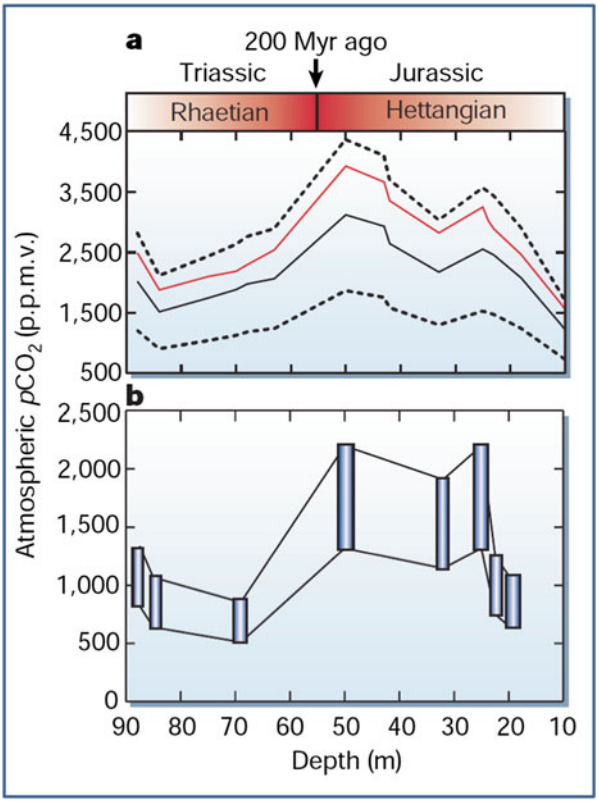

Fig. 2.11 Palaeo-atmospheric CO_2 variations across the Triassic–Jurassic boundary at 208 Ma. (**a**) Atmospheric CO_2 changes calculated using $\delta^{13}C$ values and a constant Triassic paleosol carbonate value up to the Triassic–Jurassic boundary and a constant Jurassic paleosol value; (**b**) Atmospheric CO_2 changes reconstructed from the stomata of fossil leaves. *Vertical bars* denote the upper and lower range for any given depth calculated using this technique (Beerling 2002a; Nature, by permission)

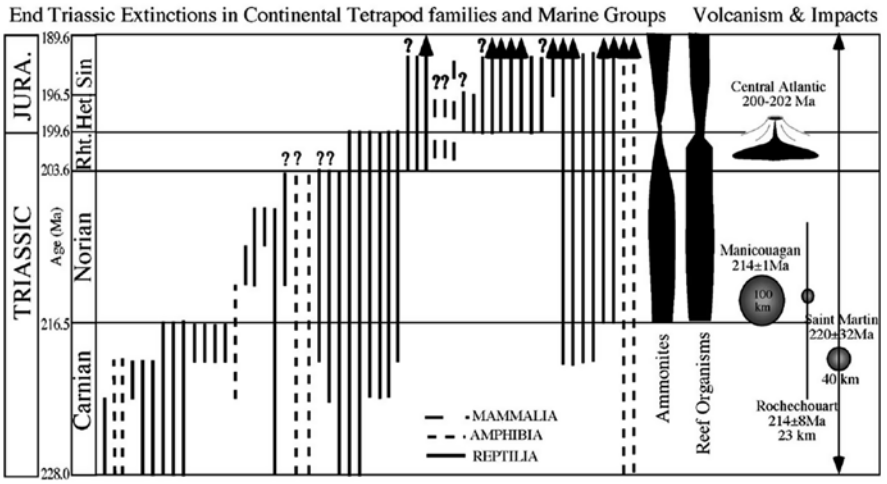

Fig. 2.12 Mass extinction, impacts and volcanism across the Triassic – Jurassic transition. Fauna changes modified after Hallam and Wignall (1997); volcanism after Courtillot and Renne (2003). (Keller 2005; Australian Journal of Earth Science, by permission)

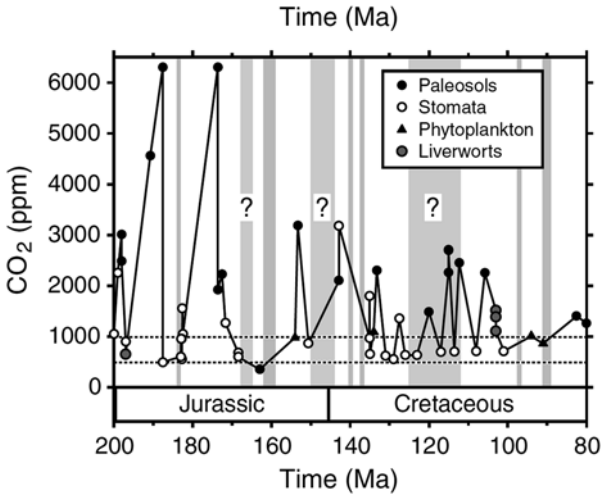

Fig. 2.13 CO_2 and temperature records for the Jurassic to late Cretaceous (~200–80 Ma). Cold periods with evidence for geographically widespread ice are marked with shaded bands. The *horizontal dashed lines* at 1000 and 500 ppm CO_2 represent the proposed CO_2 thresholds for, respectively, the initiation of globally cool events and full glacial periods (Royer 2006; Elsevier, by permission)

nitrogen fertilization and/or eutrophication induced by sulphide. The authors suggest the high productivity recorded in the K–T boundary clays imply that, by contrast to marine environments, freshwater environments re-recovered rapidly from the effects of impact. At a second K-T impact boundary site of Dogie Creek a positive shift of δ^{13}Corg is observed (Fig. 2.14) similar to other continental sites in North America. Variations between the sections suggest the effects of local environments such as anoxia and reactions with sulphide and sulphate related to acid rain effects of the impact.

Kaiho et al. (1999), reporting 36 isotopic analyses of K-T boundary samples from Caravaca, Spain, observe a rapid reduction in the gradient between δ^{13}C values in fine fraction carbonate and benthic foraminiferal calcite in sediments immediately above the K/T boundary, implying an abrupt extinction of pelagic organisms leading to a significant reduction in the flux of organic carbon to the seafloor. Variations in sulphur isotope ratios at Caravaca, Japan and New Zealand imply a rapid decrease in oxygen coincident with the δ^{13}C shift. A three-fold increase in the kaolinite/illite ratio and a 1.2‰ decrease in δ^{18}Ocarb recorded in the basal 0.1–2 cm of Danian sediments indicate atmospheric and marine warming up to 3000 years following the δ^{13}C event. Recovery in the δ^{13}Ccarb and commenced some 13,000 years kyr following the K-T event.

During periods when both asteroid impacts and volcanic eruptions occurred the respective roles of these events in driving mass extinctions is difficult to estimate

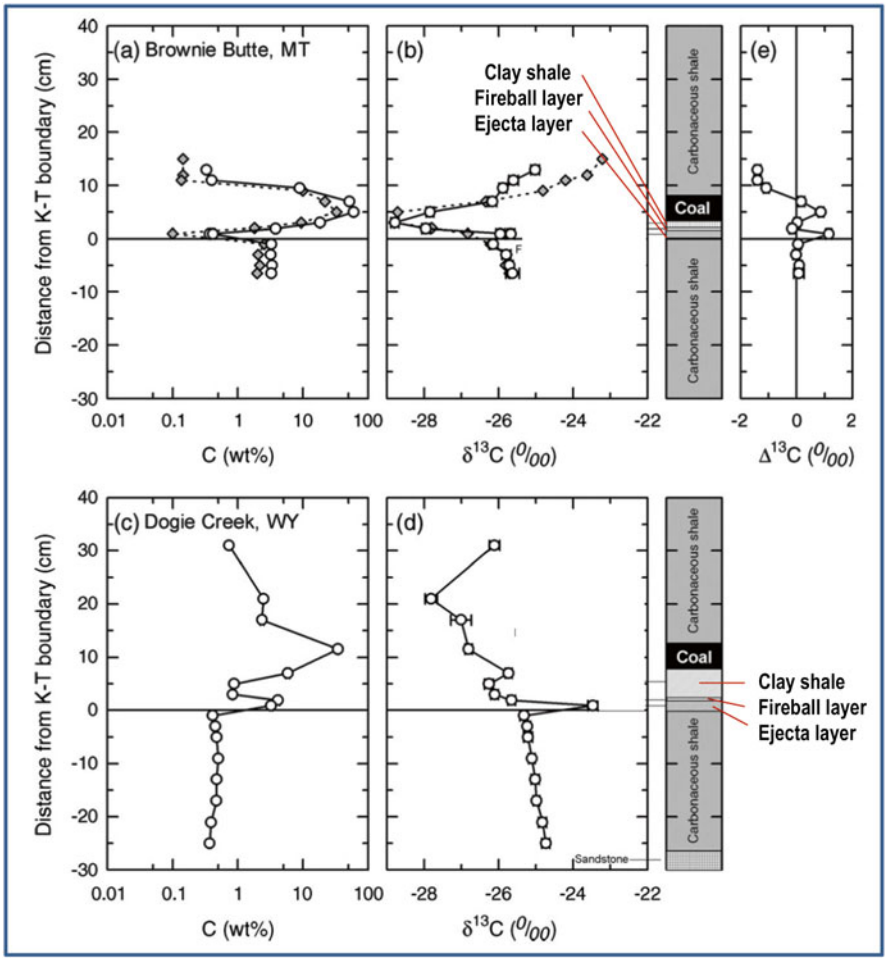

Fig. 2.14 Chemostratigraphic profiles for a organic carbon concentrations and b $\delta^{13}C$ values of bulk organic carbon for the Brownie Butte samples and for c organic concentrations and $\delta^{13}C$ values of bulk organic carbon for the Dogie Creek samples. *Open circles* and *gray diamonds* represent data obtained by Maruoka et al. (2007) and those obtained by Gardner and Gilmour (2002), respectively (Maruoka et al. 2007, Fig. 4; Elsevier, by permission)

and a relatively small number of asteroid impact structures have been accurately dated (Jourdan et al. 2012). The following temporal associations between volcanic and/or asteroid events and mass extinction are relevant (Fig. 2.1; Tables 2.1 and 2.2):

1. Acraman/Bunyeroo ~580 Ma asteroid impact and Acritarch radiation (Grey et al. 2003; Grey 2005) (Fig. 2.2).
2. Late Devonian (Frasnian-Fammenian) ~374 Ma Viley volcanism and mass extinction.

Table 2.1 Geological stage boundaries, large asteroid impact events, large volcanic provinces and percent mass extinction of species

Stage boundaries/ epochs	Large asteroid impacts	Large volcanic provinces	% Mass extinction of genera
Mid-Miocene Langhian 15.97 Ma	Ries (24 km) 15.1 ± 1.0 Ma	Columbia Plateau Basalt 16.2 ± 1 Ma	6
Eocene–Oligocene boundary 33.9 ± 0.1 Ma	Popigai (100 km) 35.7 ± 0.2 Ma; Chesapeake Bay (85 km) 35.5 ± 0.3 Ma Mount Ashmore: E-O Boundary	Ethiopian Basalts 36.9 ± 0.9 Ma	10
KT boundary 65.5 ± 0.3 Ma	Chicxulub (170 km) 64.98 ± 0.05 Ma Boltysh (25 km) 65.17 ± 0.64 Ma	Deccan Plateau Basalts. 65.5 ± 0.7 Ma (pooled Ar Ages: 65.5 ± 2.5 Ma)	46
Cenomanian–Turonian 93.5 ± 0.8 Ma	Steen River (25 km) 95 ± 7 Ma	Madagascar Basalts 94.5 ± 1.2 Ma	17
Aptian (Early Cretaceous) 125–112 Ma	Carlswell (39 km) 115 ± 10 Ma; Tookoonooka (55 km; 125 ± 1 Ma); Talundilly (84 km; 125 ± 1 Ma); Mien (9 km) 121 ± 2.3 Ma; Rotmistrovka (2.7 km) 120 ± 10 Ma	Ontong-Java LIP 120 Ma Kerguelen LIP 120–112.7–108.6 Ma Ramjalal Basalts, 117 ± 1	14
End-Jurassic 145.5 ± 4 Ma	Morokweng (70 km) 145 ± 0.8 Gosses Bluff (24 km) 142.5 ± 0.8 Ma; Mjolnir (40 km) 143 ± 2.6 Ma	Dykes SW India 144 ± 6 Ma	20
End-Pliensbachian 183 ± 1.5 Ma		Peak Karoo volcanism Start 190 ± 5 Ma; Peaks 193, 178 Ma; Lesotho 182 ± 2 Ma	19
End-Triassic 199.6 ± 0.3 Ma		Central Atlantic Igneous Province: 203 ± 0.7 to 199 ± 2 Ma Newark Basalts 201 ± 1 Ma	18
Norian/Rhatian 216.5	Manicouagan (100 km) 214 ± 1 Ma; Rochechouart (23 km) 213 ± 8 Ma;		34
Permian–Triassic: 251 ± 0.4 Ma; 251.4 ± 0.3 to 250.7 ± 0.3 Ma	Araguinha (40 km) 252.7 ± 3.8 Ma,	Siberian Norilsk 251.7 ± 0.4 to 251.1 ± 0.3 Ma	80
Late to end Devonian 374–359 Ma	Woodleigh (120 km) 359 ± 4 Ma; Siljan (52 km) 361 ± 1.1 Ma; Alamo breccia (~100 km) ~360 Ma; Charlevoix (54 km) 342 ± 15 Ma	Rifting and 364 Ma Pripyat–Dneiper–Donets volcanism	30 58
End-Ordovician 443.7 ± 1.5 Ma	Several small poorly dated impact craters		60
End-Early Cambrian 513 ± 2 Ma	Kalkarindji volcanic Province, northern Australia 507 ± 4 Ma		42

Table 2.2 Comparison of mean global temperature rise rates during the Cenozoic, including the K-T impact events (Beerling et al. 2002), the 55.9 Ma PETM hyperthermal event (Zachos et al. 2008), end-Eocene freeze and formation of the Antarctic ice sheet (34–32 Ma) (Zachos et al. 2001), Oligocene (Zachos et al. 2001), Miocene (Kurschner et al. 2008) and end-Pliocene (Zachos et al. 2001; Beerling and Royer 2011) thermal rises, glacial terminations (Hansen et al. 2007) Dansgaard-Oeschger cycles (Ganopolski and Rahmstorf 2002; Jouzel 2007), 8.2 kyr event (Wagner et al. 2002) intra-Holocene events (IPCC-AR4 2007) and Anthropocene climate change (IPCC-AR4 2007)

Age	Interval	Mean global land and sea temp change (C)	Warming rate (C/year)	CO_2 change (ppm)	CO_2 change rate (ppm/year)	Reference	Proxy methods
K-T impact 64.98 Ma	Instant to 10,000 years	Short freeze followed by ~+7.5C	~0.00075	~400 to 2300	Instantaneous to 0.19 ppm/yr	Beerling et al. 2002	Gingko stomata
PETM 54.9 Ma	~10,000 years	~ +5–9C	~0.0005	~1800 to 4000 ppm	~0.22 ppm/yr	Zeebe et al. 2009	Deep sea carbonate dissolution
Eo–Ol freeze 34.2–34.0	~200,000 years	~ −5.4C	−0.000027	~1120 to 560 ppm in 10×10^6 years		Liu et al. 2009; Pollard and DeConto 2005	TEX86; δ18O of benthic foraminifera; Boron and alkenones model
End-Oligocene ~24.7	~200,000 years	~ +4C	0.00002	500–900 ppm	0.002	Pekar and Christie-blick 2007	$\delta^{13}C$ data from alkenones
Mid-Miocene 20–18 Ma	~200,000 years	~ +1.5C	0.000007	~300–520 ppm	0.0011	Kurschner et al. 2008	Multiple-species stomatal frequency record
End-Pliocene	4–3 Ma	~ +1C	0.000001	~250 to 400 ppm	0.00015	Zachos et al. 2001; Beerling and Royer 2011	Stomata pores; $\delta^{13}C$ plankton
Glacial terminations/Eemian	11,000 years	+ ~5C	0.0004	+100 ppm	0.009	Hansen et al. 2007; Petit et al. 1999; EPICA 2004	Ice cores

(continued)

Table 2.2 (continued)

Age	Interval	Mean global land and sea temp change (C)	Warming rate (C/year)	CO_2 change (ppm)	CO_2 change rate (ppm/year)	Reference	Proxy methods
Dansgaard-Oeschger – 21 cycles of ~1500 years each	~75–15 kyr	~3.5C	**0.01–0.2**	+20 ppm	0.2	Ganopolski and Rahmstorf 2002; Jouzel 2007	Greenland ice cores
Younger dryas Interglacial stadial	12.9–11.7 kyr	~ −15C in GISP2 ice core		−7 ppm			Greenland ice cores
8.2 kyr stadial	~100 years	−3.3C in the North Atlantic		−25 ppm in ~300 years	−0.08	Wagner et al. 2002	Greenland ice cores
Medieval warm period (MWP)	~400 years	~0.4–0.5C	**~0.001**	5 ppm	~0.012	IPCC-AR4 2007 Chap. 4	Ice cores, tree rings, cave deposits
Little ice age (LIA)	~60 years	~ −0.4C	**~ −0.006**	−5 ppm		IPCC-AR4 2007 Chap. 4	Ice cores, tree rings, cave deposits
Post-1750	263 years	+0.9C +2.3C potential (with no aerosol masking)	**~0.0034 ~0.008**	280–400 ppm	~0.45	IPCC-AR4 2007	Instrumental
1975–2012	37 years	+0.6C	**~0.016**	330–394.28 ppm	~1.73	NASA/GISS IPCC-AR4 2007	Instrumental
March 2012–March 2013	1 year			**2.89 ppm**	**2.89**	NOAA 2013	

3. End-Devonian ~360 Ma impact cluster (Woodleigh, Siljan, Charlevoix, Alamo) and the destruction of reefs (McGhee 1996; Balter et al. 2008).
4. Permian-Triassic boundary ~ 251 Ma volcanic (Norilsk) and asteroid impact (Araguinha) events and mass extinction of species (Renne et al. 1995; Ross and Ross 1995; Wignall and Twitchett 1996; Twitchett et al. 2001; Racki 2003; Ward 2007).
5. Late-Triassic ~216 Ma impact (Manicouagan, Rochechouart) and mass extinction.
6. End-Triassic ~200 Ma opening of the Atlantic Ocean, extensive volcanism and extinction (Olsen and Sues 1986; McElwain et al. 1999; Jourdan et al. 2009; Whiteside et al. 2010
7. Early Jurassic (Pliensbachian) ~183 Ma Karoo volcanism and extinction
8. End-Jurassic ~145 Ma impact cluster (Morokweng, Gosses Bluff, Mjolnir), opening of the Indian Ocean and extinction (McElwain et al. 1999).
9. Cretaceous-Tertiary boundary ~65 Ma impacts (Chicxulub, Boltish), Deccan volcanism and mass extinction.

2.1 Acraman Impact and Acritarchs Radiation

The ~580 Ma Acraman impact structure, estimated as ~90 km in diameter (Gostin et al. 1986; Gostin and Zbik 1999; Williams et al. 1996; Williams and Gostin 2005), and its ejecta layer found up to 550 km away from the crater, postdate the Marinoan glaciation (650–635 Ma). The impact was closely followed by radiation of Acritarch phytoplanktons, including an abrupt change from Ediacaran leiosphere palynoflora (ELP) to Ediacaran complex Acritarchs palynoflora (ECAP), presenting the oldest example of biological radiation following large catastrophic events (Grey et al. 2003; Grey 2005) (Fig. 2.2). The sequence from the terminal glacial sediments of the Cryogenian (~635 Ma) to the base Cambrian includes (1) cap carbonates, representing likely greenhouse gas-driven glacial collapse; (2) clastic sediments; (3) the ~580 Ma Acraman impact ejecta overlain by the Acritarchs-radiation horizon; (4) Ediacara fauna ~550 Ma (Fig. 1.14) and (5) ~544 Ma base Cambrian. The Acraman event is associated with marked negative $\delta^{13}C$ anomalies which signify increased deposition of organic matter (Calver 2000; Walter et al. 2000).

2.2 Cambrian and Late Ordovician Mass Extinction

The end-Ordovician period, marked by a glaciation about ~445.6–443.7 Ma and possibly longer (Frakes et al. 1992), saw two phases of extinction involving ~57 % of genera (Hallam and Wignall 1997), including pelagic graptolites and most benthic groups (trilobites, brachiopods, bryozoans, echinoderms) (Fig. 1.15).

Factors driving the extinction included cooling, glaciation, sea-level regression and major changes in oceanic circulation, leading to extinction of pelagic groups including graptolites and conodonts. The second phase appears to have been related to warming and ocean bottom anoxia eliminating shelf habitats (Hallam and Wignall 1997; Keller 2005). According to Kump et al. (1999) CO_2 levels declined during the glaciation from 5000 to 3000 ppm, high levels compensated by low insolation about 4 % lower than at present level of 342 Watt/m^2.

2.3 Late and End-Devonian Mass Extinctions

Possible factors associated with late Devonian mass extinctions include volcanism of the Viluy Traps, East European platform, estimated as >510,000 km^3 and dated in the range 377 and 350 Ma (Keller 2005) (Fig. 2.1). The end-Devonian at ~360 Ma was marked by a large asteroid impact cluster including Woodleigh (D = 120 km), Alamo (D = 100 km), Charlevoix (D = 54 km) and Siljan (D = 52 km) and possibly Warburton East and Warburton West (D ~400 km) (Glikson et al. 2013). Devonian mass extinction events (McGhee 1996; Hallam and Wignall 1997) include a ~387 Ma extinction (~30 % of Genera) and ~374 Ma extinction (58 % of Genera) affecting pelagic fauna (Ammonoids, Cricoconaids, Placoderms, Conodonts, Agnathans) and benthic groups (Rugose corals, Trilobites, Ostracods and Brachiopods). The extinction involved collapse of Stromatoporoid reefs (Keller 2005). End-Devonian ~359 Ma extinction (~30 % of Genera) affected fish (Placoderms), ammonoids, conodonts, stromatoporoids, rugose corals, trilobites and ostracods. Major factors included ocean anoxia, declining biological activity (high $\delta^{13}C$), and warming (low $\delta^{18}O$) (Balter et al. 2008). The late Devonian mass extinctions are superposed on a protracted cooling trend associated with a decline in CO_2 levels from a range of ~3200–5200 ppm to below ~500 ppm. Concomitant decline in $\delta^{13}C$ from ~22 to ~15‰ from ~405 Ma to 280 Ma is indicated by paleosols (Mora et al. 1996). The development in the Late Devonian of plant megaphyll leaves with their branched veins containing high stomata density allowed vegetation to adapt to the cool low-CO_2 conditions of the Carboniferous-Permian (Rothwell et al. 1989; Beerling et al. 2001).

2.4 Late Permian and Permian-Triassic Mass Extinctions

Major eruptions of the Siberian Norlisk magmatic province and Emeishan volcanism (Renne et al. 1995; Wignall and Twitchett 1996; Wignall 2001) about ~251 Ma (251.7 ± 0.4 to 251.3 ± 0.3 m.y., Kamo et al. 2003) and a large asteroid impact (Araguinha, Brazil, D = 40 km, ~247.8 ± 3.8 Ma; Tohver et al. 2012), which excavated carbonates and shale (Table 2.1), has led to a rise of atmospheric CO_2 levels to ~3400 ppm (Royer 2006) (Fig. 2.8), associated with the greatest mass extinction recorded in geological history (Figs. 2.9 and 2.10).

Two major extinction phases are defined:

A. ~50 percent of genera extinguished at the ~260 Ma Late Permian Maokouan Stage. Tropical zones saw the extinction of echinoderms, corals, brachiopods, sponges, fusulinid foraminifera and ammonoids (Ross and Ross 1995; Keller 2005) (Table 2.1; Fig. 2.9).
B. ~78 percent of genera extinguished at the ~251 Ma end-Permian Changhsingian Stage, effecting abrupt extinction of the Rugose Corals, Bryozoans, complex Foraminifera, many Gastropod and Bivalve families, radiolarians and many Ammonoid families (Hallam and Wignall 1997; Racki 2003) (Table 2.1, Fig. 2.9).

The two events were separated by the Capitanian and Wuchiapingian Stages (265.8–253.8 Ma) (Keller 2005). An abrupt nature of these events is indicated by their short duration of $10–50.10^3$ years and negative $\delta^{13}C$ excursion indicating deposition of fauna and flora remains (Twitchett et al. 2001). Nektonic (free swimming) fauna, including fish, conodonts and nautiloids survived better thanks to their mobility in the upper water column above anoxic bottom water (Keller 2005). Anoxia is evidenced by sulphide-rich and black clay sediments and negative $\delta^{13}C$ anomalies testifying to mass settling of organic matter. Grasby et al. (2011) suggested a link between extinction and a release of carbon ash/char derived from the combustion of Siberian coal and organic-rich sediments by flood basalts, which was dispersed globally and created toxic marine conditions.

Berner (2005) investigated geochemical trends across the Permian-Triassic boundary from isotopic $\delta^{13}C$ and $\delta^{34}S$ mass balance and estimates of weathering and burial of carbon and sulphur. A drop in the rate of organic burial from the late Permian to the mid-Triassic is attributed to rising aridity and decrease in biomass due to a transition from forests to herbaceous grassland. A major drop in oxygen from 30 % to 13 % was associated with an increase in the ratio of pyrite to organic carbon and in development of marine euxinic basins. Consequences included extinction of vertebrates and loss of giant insects and amphibians. According to Ward (2007) ocean acidification due to rising CO_2 levels, polar ice melt, reduced ocean current system and the conveyor belt which provides oxygen, consequent anoxia, production of H_2S by sulphur-reducing microbes and its release to the atmosphere, constituted critical factors in sea and land mass extinction.

2.5 End-Triassic Mass Extinction

The opening of the Central Atlantic magmatic province by the end-Triassic at ~200 Ma, involving copious basaltic volcanism (Hames et al. 2003; Courtillot and Rennes 2003; Jourdan et al. 2009) affected a major mass extinction event represented by a large negative carbon isotope excursion, reflecting perturbations of the carbon cycle including an increase in CO_2 (Beerling 2002a; Whiteside et al. 2010) (Fig. 2.11). The end-Triassic was preceded by a Norian (~216–213 Ma) extinction associated with the large Manicouagan impact (D ~ 100 km; 214 ± 1 Ma) (Table 2.1).

The extinction affected ammonites, which radiated back in the early Jurassic, reef organisms, conodonts and bivalves, as well as a crisis in terrestrial plants (Hallam and Wignall 1997; Keller 2005) (Fig. 2.12). The duration of the extinction is variously estimated as between 50 and 200 kyr (Olsen and Sues 1986). According to Beerling (2002a), depending on the proxy used, CO_2 levels rising from the Rhaetian (~204 Ma) reached about ~1300–2200 from leaf stomata and a wider range from carbon isotopes, just above the Rhaetian-Hettangian (early Jurassic) boundary (Fig. 2.11), signifying an extreme greenhouse event of ~34 % of genera.

2.6 Jurassic-Cretaceous Extinction

The Triassic-Jurassic boundary marks a major faunal mass extinction (Fig. 2.13), but records of accompanying environmental changes are limited. Paleobotanical evidence across the boundary indicates a marked increase in atmospheric CO_2 and associated temperature rise of 3–4 °C. These environmental conditions are calculated to have raised leaf temperatures above a highly conserved lethal limit, perhaps contributing to the >95 % species-level turnover of Triassic-Jurassic megaflora (McElwain et al. 1999).

2.7 K-T (Cretaceous-Tertiary Boundary) Mass Extinction

The K-T boundary (64.98 ± 0.05 Ma) marks the second largest mass extinction of species recorded in Earth history, when some 46 per cent of living genera disappeared (Keller 2005, 2012) (2.1, 2.15, 2.16, 2.17). Alvarez et al. (1980) discovered a hiatus across the Cretaceous-Paleocene boundary in Italy, where a foraminifera-rich white limestone facies containing large-scale *Globotruncana contusa* is abruptly replaced by overlying clay-rich red limestone termed Scaglia rossa containing smaller foraminifera (*Globigerina eugubina*) and micron-scale algal coccoliths (Fig. 2.17). At the classic locality at Gubbio a ~1 cm-thick boundary clay layer consisting of a lower ~5 mm-thick grey clay zone consists of clastic material and an upper ~5 mm-thick red clay zone termed 'fire layer'. This layer contains an Iridium anomaly of up to ~9 ppb and similar relations are observed elsewhere (Figs. 2.15, 2.16, and 2.17). The boundary coincides with a major geomagnetic reversal correlated with a marine magnetic anomaly sequence dated with foraminifera. The parent craters of the K-T event have been identified, including Chicxulub (170 km in diameter, Yucatan Peninsula, Mexico) and Boltysh (~25 km in diameter; 65.17 ± 0.64 Ma, Ukraine). Since the initial discovery of K-T impact ejecta, best preserved in deep water environment, 101 sites have been identified along the Maastrichtian – Danian boundary around the globe (Claeys et al. 2002). Around the Gulf of Mexico and the Atlantic Ocean the ejecta layer coincides with erosion of Maastrichtian sediments and is overlain by clastic sediments and breccia attributable to seismic and tsunami effects.

A panel of 41 international experts from 33 institutions concluded the evidence for a cause and effect relation between asteroid impact and mass extinction at the

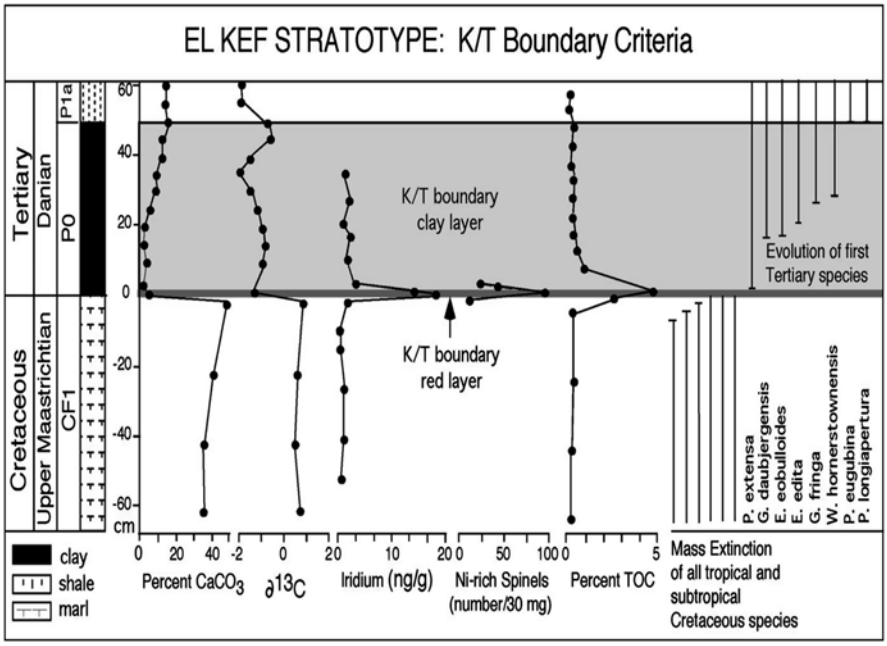

Fig. 2.15 K/T boundary at the El Kef , Tunisia, defined by a dark organic-rich boundary clay with thin red layer at its base (see fig. 2.17) enriched in iridium, nickel rich spinels, pyrite and rare clay spherules, a negative $\delta^{13}C$ excursion, high Total Carbon Contents (TOC) and low $CaCO_3$, and extinction of tropical and subtropical species (Keller 2005; Australian Journal of Earth Science, by permission)

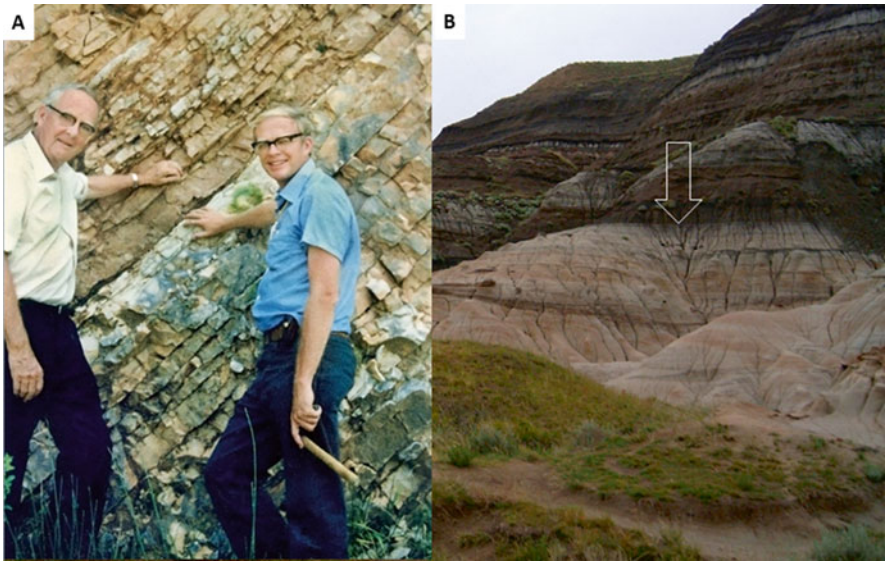

Fig. 2.16 (**a**) Walter and Louis Alvarez at the KT boundary at Gubbio. http://en.wikipedia.org/wiki/Luis_Walter_Alvarez#mediaviewer/File:LWA_with_Walt.JPG; (**b**) the KT boundary near Drumheller, by Glen Larson. Wikipedia Commons. http://commons.wikimedia.org/wiki/File:KT_boundary_054.jpg

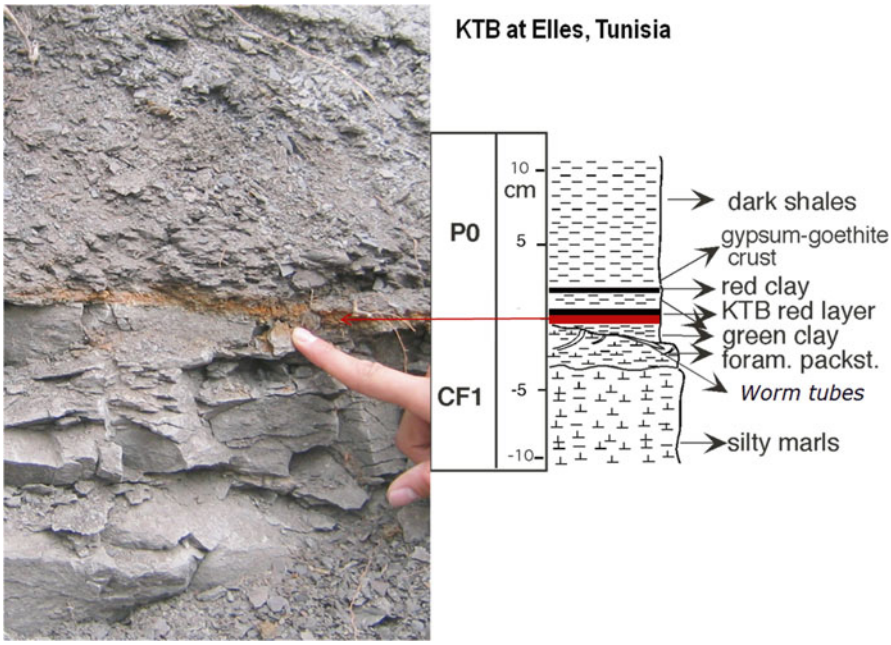

Fig. 2.17 The K/T boundary at Elles, Tunisia (Courtesy G. Keller)

K-T boundary is overwhelming (Schulte et al. 2010). The Chicxulub impact and Boltysh impacts occurred during an active volcanic period which saw continuing eruptions in the Deccan (northwest India) volcanic province recently dated by U-Pb ages (Schoene et al. (2015) to have commenced approximately ~250,000 years before the K-T boundary. The Deccan volcanism produced >1.1 million km^3 of basalt during ~750,000 years, inducing environmental changes preceding the terminal effects of the extraterrestrial bombardment. Stomata leaf pore-based estimates of atmospheric CO_2 during these events indicate an abrupt rise from ~350–500 ppm to at least ~2300 ppm within about 10,000 years, consistent with instantaneous transfer of ~4,600 Gigaton Carbon (GtC) to the atmospheric reservoir. Climate models suggest consequent forcing of 12 Watt/m^2, sufficient to warm the Earth's surface by ~7.5 °C in the absence of counter forcing by sulphate aerosols (Beerling et al. 2002). According to these authors a CO_2 rise of ~1800 ppm and temperature rise occurred over a period of ~10,000 years, namely at rates of ~0.18 ppm/year and 0.00075 °C/year.

Short term effects of the K-T asteroid impact include incineration of large land surfaces from the heat pulse of the incoming projectile, from the explosion and settling of ejecta and microkrystite spherules (Wolbach et al. 1990), ejection of dust and water vapor and oxidation of atmospheric nitrogen and consequent ozone depletion. Longer term effects included release of CO_2 and other greenhouse gases with consequent warming, ocean acidification and anoxia (McCracken et al. 1994; Covey et al. 1997). The K-T mass extinction involved phytoplankton, calcareous

nanoplankton, planktonic foraminifera, benthic foraminifera, 54 % of diatoms, marine invertebrates, crustaceans, ostracods, 98 % of tropical colonial corals, 60 % of late Cretaceous Scleractinia coral, echinoderm, and bivalve genera, numerous species of the molluscan and Cephalopoda and all cephalopod species, belemnoids and ammonoids, 35 % of echinoderm genera, rudists (reef-building clams), inoceramids (giant relatives of modern scallops), jawed fishes, cartilaginous fishes. Survivors included approximately 80 % of the sharks, rays, and skates families. In North America, approximately 57 % of plant species became extinct. All Archaic birds and non-avian dinosaurs became extinct. Cretaceous mammalian lineages, including egg-laying mammals, multi-tuberculates, marsupials and placentals, dryolestoideans, and gondwanatheres survived. Marsupials mostly disappeared from North America and Asian deltatheroidans became extinct. Many of these extinctions constituted proximal instantaneous consequences of the fire ball and asteroid explosion, while distal habitats were affected by more protracted consequences.

2.8 Paleocene-Eocene Extinction

The Paleocene-Eocene thermal maximum (PETM) at ~55.9 Ma involved a release of some ~2000 billion ton carbon (GtC) as methane, elevating atmospheric CO_2 to near-1800 ppm at a rate of 0.18 ppm/year, and mean temperature rise of ~5 °C (Zachos et al. 2008; Panchuk et al. 2008; Cui et al. 2011). Elevated CO_2 led to acidification of ocean water from ~8.2 to ~7.5 pH and the extinction of ~35–50 % of benthic foraminifera during a period of ~1000 years (Zachos et al. 2008). Other consequences included a global expansion of subtropical dinoflagellate plankton, appearance of modern orders of mammals, including primates, a transient dwarfing of mammalian species, and migration of large mammals from Asia to North America.

2.9 The End-Eocene Freeze

The incidence of an asteroid impact cluster about 35.7–35.6 Ma (Popigai, Siberia-~100 km-diameter; Chesapeake Bay, off-shore Virginia – 85 km-diameter; Mount Ashmore, Timor Sea – >50 km-diameter; the related North American strewn tektite field) and the abrupt decline in temperatures about ~33.7–33.5 Ma can be expected to have triggered major environmental and biotic transformations. Abrupt cooling (Pearson et al. 2009) was associated with elimination of warm-water planktonic species (Keller 1986, 2005). Alvarez (2003) and Poag (1997) suggested impact-related extinctions during the late Eocene and the E-O transition, whereas Keller (2005) ruled out impact-triggered extinction. Isotopic $\delta^{13}C$ and $\delta^{18}O$ studies of late Eocene Iridium-rich ejecta layers at Massignano, Italy, indicate increase in temperature and in organic matter associated with the impacts, possibly reflecting release of methane hydrates by impact excavation (Monechi et al. 2000; Bodiselitsch et al. 2004).

Chapter 3
Cenozoic Biological Evolution (by Colin Groves)

Abstract Ancestors of mammals separated from reptiles and birds during the Carboniferous. Early members of the mammalian lineage, called "mammal-like reptiles" as they lack mammalian specializations, flourished during the Permian. Survivors of the Permian-Triassic boundary mass extinction progressively developed mammalian characters. The basic characteristic whereby the Mammalia are defined is the structure of the middle ear. In "reptiles", including mammal-like reptiles, the lower jaw consists of several bones, one of which, the dentary, contains the teeth, another, the articular, forms a joint with a bone called the quadrate in the cranium, and there is only a single bone, the stapes, in the middle ear. Through the Miocene and Pliocene, mammalian lineages seem to have undergone diversification and extinction at rates that had characterised most of the Cenozoic. It was only the Pleistocene that saw elevated extinction rates, mainly affecting large mammals. The human lineage may have separated from that of chimpanzees some 6–7 million years ago, but about 4 million years ago there was an episode of interbreeding between the two lineages, leaving humans with an X chromosome that is markedly more chimpanzee-like than the rest of the genome. Comparative morphology and DNA analysis agree chimpanzeesare the closest living relatives of humans, followed by gorillas, then orangutans and then gibbons. Most molecular clock calculations indicate that the human and chimpanzee lineages separated some 6 million years ago. *Sahelanthropus tchadensis* is plausibly promoted as the earliest member of the Hominini.

3.1 The Evolution of Mammals

The dinosaurs ruled the earth in the Jurassic and Cretaceous, then an asteroid hit the earth and wiped them out, and we started the Age of Mammals. So goes the story: is it true? It is in a way, but it is much more complicated than that. First, it is necessary to appreciate that Jurassic and, especially, Cretaceous mammals were abundant: they were poorly known until about the middle of the twentieth century, partly because their fossils, smaller and less spectacular than those of the dinosaurs and the other giant reptiles, were probably missed during many excavations, and partly because they really do seem to have been rarer than other groups of land vertebrates.

A.Y. Glikson, C. Groves, *Climate, Fire and Human Evolution*, Modern Approaches in Solid Earth Sciences 10, DOI 10.1007/978-3-319-22512-8_3

Secondly, the end-Triassic Mass Extinction also seems to have played its part. And thirdly, there is a lively controversy about when the modern mammalian orders began to separate and diversify. The ancestors of mammals separated from those of reptiles and birds during the Carboniferous. Because they lack mammalian specializations, these early members of the mammalian lineage have commonly been called "mammal-like reptiles". They flourished during the Permian, and those which survived the massive end-Permian Mass Extinction progressively developed mammalian character.

The basic character whereby the Mammalia are defined is the structure of the middle ear. In "reptiles", including mammal-like reptiles, the lower jaw consists of several bones, one of which, the dentary, contains the teeth, another, the articular, forms a joint with a bone called the quadrate in the cranium, and there is only a single bone, the stapes, in the middle ear. Whereas in mammals the lower jaw consists of the dentary alone, which forms its own joint with the squamosal bone of the cranium, and there are no articular or quadrate, while there are three bones in the middle ear, the malleus and incus as well as the stapes. In mammalian embryos, there is a strut along the inner (lingual) side of the mandible called Meckel's Cartilage, and the articular bone is the posterior end of it, together with a semicircular bone called the angular; the articular becomes part of the middle ear as the malleus, and it and the incus become surrounded by the angular, which develops into the tympanic bone.

If, as late nineteenth century evolutionary theory claimed, "ontogeny recapitulates phylogeny" (broadly speaking, an embryo climbs up its family tree as it develops), we should expect to see fossils at the reptile-mammal transition which have an ossified Meckel's Cartilage and demonstrate the articular and quadrate becoming the malleus and incus, the angular becoming the tympanic, and the dentary at the same time developing a joint with the squamosal. And this is indeed what we do see: fossils like *Morganucodon*, from the earliest Jurassic, have an ossified Meckel's Cartilage and have both the old, "reptilian" quadrate-articular joint and a new, mammal-style dentary-squamosal joint (because they have this new joint, they are classified as mammals), and quite a number of Jurassic fossils demonstrate the articular detaching from the ossified Meckel's Cartilage and disappearing into the middle ear and the angular surrounding the middle ear, and becoming the tympanic. If this sounds odd – large jawbones becoming tiny ear ossicles, and the period in which there were two joints between the lower jaw in the cranium – it is worth emphasizing that the fossil record is very clear about this, and the latest evidence even suggests that it may have happened twice, independently (Bi et al. 2014)! Mammals with an ossified Meckel's Cartilage are still found in the early Cretaceous, even though the malleus had long since detached from it and was already incorporated into the middle ear (Wang et al. 2001).

All this began to happen after the end-Triassic Mass Extinction. It is difficult to say whether this timing is relevant or coincidental. Living mammals are divided into Prototheria and Theria. The Prototheria are the monotremes: the platypus and echidna, today confined to Australia and New Guinea, but Palaeocene monotreme

fossils are known also from South America. They differ from all other mammals in that they lay eggs, they lack nipples but secrete milk for the young, and they retain many bones in the skeleton which have been lost (typically by fusing with other bones) in the Theria. The Prototheria have a sparse fossil record; earliest representatives are known from the Middle Jurassic. The separation between platypus and echidna, however, is not very old, probably Oligocene (Phillips et al. 2009).

As the Prototheria and Theria are, in biological jargon, "sister groups", they must have arisen from a common ancestor, and this plausibly lived in the Early Jurassic (Luo 2007). Most of the very numerous Jurassic and Cretaceous fossil mammals are thought by Zhe-Xi Luo to be more closely related to the Theria, but it was not until the early Cretaceous that the last common ancestor of the two modern groups of Theria, the Eutheria (placental mammals) and Metatheria (marsupials), lived.

Three hypotheses of the origin of modern placental mammal orders have been proposed: "explosive", "long fuse" and "short fuse". According to the "explosive" hypothesis, the Eutheria may have separated from the Metatheria in the Early or Middle Cretaceous, but it was only after the Mass Extinction of the K/T boundary that the modern orders began to diverge from each other. In the "long fuse" hypothesis, the orders of placental mammals diverged well back in the Cretaceous, and it was the divisions within the orders that diversified after the K/T boundary. The "short fuse" hypothesis maintains that not only did the orders of Eutheria diverge well back within the Cretaceous, but the divisions within them also diverged within the Cretaceous. Thus, in two of these models, the end-Cretaceous Mass Extinction clears the way for the survivors – in this case, the placental mammals – to undergo an adaptive radiation and fill the ecological niches that had been left vacant by those land animals that had become extinct.

Ji et al. (2002) described the Middle Cretaceous (about 125 Ma) *Eomaia*, from Liaoning Province, northern China, as "the earliest known eutherian mammal", but some of the describers of that fossil later revised their opinion: Wible et al. (2007) did not consider *Eomaia* to be a eutherian, describing *Maelestes*, from the Late Cretaceous (75–71 Ma) of Mongolia, as the earliest member of the *Eutheria*, and Luo (2007) concurred. Both sets of analysis reject any known Mesozoic mammal as belonging to any of the living mammalian orders; they thus support the "explosive" model, as both of the other models require long "ghost lineages" (lineages not supported by any fossils) (There has been less discussion about the origin of the orders of marsupials, but probably they also diversified around the K/T boundary). Meanwhile Bininda-Emonds et al. (2007), using supertree methodology, supported the "long-fuse" model. Later, some of the Chinese and American palaeontologists who had described *Eomaia* and *Maelestes* revised their opinion yet again, after the discovery of *Juramaia*, also from Liaoning, from the Middle-Late Jurassic, dated at 160.7 ± 0.4 Ma, which they interpreted to be the earliest member of the Eutheria, and they dated the initial diversification of both placentals and marsupials to around 100 million years ago, i.e. supporting the "short-fuse" hypothesis (Luo et al. 2011). More recently a study based on both molecular and morphological data once again supported the "explosive" model (O'Leary et al. 2013).

It is still unclear which model of mammalian evolution applies; the "molecular clock" seems to support the short-fuse model, but the fact remains that there are no fossils in the Cretaceous, let alone the Jurassic, that can be argued to belong to any of the living orders of either placentals or marsupials. Although "absence of evidence is not evidence of absence", one really would have thought that fossils of the living orders would have begun to turn up by now if they really existed.

During the Late Cretaceous, the continents were divided into Laurasia (Northern) and Gondwana (southern), but by the end of the Cretaceous Gondwana had already begun to split up: Africa, India and Madagascar were drifting north, whereas South America, Antarctica and Australasia still formed a single land mass. Most of the modern orders are known from the Palaeocene, and their relationships reflect the prevailing geography. The placentals are divided into Afrotheria (elephants, hyrax, "elephant shrews", aardvark) originating in Africa, Boreoeutheria (rodents, primates, shrews, hedgehogs, bats, carnivores, perissodactyls, artiodactyls) originating in Laurasia, and Xenarthra (sloths, armadillos, anteaters) in South America. Meantime the marsupials were spread through Australasia and South America, and some Palaeocene fossils are known from Antarctica; and what we know of the monotremes indicates that in the Palaeocene they occurred in South America as well as Australasia. Marsupials and the placental order Xenarthra thus shared South America.

The Palaeocene fossil placentals include members of our own order, Primates. The division between the two living suborders, Strepsirrhini (lemurs and lorises) and Haplorrhini (tarsiers, monkeys, apes and humans), dates to the Eocene, but a few sparse fossils suggest that may have begun during the Palaeocene; nonetheless, all the well-represented Palaeocene primates belong to extinct families, mostly already highly specialised and placed in a separate suborder, Plesiadapiformes. During the Eocene, both Strepsirrhini and Haplorrhini diversified enormously, spreading through North America, northern Eurasia and North Africa. Among the Haplorrhini, a few Eocene fossils are recognisable as primitive tarsiers, the sister-group of the anthropoids, restricted today to island Southeast Asia; and it is around the Early/Middle Eocene, in Algeria, that the first definitive anthropoids, *Algeripithecus* and *Tabelia*, are known, and from the Middle Eocene fissure deposits in China come fossils of the tiny (67–137 g) basal anthropoid *Eosimias*.

During the Late Eocene and Early Oligocene there was a major diversification of anthropoids, known from both Southeast Asia (Burma, Thailand) and North Africa/Middle East (Egypt, Oman), and these include the earliest known Catarrhines (the group that includes the living Old World monkeys and the Hominoidea, i.e. apes and humans), one of which, *Aegyptopithecus*, from 33.1 to 33.4 Ma deposits in the Faiyûm, Egypt, is known from several skulls and most parts of the skeleton, and is a good candidate for an early common ancestor of Old World monkeys, hominoids, and a variety of "sidelines", some of which survived until the late Middle Miocene in both Africa and Europe.

The Old World monkeys (Cercopithecoidea: baboons, macaques, guenons, langurs, colobus, the monkeys of Africa and Asia) are easy to recognise as fossils by their highly specialised molar and premolar teeth, whereas the Hominoidea have more

primitive dentition but more specialised postcranial skeleton. Remains of each are known from as early as 19–20 Ma in East Africa, and they both rapidly spread to Asia and Europe; at first, the *hominoids* appear to have been commoner, but with time they dwindled, while the cercopithecoids became both more diverse and more abundant. Sivapithecus, the earliest identified ancestor of the modern orangutan, is first known from the Siwalik Hills of north-western India and Pakistan at about 12.5 Ma, and the orangutan lineage underwent a minor radiation in the latest Miocene in mainland Southeast Asia and southern China. In Africa, the poorly known Chororapithecus from Ethiopia, dated at 10.5 Ma, has been proposed as an ancestor to the gorilla, but the evidence is not good, and some broken teeth from Lukeino at about 6 Ma seem so far to be the only fossils definitely attributable to the gorilla lineage. It is even worse for the chimpanzee, for which no fossil ancestors are known until a handful of teeth from Kenya dated at ±250 ka.

The other orders of placental mammals likewise began to diversify during the Eocene. In the Late Eocene and Early Oligocene some lineages underwent an enormous increase in size; in particular, the order Perissodactyla, today represented by horses, tapirs and rhinos, included several gigantic forms. The North American and Asian family Brontotheriidae, characterised by having a bifurcated bony horn like protrusion on the snout, rapidly developed into giants, as much as 2.5 m in height; they disappeared in the Oligocene, about 34 Ma. Even larger forms were the hornless rhinos of the family Indricotheriidae, among which Paraceratherium, from the Oligocene, 34–23 Ma, of central Asia, reached a height of 6 m and was as far as we know the largest land mammal that ever existed.

One of the most remarkable advances in understanding of mammalian evolution began with the discovery, in the 1990s, that the closest relatives of cetaceans (whales and dolphins) are, according to genetic data, hippos. The fossil record of the hippopotamus lineage is, until the Late Miocene, extremely poor, but their probable ancestors, known as anthracotheres, are known as far back as the Middle Eocene. Until the 1990s, nothing was known of the evolution of cetaceans from land mammals; but the exploration of mainly Middle Eocene deposits in Pakistan and Northwest India has uncovered an almost complete lineage from the small semiterrestrial Pakicetus, 50 Ma, via Ambulocetus, the remingtonocetids, and the protocetids, to Basilosaurus, the earliest fully aquatic whale, at 42 Ma. The story of how whales became whales, in such an astonishingly short period of time in the middle of the Eocene, is told by Thewissen (2014).

As the Cenozoic progressed, marsupial and placental mammals became recognisably modern in general appearance. 25 Ma levels at the site of Riversleigh in North Queensland, for example, has yielded fossils representing almost all modern families of Australasian marsupials; and modern placental families arose around the same time.

Through the Miocene and Pliocene, mammalian lineages seem to have undergone diversification and extinction at rates that had characterised most of the Cenozoic. It was only the Pleistocene that saw elevated extinction rates, mainly affecting large mammals.

These extinctions began in Africa. *Loxodonta atlantica* disappeared in the Middle Pleistocene, perhaps around 400 ka, and *Elephas recki* about the same time, although a descendant species *Elephas iolensis* persisted in far northern and far southern Africa until the end of the Pleistocene (Sanders et al. 2010). The giant buffalo *Syncerus antiquus* survived until after 18 kyr in East Africa, until the early Holocene in South Africa, and until after 4000 kyr in North Africa (Gentry 2010). Two species of springbok, *Antidorcas bondi* and *A.australis*, survived in South Africa until the early Holocene (note that there is some question about their validity, according to Gentry 2010). A species of Hippotragini went extinct during this period, *Parmularius angusticornis* during the Middle Pleistocene; and the alcelaphines *Damaliscus niro, D.hypsodon, and Rusingoryx atopocranion* in the Late Pleistocene (Gentry 2010; Faith et al. 2011, 2012, 2014), while a large species of alcelaphine, *Megalotragus priscus*, survived in South Africa until perhaps 7500 BP (Gentry 2010). The giant hippopotamus *Hippopotamus gorgops* survived well into the Middle Pleistocene in South and East Africa (Weston and Boisserie 2010). *Theropithecus oswaldi*, known as early as 2 Ma, survived until 250 kyr in Kenya. (Jablonski and Frost 2010).

When we look at the pattern of these extinctions, we find them more or less clustered into two periods: the middle Middle Pleistocene, and the Pleistocene/Holocene boundary. What we see elsewhere in the Old World tropics (India, Sri Lanka, Southeast Asia, even the Levant) seems consistent with this, with perhaps fewer terminal Pleistocene extinctions – that is to say, from the late Middle Pleistocene until the present day we find an essential continuity of the mammalian fauna (Roberts et al. 2014). Indeed, Africa, at least as far as the terminal Pleistocene is concerned, actually shows a higher faunal turnover than other parts of the tropical Old World, and one wonders whether this is simply due to the complete or local disappearance of certain habitats (as suggested by Faith et al. 2011) – or does it relate to an increased impact of human activity?

In East Asia, Pleistocene faunal turnovers have been recently documented by Jin et al. (2014). Species like the ancestral giant panda *Ailuropoda microta* replaced the earliest Pleistocene mammals around 1.8 Ma, and were themselves replaced by larger descendant species from about 1.2 Ma, and these in turn were replaced by their own still larger descendant species from about 0.8 Ma; one of the species that increased in size, along with giant pandas and the elephant-like *Stegodon*, was the giant ape *Gigantopithecus blacki*, the largest primate that ever lived (as far as we know!). Early humans and primitive orangutans, both known only by their teeth, lived alongside these giants, but *Gigantopithecus* was last recorded in a cave in Vietnam at 475,000 Ma.

Global temperatures began to drop markedly from the Late Pliocene, and the 41 ka periodicity of the temperature fluctuations gave way around 900 ka to 100 ka periodicity; at the same time, the Tibetan Highlands were beginning to rise. As a consequence of these changes, a cold arid steppe fauna and a separate arid tundra fauna began to differentiate, and by about 460 ka the two zones coalesced into a circumpolar steppe-tundra biome, characterised by such fauna as mammoth, woolly rhinoceros, muskox, reindeer, saiga antelope, wild horse, Arctic Fox, cave lion, and

cheetah (Kahlke 2014). The collapse of the steppe-tundra biome at the end of the Pleistocene resulted in the extinction of some of these characteristic species (mammoth, woolly rhino, cave lion) and a drastic range shrinkage of most of the others.

So, even without this talking about major extinction periods, species have become extinct, either individually or in groups, throughout the Cenozoic, especially throughout the Middle and Late Pleistocene (although of course, we know more about the later Pleistocene because we can examine the record in finer detail than earlier records). Species become extinct because their habitats disappear – perhaps only locally, but, by implication, they are unable to migrate to similar habitats elsewhere. They become extinct because competitors spread into their habitats, and do things slightly better. And they become extinct because they get over-exploited by their predators, especially human beings. It is very difficult to disentangle different effects in the major tropical continental faunas, but when we look at what happened when people entered new regions for the first time, we may get a clue. When people first entered Australia, the larger indigenous mammalian species (the so-called Megafauna) crumbled before them. The same occurred in North America, and apparently also in South America. The same occurred on once isolated islands: Madagascar, Fiji, New Zealand, for example. It is simply human nature: people find a rich new resource, and act as if there is no tomorrow (Flannery 1994). This in turn suggests that humans might have had a hand in the demise of the Eurasian steppe-tundra Megafauna, as they gradually became more tolerant of the aridity and bitter cold towards the end of the Pleistocene, and might even suggest that technological advances in Africa around the same time could have resulted in the local extinctions that occurred there. All this does not exclude the likelihood that "natural" factors like climatic fluctuations could have constricted the ranges of some species, making them more vulnerable to human impacts.

What does this mean for the future? As recently discussed by Blois and Hadly (2009), community structure lends considerable stability to the persistence of mammalian species, but what we are beginning to see under the present climate change regime is something more extreme and more rapid than documented in the fossil record. Besides this, the persistence of a species in the face of climate change depends on the persistence of the sort of habitat to which it is adapted, even though the distribution of that habitat may move back and forth: but the human population in recent times has expanded to an unprecedented degree, cutting off potential "escape routes", which might have allowed habitats to track the changing climate. Even if they do not finish off many species simply by hunting.

3.2 From Primates to Humans

The story of human evolution has been told and retold. Two very thorough recent sources are Cartmill and Smith (2009) and Stringer and Andrews (2011). The human lineage may have separated from that of chimpanzees some 6–7 million years ago, but about 4 million years ago there was an episode of interbreeding

between the two lineages, leaving humans with an X chromosome that is markedly more chimpanzee-like than the rest of the genome. We simply don't know what phase of the human fossil record may document this brief, unexpected togetherness.

Sahelanthropus tchadensis is plausibly promoted as the earliest member of the Hominini (of the human clade), at somewhat more than 6 million years ago, a date which unfortunately is rather poorly substantiated; this is because the site where it was found (in Chad, west-central Africa) is geologically stable, and one must try to link associated mammalian fossils with those from datable sites in East Africa, and because its stratigraphy at that site is unclear. It is represented mainly by a complete but distorted cranium, although there are mandibular and other fragments. The facial skeleton appears rather short, but sits below an enormous, continuous supraorbital torus (brow ridge). The cranial capacity is estimated at 320–380 cc, within the chimpanzee range. Canines seem short; the palate is rectangular; the foramen magnum (the holes through which the spinal cord enters the cranium) appears to be further forward than in chimpanzees, suggesting that the skull could have been balanced on top of an upright vertical column – i.e., it may have stood and moved upright. Contemporary or slightly later, at about 6 million years ago, is *Orrorin tugenensis* from central Kenya; it is difficult to compare this with *Sahelanthropus* because the best preserved parts are femora, which do however tell us that it potentially stood and walked upright. The near-contemporary Ethiopian *Ardipithecus kadabba* is again represented by non-comparable parts, and may be the same animal as one or both of the others. A later fossil, *Ardipithecus ramidus*, also from Ethiopia, is known by one complete and one partial skeleton and numerous "scraps"; unfortunately, its interpretation is in many respects controversial, although biped it certainly was.

From some 4 Ma onwards we enter the age of the "australopithecines". This term is given to any member of the Hominini that is not customarily classed as *Homo* (Fig. 3.1), and so has a weak heuristic value, not a taxonomic one, despite its central genus, *Australopithecus*, being customarily misused as if it were of taxonomic value. *Australopithecus anamensis*, from 3.9 to 4.2 Ma in northern Kenya, is known from jaws and limb bones. Far better known, from sites in Ethiopia, Kenya and Tanzania, is *Australopithecus afarensis*, which lasted with little change from 3.75 to 3.00 Ma; the cranial capacity was 350 to 500 cc, combined with prognathism (jutting jaws), large cheekteeth, canines only slightly larger than those of humans, and adaptations for upright posture and gait: flaring pelvis, shortened lumbar spine, valgus knee. It is controversial whether the species also was a capable climber.

Recent analysis (Su and Harrison 2015) suggests that *Australopithecus afarensis* was capable of subsisting in quite a wide variety of environments. At Laetoli in Tanzania, dated to about 3.6–3.85 Ma, representatives of the species lived in a very dry environment dotted with shrubby thickets and some open woodland, with some gallery forest around the small and seasonal streams, in contrast to the contemporary population at Woranso-Mille in Ethiopia which lived in more dense woodland with some grassy areas, with permanent water nearby. At the later sites of Hadar Maka and Dikika in Ethiopia, and Koobi Fora in Kenya, dating approximately to between 3 and 3.4 Ma, populations of th e same species lived in comparatively well-watered environments with woodland mixed with edaphic grassland.

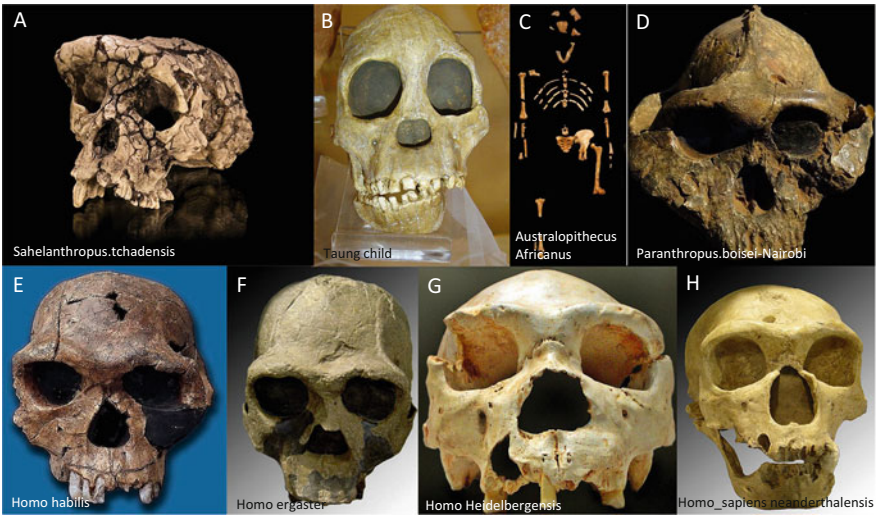

Fig. 3.1 Cranium of (**a**) *Sahelanthropus.tchadensis* (http://en.wikipedia.org/wiki/File:*Sahelanthropus_tchadensis*_-_TM_266-01-060-1.jpg), (**b**) Taung Child (http://en.wikipedia.org/wiki/Taung_Child), (**c**) skelleton of *Australopithecus afarensis* (Lucy) (http://en.wikipedia.org/wiki/File:Lucy_blackbg.jpg); (**d**) cranium of *Paranthropus boisei*-Nairobi (http://en.wikipedia.org/wiki/File:Paranthropus boisei-Nairobi.JPG); (**e**) cranium of *Homo habilis* (http://en.wikipedia.org/wiki/Homo_habilis); (**f**) cranium of *Homo ergaster* (http://en.wikipedia.org/wiki/Homo_ergaster); (**g**) cranium of *Homo heidelbergensis* (http://en.wikipedia.org/wiki/File:Homo_heidelbergensis-Cranium); (**h**) cranium of *Homo sapiens-neanderthalis* (http://en.wikipedia.org/wiki/File:Homo_sapiens_neanderthalensis.jpg) (Wikipedia/Creative Commons)

The odd, flat-faced *Kenyanthropus platyops* is known from a single site, in Kenya, a rare contemporary of *A.afarensis*. In Chad, a related species, *Australopithecus bahrelghazali*, lived at a similar time. Between 2 and 2.5 Ma another species, *Australopithecus africanus*, is known from plentiful material from Sterkfontein and elsewhere in South Africa. The so-called "robust australopithecines", assigned to separate genus *Paranthropus*, had shortened jaws with a combination of huge premolars and molars with tiny incisors and canines, an evident specialisation for heavy (especially hypogeous) vegetation. They outlived the other australopithecines and were found alongside early *Homo* in East African sites (Koobi Fora, Omo, Olduvai) as well as in the South African caves of Swartkrans and Kromdraai, all of them dated between 2 and 1 Ma.

The origin of *Homo* has been much debated, although, truth to tell, there are some fossils that are hard to allocate to one or the other. The poorly known *Australopithecus garhi*, from 2.5 Ma in Ethiopia, has been proposed as transitional to early *Homo*, but its enormous molars would seem to rule it out. The late South African *Australopithecus sediba* has some claimed "advanced" characters, but is not likely to be ancestral to *Homo* (its date is 1.977 ± 0.002 Ma). One of the Sterkfontein fossils has also been supposed to be early *Homo*, rather than *Australopithecus*, and this may be plausible, but the recent discovery of the Ledi-Geraru jaw indicates that the origin of our genus was quite far back.

The earliest site containing a fossil (a hemimandible) with characters of *Homo*, Ledi-Geraru in the Afar Triangle of Ethiopia (2.80–2.75 Ma), indicates a more open, arid habitat (DiMaggio et al. 2015). This is of course strongly consistent with the hypothesis first laid out in detail by Potts (2012): in regions like Lake Turkana, in far northern Kenya, perhaps the world's pre-eminent source of fossils documenting human evolution, the lake rose and fell, the climate switched from wet to dry, and still *Homo* was there – what characterised *Homo* was above all an ability to cope with extreme climatic variability. This "climatic pulse" hypothesis has been recounted in detail by Maslin et al. (2014).

At least three species of early *Homo* occurred in East Africa from a little over 2 million years ago, and it is very interesting that at the same date comes the first appearance of an Indian Ocean species of stingray: that is to say, Lake Turkana was connected to the Indian Ocean, with all that implies for climate and geography.

The three species were: First, the long-faced but large-brained (750 cc) *Homo rudolfensis*, known from only this time frame. The type specimen of *Homo rudolfensis*, the cranium ER 1470, is now dated cleanly at 2.058 ± 0.034 Ma. Other known fossils of the species (ER 62000, 1801 1482), as well as an enigmatic jaw, ER 1802, at one time ascribed to the species but recently (Spoor et al. 2015) removed from it, have been shown to date between 2.058 ± 0.034 and 1.945 ± 0.004 Ma, except for ER 60000 which is slightly younger at 1.78–1.87 Ma (Joordens et al. 2013). This was, in its known parts (only skulls), quite unlike other species of *Homo* – indeed, there is a school of thought that argues that it is descended from *Kenyanthropus*.

The smaller *Homo habilis* (Fig. 3.1e), which according to the latest data (Spoor et al. 2015) may have had an equally large brain, lasted until some 1.4 Ma. Before the relative dating was sorted out, this species appeared to be earlier in time than *H. ergaster* (Fig. 3.1f), and potentially ancestral to it; but the evidence is now clear that, from their first appearances, they lived side by side for at least half a million years.

Finally *Homo ergaster* (Fig. 3.1f) with a somewhat larger cranial capacity (800–900 cc) and skeleton indicating a near-modern striding gait, was plausibly a "main line ancestor". The oldest postcrania ascribed to *Homo ergaster* (Fig. 3.1f) are femur ER 1481 (slightly $> 1.945 \pm 0.004$) and innominate ER 3228 (1.92 Ma), and there are some skull fragments of this same general age (Joordens et al. 2011, 2013), but the species is best known from a complete cranium, two incomplete crania, and several mandibles from Koobi Fora (1.7–14 Ma), the nearly complete skeleton of a boy from Nariokotome, west of Lake Trukana (1.5 Ma), a huge calvaria from Olduvai in Tanzania (about 1.4 Ma, but uncertain), and calvariae from Daka in Ethiopia and Olorgesailie in Kenya (both about 1 Ma). What the disparity of sizes seems to indicate is that this, our presumed ancestor, was strongly sexually dimorphic, the remains of males being much rarer than those of females – which is comprehensible given that other sexually dimorphic mammals (including primates, such as the gorilla) tend to live in "harems", or one-male groups.

Although all known hominins were evidently efficient bipeds, when comparing the two most complete fossil skeletons, it is clear that KNM-WT 15,000, *Homo ergaster* (Fig. 3.1f), was a much more efficient long-distance bipedal walker than AL288, the *Australopithecus afarensis* skeleton nicknamed "Lucy" (Wang et al. 2004).

Yet all is not clear about these three species. The crania are distinct, but questions such as which are their respective postcranial remains, and even, in some cases, which mandible belongs to which species, are still mostly unresolved.

Using strontium isotope ratios of fossil fish, Joordens et al. (2011) were able to place important hominin fossils from the Lake Turkana region in their climatic context, showing that between about 2 and 1.85 Ma the Omo River flowed continuously with fluctuations of no more than 5–10 % such that the region was continuously well-watered, lacking the droughts that characterised other regions of the Eastern Rift such as Olduvai and Olorgesailie, so that it could have acted as a refuge area. This means either that the three species, *Paranthropus boisei* (Fig. 3.1d), *H. habilis* (Fig. 3.1e) and *H. ergaster* (Fig. 3.1f) whose ranges encompassed all these sites, were adapted to high environmental variability, or else that they were adapted to somewhat different climatic regimes, their ranges moving back and forth according to the prevailing environment – possibly they never even encountered one another.

Early hominins spread their range outside Africa at a surprisingly early date. The remarkable finds from Dmanisi, in Georgia, date to 1.75 Ma; they represent something different from any of the African fossils, somewhat intermediate between *H. habilis* (Fig. 3.1e) and *H. ergaster* (Fig. 3.1f). A separate species, *Homo georgicus*, has been proposed for this population.

At very little later, hominin remains occur in both Java and China. The Javanese species, *Homo erectus*, which goes back to about 1.6 Ma (though this is controversial), had enormous brow ridges, nearly continuous from side to side, and very low, flat, angular braincases. The first specimen was discovered in 1891, and it is understandable that all subsequent fossils from this general period have been compared with the species, although actually calling *Homo ergaster* "African *Homo erectus*" is incorrect (given that the two species do actually differ consistently), not to mention unhelpful from many points of view; for example, from Java we know only a few femora, mostly fragmentary, and it is simply wrong to refer to "the *Homo erectus* skeleton" (referring to the Turkana Boy) when we know almost nothing about the general skeleton of the real *Homo erectus.*

What we do know about *Homo erectus* is that it persisted in Java, with minimal change, until under 500 ka: an example of evolutionary stasis recalling that shown by *Australopithecus afarensis* much earlier. The earlier specimens, >1 Ma, have a cranial capacity of about 900 cc; the later ones, about 1150 cc. Then the species disappeared: whether it was out-competed by a newcomer (perhaps even *Homo sapiens*, if *H. erectus* persisted that long as some still think), or simply died out naturally.

The earliest fossil from China is from Gognwangling and has recently been dated to 1.63 Ma. It consists of a very low, flat calvaria, reminiscent of some of the Dmanisi skulls. Much better known are the series (6 calvariae, plus numerous fragments of facial skeletons, jaws and postcranial bones) from Zhoukoudian, near Beijing, well-known as "Peking Man". They show consistent differences from all other samples, and have been placed in a separate species, *Homo peklinensis* (as with the African and Georgian fossils, it is incorrect and unhelpful to refer them to *Homo erectus* as has all too frequently been done).

As the Middle Pleistocene record of Africa and Europe becomes better known, it seems evident that the descendants of *Homo ergaste*r (Fig. 3.1f) spread to both continents, evolving into a larger-brained species, *Homo heidelbergensis* (Fig. 3.1g). The earliest specimen of this species is the 600 ka cranium from Bodo, Ethiopia. Some half million years ago the populations of the two continents became separate; the European/West Asian branch evolved into the stocky, big-brained Neandertals (*Homo neanderthalensis*) (Fig. 3.1h), and the African branch into *Homo sapiens*. There appears to have been first a *H. heidelbergensis* then a proto-Neanderthal dispersal as far east as China; specimens from Dali and Jinniushan (both dated rather vaguely to Middle Pleistocene) fall within the range of *H. heidelbergensis* (Fig. 3.1g), while the partial cranium from Maba, as well as one from Hathnora in India, resemble – but are not identical to – *Homo neanderthalensis*, which otherwise is known from Europe, the Middle East, Central Asia, and western Siberia.

The earliest specimens identifiable as *Homo sapiens* are from Florisbad in South Africa and Guomde in Kenya, both about 260 ka; until about 60 ka, all fossils of our own species are in Africa, then there was a dispersal, via Sinai or southern Arabia or both, into tropical Asia and Australia, then northwest into Europe, and into the Americas only towards the end of the Pleistocene.

DNA, both mt and nDNA, has been extracted from Neandertal remains, and the curious finding is that modern non-African *Homo sapiens* people are 4 % closer to Neandertals than are Africans, strongly implying that, when modern humans moved through the Middle East, they intrebred (to a very limited extent) with the Neandertals that already lived there. But there is a further wrinkle: in Denisova cave, in the Altai Mountains of western Siberia, dating to about 41 ka, a molar tooth and a finger bone have been discovered whose DNA is unlike either modern humans or Neandertals, but somewhat closer to the latter (We have no better fossils of this hitherto unknown population – perhaps Maba could be one of them?). The nDNA of modern Australomelanesian people is slightly closer to Denisovans than are other modern peoples', implying that there had been a slight degree of interbreeding. We know nothing definitive about the Denisovans except for that one finger and that one tooth from western Siberia, but since people of Australomelanesian affinity still live in parts of Southeast Asia, it does imply that Denisovans were widespread through eastern Asia by the time modern humans were spreading through that region.

Fossils dating as late as 14.5–11.5 ka were found in two sites, Maludong (Red Deer Cave) and Longlin, in southwestern China (Curnoe et al. 2012). They are not precisely *Homo sapiens*, yet they do most closely resemble modern humans, but have some unique features, and their discoverers have suggested that they could be the enigmatic Denisovans or, perhaps more likely given their *Homo sapiens* overall morphology, hybrids between Denisovans and modern humans.

The idea that modern humans, during their spread out of Africa, not only met and displaced their non-modern predecessors but even to a small extent interbred with them, surprises some people. Yet we know from DNA studies that hybridisation between different species other than primates has occurred frequently; this simply reminds us that humans, too, are animals.

But one other species is known to have been present where *Homo sapiens* was spreading. This is the notorious "Hobbit", *Homo floresiensis*, known from a complete skeleton and other remains from Liang Bua, a cave in Flores, southeastern Indonesia. The remains are reported to be from about 17–95 ka. The species was diminutive, of the order of 1 m tall, with a cranial capacity (in the one known skull) of 428 cc; the features of cranium, mandible and postcranial skeleton recall *Homo habilis* (Fig. 3.1e) or *australopithecines* (Fig. 3.1c), although it has also been argued that the species was descended from *Homo erectus*, dwarfed through long isolation on a relatively small island. A few authors, have maintained that either the type specimen (the complete skeleton) or the whole series actually consist of pathological modern humans: microcephalic dwarves, cretins, or sufferers from Down's Syndrome. One recalls that, ever since the early days of palaeoanthropology, "denialists" have sought to get rid of Neandertal, *Homo erectus*, Australopithecus africanus and other important fossils in just such a fashion.

3.3 From Genetic Evolution to Cultural Evolution

Both comparative morphology and DNA analysis agree that chimpanzees are our closest living relatives, followed by gorillas, followed by orangutans, then gibbons, the Old World monkeys – and so on. Most molecular clock calculations indicate that the human and chimpanzee lineages separated some 6 million years ago.

One must remember that we are not descended from chimpanzees – we and they diverged from a common ancestor. So it is not likely that the chimpanzee mind is not simply the human mind "writ small": they are likely to have different cognitive skills. We are only just beginning to learn about this, but Matsuzawa (2012 and elsewhere) has shown that chimpanzees' working memory is strikingly superior to humans, which may be connected to their need for instant decision-making in the natural habitat. A comparative study of detailed aspects of the cognition of chimpanzees, gorillas and orangutans would be very revealing; mental characteristics in common between, for example, chimps and gorillas are likely to have been present in the chimp-human last common ancestor.

There seems to be a definite hiatus between great ape cognition and that of monkeys, gibbons and other primates. In acknowledging this, we must at the same time acknowledge that there is a hiatus between human cognition and that of (other) apes (The Gap: Suddendorf 2012). The very mention of the Metamind of great apes implies to some that chimpanzees, gorillas and orangutans can do everything that humans can do: nonsense, of course, but it does remind us that we did not evolve our special human cognition from a standing start, so to speak: (other) great apes are already some way there. It is our task to deduce how much further we had to go – and perhaps why.

Tool-making is by now well known throughout the wide African range of chimpanzees, and different tool-use and tool-making traditions have become characteristic of different populations – "culture areas", in a limited sense (these are not

restricted to tools, but apply to differential behaviour patterns in general). Mainly, tools are of wood (e.g. for digging), grass stems (especially for termiting), leaves (to make "sponges" to get water from tree holes), and other vegetable material. In West Africa, however, stones are used to crack certain nuts, one being the anvil, another the hammer, and it has been found that, in one locality at least (Bossou, in Guinea), each individual has his or her preferred anvil stone; and archaeological excavation of a modern nut-cracking site has found that this activity has been going on there for at least 500 years. Strikingly, stone, in contrast to vegetable material, is not modified by chimpanzees; humans may no longer be the only toolmaker, but seem still to be the only stone-toolmaker. What, one asks, is the cognitive significance of this gap?

It has been found that transmission of basic tool-making skills is much better with teaching, especially with language, than with simple imitation (Morgan et al. 2015). While apes do plan, it is for only the short-term future – for example, bringing two different types of sticks to a termite mound, a sturdy one to dig into the mound and a long, flexible one to insert afterwards in order to extract termites to eat. Forward planning, to form a coalition and achieve political dominance, or to retrieve food before others can discover it, is also commonplace – but this too is rather short-term. In the words of Matsuzawa (2012), their range of mental time- and space-travel is limited. This may relate to chimpanzees' failure to build upon their cultural base: they do not, apparently, use one tool to make another, nor learn extensive new skills from each other – the "ratchet effect" of Tomasello (1999).

The whole of human ontogeny is geared towards manipulation and learning, especially social learning. Matsuzawa (2012) makes much of the finding that only human infants have a stable supine posture: other apes, on being placed on their backs, try to assume a clinging posture. A supine posture in human infants opens them up to manipulation, communication, and vocal exchange. As they grow, these early experiences are built upon, not least by interaction with a wide range of peers: not only are human societies typically much larger than those of chimpanzees, but birth intervals are less so that, unlike in chimpanzees (or gorillas, or orangutans), there is the potential for constant stimulation from siblings.

Humans, of course, live longer than chimpanzees or other apes. Citing Life Expectancy is misleading, because high rates of infant mortality bring life expectancy well down, even in societies where there are demonstrably a lot of very old men and women. It is much more revealing to calculate age at which the chance of dying begins to exceed the chance of surviving, and this, in all modern human societies (with the possible exception of Pygmy people) turns out to be 70 years or a little more. There is, moreover, the peculiarly human occurrence of menopause. While female chimpanzees may eventually, if they live long enough, cease to breed, it is only in humans fertility cessation is an actual event. The importance of post-menopausal women in child-rearing and socialisation, freeing their still-fertile daughters to gather food (very likely carrying their latest infants with them), is known as the Grandmother Effect.

What else distinguishes us humans from our nearest relatives? Often mentioned is language, but we must be careful to distinguish the different aspects of language. First, it is symbolic of objects and actions (nouns and verbs, elaborated by other

parts of speech). Yet chimpanzees, gorillas and orang-utans have proved capable of using hand signs or computer lexigrams symbolically to represent objects and actions; what they cannot do is to put them together in anything but a rudimentary string. Syntax, in other words, is specifically human. The openness of language, its infinite flexibility, is specifically human in its fullest extent, but again, the rudiments of this it seems can be grasped by our closest relatives: vocal learning does occur in chimpanzees (Watson et al. 2015). An orangutan learned to produce both voiced and voiceless calls with speech-like rhythm, both clicks (with lip and tongue movements) and "faux-speech", with harmonic and formant modulations (Lameira et al. 2015).

Humans are notoriously interested in aesthetic activities; art (including music, poetry and story-telling) is practised in all societies. Zoo chimpanzees, gorillas and orangutans have all been introduced by human friends to practice of painting or scribbling on paper, and have generally shown an interest in this activity for its own sake, as opposed to for any reward. Perhaps they simply find this an interesting diversion in otherwise humdrum lives; but in many cases their housing and husbandry seem to be rather superior, and interesting in their own right, and it is difficult to avoid the impression that they simply enjoy making art (incidentally, they likewise generally prove eager to undergo psychological testing: intellectual as well as aesthetic stimulation). It would seem that, like toolmaking and language, the predisposition for art may already have been there in the human lineage when it separated from the chimpanzee lineage.

Of course, much art is ephemeral – body painting and other body decoration, sand painting, bark painting, string figures and so on. In the archaeological record, we must look for constructions in stone, or cave paintings. The earliest archaeological records of art may be Middle Pleistocene. Petroglyphs have been claimed in two caves in Central India (Auditorium Cave and Daraki-Chattan Cave), and two "Venus figurines", which may however be natural formations mimicking human-modelled forms; from Israel (Berekhit Ram), and from Morocco (Tan-Tan). Less controversial is the very recent announcement of geometric engravings on a mollusc shell at Trinil, dating to approximately half 1 million years ago (Joordens et al. 2015); nonetheless, this case is surprising because of the general view that *Homo erectus*, the only *hominin* species so far known from Trinil, is not supposed to be on the lineage leading to modern humans. The next oldest art comes from Blombos Cave in South Africa, dating to 70 ka, followed by several sites in Europe dating to perhaps up to 40 ka, certainly to 33 ka (the latter being the famous cave paintings of Chauvet Cave and the Swabian Jura ivory carvings. Interestingly, there are also claims of cupules from La Ferrassie, whose inhabitants were Neanderthals. It may well be, therefore, either that there was independent aesthetic exploration in different lineages; or more probably that some early common ancestor of *Homo erectus, Homo neanderthalensis* (Fig. 3.1h) and *Homo sapiens*, 1.5 million years ago or more, began to modify natural features for aesthetic reasons, and that this propensity was carried on in several descendant lineages.

And this brings us to the devil's bargain: fire. In Greek mythology, the Titan Prometheus stole fire from the sun god's chariot and snuck it down to earth to give

to humanity. When Zeus, king of the gods, discovered this, he chained Prometheus to a rock in the Caucasus and tortured him by sending an eagle to feed on his liver – a never-ending torture, because the liver grew back every night, in preparation for the eagle next morning. Finally, Zeus's son Herakles shot the eagle and freed Prometheus. But it is no myth that the consequences of the discovery of fire are a devil's bargain.

The earliest traces of fire are disputed. Traces of apparent fire occur at Swartkrans, where both early *Homo* and *Paranthropus* (Fig. 3.1d) are found; but too little is known of what sort of *Homo* lived there, and the fire traces are disputed. The site that has satisfied all archaeologists is Wonderwerk Cave, South Africa, where a distinct lens, implying a sort of fireplace, is clearly marked at a level of 1 million years BP. Further occurrences of fire have been claimed over the following 650,000 years, including, interestingly enough, at Zhoukodian in China, where it is associated with *Homo pekinensis*, a species that was definitely not on the modern human line. Whatever the earliest use of fire, it has been recently well argued from Middle Eastern sites, especially Tabun, at the foot of Mount Carmel in Israel, that it was being habitually used some 350,000 years ago.

Chapter 4
Fire and the Biosphere

Orlando's Vision

Strained wire-like fingers strum a guitar
White strings of pain take you afar
Blue visions tall angel by the gate
Leads down steps where fate awaits
A door swings brilliant light engulfs
A huge hall's walls cryptic hieroglyphs
Bright ray beams flash pierce toward
A radiant core's mortal reward
Where the eternal cosmic flame
Creates the life it shall reclaim.

(Andrew Glikson)

Abstract The advent of plants on land surfaces since about 420 million years-ago has created an interface between carbon-rich organic layers and an oxygen-rich atmosphere, inevitably leading to recurrent fires triggered by lightning, volcanic eruptions, high-temperature combustion of peat and, finally, ignition by humans, constituting the blueprint for the Anthropocene. According to Scott et al. (Fire on earth: an introduction. Wiley Blackwell, Oxford, 413 pp, 2014) (*Fire on Earth: An introduction*): "*Earth is the only planet known to have fire. The reason is both simple and profound: fire exists because Earth is the only planet to possess life as we know it. Life created both the oxygen and the hydrocarbon fuel that combustion requires, it arranges these fuels according to processes of evolutionary selection and ecological dynamics and, in the form of humanity, it supplies the most abundant source of ignition. Fire is an expression of life on Earth and an index of life's history. Few processes are as integral, unique, or ancient*". Since the mastery of fire by humans some 2 million years ago, and in particular the onset of the Neolithic, cultivation and agriculture-based civilizations, concentrating along rivers or above groundwater reservoirs, applied large-scale burning, with major effects on the atmosphere. Civilization, dependent on climate and water, including annual river rhythms, is founded on transformation of nature through its effects on forests, soil erosion and chemical contamination. For a species to be able to control ignition and energy output and entropy in nature higher by orders of magnitude than its own physical energy outputs, the species would need to be perfectly wise and responsible. No species can achieve such levels.

A.Y. Glikson, C. Groves, *Climate, Fire and Human Evolution*, Modern Approaches in Solid Earth Sciences 10, DOI 10.1007/978-3-319-22512-8_4

4.1 An Incendiary Biosphere

High-temperature carbon oxidation processes, including open flame-producing fire and confined smoke-producing combustion, inherent in the continental biosphere, constitute the direct product of photosynthesis producing terrestrial carbon-rich land surfaces and atmospheric oxygen. Non-organic combustion processes arising from breakdown of molecules, atomization and re-combination of metals, including hydrogen fusion, can be triggered by extreme temperatures induced by lightning, volcanism, extraterrestrial impacts, chemical disintegration and subsequent explosion of molecules which contain both oxidizing and oxidized elements, cf. nitroglycerin, and nuclear chain reactions.

Photosynthesis, a process elevating the potential energy of plants, operating in the opposite direction to entropy, is closely followed by oxidation which reduces the energy potential of plants and organisms, magnifying entropy. In plants the control by stomata pores of CO_2-intake rates for photosynthesis and of the oxygen intake rates for respiration regulates the rates of these processes and the energy balance of plants. Likewise a regulation of slow oxidation rates applies equally to animals' food intake, breathing and exhalation. Thus, whereas human respiration dissipates 2–10 calories per minute, a camp fire covering one square meter releases approximately 2×10^5 Calories/minute, magnifying the human-triggered energy output rate by more than 4 orders of magnitude. The output of a 1000 megawatt/hour power plant, expending some 2.5×10^9 calories/minute, surpasses the human energy release rate by more than 8 orders of magnitude. By harnessing the fast-oxidation process of fire the genus *Homo* has overcome a fundamental barrier of mastering and releasing energy at rates suitable for its purposes – warmth, cooking and industry – with consequences leading to a new geological era – the Anthropocene (Part E).

Oxygenation reactions through fire and by plant-consuming organisms enhance degradation and entropy. From this stage the decay of plants and deposition of charcoal from fires, permeating soils and coating many parts of the land with carbon-rich layers, coupled with the carbon located in cellulose of trees and grasses, in methane hydrate and methane clathrate deposits in bogs, sediments and permafrost, provided fuel for extensive fires which, in turn, lead to progressive modification of the composition of the atmosphere.

Wildfires were ignited by lightning, incandescent fallout from volcanic eruptions, meteorite impacts and combustion of peat. Consuming vast quantities of biomass, fires have an essential role in terrestrial biogeochemical cycles (Belcher et al. 2010), including consequences for the oxygen cycle and the evolution of biodiversity over geological timescales. Subsequent burial of carbon in sediments stored the fuel over geological periods, affecting the carbon and oxygen cycle in favor of oxygen. The appearance of diverse flora in the Silurian (Fig. 4.1) followed by extensive fires during the Paleozoic and Mesozoic (Fig. 4.2, 4.3, and 4.4), is represented by charcoal remains whose pyrogenetic origin is identified by high optical refractive indices. Experiments and models by Belcher et al. (2010) suggest fire is suppressed below 18.5 % O_2, switched off below 16 % O_2 and enhanced between 19 % and 22 % O_2.

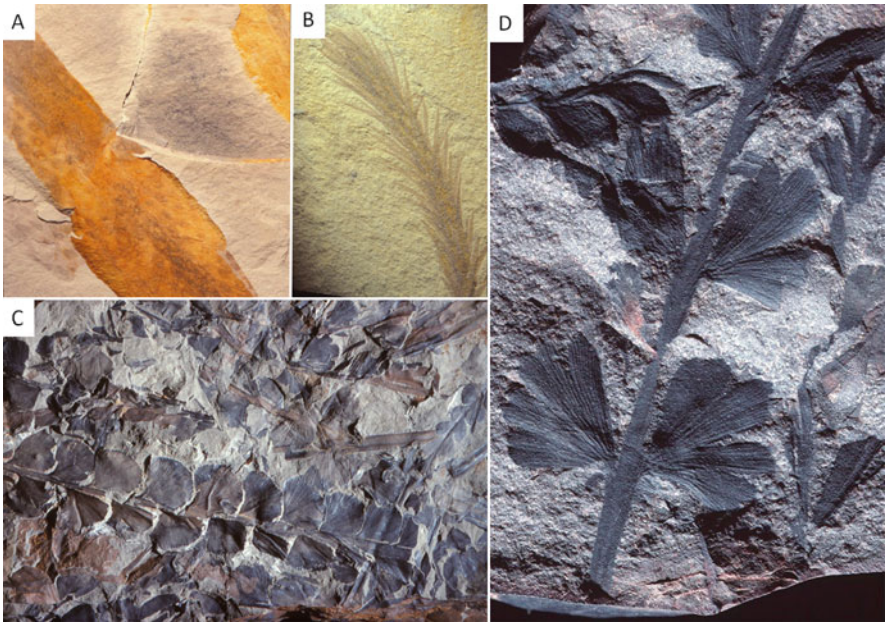

Fig. 4.1 Fossil Palaeozoic plants. (**a**) *Baragwanathia longifolia* (Silurian); (**b**) *Baragwanathia longifolia* – Silurian, Yea in Victoria; (**c**) *Rhacopteris ovate* (Carbonifierous); (**d**) *Rhacopterid* with partly divided leaves (Carboniferous). Courtesy Mary White (From 'Greening of Gondwana' 1986, Reed Books, French's Forest. Photograph by Jim Frazier)

Fires reached maximum influence during ~350–300 Ma and 145–65 Ma, intermediate effects during the 299–251 Ma, 285–201 Ma and 201–145 Ma and low effects between 250 and 240 Ma (Belcher et al. 2010). During the Carboniferous-Permian period, when atmospheric oxygen levels reached ~31 % or higher (Beerling and Berner 2000; Berner et al. 2007), instantaneous combustion affected even moist vegetation (Scott and Glasspool 2006; Bowman et al. 2009). Thus Permian (299–251 Ma) coals may contain charcoal concentrations as high as 70 % (Bowman et al. 2009).

Above critical thresholds of atmospheric oxygen fires would constrain the development of forests, constituting strong negative feedback against excessive rise of atmospheric oxygen (Watson et al. 1978). Conversely a decline of oxygen reduces the frequency and intensity of fires. The association of fossil charcoal with fossil trees suggests O_2 levels continued to be replenished, whereas the upper oxygen limit of Phanerozoic atmospheres is uncertain. Robinson (1989) pointed to Paleobotanical evidence for a higher frequency of fire-resistant plants during the Permo-Carboniferous, supporting a distinctly higher O_2 level at that time. Model calculations of the interaction between terrestrial ecosystems and the atmosphere by Beerling and Berner (2000) suggest the rise from 21 % to 35 % O_2 during the Carboniferous resulted in a decline in organic productivity of about 20 % and a loss of more than 200 GtC (billion ton carbon) in vegetation and soil carbon storage.

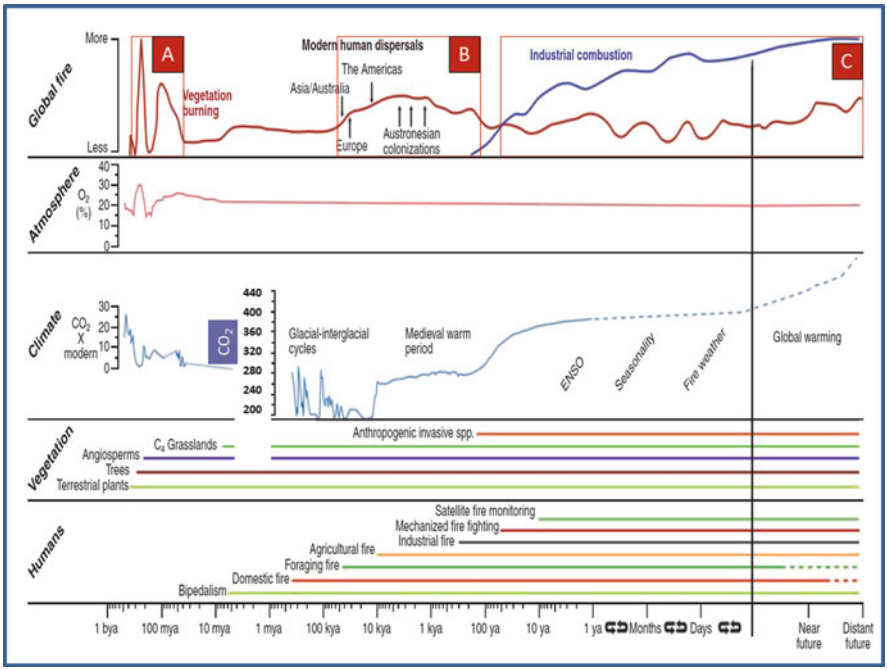

Fig. 4.2 Qualitative schematic of global fire activity through time, based on pre-Quaternary distribution of charcoal, Quaternary and Holocene charcoal records, and modern satellite observations, in relation to the percentage of atmospheric O_2 content, CO_2 (in parts per million), appearance of vegetation types, and presence of Hominins. *Dotted lines* indicate periods of uncertainty. (**a**) Mesozoic and Paleozoic flammability peaks; (**b**) prehistoric flammability period, in part related to human-lit fires; (**c**) Anthropocene fuel combustion; (Bowman et al. 2009 Courtesy D. Bowman; American Association for Advancement of Science, by permission)

This occurred due to burning in an atmosphere of ~300 ppm CO_2. However in a CO_2-rich atmosphere of ~600 ppm carbon fertilization of the soil ecosystem productivity increases lead to the net sequestration of 117 GtC. In both cases these effects resulted from strong interaction between O_2, CO_2 and climate in the tropics.

4.2 The Deep-Time History of Fire

The emergence of land plants in the late Silurian ~420 Ma, the earliest being vascular plants (*Cooksonia, Baragwanathia*) and later Cycads and Ginkgo in the Permian (299–251 Ma), combined with the rise in photosynthetic oxygen above 13 %, with consequent juxtaposition of carbon-rich land surfaces and rising atmospheric oxygen, set the stage for extensive fires. Fires became an integral part of the atmosphere/land carbon and oxygen cycles and have led to development of fire-adapted

(pyrophyte) plants, enhancing the distribution of seeds and control of parasites. With the exception of anaerobic chemo-bacteria which metabolize sulphur, carbon and metals, photosynthesis has become the basis for the land-based food chain.

Initial difficulties in discriminating between charcoal products of fires and coal products of plant decay hampered early studies of the history of fire, a problem largely resolved through experimental studies of the relations between charring temperatures and optic reflectance indices (Scott and Glasspool 2006, Scott et al. 2014). Charcoal, a proxy for fire, occurs in the fossil record from the Late Silurian ~420 Ma. Scott and Glasspool (2006) and Glasspool and Scott (2010) document Silurian through to end-Permian charcoal deposits with reference to the frequency of Paleozoic fires in relation to atmospheric oxygen concentrations. Only weak signatures of fire occur at this stage, in part due to the small size of plants producing only primary tissues and no secondary wood (Scott et al. 2014). Late Silurian to early Devonian charcoal indicates the burning of diminutive rhyniophytoid vegetation. Early Devonian plants are also found as charcoal (Scott and Glasspool 2006). There is an apparent paucity of charcoal in the Middle to Late Devonian (~375–350 Ma) coinciding with low atmospheric oxygen of approximately 15–17 %, although fire records increase toward the late Devonian in both marine and terrestrial sediments, including charcoal derived from ferns (Scott et al. 2014). As atmospheric oxygen levels rose from ~13 % in the Late Devonian to ~30 % in the Late Permian, fires progressively occur in an increasing diversity of ecosystems. This included macroscopic charcoal fragments in terrestrial sediments as well as wind-blown microscopic particles of charcoal (inertinite) in marine sediments. According to Berner et al. (2003) the evolution of secondary wood containing ~70 % cellulose and ~30 % lignin, enhancing the formation of fire-produced charcoal and burial of organic matter and thus of weathering rates, had a profound effect on the composition of the atmosphere. The transition from spore-bearing trees to seed-bearing trees in the late Devonian allowed trees to spread from wet to dry areas where fires are more common.

Charcoal-rich units and charcoal-bearing shales become widespread in the Early Mississippian (Lower Carboniferous) and in the Middle Mississippian. SEM analysis of charcoal has disclosed remnants of herbaceous lycopsids and seed plants (Scott et al. 2014). Examples are from middle Mississippian (~310 Ma) marine estuarine sediments of west Ireland where charcoal concentrations derived by erosion and re-deposition of woody plants and lycopsids reach ~10 %, interpreted in terms of extensive fires burning over 70,000 km^2 (Nichols and Jones 1992). During the Pennsylvanian (Upper Carboniferous) oxygen rose toward levels above 30 %, possibly reaching a peak of ~35 %, consistent with the abundance of charcoal in fossil peat, in some instances over 20 % charcoal. Likely some plants developed thick bark as protection from fire (Scott et al. 2014). The appearance of conifer trees in the late Carboniferous signifies spreading of vegetation into arid and semi-arid regions where fire was widespread (Scott et al. 2010).

Charcoal is recorded in upland settings and is important in many Permian mire settings, suggesting the burning of conifers and seed plants, including moist vegetation.

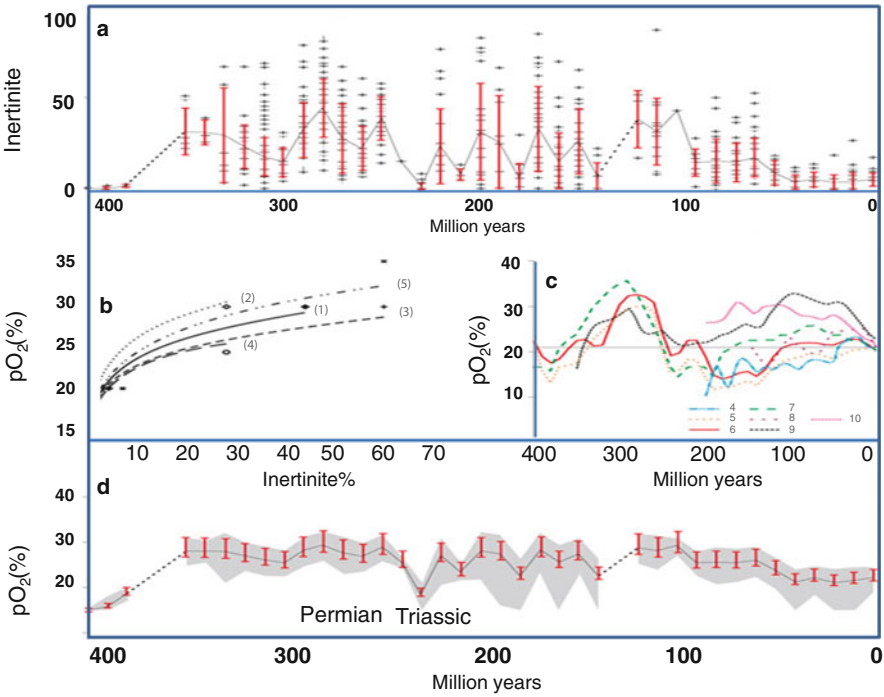

Fig. 4.3 Inertinite abundance – 400 Myr to the present. (**a**) bin mean. Error bars 1 s.d. from mean. Lower axis; seams/samples per bin; (**b**) Power-law regressions for conversion of Inertinite % to pO_2; (**c**) Biogeochemical predictions of Phanerozoic pO_2 published to 2009 (refs 4, 5, 6, 7, 8, 9, 10). Lines: publication references in key. (**d**) Prediction of pO_2 from Inertinite %. Line – best estimate based on late Palaeozoic pO2 maxima of 30 %. Error bars 1 s.d. from mean. Shaded area – estimate of maximum error assuming Phanerozoic pO_2 maxima of 35 % + 1 s.d. (*upper margin*) and 25 % – 1 s.d. (*lower margin*) (Scott and Glasspool 2006; Elsevier by permission)

Some Permian coals reach near ~70 % of charcoal in both Gondwana and northern hemisphere sediments, consistent with extreme level of atmospheric O_2 higher than 30 %, testifying to extensive fires (Figs. 4.3 and 4.4). Late Permian coals in Siberia indicate domination of the flora by aborscent gymnosperms. Studies of charcoal horizons suggest fire frequencies higher than modern rates (Hudspith et al. 2012).

The Permian-Triassic mass extinction event signifies a collapse of vegetation and thereby of photosynthesis, production of atmospheric oxygen and of charcoal (Abu Hamad et al. 2012) widely attributed to the eruption of the Siberian trap basalts with attendant release of CO_2 and SO_2, and elevation of temperature by about 8 °C (Ward 2007). Long-term consequences of this event are represented by a gap of coal and charcoal records during the early Triassic, with charcoal levels rising toward the upper and end-Triassic. A major rise in atmospheric CO_2 and temperature across the Triassic-Jurassic boundary saw a rise in fire regimes, in part related to a shift from broad-leaf vegetation to narrow-leaf vegetation more prone to burning (Belcher et al. 2010; Scott et al. 2014). The Triassic-Jurassic boundary is marked by

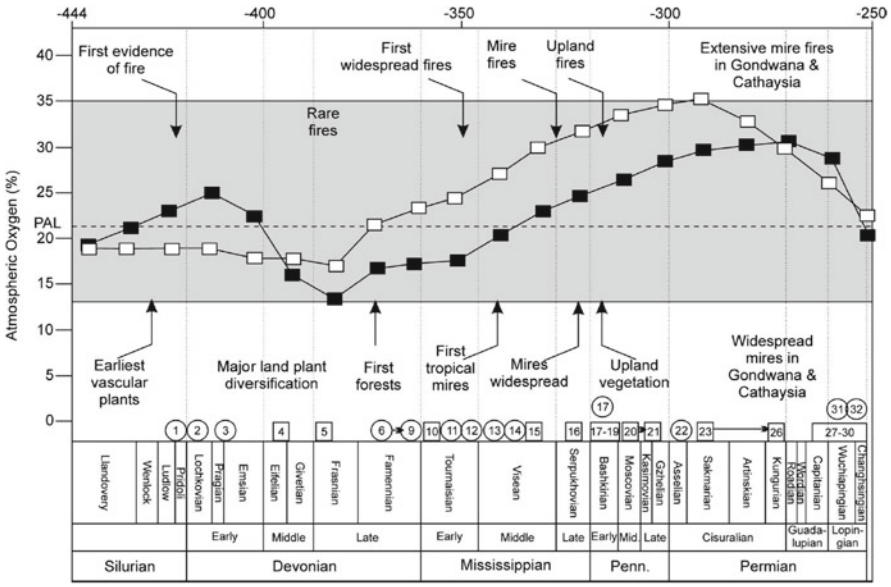

Fig. 4.4 Modeled fluctuations in Late Paleozoic atmospheric oxygen concentration in context with the timing of key terrestrial ecological events and major trends in wildfire occurrence (text and *arrows* toward top). *Shaded area* indicates the fire window. The charcoal inertinite data used to support interpretations are differentiated into clastic sediments (*numbered circles*) and coals (*numbered squares*) (Scott and Glasspool 2006; PNAS by permission)

a sharp decline in oxygen, followed by a rise in oxygen toward the end of the Jurassic and the early Cretaceous (Brown et al. 2012) (Figs. 4.5 and 4.6).

Early studies by Harris (1958) documented charcoaled conifers in Jurassic cave limestone. Mid-Jurassic sediments contain gymnospermous wood, cycad and cycadeoid charcoals (Scott et al. 2014). High atmospheric CO_2 levels during much of the Cretaceous leading to 'greenhouse Earth' conditions (Scott et al. 2014), an absence of polar ice and sea levels some ~70 m higher than at present resulted in global distribution of conifer forests (Brown et al. 2012) (Fig. 4.5). An abundance of charcoal in Cretaceous sediments indicates widespread fires linked to high atmospheric O_2 levels in the range of 21–25 % (Brown et al. 2012). During the Cretaceous further rise in oxygen above present-day levels was related to extensive occurrence of conifers, pteridphytes, cycads, bennettitaleans, gingophytes and flowering plants (angiosperms). The latter, dominating the upper Cretaceous, evolved from sheltered undergrowth habitats to open weed-like distribution, covering a wide latitudinal range. The abundance of vegetation in the Cretaceous is represented by widespread charcoal deposits, militating for extensive fires triggered by high O_2 levels and high temperatures (Brown et al. 2012). Cretaceous fire-adapted vegetation is recorded by He et al. (2012). Charcoal remains in the Campanian indicate catastrophic dinosaur bone bed accumulations may have ensued from post-fire erosion-deposition (Brown et al. 2012).

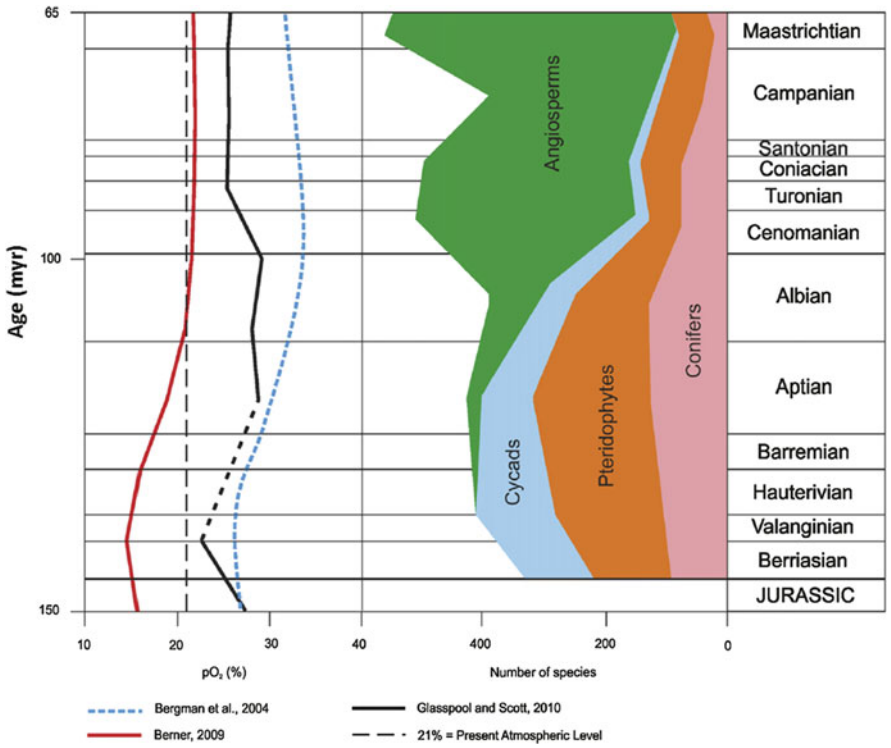

Fig. 4.5 Plant species and oxygen levels during the Cretaceous, modelled (Bergman et al. 2004; Berner 2009) and calculated (Glasspool and Scott 2010) atmospheric oxygen concentrations in the Cretaceous with the global change in vegetational composition (after Niklas et al. 1985; Crane and Lidgard 1989). Time scale after 2010 ICS/IUGS (Brown et al. 2012; Elsevier, by permission)

The K-T boundary impact (Sect. 2.7), dated as 65.5 ± 0.3 Ma, is thought by some to have been accompanied by extensive wild fires triggered by the impact, evidenced by layers of soot including polycyclic aromatic hydrocarbons (PAH) (Wolbach et al. 1990) estimated at a global distribution of 2.2 ± 0.7 mg/cm^2. Melosh et al. (1990) suggested thermal radiation of re-entering ejecta was adequate for the ignition of forests producing ~50 kWm^{-2}. Hildebrand et al. (1990) suggested that at distances of ~1000–2500 km the thermal pulse was higher by two to three orders of magnitude. Kring and Durda (2002) suggested that shock heating of the atmosphere occurred in pulses, igniting fires across several continents, for example in Colorado where they model a pulse of 150 kW m^{-2} which would result in burning of even wet vegetation. Wildfires ignited by fallout of incandescent ash could also have been ignited by lightning storms related to the impact. The suggestion of extensive fires at the KT boundary was questioned by other authors. Thus Belcher (2009) argues the total amount of charcoal is less than that in both older and younger sediments. Soot may also have been derived from combustion of hydrocarbons in the impacted

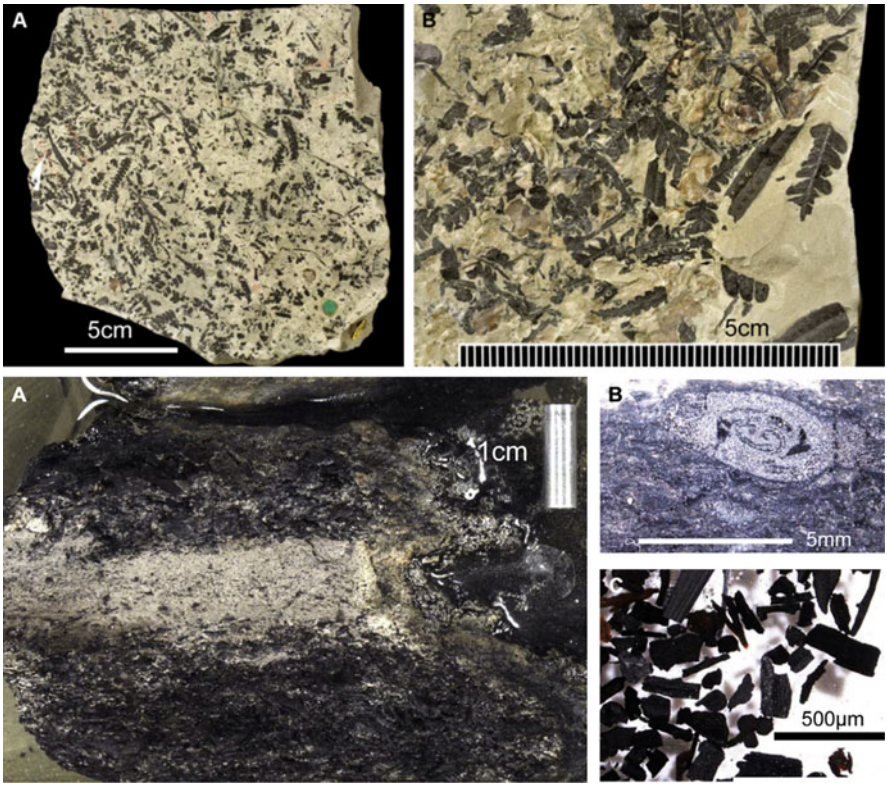

Fig. 4.6 Cretaceous fern-dominated charcoal from the Wealden of Beare Green, Surrey, UK. Scales in mm. Upper part of figure: (**A**) block of siltstone with abundant charred fern pinnules; Natural History Museum, London; NHMUK V.60444. (**B**) Detail of another block showing charred pinnules of *Weichselia* and *Phlebopteris*; NHMUK V.60435. Lower part of figure: (**A**) Fern-dominated charcoal from the Wealden of Hautrage, Belgium. Reworked litter layer block (rip-up clast) from sandstone channel composed of two fern-dominated charcoal layers with clay-rich layer between; (**B**) fern rachis TS from polished block of specimen. Macro- and meso-charcoal fragments macerated from the charcoal layers illustrated in **e** (Brown et al. 2012; Elsevier by permission)

target rocks. According to Belcher et al. (2003) the KT impact resulted in ground temperatures of ~325 °C with short-lived peaks of <545 °C implying thermal radiation of less than 19 kW m^{-2}, significantly less than estimates by Kring and Durda (2002). Goldin and Melosh (2009) modelled the thermal radiation history of impact spherules and its effects on ground temperatures, including the effects of impact-generated dust, estimating a thermal flux of 5 kW m^{-2} and surface temperatures of <325 °C associated with spherule settling.

Peak global temperatures associated with the Paleocene-Eocene Thermal Maximum (PETM) (Zachos et al. 2008) (Sect. 2.8). As based on remnants of ferns on lignite Collinson et al. (2007), periods of fires interchanged with fire-free periods.

Scott et al. (2014) point out charcoal is relatively rare during the Eocene (55–34 Ma), a period dominated by fire-resistant angiosperm rainforests. Berner et al. (2007) indicate atmospheric oxygen levels increased to ~21 % O_2 through the Eocene to the present. The spread of C4-grass dominated savannah during the late Cenozoic was associated with extensive grass fires represented by charcoal deposits in marine sediments (Bond and Keeley 2005).

4.3 Fire and Pre-historic Human Evolution

Studies of pre-historic fires from approximately 2 million years ago, based on associations of charcoal fragments and pollen in lake and peat sediments indicative of plant habitats, suggesting the opening of savannah since the Miocene (~23–5.3 Ma) was associated with proliferation of grass fires. Grasses were dominated by tropical C4 photosynthetic pathways adapted to warm, arid and low-CO_2 conditions, related to overall cooling (Hoetzel et al. 2013). These authors studied pollen, charcoal and stable isotopic composition of plant waxes from marine sediments off-shore Namibia in relation to plant composition during the late Miocene and Pliocene, observing expanding C4-grass-cominated habitats with increasing aridity and fire regimes, a trend enhanced in the Pliocene. Large-scale release of carbon through extensive fires acted as a feedback, counter-acting the decline in atmospheric CO_2.

Estimates of fire frequencies and intensity of fires observed in the context of studies of charcoal fragments associated with lake sediments and fossil plants and pollen are greatly enhanced in studies of post-70,000 year systems by the Carbon ^{14}C dating method and for post-3000 years-ago by tree ring counts (Power 2013). When combined with paleo-climate indicators from ice cores, deep ocean drill cores, corals, cave deposits and other paleo-climate criteria, the frequency of paleo-fires correlates with climate changes, including the upper Pleistocene trends and peaks (Marlon et al. 2008, 2009; Power et al. 2008) (Figs. 4.7 and 4.8):

1. A marked charcoal flux is indicated in deep sea sediments from about 10 million years ago exceeding previous fluxes during the Cainozoic by at least a factor of 5 (Herring 1985).
2. The last glacial termination (LGT) was followed from about 15 kyr by a gradual rise in influx of charcoal in North American sediments during the warm *Bolling-Allerod* (~14.7–12.9 kyr), flattening during the cold *Younger–Dryas* (~12.9–11.7 kyr) and rising again during the earliest Holocene (11.6–10.0 kyr) (Marlon et al. 2009) (Fig. 4.7).
3. Variations in the charcoal flux follow closely changes in average global temperatures over the last two millennia. A gradual decline in temperatures during ~2000–1000 years before present (BP) was followed by stabilized to slightly warmer (average of +0.2 °C) climates during ~850–1400 AD (The *Medieval Warm Period* – MWP), a cool period during 1550–1750 AD (The *Little Ice Age* – LIA), an abrupt rise from ~1850 AD and fire suppression associated with modern agricultural practices since about ~1900 AD (Marlon et al. 2008) (Fig. 4.8).

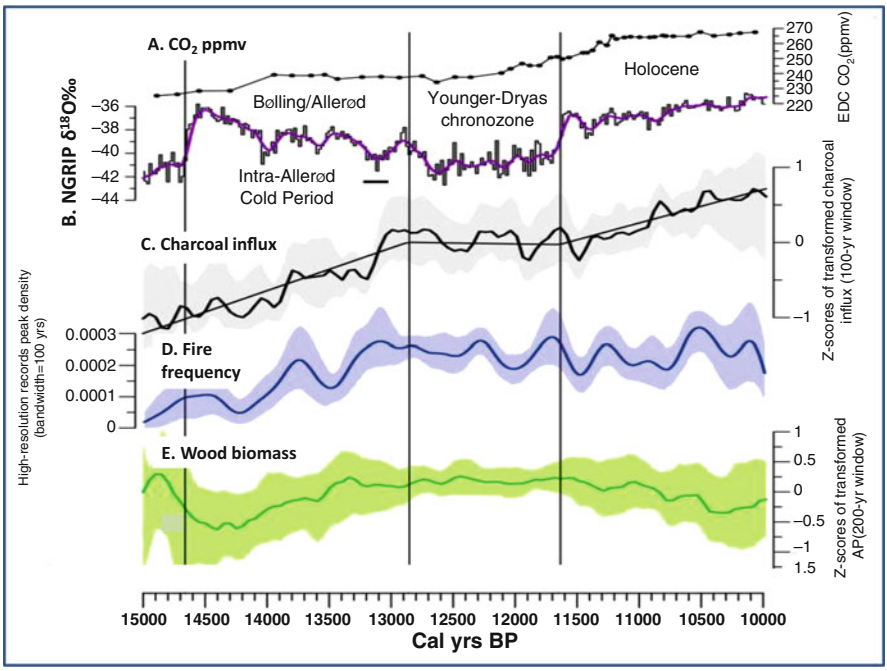

Fig. 4.7 Reconstructions of biomass burned, fire frequency, and woody biomass levels during 15–10 kyr in North America: (**a**) CO_2 ice-core record from Antarctica; (**b**) The NGRIP (North Greenland Ice Core Project) $\delta^{18}O_{ice}$ record, a proxy for North Atlantic temperatures; (**c**) Reconstruction of biomass burned based on 35 records; the *straight lines* are segmented regression curves, and the *smooth curves* are local-regression fitted values; (**d**) Reconstruction of fire frequency based on 15 high-resolution records expressed as the density of peaks per site-year; (**e**) Trends in woody biomass based on 35 records; After Marlon et al. (2009) (Proceedings American Association of Science, PNAS by permission)

Progressive overall and intermittent cooling through the early Pleistocene, culminating with the ice ages, saw the retreat of tropical rainforests and the opening of savannah, heralding a fundamental shift in the terrestrial habitats, the rise of hominins in Africa and subsequent migrations of a succession of human species (Klein and Edgar 2002; Klein 2009; Henn et al. 2012). Once humans became hunters in the open savannah, they became affected by climate and environment variability factors which affected their prey, as indicated by the extinction/radiation relations of bovids (Fig. 4.9) (deMenocal 2004).

The genus *Homo* is defined by its specialized bipedalism, an increase in its cranial volume from Australopithecines (*A. garhi* ~450 cc) [~2.3–2.4 Ma], to *Homo* (*H. habilis* ~600 cc [2.4–2.3 Ma]; *H.ergaster* (700-1935 cc) [2.0–1.0 Ma], *H. erectus* 950–1300 cc [1.6–0.5 Ma]; *H. heidelbergensis* ~1100–1400 cc [~0.6 Ma]; *H. neanderthalensis* 1200–1700 cc and *H. sapiens* 1350–1400 cc) (Groves 1993; Klein and Edgar 2002; Zimmer 2005; McHenry 2009) (Fig. 4.10). The type of tools became

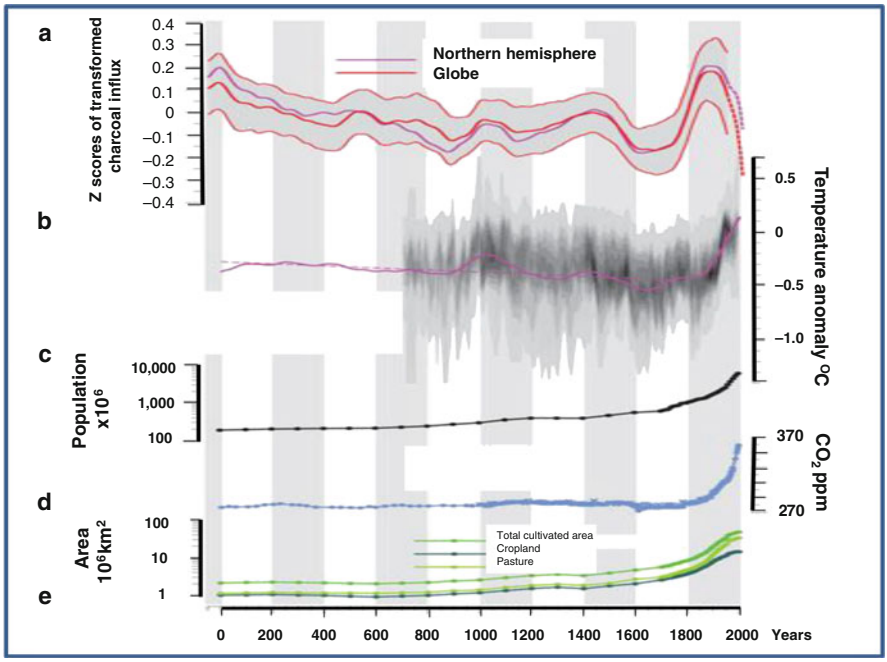

Fig. 4.8 (**a**) Reconstruction of global (*red line*) and Northern Hemisphere (*purple line*) biomass burning with confidence intervals based on bootstrap resampling by site. A *dashed line* is used to represent increased uncertainty in late twentieth century changes in biomass burning; (**b**) Reconstructions of Northern Hemisphere climate with mean temperature values (*purple line*) of available reconstructions, trend line (*dotted line*) for first part of record and overlap of uncertainty ranges of ten Northern Hemisphere temperature reconstructions after AD 700 (*grey shading*); (**c**) World population (from the HYDE 3.0 database); (**d**) Atmospheric CO_2 concentration; (**e**) Global agricultural land cover (After Marlon et al. 2008. Nature Geoscience, by permission)

more and more sophisticated; of course, as we have already noted, the use of tools, and even to some extent their manufacture, is not unique to *Homo*, as it is shared by other biological genera, including Chimpanzees, beavers, birds and insects. What truly makes us unique, however, is the mastery of fire.

Physical criteria used to distinguish *Homo* from animals do not adequately explain the unique nature of the genus. Partial bipedalism, including a switch between two and four legged locomotion, is common among mammals, cf. bears, meerkats, lemurs, gibbons, kangaroos, sprinting lizards, birds and their dinosaur ancestors. *Homo sapiens'* brain mass is lower than that of whales and elephants but the brain to bodyweight ratio is one to two orders of magnitude higher (human brain ~1.3–1.4 kg; average body ~70 kg/ratio ~0.02; sperm whales' brain ~7.8 kg, body 40,000 kg; ratio 0.0002; elephants' brain ~4.8 kg, body ~5000 kg; ratio ~0.001) (Fig. 4.11). The human brain/body mass ratio is similar to that of mice but lower

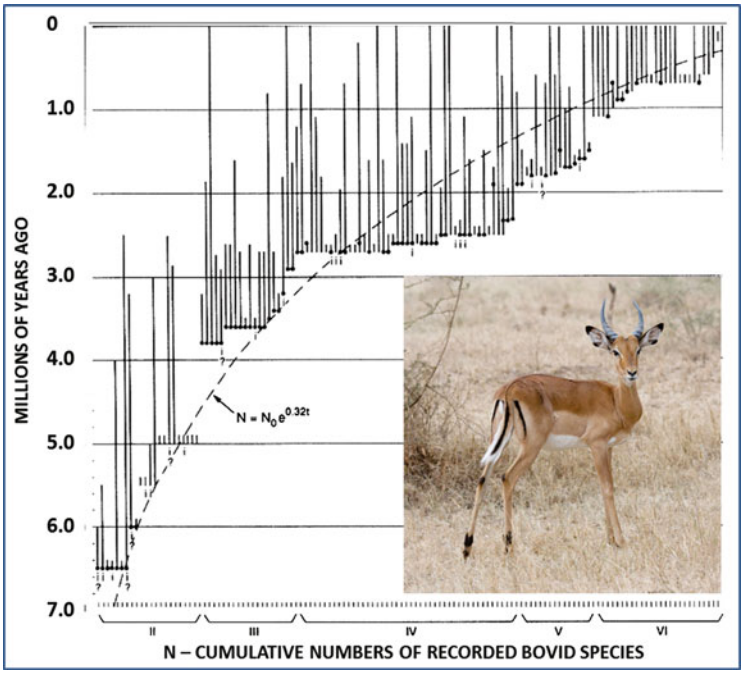

Fig. 4.9 Africa-wide occurrences of fossil bovids (antelope) over the last 7 Ma. Pronounced faunal turnover pulses occurred about ~2.8 Ma and ~1.8 Ma were associated with onset of arid-adapted fauna and were more gradual in some areas (deMenocal 2004; Elsevier, by permission. Photograph of Impala (stock.xchng Image ID: 1420956 – http://www.sxc.hu/photo/1420956 http://www.sxc.hu/help/7_2)

than that of birds (~0.08). The high neocortex to brain ratio (the so-called 'Dunbar index') of birds has been related to their high sociability and enhanced communications (Dunbar 1996) (Fig. 4.12). The evolution of hominins, corresponding to the brain weight to body weight ratio, is represented by the emergence of species from about 7 million years-ago (brain case 320–380 cc) to *Homo neanderthalensis* (brain case ~1200–1500 cc) (see Chap. 3) (Figs. 4.11 and 4.12).

Numerous organisms use tools and construct articulate structures, examples being the elaborate architecture of termite nests, bee hives, spider webs, and beaver dams, and, as we have already mentioned in the previous chapter, the use of rudimentary tools by some primates, including chimpanzees and oran-utans. Examples of sophisticated language among animals include the bee dance, bird songs and the echo sounds of whales and dolphins, possibly not less complex than the languages of original prehistoric humans, if not that of Shakespeare some 2 million years later (Patterson et al. 2006). Other features unsurpassed by humans include the visual memory of birds and navigation by ants, birds, fish, whales and insects (Griffin 1992; Narby 2005).

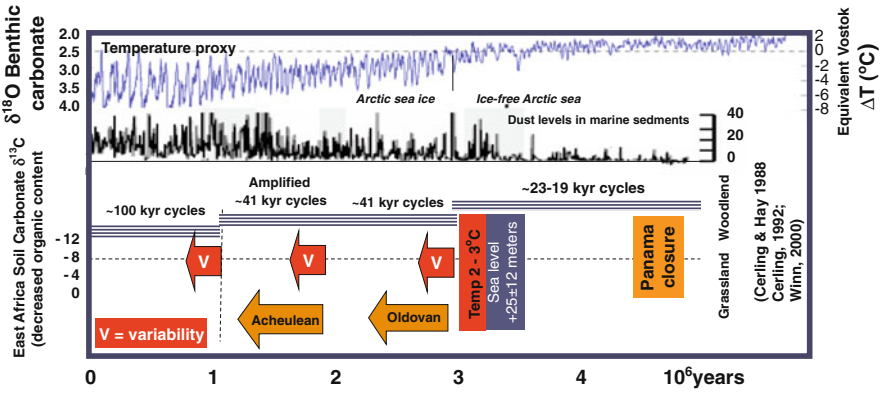

Fig. 4.10 Paleoclimate and hominin evolution events during the Pliocene-Pleistocene. Marine paleoclimate records indicate that African climate became progressively more arid after step-like shifts near ~2.8 Ma, and subsequently after ~1.7 Ma and ~1.0 Ma, coincident with the onset and intensification of high-latitude glacial cycles. Consequences included changes toward dry-adapted African faunal compositions, including steps in hominin speciation, adaptation, and behaviour. Soil carbonate carbon isotopic data from East African hominin fossil localities document the Pliocene-Pleistocene progressive shifts from closed woodland forest C3-pathway vegetation to arid-adapted C4-pathway savannah grassland vegetation (Modified after deMenocal 2004; Elsevier, with permission)

The appearance of a species which has learnt how to kindle fire (Figs. 4.13, and 4.14) meant that, for the first time, the flammable carbon-rich biosphere could be ignited by a living organism. The mastery of fire in the mid-Pleistocene about ~2.0–1.0 Ma coincides with accentuation of intermittent glacial conditions associated with the amplification of the 41 kyr-long Milankovic cycles at about 1.8–1.5 Ma, a period of increased climate variability (Figs. 1.27 and 1.30). It is likely that, like other major inventions, the mastery of fire was driven by necessity, under acute environmental pressures associated with the descent from warm Pliocene (5.2–2.6 Ma) climate to Pleistocene (2.6–0.01 Ma) (deMenocal 2004), which involved global temperature oscillations of up to ±5 °C.

Examples of the effects of climate on early human evolution come from East African rift valleys, where climates were controlled by major tectonic changes, global climate transitions, and variations in orbital forcing (Maslin and Christensen 2007). The appearance of C4 plants, signifying open savannah conditions, represent global cooling and a long-term drying trend. Uplift related to formation of the East African Rift Valley resulted in changes in wind flow patterns from a more zonal to a more meridional direction. Evidence from lake, speleothem, and marine paleoclimate records manifests a long-term drying trend punctuated by episodes of short alternating periods of extreme wetness and aridity, involving appearance and disappearance of large, deep lakes. The extreme climate variability has been related to the 41 kyr-long precession cycles and related wind patterns associated with the

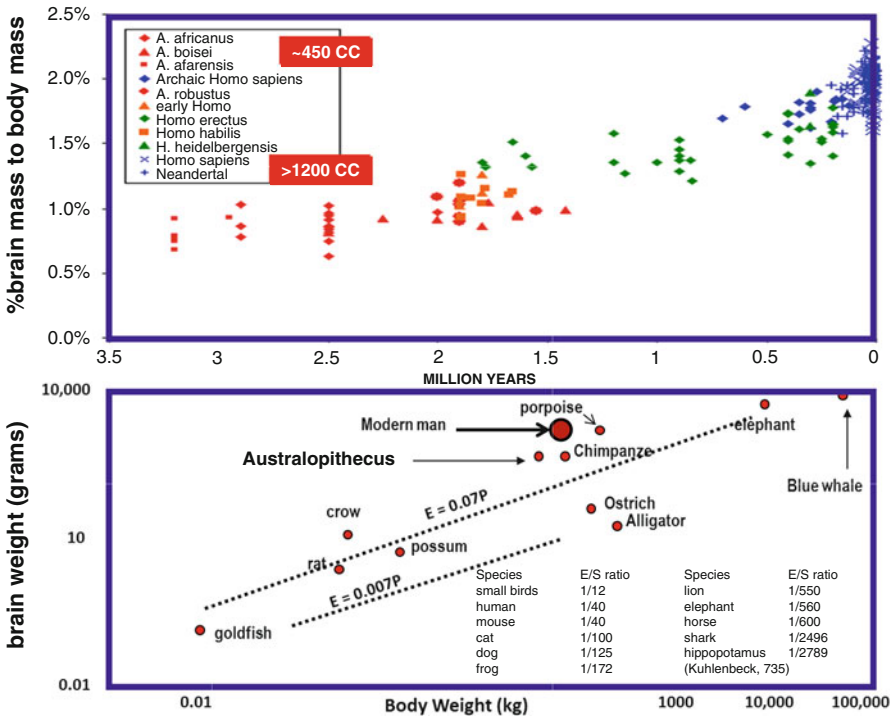

Fig. 4.11 (**Upper part**) Evolution of the human brain. Brain mass as a percentage of body mass. after Miguel and Henneberg (2001) (Elsevier, by permission) processed by Nick Matzcke of NCSE http://www.pandasthumb.org/archives/2006/10/fun-with-homini-2.htmlhttp://www.pandasthumb.org/archives/images/Henneberg_de_Miguel_2004_Homo_hominins_single_lineage_fig1.png; (**Lower part**) Comparison between human brain weight/body mass weight and that of animals and birds (Reproduced (or adapted) with permission from http://www.brains.rad.msu.edu, and http://brainmuseum.org, supported by the US National Science Foundation. http://serendip.brynmawr.edu/bb/kinser/Int3.htmlwww.neurophys.wisc.edu)

intensification of Northern Hemisphere glaciation (2.7–2.5 Ma), the Walker Circulation (1.9–1.7 Ma), mid-Pleistocene climate transition (1–0.7 Ma) and compression of the Intertropical Convergence Zone, resulting in rapid shifts from wet to dry conditions (Maslin and Christensen 2007; Trauth et al. 2007; Maslin and Trauth 2009). This extreme climate variability constituted a catalyst for evolutionary change and has driven key speciation and dispersal events amongst mammals including hominins, which either originated or became extinct during climate upheavals.

Small human clans reacted to extreme climate changes during the Pleistocene—including cold fronts, storms, droughts and sea level changes—through migration within and out of Africa. *Homo sapiens* emerged during the glacial period which preceded the 124,000 years-old (124 kyr) Eemian interglacial, when temperatures

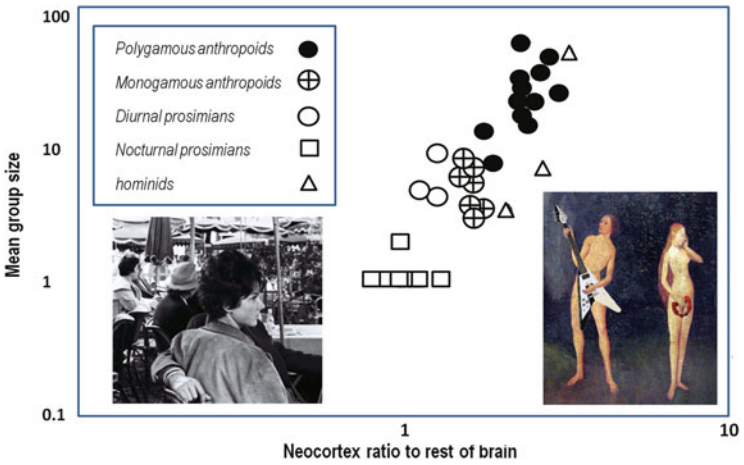

Fig. 4.12 Mean group size for individual genera plotted against neocortex ratio relative to rest of brain, including polygamous anthropoids, monogamous anthropoids, diurnal prosimians (primate that include lemurs, lorises, bushbabies, and tarsiers), nocturnal prosimians and hominoids ((Dunbar 1992; Elsevier, by permission). Adam & Eve – Hieronymus Bosch http://www.flickr.com/photos/oddsock/92105811/ http://creativecommons.org/licenses/by/2.0/deed.en; Woman's profile – photograph by Arthur Glikson)

Fig. 4.13 Camp fire http://commons.wikimedia.org/wiki/File:Camp_fire.jpg

rose temporarily by ~5 °C to nearly +1 °C higher than late-Holocene pre-industrial temperature, while sea levels were 6–8 m higher than the present (Hansen and Sato 2012a). However, the emergence of agriculture, and thereby of Neolithic human civilization, did not occur until the climate stabilized between ~10,000 and

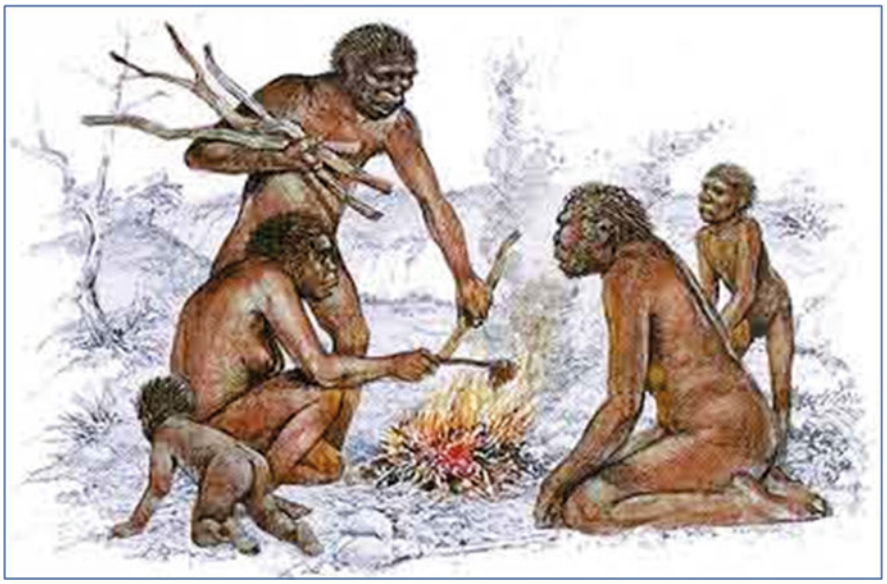

Fig. 4.14 6-5B *Homo pekinensis* lighting fire http://4.bp.blogspot.com/-2QaPsqNs83g/T7vyIhIk3bI/AAAAAAAABlM/6IBvkzVI00s/s1600/Homo+Erectus.jpg http://www.thesubversivearchaeologist.com/2012_04_29_archive.html http://creativecommons.org/licenses/by-nd/3.0/deed.en_US

7000 years-ago, when large-scale irrigation along the great river valleys– the Nile, Euphrates, Indus and Yellow Rivers– became possible thanks to regulated river flows allowed by accretion and melting of snow in source mountain terrains.

It may never be known how fire was originally mastered, whether by percussion of flint stones or fast turning of wooden sticks, and whether this technique was developed in one or several places. During the earliest Paleolithic (~2.5 Ma) mean global temperatures were at least 2 °C warmer than the Holocene, allowing human migration through open vegetated savannah in the Sahara and Arabian Peninsula. Confident evidence has emerged for the use of fire at ~1 Ma in the Wonderwerk Cave, Kuruman Hills, Cape Province, South Africa, from the study of palaeotemperatures of burnt bones (Berna et al. 2012) (Fig. 4.15) (Table 4.1). Possible records of ~1.7–1.5 Ma-old fire places were recovered in excavations at Swartkrans (South Africa), Chesowanja (Kenya), Xihoudu (Shanxi Province, China) and Yuanmou (Yunnan Province, China) (Table 4.1). These included black, grey, and greyish-green discoloration of mammalian bones suggestive of burning. Clear evidence has been uncovered of the use of fire by *Homo pekinensis* and *Homo heidelbergensis* at least 300 thousand years (kyr)-ago in Africa, the Middle East and China. Evidence for fire in sites as old as 1.4 Ma in Kenya and 750 kyr in France is controversial (Hovers and Kuhn 2004; Stevens 1989). Penetration of humans into central and northern Europe, including by *H. heidelbergensis* (400–30 kyr) and

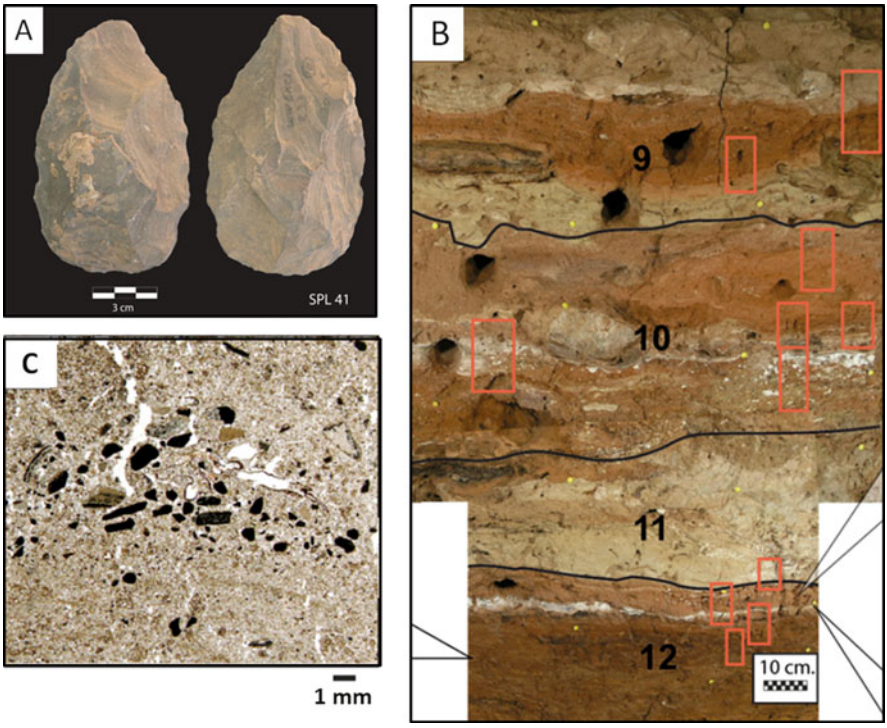

Fig. 4.15 Wonderwerk Cave (Berna et al. 2012): (**a**) Hand axes characteristic of the Acheulean of stratum; (**b**) Photograph of the east section in excavation where charred bones were found; (**c**) Representative micrograph of low-energy, water-bedded silt, sand, and 0.5-cm-thick gravel dolostone and flowstone where charred remains were found (Proceedings National Academy of Science USA, by permission)

H. neanderthalensis (600–30 kyr) was facilitated by the use of fire for warmth, cooking and hunting. According to Roebroeks and Villa (2011) evidence for the use of fire, including rocks scarred by heat and burned bones, is absent in Europe until around 400 kyr. Unless older charcoal beds were missed in north European sites, this would lead to the extraordinary conclusion that humans penetrated northern latitudes with no fire to keep them protected from the freezing conditions of the glacial periods.

Fire allowed humans to migrate to harsh climate zones. Intensification of glacial-interglacial cycles drove intermittent dispersal of fauna, including humans, between Africa, the Middle East, southern and south-eastern Asia and southern Europe (Dennell and Roebroeks 2005) (Fig. 4.16), likely following the animals (Fig. 4.9). By at least ~1.8–1.6 Ma *hominins* arrived in Western Asia (Dmanisi ~1.85 Ma), Eastern Asia (Yuanmou ~1.7 Ma; Nihewan ~1.66 Ma) and southeastern Asia (Sangiran, Java) ~1.66 Ma) (Smithsonian 2012). Evidence for widespread use of fire in the late Paleolithic is indicated by charred logs, charcoal, reddened areas,

Table 4.1 Prehistoric sites containing evidence or possible evidence of human use of fire

1.7 Ma	Yuanmou, Yunnan Province	Blackened mammal bones
1.5 Ma	Swartkan, South Africa	Burnt bones were found among Acheulean tools, bone tools, and bones with hominin-inflicted cut marks
1.42 Ma	Chesowanja, Kenya	Red clay shards. heated to 400C to harden but re-interpreted as bushfire
1.5 Ma	Koobi Fora Kenya	Red clay shards heating at 200–400C
	Olorgesailie Kenya	"Hearth-like depression". microscopic charcoal
	Gadeb, Ethiopia	Welded tuff near Acheulean artefacts
~1.0 Ma	Wonderwerk Cave, Northern Cape province, South Africa	Burned bone and ashed plant remain: carbonate-hydroxylapatite – undergoes characteristic recrystallization at approximately >500 °C
0.79–0.69 Ma	Bnot Yaakov Bridge Israel	Burnt flintstones; probably *H. ergaster*
0.83–0.5 Ma	TJava	*H. erectu*s fossils; blackened bone and charcoal deposits
	Xihoudu in Shanxi Province	Evidence of burning by the black, grey, and greyish-green discoloration of mammalian bones
0.7–0.2 Ma	Cave of Hearths in South Africa	
130,000–120,000 BP	Klasies River Mouth	
110,000–61,000 BP	Kalambo Falls in Zambia	Artefacts related to the use of fire by humans: charred logs, charcoal, reddened areas, carbonized grass stems and plants, and wooden implements which may have been hardened by fire
72,000 BP	Stillbay culture. South Africa	Fire was used to heat treat silcrete stones to increase their workability before they were knapped into tools

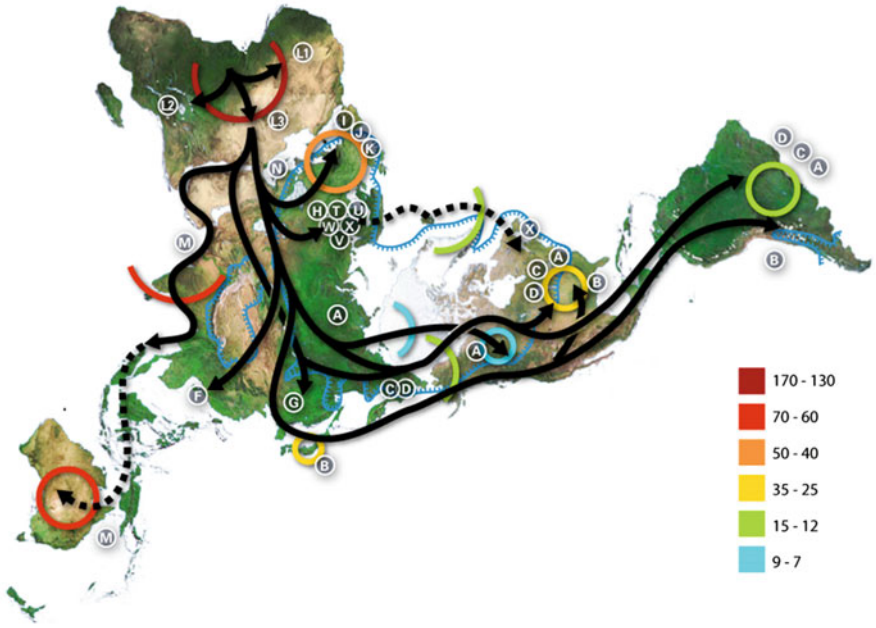

Fig. 4.16 A model of human migration based on mitochondrial DNA the letters are the mitochondrial DNA haplogroups (pure motherly lineages); Haplogroups can be used to define fine genetic population often geographically oriented. The following are common divisions for mtDNA haplogroups: African: L, L1, L2, L3' Near Eastern: J, N; Southern European: J, K; General European: H, V; Northern European: T, U, X; Asian: A, B, C, D, E, F, G (note: M is composed of C, D, E, and G) Native American: A, B, C, D, and sometimes X. http://en.wikipedia.org/wiki/File:Map-of-human-migrations.jpg (http://www.mitomap.org/pub/MITOMAP/MitomapFigures/WorldMigrations.pdf) (license GNU Operating Systems: http://www.gnu.org/copyleft/fdl.html)

carbonized grass stems and plants, and by wooden implements which may have been hardened by fire. Reliable evidence for the use of fire comes from the Bnot Yaakov Bridge, Israel, where between 790 and 690 kyr *H. ergaster* or a descendant species produced stone tools, butchered animals, gathered plant food and controlled fire (Goren-Inbar et al. 2004). Wood of six taxa was burned at the site, at least three of which are edible – olive, wild barley, and wild grape. The distribution of small burned flint fragments suggests that burning occurred in specific spots, possibly indicating hearth locations.

Darwin considered language and fire the two most significant achievements of humanity. Wrangham (2009) attributed the increase in brain size and the drop in tooth size of what he dubbed *Homo erectus* (correctly *H. ergaster*) at 1.9–1.7 Ma, relative to *H. habilis* (see Chap. 3.2), to the onset of cooking of meat. Cooking allowed easier digestion of raw vegetables and of proteins, greatly improving the calorie intake and relieving early humans from energy-consuming chewing and

enhancing the brain blood supply. As expressed by Adler (2013) "*Cooking breaks down collagen, the connective tissue in meat, and softens the cell walls of plants to release their stores of starch and fat. The calories to fuel the bigger brains of successive species of hominids came at the expense of the energy-intensive tissue in the gut, which was shrinking at the same time—you can actually see how the barrel-shaped trunk of the apes morphed into the comparatively narrow-waist Homo sapiens. Cooking freed up time, as well; the great apes spend four to seven hours a day just chewing, not an activity that prioritizes the intellect.*"

It is since their mastery of fire that hominins grew taller and leaner, shedding much of their original hair cover, allowing perspiration, cooling and the long range chase and hunt of animals. According to Adler (2013) "*Wherever humans have gone in the world, they have carried with them two things, language and fire. As they traveled through tropical forests they hoarded the precious embers of old fires and sheltered them from downpours. When they settled the barren Arctic, they took with them the memory of fire, and recreated it in stoneware vessels filled with animal fat*". Twomey (2011) inferred a high degree of human cognition and cooperation required for fire use and control. Examples include the specific technologies of igniting, preserving and transporting fire, the planning of cooking requiring collection of firewood, the delay of gratification required during cooking, precautionary measures of avoiding burn and fire-spreading, amounting to sound behavioral patterns in the context of fire-related tasks. Thus, to keep fires going, humans needed to undertake long-range planning further than needed for sculpting stone tools or hunting, including collection of firewood in advance and the protection of fire from wind, rain and storms.

Some of the best information regarding prehistoric fire cultures is related to burning strategies by native people in Africa (Laris 2002; Sheuyange et al. 2005), North America (Stephens et al. 2007) and Australia. Aboriginal 'fire-stick farming' associated with maintenance of small-scale habitat mosaics increased hunting productivity and foraging for small burrowing prey, including lizards (Gammage 2012). This led to extensive habitat changes, possibly including the extinction of mega-fauna, a debated issue (Miller 2005; Surovell and Grund 2012). The paucity of archaeological evidence for connections between hunting and mega-fauna extinction led some to invoke abrupt climate change, or even an extra-terrestrial impact, for which there is no direct evidence, as drivers of the mega-fauna extinction. However, since the last glacial termination (LGT) bears close similarities to earlier terminations which mega-fauna survived, the LGT hardly explains the disappearance of mega-fauna such as diprotodons, giant kangaroos, marsupial tapirs, or über-echidna (Surovell and Grund 2012; Johnson 2013).

Maori colonization of New Zealand 700–800 years-ago led to loss of half the South Island's temperate forest (McGlone and Wilmshurst 1999). These practices intensified upon European colonization, with extensive land cultivation and animal husbandry.

The harnessing of fire by humans, elevating the oxygenating capacity of the species by many orders of magnitude through utilization of solar energy stored by photosynthesis in plants (Kittel and Kroemer 1980), elevated planetary entropy to

levels on a scale analogous to volcanic events and asteroid impacts. The effect on nature of anthropogenic combustion is tracking toward a similar order of magnitude. The decrease in entropy inherent in photosynthetic reactions, which locally and transiently raise potential energy levels stored in plants, is dissipated through the energy output by plant-metabolizing organisms, from microbes to herbivors to complex technological civilizations. Since the industrial revolution, further to devastating the world's bio-diverse forests, the oxidation of fossil carbon of ancient biospheres has increased the release of energy by orders of magnitude. In 2011 fossil fuel burning, cement production and land clearing released a total of 9.5 ± 0.5 GtC to the atmosphere (Global Carbon Project 2012), 54 % higher than in the 1990 Kyoto Protocol reference year. In 2011 coal burning was responsible for 43 % of the total emissions, oil 34 %, gas 18 %, and cement 5 %, with far reaching consequences for the atmosphere-ocean-cryosphere-biosphere system.

Inherent in ancient fire mythologies is the illegitimate nature of the acquisition of fire by humans, symbolized by Prometheus, the Titan who, after breathing life into human clay figures, stole the fire from the gods in a fennel stalk and gave it to the human beings he had created. According to the Rig Veda the hero Mātariśvan recovered fire which had been hidden from mankind. In Cherokee myth, after Possum and Buzzard had failed to steal fire, grandmother Spider used her web to sneak into the land of light and stole fire, hiding it in a clay pot. Among various Native American tribes of the Pacific Northwest and First Nations, fire was stolen and given to humans by Coyote, Beaver or Dog. According to some Yukon First Nations people, Crow stole fire from a volcano in the middle of the water. According to the Creek Indians, Rabbit stole fire from the Weasels. In Algonquin myth, Rabbit stole fire from an old man and his two daughters. In Ojibwa myth, Nanabozho the hare stole fire and gave it to humans. In Polynesian myth, Maui stole fire from the Mudhens. In the Book of Enoch, the fallen angels and Azazel teach early mankind to use tools and fire. Because fire allows humans warmth, protection from animals, cooking, pottery and migration to cold parts of the planet, the underlying warnings implicit in these legends is perplexing. Over the millennia, culminating in the Anthropocene (Ruddiman 2003; Steffen et al. 2007), however, the hidden meaning of these forewarnings has become progressively manifest.

The effects of fire on the human mind are known to those who have camped for long periods around campfires, as the senior author has on-and-off for 40 years. For hundreds of thousands of years, gathered during long nights around camp fires, captivated by the flickering life-like dance of the flames, humans developed imagination, insights, cravings, fears, premonitions of death and thereby aspirations of immortality, omniscience, omnipotence and concepts of supernatural being, or gods. Pantheistic beliefs revered the Earth, its rocks and living creatures. In similar vein, the junior author's long-ago experience of campfires in Kenya was on one occasion enhanced by the late-night visit of a small herd of elephants which filed past on either side, each one stopping briefly to examine us, its eyes glittering in the dancing firelight.

Fear, an instinctive sense arising in animals when endangered, is created in the human mind allowing it to foresee risks in advance (Fig. 4.17). Since at least

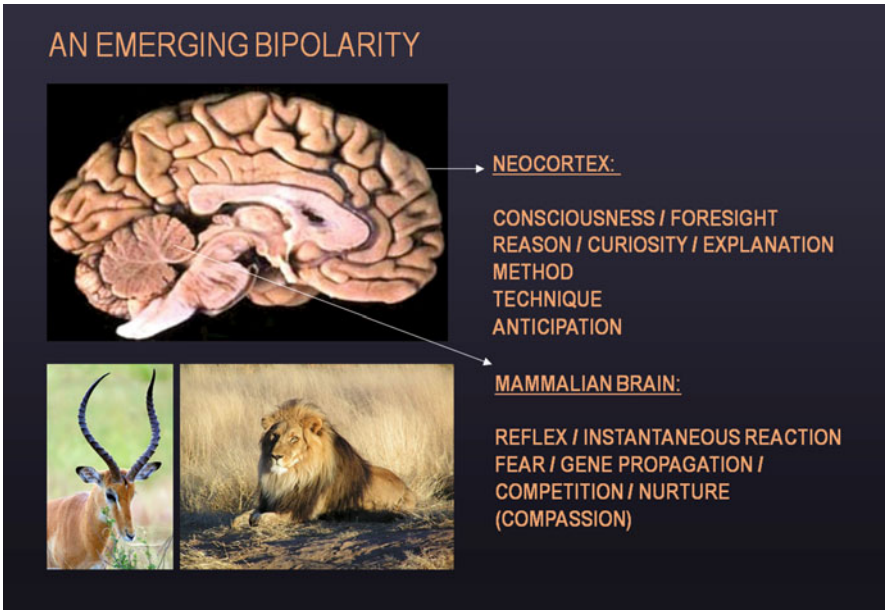

Fig. 4.17 An emerging bipolarity – the conflict between the Neocortex (consciousness, foresight and reason) and the mammalian brain (reflex/instantaneous reaction). On the surface of it no such conflict exists among animals, operating on instinct when faced with danger. Impala (http://en.wikipedia.org/wiki/File:Male_impala_profile.jpg); Wikipedia commons. Lion (http://commons.wikimedia.org/wiki/File:Lion_waiting_in_Namibia.jpg)

130,000 years-ago the recognition of death and a yearning for immortality have been expressed in ritual burial (Fig. 4.18). An example is the Skhul cave, Mount Carmel, Israel, where skeletons painted in red ochre are surrounded by tools (Hovers and Kuhn 2004). Cremation constituted a special way of merging the spirit of the deceased with fire, allowing a passage of the soul to eternity. When civilization rose, burial rituals evolved into grand monuments for the afterlife, represented by the Egyptian pyramids (Fig. 4.26) and Chinese imperial burial caves, the latter including entombed entourages intended to serve the ruler in the hereafter, such as Emperor Qin Shi Huang's terracotta army (Wood 2008).

The human premonition of death has led to tension between foresights acquired by the neocortex and the instant reflexes of the mammalian brain (Koestler 1986) (Fig. 4.17). Where the cerebral neocortex invents tools and techniques and identifies future dangers, the primitive brain reacts instinctively through defensive/aggressive impulses (Dawkins 1976), with ensuing conflict. When equipped with weapons designed by the intelligent brain, such responses lead to destructive violence, translated from the individual scale into tribal and global wars. By analogy to infanticide experienced by rival baboons, running through human history are mass sacrifices of the young, children thrown into the Moloch's fire, the Maya blood cult

Fig. 4.18 Mungo man No. 3, the skeleton of a tall middle-aged man, was excavated in March, 1974, by a team led by the late Alan Thorne (Photo C. Groves)

(Clendinnen 1995), all the way to generational sacrifice as in World War I and II – called '*war*', under tribal or religious flags, appeasing the angry gods in a quest for immortality.

A Maya war song (1300–1521 AD):

> There is nothing like death in war,
> Nothing like flowering death, so precious to him who gives life,
> Far off I see it, my heart yearns for it.

With the onset of space exploration, from the Sputnik to the lunar landings, the Galileo space craft and Voyager's interstellar mission, religious mythologies evolved into a space cult, alluding to colonization of the planets where, presumably, *H. sapiens* would proceed to overwhelm new environments. The suggestion by space race proponents as if life has been seeded on Earth by comets appears to be as

ideologically motivated as it is lacking in evidence. Thus, while hosting amino acids, comets and space dust are not known to contain biomolecules. The allusion of the space cult to panspermia and human propagation to other planets and solar systems ignores the central observation arising from planetary exploration—barring possible presence of microbes.

Ancient DNA sequences suggest that earlier than 400 kyr-ago *Homo neanderthalensis* diverged from the ancestors of modern humans (Endicott et al. 2010). *Homo sapiens* is thought to have evolved in Africa during the glacial period which preceded the Eemian interglacial period (~130–114 kyr) (Klein 2009): the earliest dates for fossils acknowledged to be modern in form are 195 kyr, possibly as early as 259 kyr (see Chap. 3.2). During this period and early parts of the last glacial, anatomically near-modern humans occupied the Levant (Bar-Yosef 2000), although for a long while they seem to have alternated with Neandertals (see Chap. 3.2) and it is only after 50 kyr that humans of near-modern behaviour occur in the archaeological record in the Near East. The major expansion of *H. sapiens* out-of-Africa probably occurred between 60 and 45 kyr (Henn et al. 2012) and human expansions outside of Africa were likely associated with climatic fluctuations (Stewart and Stringer 2012). Significantly this migration occurred following the coldest temperatures recorded in Greenland and Antarctic ice cores and related to the sun-blocking effects of the Toba volcanic eruption, dated by $^{40}Ar/^{39}Ar$ as 73.88 ± 0.32 kyr (Storey et al. 2012) (Fig. 4.19). The eruption is followed by ~10 °C drop in Greenland surface temperature over ~150 years, as related to the climatic impact of volcanic aerosols. The Toba super-eruption is estimated to have produced some 2500–3000 km^3 of lava and pyroclastics, probably injecting at least 10^{15}gr of fine ash into the stratosphere (Rampino and Self 1993; Gathorne-Hardy and Harcourt-Smith 2003). Ash and sulphate aerosols were deposited in both hemispheres, forming a time-marker horizon that can be used to synchronize late Quaternary records globally (Storey et al. 2012). The discovery of stone artifacts covered by Toba volcanic ash in Malaysia and India indicates that by 74 kyr *H. sapiens* or Denisovans had reached Southeast Asia (Petraglia et al. 2007; Timmreck et al. 2012). If so, survivors of the Toba eruption may have been able to migrate eastwards following the eruption, taking advantage of the low sea levels and newly exposed continental shelf and land bridges (Storey et al. 2012) (Fig. 4.16).

According to Ambrose (1998) Toba's volcanic winter could have nearly destroyed most modern human populations, especially outside isolated tropical enclaves (Fig. 4.19). The release from this population bottleneck could have occurred at the end of this phase, or about 10,000 years after the eruption, with most survivors found in the tropical refugia in equatorial Africa. DNA re-sequencing studies estimate the size of the ancestral population bottleneck in Africa as 12,800–14,400 individuals during ~65–50 kyr. It is suggested that a small group/s of only ~1000 to 2500 individuals moved from the African continent into the Near East (Henn et al. 2012). The 'Volcanic winter' effects of Toba may have reduced populations to levels low enough for 'founder effects', where local adaptations produced rapid differentiation at about 70 kyr. Around 50 kyr growth occurred within dispersed populations that were genetically isolated from each other.

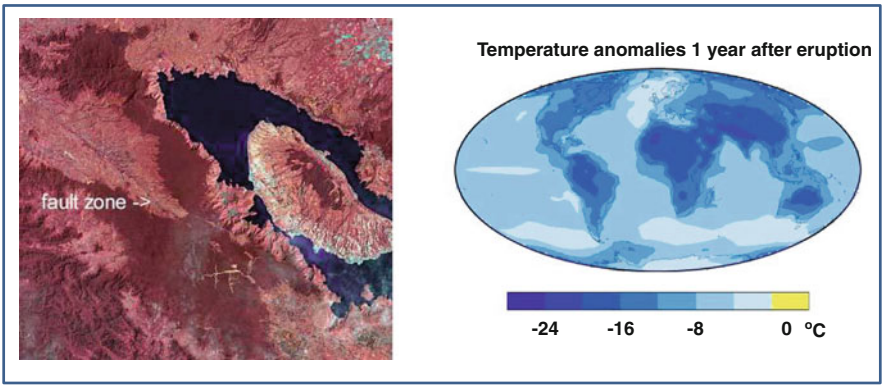

Fig. 4.19 The Toba volcanic eruption of ~77–69 kyr-ago: (**Left**) Landsat image of Toba caldera (Landsat Pathfinder Project); (**Right**) Annual near-surface temperature anomalies for the year following a super-volcanic eruption like the Toba eruption if it were to occur today. Most land areas cool by 12 °C compared to average. Some areas, like Africa, cool by 16 °C (Jones et al. 2005; Springer, by permission)

Gathorne-Hardy and Harcourt-Smith (2003) raise questions regarding a human population bottleneck following Toba and suggest there has been no mammal extinction associated with Toba. Human genome studies analyzing the Y-chromosome and mitochondrial DNA support the existence of a bottleneck in human evolution but the age of this bottleneck remains uncertain. Consistent with this view, archaeological finds (McBrearty and Brooks 2000) show that by 73.5 kyr modern humans occupied a diverse range of habitats over the whole African Continent, with complex tool-kits and ability to hunt and forage for a variety of different taxa over extensive areas (McBrearty and Brooks 2000; Gathorne-Hardy and Harcourt-Smith 2003).

By about 20,000 years-ago, toward the end of the last glacial age, *Homo sapiens* spread over much of Asia, Australasia and Europe. From paleo-anthropological and DNA evidence, the species interbred and replaced archaic human species, including the Neanderthals in Europe, the Denisovans in Siberia and *Homo floresiensis* on the Indonesian island of Flores (Brown et al. 2004; Stewart and Stringer 2012, and see Chap. 3.2). These authors pointed to the relation between the phylo-geographic (genetic bio-geographical), paleontological and DNA records of extant animals and human migration patterns by the end-Pleistocene, including evidence of extinctions. The genetics of human parasites, morphology and linguistics suggest the *H. sapiens* takeover involved an overall loss of genetic diversity. Thus whereas genomes from African populations retain a large number of unique variants, a dramatic reduction is observed in genetic diversity of people outside of Africa (Henn et al. 2012).

The long time gaps between the appearance of *Homo Habilis* with its small brain and simple Oldowan stone industry about 2.6–1.7 Ma, the emergence of burial possibly with *Homo heidelbergensis* (brain size ~1100–1400 cc) about ~0.6 Ma, and early signs of human cave rock painting, ornaments and sophisticated implements

by *Homo sapiens* (~1200–1500 cc) about ~100,000–70,000 years ago as in Blombos Cave, South Africa (Henshilwood et al. 2011), betrays log hiatus periods between these stages and uncertain correlation between brain size and the appearance of advanced cultural expressions (Ramachandran 2000). The latter author raises the question of the origin of the long gaps between the cultural evolution and brain size. Thus, what is the origin of the near to ~1 million years gap between the emergence of Oldowan stone tools and the Acheulean stone tools, and the near ~1 million years gap between the latter and the earliest signs of burial approximately ~600,000 years ago? Why has the human brain, which nearly reached its present size and intellectual level approximately 250,000 years ago, developed more modern attributes which appeared much later? Ramachandran (2000) attributes these changes to changes in neuron patterns in the human brain, including the emergence of "Mirror Neurons", present but much less abundant in greater apes, which can identify and respond to expressions by other creatures, identified by Giaccamo Rizzollati (Kohler et al. 2002) and correlated with the appearance of Acheulean stone tools at approximately ~1.76 Ma (Lepre et al. 2011). Mithen (2003) hypothesized that about 40,000 years ago three different brain modules previously isolated from each other began to communicate allowing flexibility and versatility of human consciousness. The factors underlying the episodic evolution of the Genus *Homo* remain little understood.

4.4 Neolithic Burning and Early Civilizations

In the wake of the last deglaciation (Fig. 4.20) peak pre-Holocene temperatures are represented by the ~14.7–12.9 kyr Bølling-Alerød interstadial, preceded by a cool '*Older Dryas'* phase and followed by sharp cooling at the '*Younger Dryas*' at 12.9–11.7 kyr (Fig. 4.21), succeeded by the Holocene Optimum (Shakun et al. 2012; Steffensen et al. 2008). Peak early Holocene conditions involved heavy precipitation and thereby rates of erosion (Clift et al. 2007), perhaps echoed by Noah's Ark story. At ~8.2 kyr a sharp temperature decline of several degrees Celsius in the North Atlantic was associated with discharge of cold water from the Laurentian ice sheet through Lake Agassiz (Wagner et al. 2002; Lewis et al. 2012; Wiersma et al. 2011) (Fig. 4.22). High temperatures during the Holocene maximum resulted in strong East African monsoons and higher rainfall in the Sahara relative to previous and succeeding periods, which explains the presence of animals like giraffes and elephants recorded in ancient rock paintings (Fig. 4.23). Consequently cooler and drier conditions ensued with temperature decline in the range of −1 °C to −5 °C in mid-latitudes and of −3 °C from ancient coral reef in Indonesia. Atmospheric CO_2 declined by ~25 ppm over ~300 years. About 8.2 kyr the earliest settled human communities in Catal Huyuk (southern Anatolia) were abandoned, likely due to droughts associated with the cooling, and were not reoccupied until about five centuries later when climate improved.

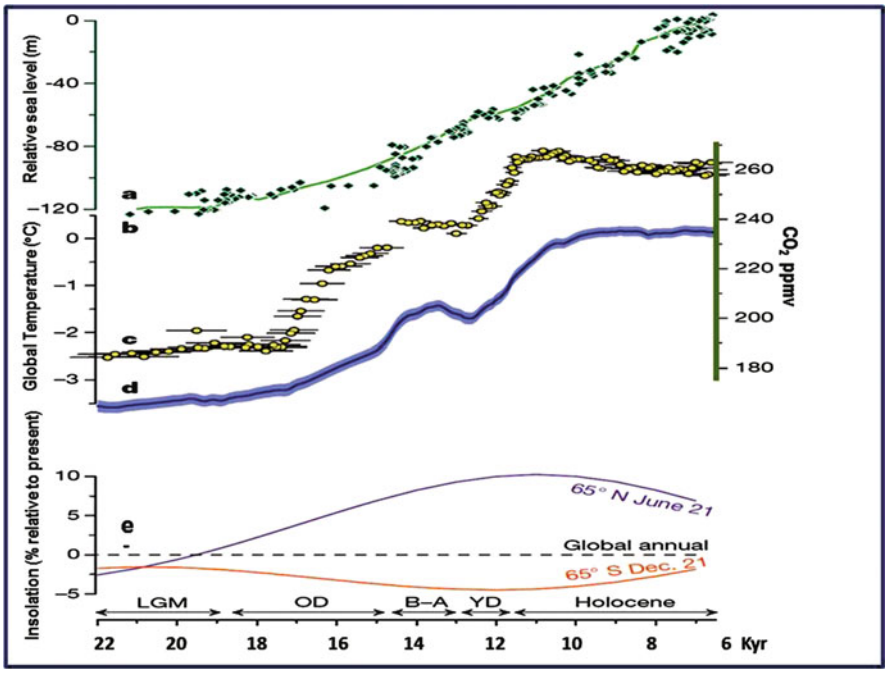

Fig. 4.20 Global temperature and climate forcings: (**a**) Relative sea level (diamonds); (**b**) Northern Hemisphere ice-sheet area (*line*) derived from summing the extents of the Laurentide, Cordilleran and Scandinavian ice sheets through time; (**c**) Atmospheric CO_2 concentration; (**d**) Global proxy temperature stack; (**e**) Insolation forcing for latitudes 65°N (*purple*) and 65°S (*orange*) at the local summer solstice, and global mean annual insolation (*dashed black*) (after Shakun et al. 2012; Nature, by permission)

A decline in CO_2 and methane following the Holocene Optimum at ~8–6 kyr was followed by a slow rise in CO_2 from ~6000 BP and methane from ~4000 BP (Fig. 4.24). According to Ruddiman (2003) the natural interglacial cycle has been overprinted by Neolithic burning and land clearing, halting a decline in CO_2 and methane and thereby an onset of the next glacial (Kutzbach et al. 2010) (Fig. 4.25). Other authors regard the mid-Holocene rise in greenhouse gases as a natural perturbation in the interglacial, comparable with features of the 420–405 kyr Holsteinian interglacial (Broecker and Stocker 2006). The late Holocene is interrupted by mild warming phase ~900–1400 AD years-ago (Medieval Warm Period) and a cool phase during ~1550–1800 AD (Little Ice Age), broadly corresponding to periods of solar insolation reaching +0.5 watt/m^2 and −0.5 watt/m^2 relative to pre-industrial levels, respectively, attributed in part to changes in insolation related to sunspot activity (Solanki 2002).

In the wake of climate disruptions associated with the last glacial termination about ~14 ~ 7.5 kyr ago, the climate stabilized between ~7 and 5 kyr when sea level reached maximum (Fig. 4.20). Of all the factors which underlie the rise and fall of ancient civilizations along the Nile, Tigris, Euphrates, Indus and the Yellow

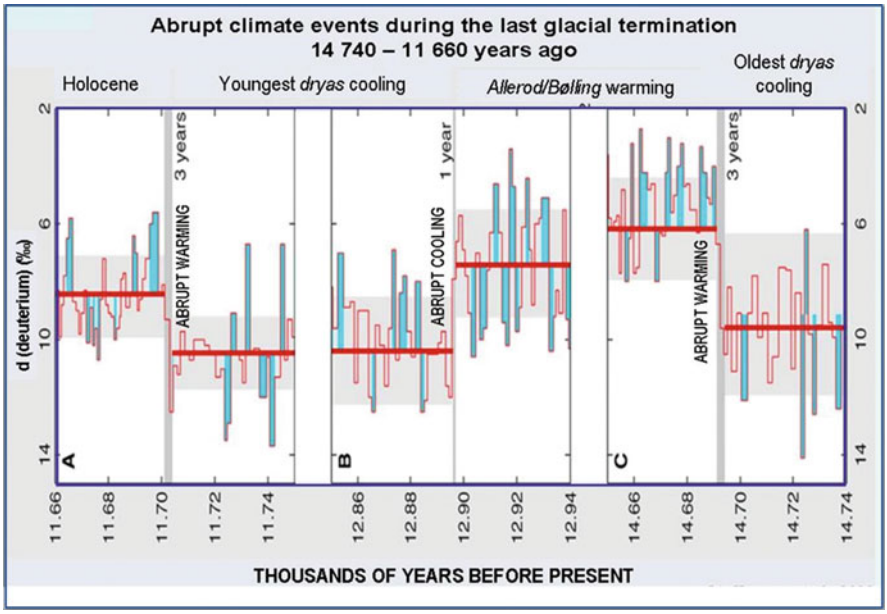

Fig. 4.21 d (deuterium)‰ variations during the last glacial termination 14,740–11,660 years-ago, marking the oldest dryas cooling, Allerod/Bolling warming, Youngest dryas cooling and Holocene optimum. The mean values are shown as *bold red lines*. Note the abrupt shifts over periods of 1–3 years between climate states (Steffensen et al. 2008; American Association for Advancement of Science, by permission)

River valleys, the main control was exerted by the seasonally regulated balance in their mountain source regions between accumulation and melting of snow. Thus cold spells would decrease river flow, resulting in droughts, whereas strong monsoons result in floods and erosion of terraces. Under stable rhythmic climate, seasonal regulation of river flow accompanied by deposition of fertile silt allowed river terrace cultivation, providing food for villages, towns and subsequently kingdoms and empires. The Nile River, fed by water from the Ethiopian Mountains, allowed a flourishing of the Old Kingdom (4660–4160 BP), Middle Kingdom (4040–3640 BP) and the New Kingdom (3550–3070 BP) (Fig. 4.26). The largest pyramids were built during the Old Kingdom. The greatest expansion of the Pharaoh's territories in the Middle East occurred during the New Kingdom.

Stages in the history of the Nile River included:

- ~20–12.5 kyr – Northeast Africa – frozen Ethiopian Mountains; stable sediment alluviation and terrace building by a low-flow river; Hunter-gatherers.
- ~12.5–8 kyr – Northeast Africa – high floods (the 'wild Nile') due to heavy rains in the Ethiopian Highlands; little rain along the Nile. Increased vegetation at the source leads to less sedimentation and thus greater erosion of river terraces; Near-disappearance of population.

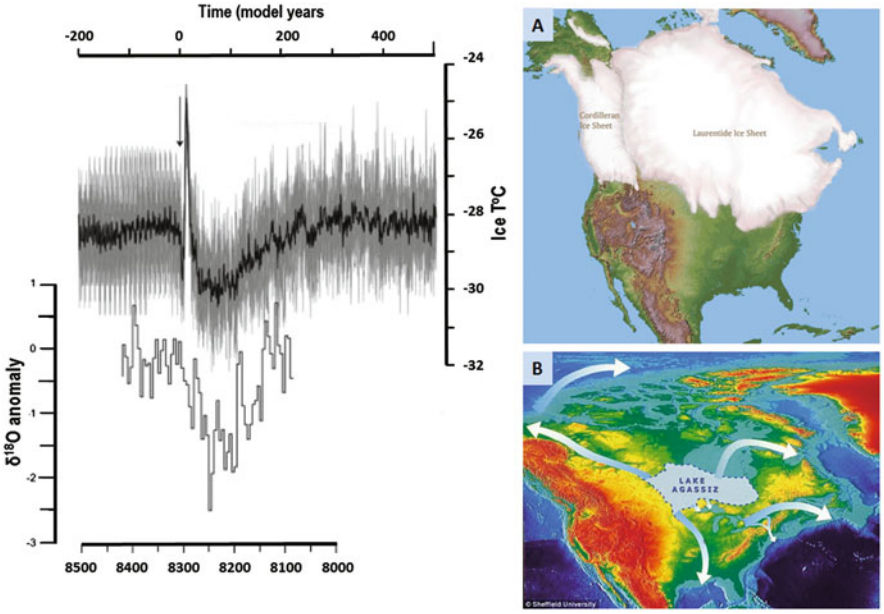

Fig. 4.22 (**Left**) Surface temperature response at Greenland Summit compared to the $\delta^{18}O$ profile as reconstructed from three Greenland ice cores. The time axes have the same scale, and the $\delta^{18}O$ profile is subjectively tied to the temperature profiles at the first decrease in both records (from Wiersma et al. 2011); (**A**) Original extent of the Laurentian ice sheet (Courtesy Randall Carlson) http://www.cosmographicresearch.org/prelim_glacial_maximum.htm); (**B**) Reconstruction of Lake Agassiz outflows south of the Laurentian ice sheet (http://www.sheffield.ac.uk/geography/about/100401) (Sheffield University based on NOAA ETOPO2 data, by permission)

- ~8–6 kyr – Seasonal climate, stabilization of the Nile and re-aggradation of alluvial terraces, allowing irrigated agriculture.
- ~7.5–5.1 kyr pre-dynastic Egypt.
- ~5.5 kyr – Retreat of the rain belt southward.
- ~4.686–4.181 kyr – Old Kingdom.
- ~4.2–4.0 kyr – Desertification.
- ~4.0–3.7 kyr – Middle Kingdom.
- ~3.570–3.069 kyr – New Kingdom
- ~3.2–2.55 kyr – Iron age cold period

The ~4.1 kyr desertification constituted one of the most severe climatic events of the Holocene period in terms of impact on civilization, and it is thought that at this time the White Nile ceased to flow continuously. It is very likely to have caused the collapse of the Old Kingdom in Egypt as well as the Akkadian Empire in Mesopotamia, and Indus Harappan cultural domain. Radiocarbon age determination from Tell Leilan, northeast Syria, uncovers evidence for an incipient collapse of the Acadian empire near 4170 ± 150 BP (Weiss et al. 1993). Deep sea core sediments

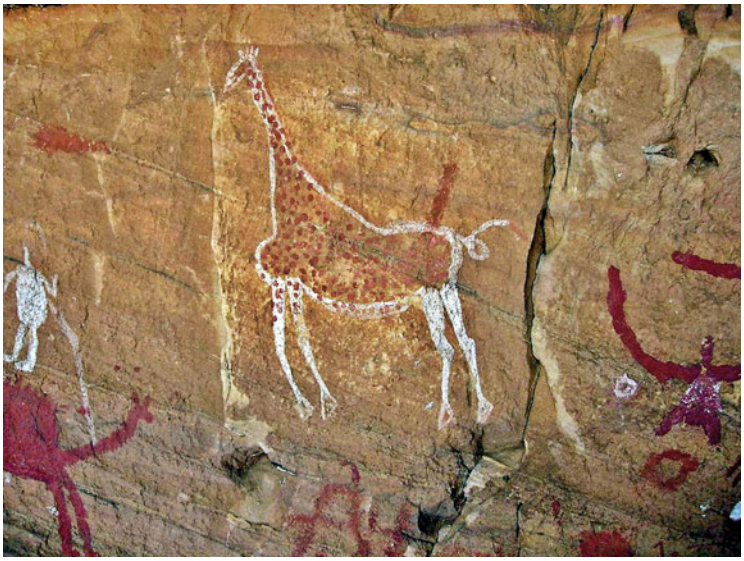

Fig. 4.23 Sahara peak Holocene rock painting. Wikipedia Commons http://en.wikipedia.org/wiki/File:Tadrart_Acacus_1.jpg. Tadrart Acacus form a mountain range in the Sahara desert of western Libya. The area is known for its rock paintings dating from 12,000 BC to 100 AD. The paintings reflect the changing environment of the Sahara desert which used to have a much wetter climate. Nine thousand years-ago the surroundings were green with lakes and forests and with large herds of wild animals as demonstrated by rock paintings at Tadrart Acacus of animals such as giraffes, elephants and ostriches (Photographer: Roberto D'Angelo (roberdan))

from the Gulf of Oman testify to a several-fold increase in wind-borne aeolian components from 4025 ± 125 BP, representing development of arid conditions in the source regions of the dust in Mesopotamia (Cullen et al. 2000).

The Tigris and Euphrates rivers, fed by the waters from the Taurus Mountains, constitute the cradle of the Mesopotamian ("Land between the rivers") civilization, where irrigation developed from about 6000 BP and Sumer cities grew between 3200 and 2350 BP, succeeded by Babylon. The Harappan civilization was developed by Dravidians people along the Indus River, fed from the Himalaya. Cultivation along the Yellow and Yangzi Rivers including the Xia, Shang and the Zhou Dynasties developed from about 7000 BP.

According to deMenocal (2001) late Holocene climate perturbations included repeated inter-annual droughts and infrequent decadal droughts. Multi-decade-long to multi-century-long droughts were rare but formed integral components of the natural climate variability. Paleoclimate and archaeological records demonstrate close relations between prolonged droughts and social collapse. Overpopulation, deforestation, resource depletion and warfare reinforced social collapse. Repeated droughts likely constituted the root factors in the downfall of the Acadian, Maya, Mochica and Tiwanaku civilizations (Shen 2012).

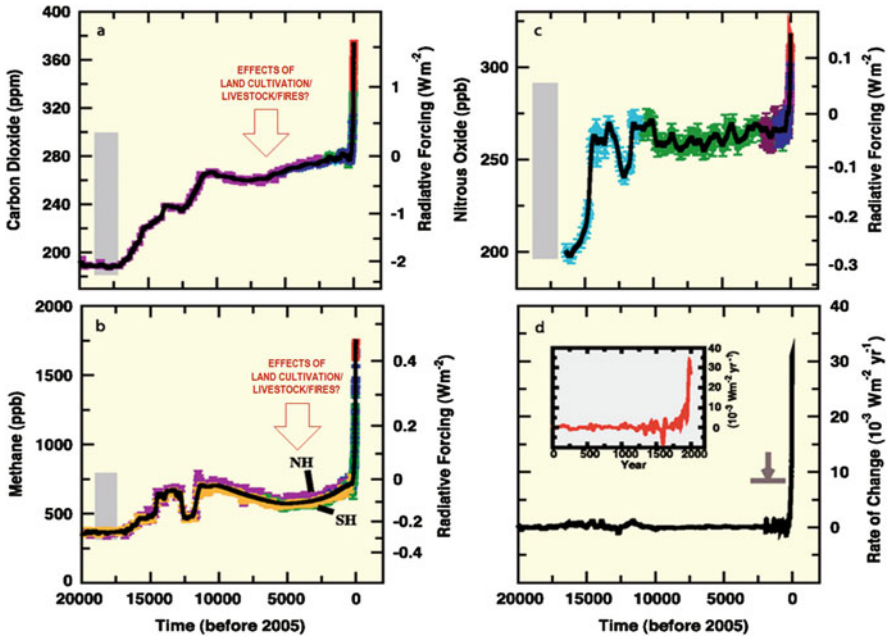

Fig. 4.24 Atmospheric concentrations of CO_2, CH_4 and N_2O over the last 10,000 years (large panels) and since 1750 (inset panels). Measurements are shown from ice cores (symbols with different colors for different studies) and atmospheric samples (*red lines*). The corresponding radiative forcing values are shown on the right hand axes of the large panels (IPCC AR4 Fig. SPM.1). Note the weak onset of CO_2 rise from about ~6 kyr-ago and CH4 about 4 kyr-ago, likely signifying the effects of deforestation, cultivation and fires. Top left - CO_2; Bottom left - methane; Top right - Nitrous oxide; Bottom right - rate of change of radiative forcing

A dry period in central America during 530–650 AD, followed by droughts during 800–1000 AD, recorded by high gypsum precipitation and high $\delta^{18}O$ in lake sediments (Lakes Chichancanab and Punta Laguna) led to collapse of the Maya civilization between 750 and 790 AD (Fig. 4.27). The last Maya monument was constructed in 990 AD (deMenocal 2001). Further confirmation of these trends is based on a paleoclimate study of Balum Cave deposits, Belize, correlated with dated Maya stone monuments (Shen 2012). The study indicates a high rainfall period during 440–660 AD followed by a drying trend between 660 and 1000 AD, leading to collapse between 1020 and 1100 AD.

A decrease in temperatures during 600–1000 AD is also recorded in the Quelccaya ice cores in Peru, showing an increase in the accumulation of ice and dust particles, signifying colder climate and a decrease in precipitation which affected the Tiwanaku civilization (300–1100 AD), leading to collapse between 1100 and 1400 AD. Based on the study of tree rings, during the fourteenth and fifteenth centuries, the Khmer Empire in Cambodia experienced decades-long droughts induced by strong El Nino events, interspersed with intense monsoons.

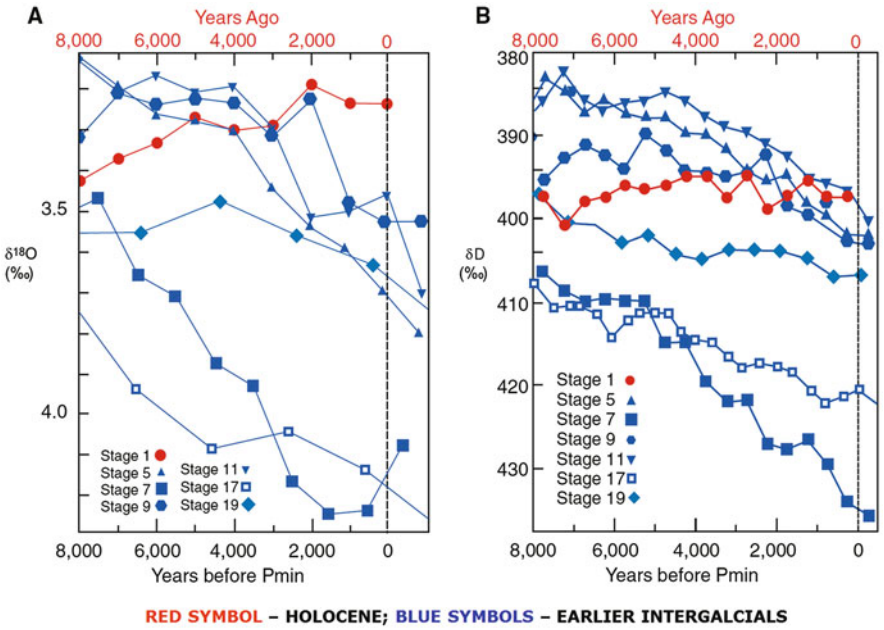

Fig. 4.25 The early Anthropocene hypothesis: (**a**) Isotopic $\delta^{18}O$ evidence for an anomalous warming trend in the late Holocene based on studies of benthic foraminifera (Lisiecki and Raymo 2005) showing a trend toward lighter $\delta^{18}O$ (warmer) values in the late Holocene, but trends toward heavier $\delta^{18}O$ (colder) values during earlier inter-glaciations; (**b**) Deuterium (δD) trend at Dome C Antarctica (Jouzel et al. 2007) shows a stable warming trend during the late Holocene, but trends toward lighter (colder) values during earlier inter-glaciations (Kutzbach et al. 2010 and Jouzel et al. 2007; Courtesy J. Jouzel; Springer, with permission; American Association for the Advancement of Science, with permission)

Increased climate variability, which damaged water supply dams and canals on which the Angkor Watt depended, led to the demise of Khmer civilization (Fig. 4.28) (Buckley et al. 2010).

The end of the 1st millennium and the first half of the 2nd millennium constituted the *Medieval Warm Period* (MWP – 900–1200 AD), which was about +0.4 °C warmer than the period ~1500–1900 AD (Fig. 4.29). The coolest century was the 17th (−0.4 °C relative to pre-industrial temperatures), including the *Little Ice Age* ~1600–1700 AD related to a near-absence of sun spots (Jones et al. 2001; Solanki 2002). Multi-proxy temperature reconstructions for the northern hemisphere show that the recent 30-year period is likely to have been the warmest of the millennium (Jones et al. 2001). Southern Hemisphere temperature reconstructions indicate cooler conditions before 1900 but the data are less reliable than northern hemisphere data. From the above, civilizations depended critically on specific climate conditions and have collapsed to a major extent due to natural climate variability

Fig. 4.26 The rise of ancient river civilizations – Egypt and Babylon. (**a**) The wheat harvest; (**b**) The Giza Cheops Pyramids 4589–4566 BP, 2,300,000 giant stone blocks over 2.5 tons, 100,000 slaves. Wikipedia Commons http://en.wikipedia.org/wiki/File:All_Gizah_Pyramids.jpg. (**c**) Tower of Babel, by Gustav Doré 1866. Wikipedia Commons http://en.wikipedia.org/wiki/File:Confusion_of_Tongues.png

which led to economic and social crises, decline in population and war (Diamond 2005; Morris 2011). Collapse may have occurred intermittently, as in Egypt and China, or become terminal as in Easter Island, the Maya.

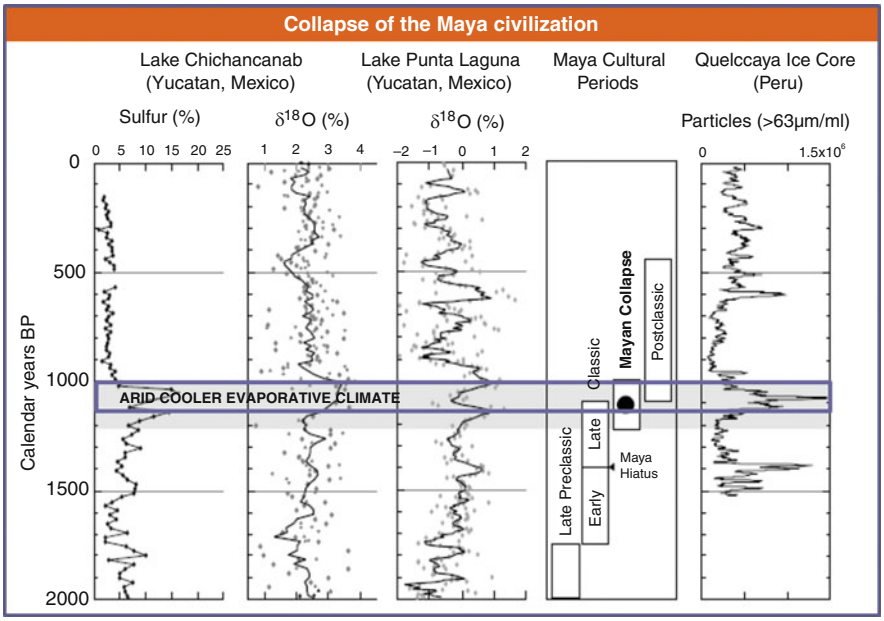

Fig. 4.27 Incipient collapse of the Classic Maya civilization near 750–790 A.D. The last Maya monument construction has been dated at 909 A.D. from the Maya Long Count inscriptions. Well-dated sediment cores from Lakes Chichancanab and Punta Laguna (northern Yucatan Peninsula, Mexico) document an abrupt onset of more arid conditions spanning 200 years between 800 and 1000 A.D., as evidenced by more evaporative (higher) $\delta^{18}O$ values and increases in gypsum precipitation signifying elevated sulphur content. Wind-borne particle concentrations from the annually dated Quelccaya ice core in the Peruvian altiplano are also shown (deMenocal 2001; Courtesy P. deMenocal; American Association for Advancement of Science, by permission)

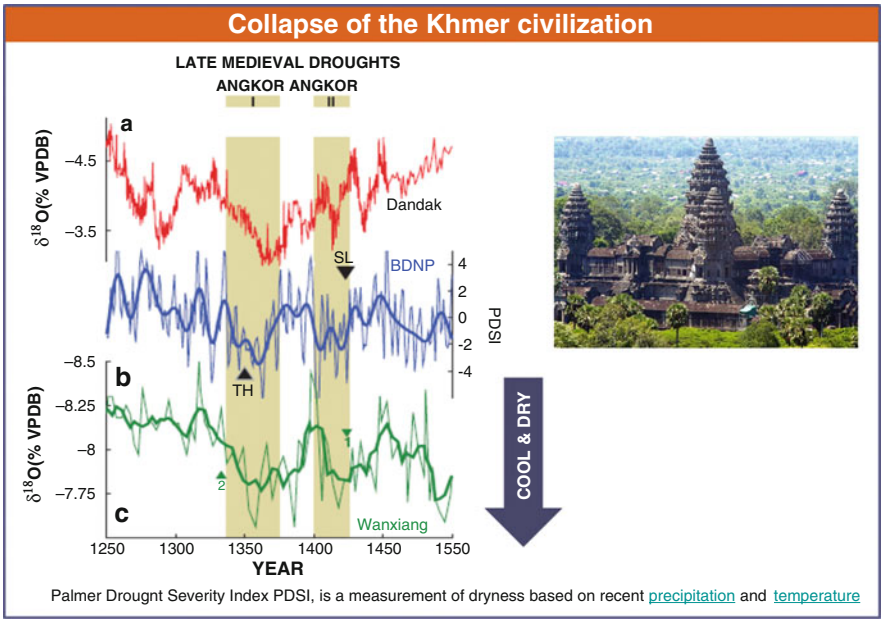

Fig. 4.28 Regional paleoclimate records of medieval drought in Southeast Asia. Dandak Cave $\delta^{18}O$ record (**a**) from the core monsoon region of India and Bidoup Nui Ba National Park (BDNP) PDSI reconstruction; (**b**) heavy line 15-year Butterworth filter from southern Vietnam, and the speleothem $\delta^{18}O$ record from Wanxiang Cave; (**c**) heavy line (five-point boxcar filter) in China. The fourteenth and early fifteenth century Angkor droughts are indicated by the *brown shaded bars*. Historical records of the fourteenth and fifteenth century droughts come from Phitsanulok in modern Thailand (TH) and Sri Lanka (SL) and are indicated by *black triangles* (Buckley et al. 2010. Proceedings National Academy of Science USA, by permission)

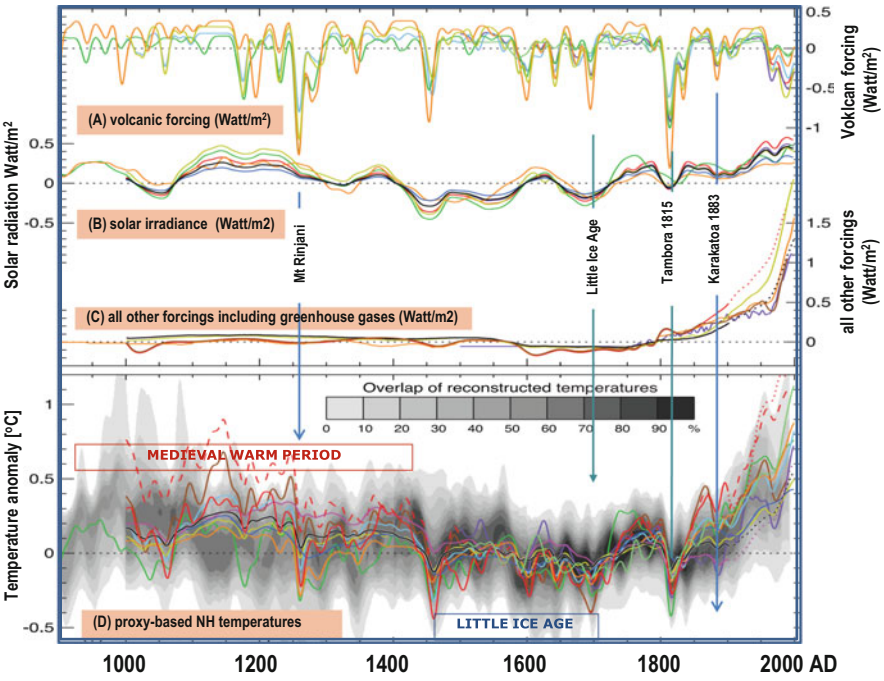

Fig. 4.29 Radiative forcings and simulated temperatures during the last 1.1 kyr. Global mean radiative forcing (Watt/m^{-2}) used to drive climate model simulations due to (**a**) volcanic activity, (**b**) solar irradiance variations and (**c**) all other forcings (which vary between models, but always include greenhouse gases, and, except for those with *dotted lines* after 1900, tropospheric sulphate aerosols). (**d**) Annual mean Northern Hemisphere temperature (°C) simulated under the range of forcings shown in (**a**)–(**c**), compared with the concentration of overlapping NH temperature reconstructions (shown by *grey shading*, modified to account for the 1500–1899 reference period. All forcings and temperatures are expressed as anomalies from their 1500–1899 means and then smoothed with a Gaussian-weighted filter to remove fluctuations on time scales less than 30 years; smoothed values are obtained up to both ends of each record by extending the records with the mean of the adjacent existing values

Chapter 5
The Anthropocene

Ozymandias

I met a traveler from an antique land
Who said: "Two vast and trunkless legs of stone
Stand in the desert. Near them on the sand,
Half sunk, a shattered visage lies, whose frown
And wrinkled lip and sneer of cold command
Tell that its sculptor well those passions read
Which yet survive, stamped on these lifeless things,
The hand that mocked them and the heart that fed.
And on the pedestal these words appear:
'My name is Ozymandias, King of Kings:
Look on my works, ye mighty, and despair!'
Nothing beside remains. Round the decay
Of that colossal wreck, boundless and bare,
The lone and level sands stretch far away".

(Percy Bysshe Shelley)

Abstract Nature includes species whose activities are capable of devastating habitats, examples include toxic viruses, methane (CH_4) and hydrogen sulphide (H_2S)-emitting bacteria, fire ant armies, locust swarms and rabbit populations. Parasitic host-destroying organisms include species of fungi, worms, arthropods, annelids and vertebrates, cf. oxpeckers and vampire bats. The mastery of fire has enabled the genus *Homo* to magnify its potential to harness and release energy by orders of magnitude, increasing entropy in nature on a scale unprecedented in the Cenozoic (since 65 Ma). Within a few thousand years since the onset of civilization in the great river valleys – the Nile, Euphrates, Indus, Ganges, Mekong and Yellow Rivers – the terrestrial biosphere has been transformed at an accelerated rate, tracking toward Pliocene-like conditions where temperatures exceed 2 ° Celsius above Pleistocene interglacial conditions. A return to greenhouse atmosphere conditions would render large parts of the continents subject to extreme weather events, unsuitable for agriculture and thereby for civilization. Rapid acidification of the oceans induced by high atmospheric CO_2 levels would seriously damage the base of the food chain and all marine life. From the mid-twentieth century, the splitting of the atom allowed individuals to trigger a chain reaction, potentially devastating much

A.Y. Glikson, C. Groves, *Climate, Fire and Human Evolution*, Modern Approaches in Solid Earth Sciences 10, DOI 10.1007/978-3-319-22512-8_5

of the biosphere. Once a species has developed sources of energy of this magnitude the species would need to be perfectly wise and responsible if it is to prevent its inventions from getting out of control.

5.1 The Modern Atmosphere

The layered atmosphere, including the troposphere, stratosphere, mesosphere, thermosphere and exosphere (Fig. 5.1) is energized by solar radiation (343.2 Watt/m^2) (Fig. 5.2) oscillating according to the 11 years sun-spot cycle (Fig. 5.3) and longer term cycles (Solanki 2002). Insolation is mitigated by greenhouse gases (H_2O, CO_2, CH_4, CO, N_2, CFC [chlorofluorocarbons]), with intermittent effects. According to Trenberth et al. (2009): "*Weather and climate on Earth are determined by the amount and distribution of incoming radiation from the sun. For an equilibrium climate, Outgoing Long Wavelength Radiation necessarily balances the incoming Absorbed Solar Radiation, although there is a great deal of fascinating atmosphere, ocean, and land phenomena that couple the two. Incoming radiant energy may be scattered and reflected by clouds and aerosols or absorbed in the atmosphere.*

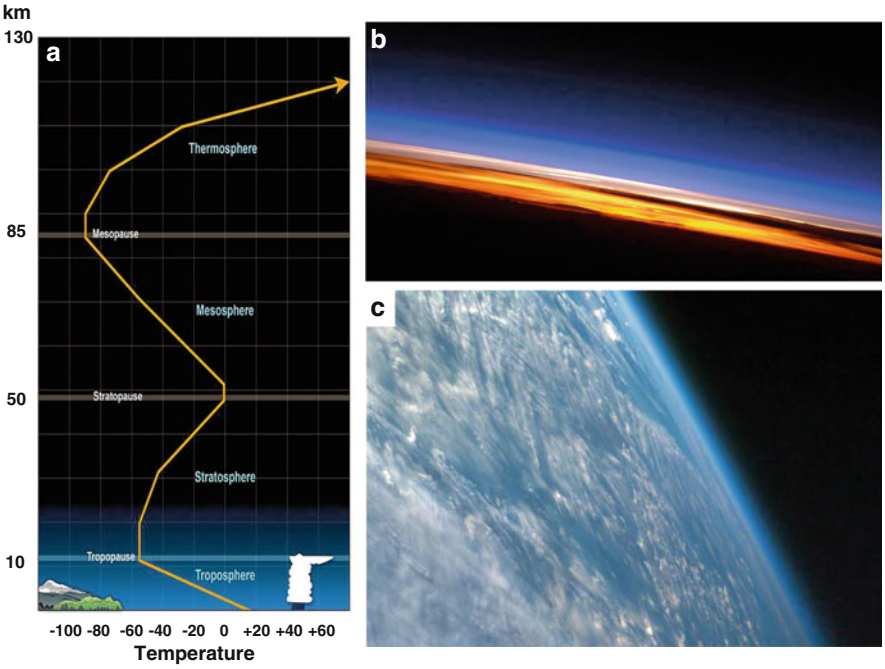

Fig. 5.1 (**a**) Vertical profile of the atmosphere http://www.srh.noaa.gov/jetstream/atmos/atmprofile.htm; (**b**) The layered structure of Earth's atmosphere visible in a sunset view from the international space station (Credit: image science & analysis laboratory, NASA Johnson Space Center http://scied.ucar.edu/shortcontent/earths-atmosphere); (**c**) Satellite view of the atmosphere http://www.grc.nasa.gov/WWW/k-12/airplane/atmosphere.html

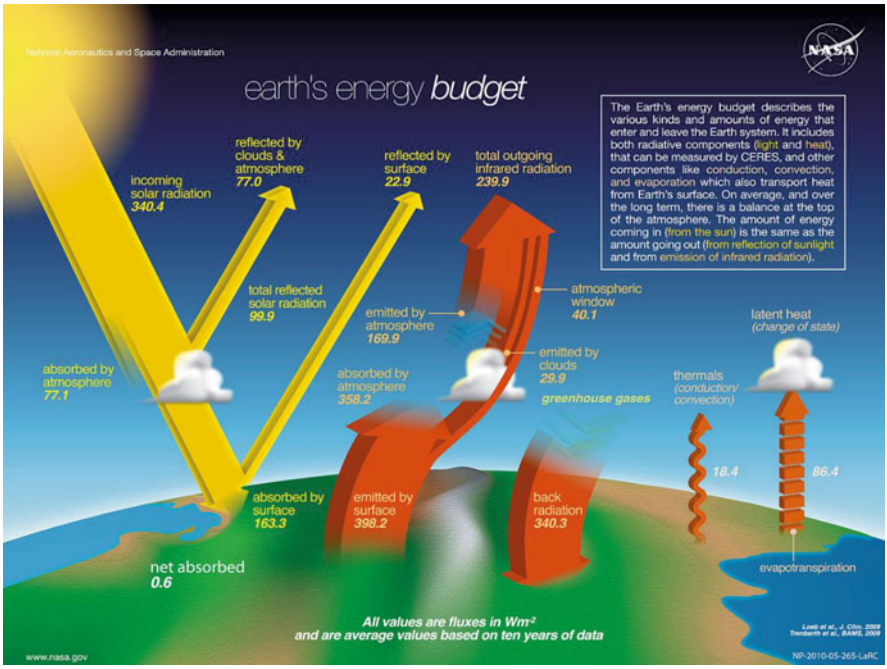

Fig. 5.2 The global annual mean earth's energy budget (NASA). Earth's climate is largely determined by the planet's energy budget, i.e., the balance of incoming and outgoing radiation. It is measured by satellites and shown in W/m² http://en.wikipedia.org/wiki/Earth's_energy_budget#mediaviewer/File:The-NASA-Earth%27s-Energy-Budget-Poster-Radiant-Energy-System-satellite-infrared-radiation-fluxes.jpg

The transmitted radiation is then either absorbed or reflected at the Earth's surface. Radiant solar or shortwave energy is transformed into sensible heat, latent energy (involving different water states), potential energy, and kinetic energy before being emitted as longwave radiant energy. Energy may be stored for some time, transported in various forms, and converted among the different types, giving rise to a rich variety of weather or turbulent phenomena in the atmosphere and ocean. Moreover, the energy balance can be upset in various ways, changing the climate and associated weather."

Solar radiation is amplified by feedback mechanisms such as ice melt, methane release and fires. Temperatures are mitigated by aerosols (SO_2, dust particles, ash, black carbon, salt particles) (Fig. 5.4) reflection from clouds and absorption by the land surface and are redistributed by wind currents (Figs. 5.5 and 5.6) and ocean currents (Fig. 5.7). The latter interact with land-sea-ocean and mountain patterns which results in a complex system of climate zones including polar regions (Fig. 5.8, 5.9). Jet streams and air and water currents, driven by temperature gradients, morphological variations, land-water patterns and the Earth's rotation (Coriolis force) give rise to major ocean gyres (Fig. 5.7c). Thermohaline currents driven by temperature and salinity variations drive cold water from the southern

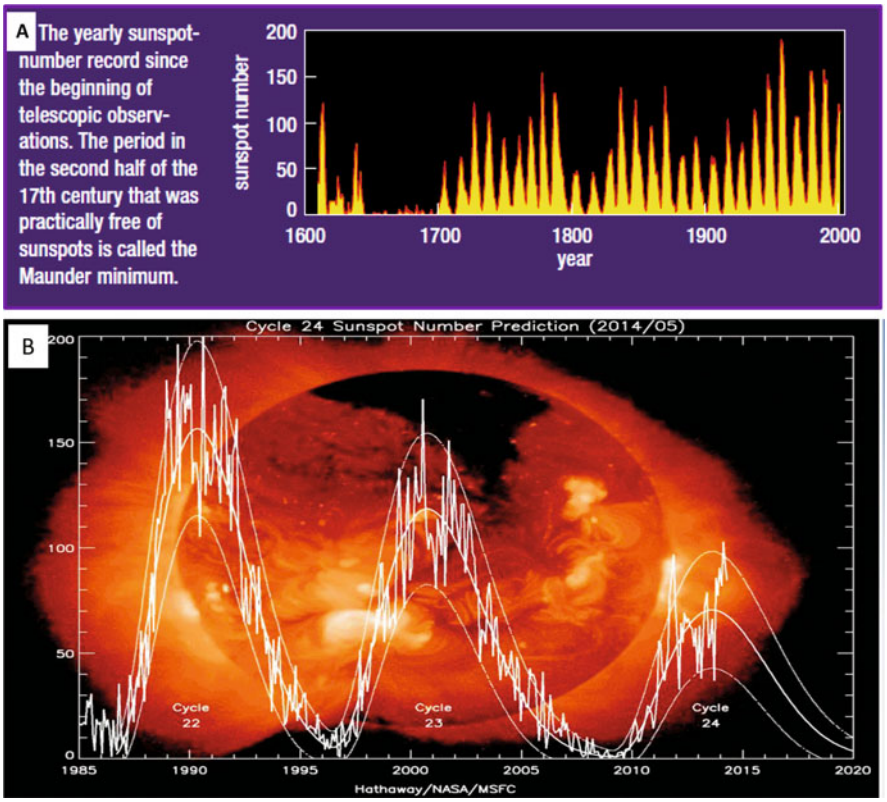

Fig. 5.3 (**A**) Variations in the 11-years sun-spot cycle since 1600 AD. Note the cessation of sun spots during 1640–1690 (Solanki 2002); (**B**) Sun spot numbers since 1985 and projections to 2020. http://www.lunarplanner.com/SolarCycles.html. The decline in maximum number of sun spots from cycle 22 to cycle 24 suggests a long term decline in sun spot activity (Image credit: NOAA/ Space Weather Prediction Center http://solarscience.msfc.nasa.gov/predict.shtml)

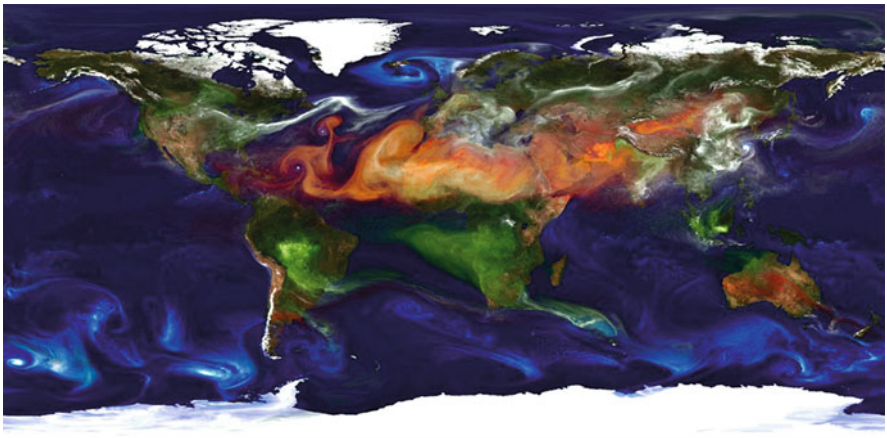

Fig. 5.4 NASA: Portrait of global aerosol distribution http://www.earthpowernews.com/nasa-portrait-of-global-aerosols/

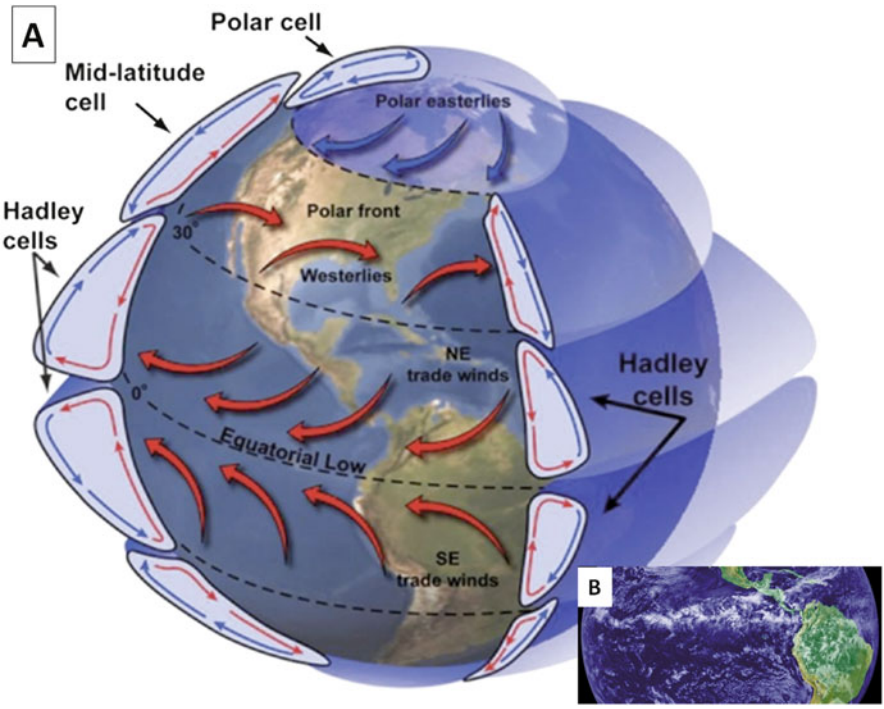

Fig. 5.5 (**a**) Wind patterns over North America and the Eastern Pacific Ocean, showing the polar easterlies, polar front, mid-latitude westerlies, NE and SE trade winds and the polar and Hadley cells. http://www.bing.com/images/search?q=NASA+global+wind+pattern&qs=n&form=QBIR&pq=nasa+global+wind+pattern&sc=0-19&sp=-1&sk=#view=detail&id=B0177F6A177DE962F5261198132A9D9198AC5010&selectedIndex=91 http://eoimages.gsfc.nasa.gov/images/imagerecords/0/703/itcz_goes11_lrg.jpg (**b**) Composite satellite image showing the cloud belt over the tropical Pacific convergence zone. http://eoimages.gsfc.nasa.gov/images/imagerecords/0/703/itcz_goes11_lrg.jpg

oceans to low latitudes and warm water from tropical oceans to high latitudes. Examples include the Humboldt Current flowing north along the Chilean and Peruvian coasts, the California Current flowing south from Alaska to the California coast and the Gulf Stream emanating from the Gulf of Mexico and flowing to the North Atlantic Ocean, where it warms higher latitude zones of Western Europe and northeast America (Fig. 5.7c, d). Driven by its high salinity the North Atlantic Thermohaline Current plunges to depths where cold water production initiates a cold southward bottom flow (Fig. 5.7c).

Major elements of the global climate system include meridional tropical low pressure cells (Hadley Cell) diverging and descending as dry air masses producing arid zones such as the Sahara Desert (Fig. 5.6). Latitudinal Pacific Ocean cells (Walker Circulation) related to the El Nino – La Nina cycle (ENSO) result in extreme weather phenomena in the eastern and western Pacific Ocean and globally (Fig. 5.5). Cold wind vortexes controlled by the Coriolis force originate from polar

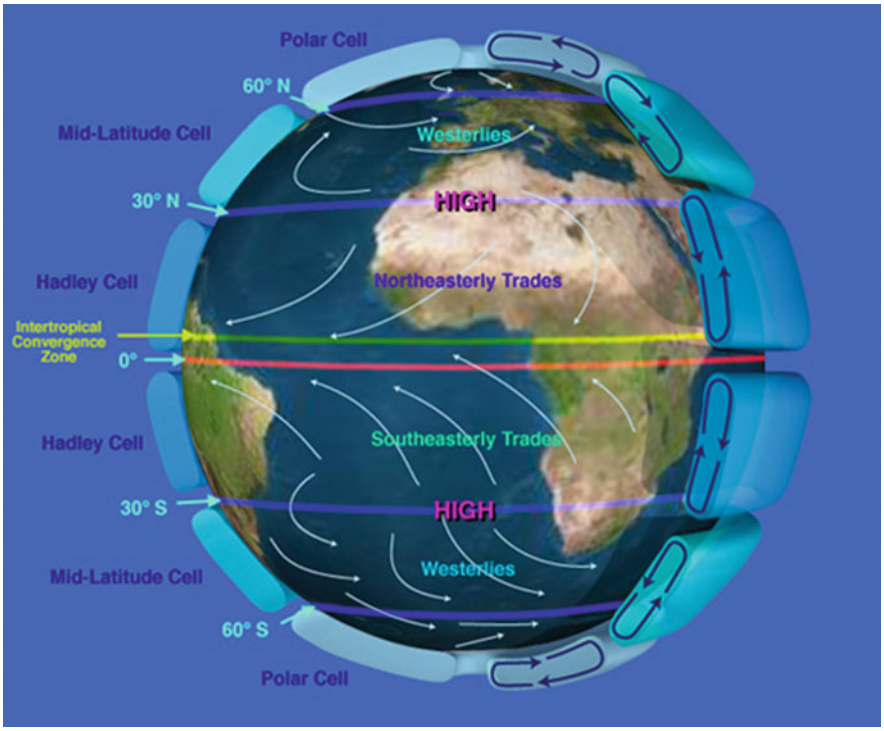

Fig. 5.6 Wind Patterns over the central Atlantic Ocean and Africa, showing the mid-latitude trade winds, westerlies, mid-latitude convergence zone, the Hadley cells, mid-latitude cells and polar cells. http://sealevel.jpl.nasa.gov/overview/climate-climatic.html

cells such as the Arctic and Antarctic vortices (Figs. 5.5, 5.6, and 5.8). Subtropical high pressure ridges (Ferrell Cell, Horse latitudes: 30 N, 30S) control SW-directed and NW-directed trade winds and NE and SE-directed Westerly winds (Figs. 5.5 and 5.6). The eastward-directed circum-Antarctic Southern Ocean, driven by the Antarctic wind vortex diverges northward along the western shores of Africa, Australia and South America, with ensuing coastal deserts in Namibia (Namib Desert) and Chile (Atacama Desert) (Fig. 5.5). Superposed on these patterns are aerosols derived from dust, salt spray, soot and sulphur dioxide emanating from industrial activities (Fig. 5.4).

Moisture-laden air masses forming over the oceans penetrate arid warm land masses during and late in summer, resulting in heavy precipitation critical for agriculture in southern and southeastern continents. Examples include the southwest Indian, west African and southeast Asian monsoons, cyclone systems off northwest and northeast Australia and cold fronts of the Antarctic wind vortex penetrating southwestern Australia (Fig. 5.8c). The Pacific Ocean gyre, including the Hadley cell, Walker Circulation and the El Nino Southern Oscillation (ENSO) cycles (Fig. 5.5), induces global effects extending as far west as India, Africa and other regions.

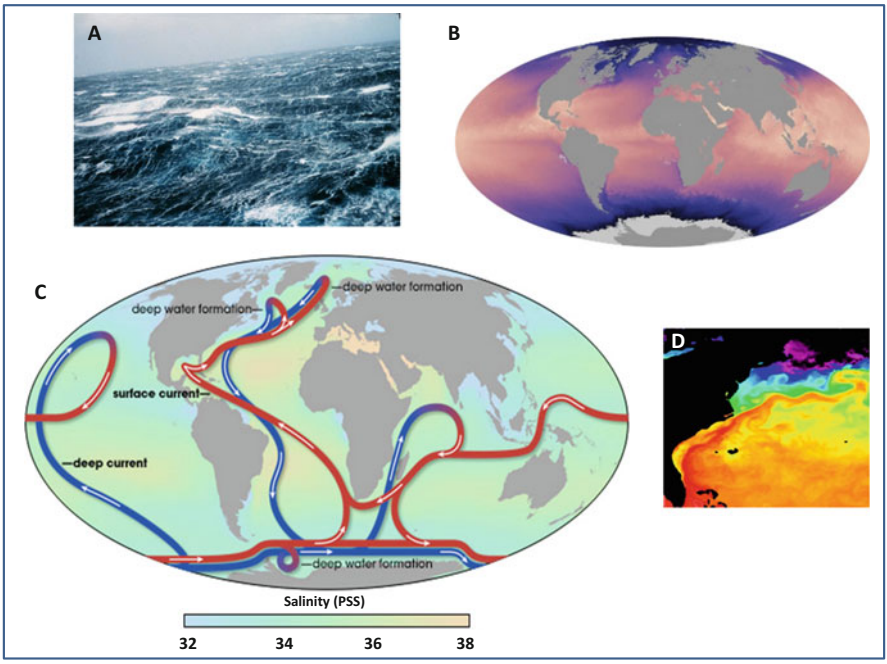

Fig. 5.7 The oceans: (**a**) Atlantic storm; http://www.giss.nasa.gov/research/news/20030903/wea00816.jpg; (**b**) Global ocean temperatures deduced from $\delta^{18}O$ isotopic ratios Animation for July 2002 to September 2014 at: http://earthobservatory.nasa.gov/GlobalMaps/view.php?d1=MYD28M; (**c**) Global ocean currents http://earthobservatory.nasa.gov/Features/Paleoclimatology_Evidence/paleoclimatology_evidence_2.php; (**d**) the Gulf stream and the North Atlantic Thermohaline Current. http://podaac.jpl.nasa.gov/sites/default/files/image/images/chartImage2final.jpg

Pulsations of the cold Humboldt current, driven northward along the western South American coast, and the effect of cold air masses, lead to cyclic polarized anomalies, including effects on the ENSO (El Nino Southern Oscillation) (Fig. 5.36):

A. The La Nina phase, with equatorial warm water driven westward by the trade winds, results in a rise (<60 cm) of warm water in the west Pacific, heavy evaporation and precipitation extending across the Indian Ocean and even east to Africa. By contrast the La Nina phase results in droughts in northwest South America and in California.
B. The El Nino phase, where warm water flows back from the western Pacific Ocean to the eastern Pacific Ocean, with consequent rain storms in northwest South America (Ecuador, Columbia) (Figs. 5.5, and 5.36).

Solar insolation associated with orbital forcing (Fig. 1.26) plays a major factor in inducing glacial terminations. Near-cessation of sun spots, representing a lull in solar magnetic storms during ~1640–1690 AD, resulted in sharp drop of temperatures

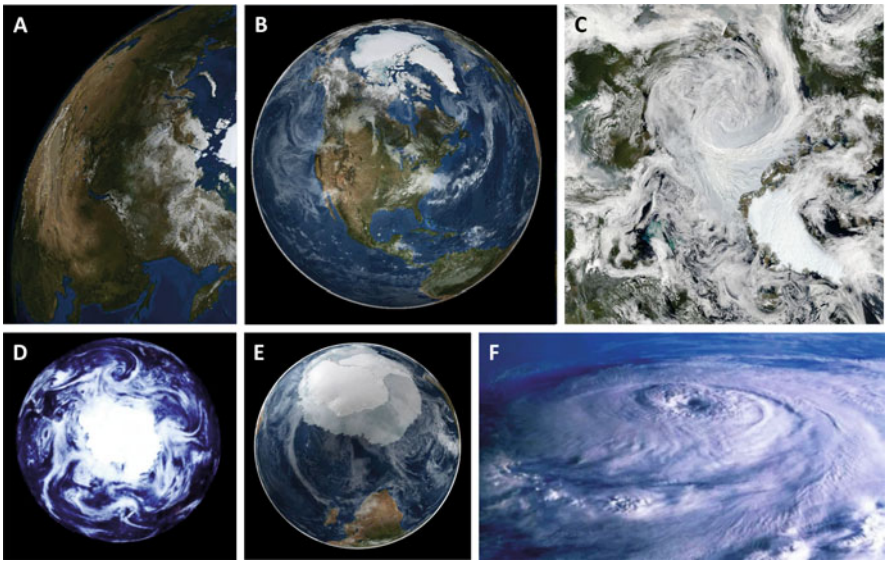

Fig. 5.8 The poles: (**A**) Composite satellite image of northern Eurasia and the Arctic circle http://www.nasa.gov/topics/earth/features/sea_ice_nsidc.html; (**B**) View of North America and the Arctic circle, September 21, 2005. http://svs.gsfc.nasa.gov/cgi-bin/details.cgi?aid=3402; (**C**) Arctic storm http://www.nasa.gov/topics/earth/features/arctic-storm.html; (**D**) Composite image of the Antarctic wind vortex (NASA, Galileo). The weather systems driven by the strong westerly winds of the Antarctic polar vortex curl over the southern continents. http://www.abc.net.au/science/news/enviro/EnviroRepublish_946924.htm; (**E**) View of the Antarctic continent and part of southern Africa, September 21, 2005. http://svs.gsfc.nasa.gov/cgi-bin/details.cgi?aid=3402; (**F**) Satellite image of the Antarctic wind vortex. NASA. http://environment-clean-generations.blogspot.com.au/2011/08/top-10-differences-between-north-pole.html

during the "Little Ice Age" (LIA). An increase in the number of sun spots during the first half of the twentieth century resulted in a rise in insolation by approximately ~0.2 Watt/m2 (Solanki 2002). From the mid-twentieth century variations in insolation were limited to the 11-years sun spot cycle in the range of ~0–150 sun spots, affecting radiative forcing in the range of ±0.2 Watt/m^2. From about 1985 the peak of sun spot activity has been declining (Fig. 5.3) yet global temperatures have been rising due to elevated GHG by as much as ~+0.6 °C (Figs. 5.19 and 5.20) leading to a rise in extreme weather events (Figs. 5.19, 5.20, and 5.30)

A major feedback for global warming is furnished by fires, bringing about major release of CO_2 (Fig. 5.10). Burning of vegetation leads to a decrease in photosynthesis (Figs. 5.11 and 5.12) and the production of oxygen (Fig. 5.13). The increase in atmospheric CO_2, with high solubility in cold high latitude and polar oceans, lowers the pH of the water (Figs. 5.33 and 5.34), with major effects on the base of the marine food chain (Fig. 5.35).

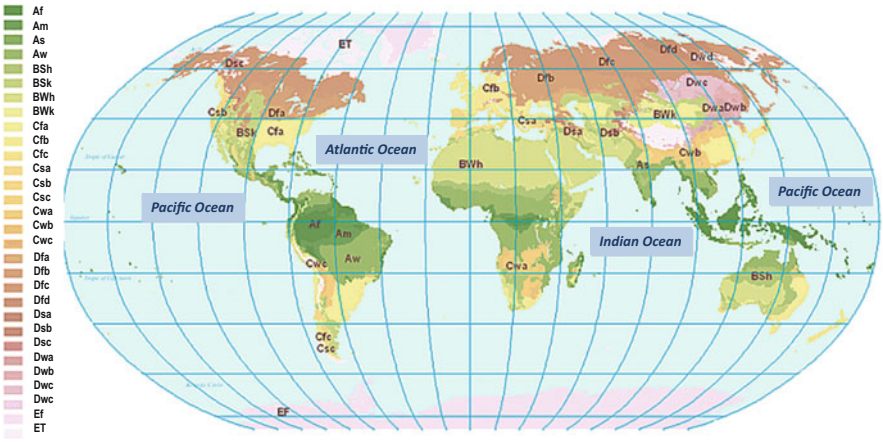

Fig. 5.9 Climate zones. Köppen further divided each major divisions (A, B, C, D, E, F, H) into smaller groups based upon precipitation and temperature patterns. http://www.srh.noaa.gov/jetstream/global/climate_max.htm; These subcategories are as follows:
Second letter add additional divisions based on precipitation pattern
f – wet year-round
s – dry summer season
w – dry winter season
m – monsoon
Third letter (lower case) add additional divisions based in temperature pattern
a – hot summer
b – warm summer
c – cool summer
d – very cold winters

The complete Köppen climates

Af	Tropical rainforest	No dry season. The driest month has at least 2.40" (61 mm) of rain. Rainfall is generally evenly distributed throughout the year. All average monthly temperatures are greater than 64°F (18°C).
Am	Tropical monsoonal	Pronounced wet season. Short dry season. There are one or more months with less than 2.40" (61 mm). All average monthly temperatures are greater than 64°F (18°C). Highest annual temperature occurs just prior to the rainy season.
Aw	Tropical savanna	Winter dry season. There are more than two months with less than 2.40" (61 mm). All average monthly temperatures are greater than 64°F (18°C).
BSh	Subtropical steppe	Low-latitude dry. Evaporation exceeds precipitation on average but is less than potential evaporation. Average temperature is *more* than 64°F (18°C).
BSk	Mid-latitude steppe	Mid-latitude dry. Evaporation exceeds precipitation on average but is less than potential evaporation. Average temperature is *less* than 64°F (18°C).

BWh	Subtropical desert	Low-latitude desert. Evaporation exceeds precipitation on average but is *less than half* potential evaporation. Average temperature is *more* than 64°F (18°C). Frost is absent or infrequent.
BWk	Mid-latitude desert	Mid-latitude desert. Evaporation exceeds precipitation on average but is *less than half* potential evaporation. Average temperature is *less* than 64°F (18°C). Winter has below freezing temperatures.
Cfa	Humid subtropical	Mild with no dry season, hot summer. Average temperature of warmest months are *over* 72°F (22°C). Average temperature of coldest month is under 64°F (18°C). Year around rainfall but highly variable.
Cfb	Marine west coast	Mild with no dry season, warm summer. Average temperature of all months is *lower* than 72°F (22°C). At least four months with average temperatures over 50°F (10°C). Year around equally spread rainfall.
Cfc	Marine west coast	Mild with no dry season, cool summer. Average temperature of all months is *lower* than 72°F (22°C). There are one to three months with average temperatures over 50°F (10°C). Year around equally spread rainfall.
Csa	Mediterranean	Mild with dry, hot summer. Warmest month has average temperature *more* than 72°F (22°C). At least four months with average temperatures over 50°F (10°C). Frost danger in winter. At least three times as much precipitation during wettest winter months as in the driest summer month.
Csb	Mediterranean	Mild with cool, dry summer. No month with average temperature of warmest months are over 72°F (22°C). At least four months with average temperatures over 50°F (10°C). Frost danger in winter. At least three times as much precipitation during wettest winter months as in the driest summer month.
Cwa	Humid subtropical	Mild with dry winter, hot summer
Dfa	Humid continental	Humid with hot summer
Dfb	Humid continental	Humid with severe winter, no dry season, warm summer
Dfc	Subarctic	Severe winter, no dry season, cool summer
Dfd	Subarctic	Severe, very cold winter, no dry season, cool summer
Dwa	Humid continental	Humid with severe, dry winter, hot summer
Dwb	Humid continental	Humid with severe, dry winter, warm summer

Dwc	Subarctic	Severe, dry winter, cool summer
Dwd	Subarctic	Severe, very cold and dry winter, cool summer
ET	Tundra	Polar tundra, no true summer
EF	Ice Cap	Perennial ice
H	Complex zone. Can encompass any of the above classifications due to the mountainous terrain.	

5.2 Neolithic Burning and Early Global Warming

Proceeding from pre-historic burning, such as fire-stick farming by the Australian Aborigines (Gammage 2012), the dawn of the Neolithic about ~10,000 years-ago saw an expansion of anthropogenic burning and clearing land for cultivation of crops. Pottery, smelting of metals (iron, bronze, copper, and gold), possibly discovered accidentally around camp fires, have led to crafting of ploughs to till the land and swords to kill enemies. Extensive burning and land clearing during the Holocene further magnified entropy. During this period biomass burning, as indicated by residual charcoal deposits, has reached levels as high as those resulting from the combustion of fossil fuels during the first part of the twentieth century (Bowman et al. 2009).

The use of fire for clearing land for farming has been central to Neolithic culture. North American Indians conducted deliberate seasonal or periodic burnings aimed at forming mosaics of resource diversity, environmental stability and the maintenance of transition zones (ecotones) (Lewis 1985). This was compounded by deliberate and incidental burnings spreading out of camp fires, hunting, smoke signals and inter-tribal wars. Controlled surface burns were broken by occasional escape of wild fires and periodic conflagrations during times of drought (Pyne 1982, 1995). So extensive were the cumulative outcomes of these fires that the overall effect of Indian occupation of the Americas replaced extensive forested land with grassland or savannah, or, where the forest persisted, opened it up and freed it from underbrush.

Major studies of North American fire regimes (Lewis 1985; Kay 1994; Russell 1983) list factors underlying deliberate and accidental ignition, including:

1. Burning aimed at diversion of big game (deer, elk, bison) for hunting, opening of prairie and meadows for host pasture and grazing and of small areas to trap other game (rabbits, raccoons, bears. ducks, geese).
2. Burning to clear areas for planting of crops like corn and tobacco, facilitate grass seed, berry and medicine plant collection, prevent abandoned fields from overgrowth, clear grass and brush to facilitate the gathering of acorns and roast mescal and obtain salt from grasses.
3. Forming fire enclaves for collection of insects (crickets, grasshoppers, moths) and collection of honey from bees.

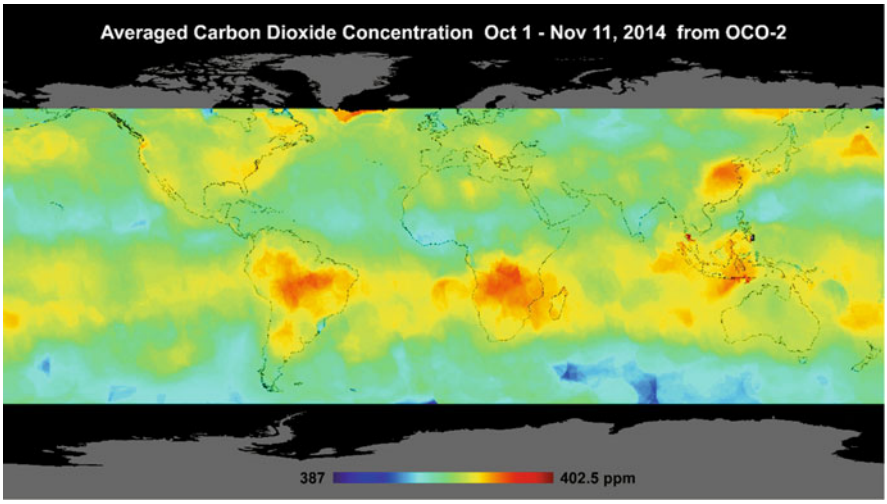

Fig. 5.10 Global maps of atmospheric carbon dioxide from NASA's new orbiting carbon observatory-2 mission showing elevated carbon dioxide concentrations across the Southern Hemisphere from springtime biomass burning from Oct 1 through Nov 11, as recorded by NASA's orbiting carbon observatory-2. Carbon dioxide concentrations are highest above northern Australia, southern Africa and eastern Brazil (Image credit: NASA/JPL-Caltech http://www.nasa.gov/jpl/oco2/nasas-spaceborne-carbon-counter-maps-new-details/index.html#.VJXC9ANAKU; http://www.nasa.gov/sites/default/files/thumbnails/image/mainco2mappia18934.jpg)

4. Back-burning for protection of settlements from wild fires.
5. Burning for protection from pests (rodents, snakes, black flies, mosquitos).
6. War and signalling, including burning strategies against enemies.
7. Burning and girdling of trees for firewood and timber.
8. Worship and spiritual rain dances.
9. Clearing undergrowth for access and travel.

Whereas burning practices by North American Indians and other people (Sheuyangea et al. 2005) were primarily aimed at land clearing for agriculture and for hunting, the rise of agricultural civilizations capable of supporting armies unleashed scorched earth strategies on a massive scale. Examples include the razing of circum-Mediterranean forests and agricultural lands by retreating armies, for example recorded by Gibbon (1788) in connection with the advance of the Emperor Julian into Mesopotamia:

> … on the approach of the Romans, the rich and smiling prospect was instantly blasted. Wherever they moved … the cattle was driven away; the grass and ripe corn were consumed with fire; and, as soon as the flames had subsided which interrupted the march of Julian, he beheld the melancholy face of a smoking and naked desert.

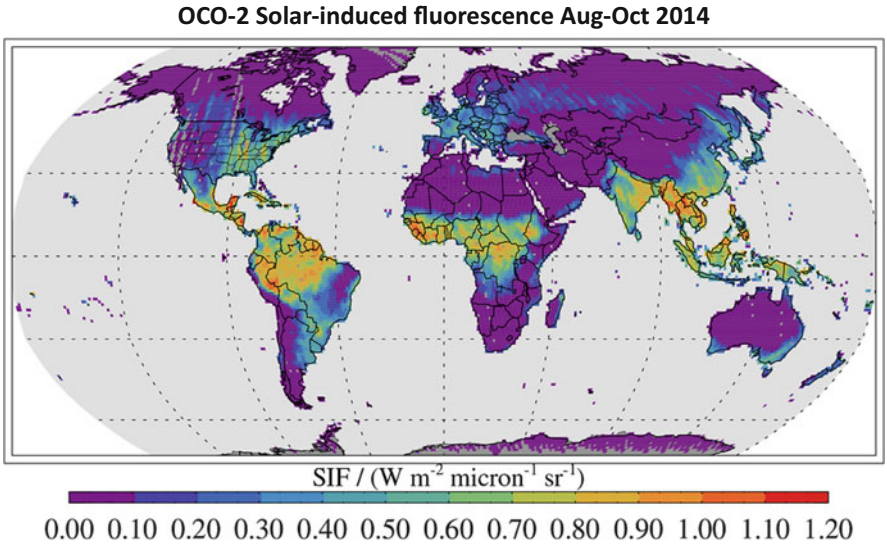

Fig. 5.11 Global photosynthesis levels affecting atmospheric oxygen levels measured by solar-induced fluorescence by NASA's orbiting carbon observatory-2 from Aug through Oct 2014, springtime in the Southern Hemisphere and fall in the Northern Hemisphere. Photosynthesis is highest over the tropical forests of the Southern Hemisphere and high over much of the U.S. Grain Belt, while the northern forests have shut down for the winter. Image credit: NASA/JPL-Caltech http://www.nasa.gov/jpl/oco2/pia18935/)

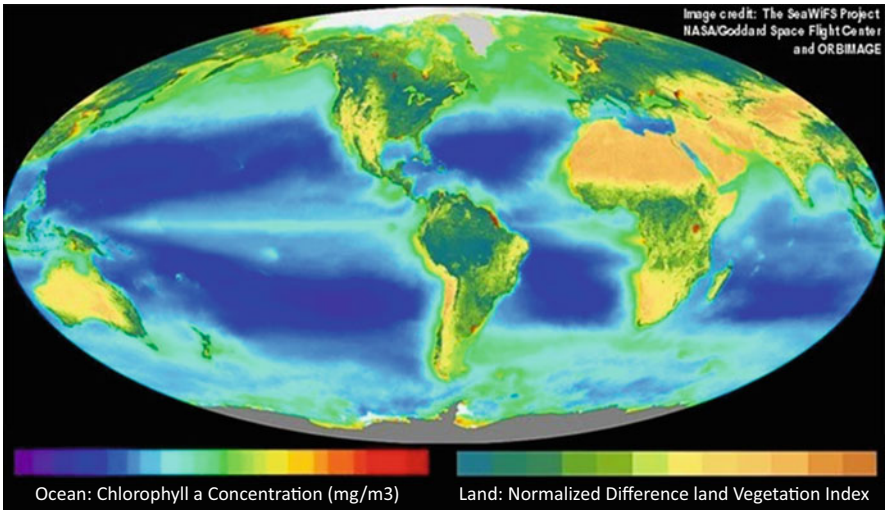

Fig. 5.12 Global chlorophyll levels. Oceans – chlorophyll concentration mg/m^3; land – normalized difference land vegetation index. http://oceancolor.gsfc.nasa.gov/REPROCESSING/SeaWiFS/R2/sea_tech.html

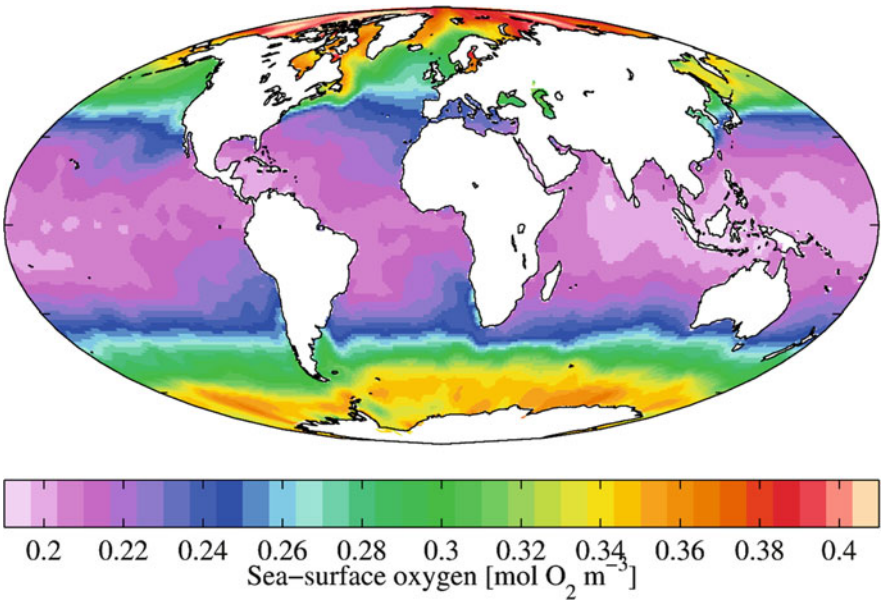

Fig. 5.13 Sea surface oxygen levels representing its temperature-dependent concentration (at 0 °C ~ 14.6 mg O_2/L; at 20 °C ~ 7.6 mg O_2/L), leading to high biological productivity in the polar oceans. Dissolved oxygen levels at the ocean's surface (Data: World Ocean Atlas 2009; photo credit: Plumbago; Wikipedia Commons) http://www.fondriest.com/environmental-measurements/parameters/water-quality/dissolved-oxygen/

Ruddiman (2003) defines the onset of a human-dominated Anthropocene era on the basis of a rise in CO_2 from about ~6000 years-ago and of methane from about ~4000 years-ago, consequent on land clearing, fires and rice cultivation. Kutzbach et al. (2010), comparing Holocene temperature variations with those of earlier interglacial periods, suggest the rise of anthropogenic greenhouse gas levels during the Holocene prevented a decline in temperatures into the next glacial cycle by as much as ~2.7 °C. By contrast Crutzen and Stoermer (2000) and Steffen et al. (2007) define the onset of the Anthropocene at the dawn of the industrial age in the eighteenth century. According to the latter classification the mid-Holocene rise of CO_2 and methane was related to a natural trend, as based on comparisons with the 420–405 kyr Holsteinian interglacial (Broecker and Stocker 2006). Other arguments which favor a non-anthropogenic rise in greenhouse gases during the mid-Holocene hinge on CO_2 mass balance calculations (Stocker et al. 2010), CO_2 ocean sequestration rates and calcite compensation depth (Joos et al. 2004). However, while the signatures of pre-industrial anthropogenic emissions and natural variability are difficult to discriminate, there can be little doubt human-triggered fires and land clearing contributed to an increase in greenhouse gases through much of the Holocene.

5.3 The Great Carbon Oxidation Event

Since the eighteenth century the onset of combustion of coal, oil and gas, which underpin the industrial age, led to the release of over >360 GtC (billion ton carbon), compounded by land clearing and fires releasing over >150 GtC to the atmosphere (Global Carbon Project 2012; Le Quere et al. 2014) (Fig. 5.14). The added >510 GtC is just under the pre-industrial atmospheric carbon level of ~590 GtC. Major consequences of atmospheric CO_2 and other atmospheric greenhouse gas levels (Figs. 5.15, 5.16, 5.17, 5.18, and 5.19) affect land and sea temperatures (Figs. 5.20, 5.21, 5.22, and 5.23). Emissions of both CO_2 and SO_2 have grown during WWI and WWII, with the largest acceleration occurring since about 1950, reflecting the post-war economic boom. Combined with other greenhouse gases this has led to an increase in the radiative forcing of the atmosphere by about +3.05 Watt/m2 (~2.3 °C). Approximately −1.2 Watt/m^2 (~0.9 °C) is masked by direct and indirect (cloud-related) effects of emitted sulphur aerosols (IPCC-AR4 2007; Hansen et al. 2011) (Fig. 5.15). Emissions continued to rise during 1978–2011, including acceleration of CO_2, and a temporary halt of methane rise during 1996–2002 resumed in 2007. By 2010 about 9 billion tons of carbon have been annually released to the atmosphere (Fig. 5.14), of which near-42 % of emitted CO_2 stay in the atmosphere, near to one quarter is absorbed by the oceans and near to one quarter is sequestered

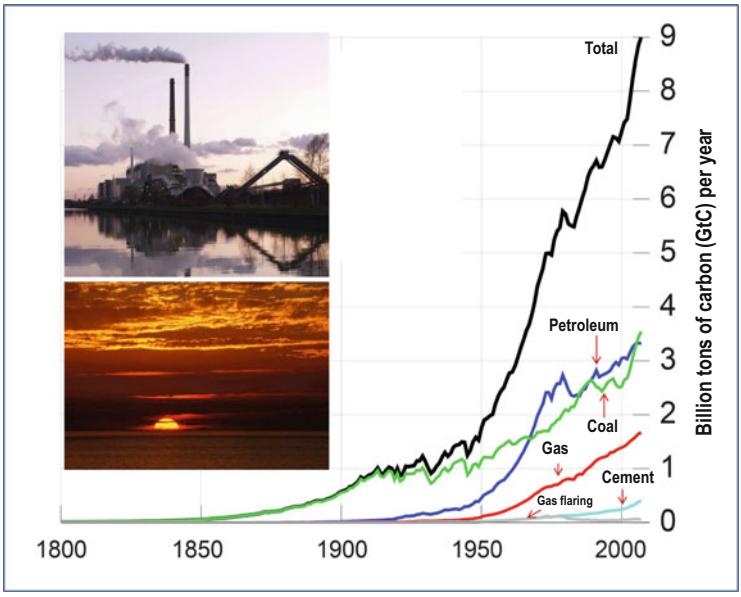

Fig. 5.14 Global CO_2 emission estimate since 1800 AD. Carbon dioxide information analysis center oak ridge national laboratory http://cdiac.ornl.gov/trends/emis/glo.html (Courtesy Tom Boden, with permission). Emission: http://www.sxc.hu/photo/975025 http://www.sxc.hu/txt/license.html; Sunset: Wikipedia Commons http://en.wikipedia.org/wiki/File:Sunset_2007-1.jpg

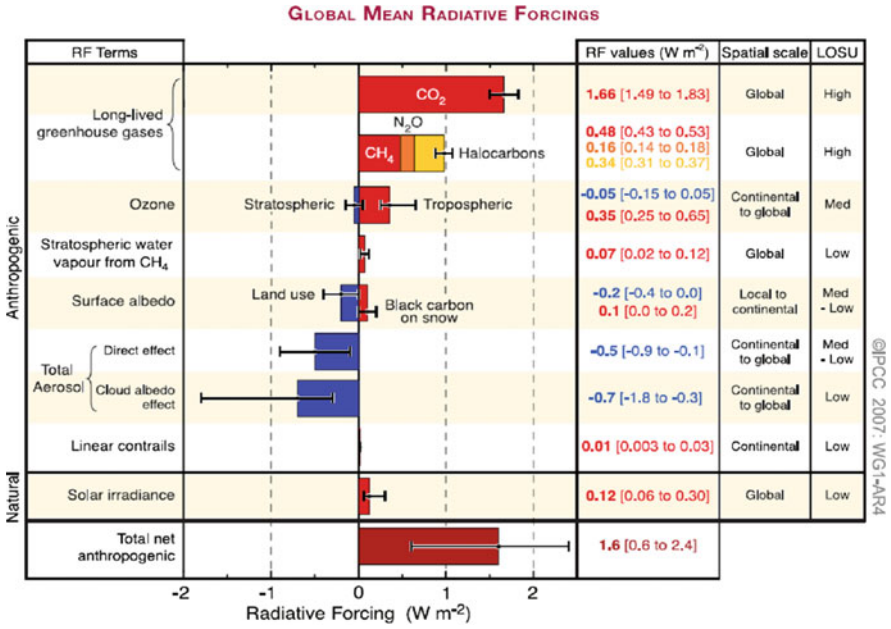

Fig. 5.15 Global mean positive and negative radiative forcings since 1750. Global average radiative forcing estimates and ranges in 2005 for anthropogenic carbon dioxide (CO_2), methane (CH_4), nitrous oxide (N_2O) and other important agents and mechanisms, together with the typical geographical extent of the forcing and the assessed level of scientific understanding. The net anthropogenic radiative forcing and its range are also shown. Volcanic aerosols contribute an additional natural forcing but are not included in this figure due to their episodic nature (IPCC-AR4 2007)

by vegetation and soils on land (Fig. 5.18). Between March 2012 and March 2013 an unprecedented rise from 394.45 to 397.34 ppm has taken place (NOAA 2012, 2013). NASA's new Space-borne Carbon Counter Maps provide global maps of the extent of photosynthesis and of oxygen (Figs. 5.11 and 5.12), achieving maximum during spring time, as well as of fires, for example during spring in the Southern Hemisphere.

The Australian CSIRO reported a rise of atmospheric CO_2 concentration from ~295 to ~380 ppm, of CO_2-e (combined CO_2 and methane equivalent) from ~300 to ~460 ppm, and of radiative forcing by more than 2.2 Watt/m^2 during 1900–2011. A mean global temperature lull and a mild degree of cooling during ~1940–1970, related to rising levels of sulphur aerosols and to a low in the 11-years sun spot cycle, were abruptly terminated by a warming trend from 1975 when atmospheric CO_2 level reached ~330 ppm and clear air policies reduced sulphur emissions (Fig. 5.21). SO_2-induced slowing-down of the rate of warming also occurs from about 2001 and is at least in part related to a rise in sulphur emissions from China (Smith et al. 2011) (Fig. 5.21). The direct and indirect negative forcing effect of sulphur aerosols since the onset of the industrial age, masking global warming, is

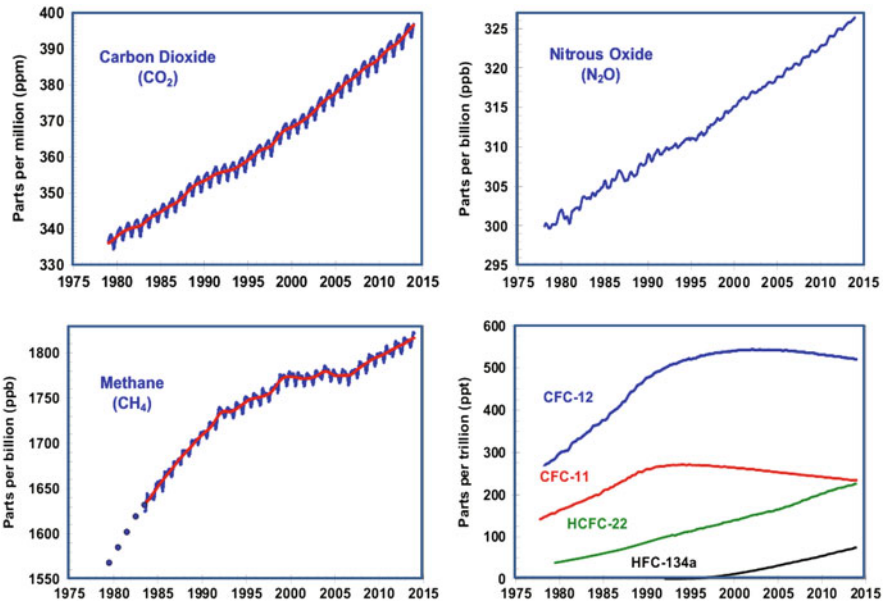

Fig. 5.16 Trends in atmospheric CO_2, methane, nitrous oxide, CFC and HFC (NOAA) http://www.esrl.noaa.gov/gmd/aggi/

estimated as −1.2 Watt/m^2 by IPCC-AR4 (2007), −1.5 Watt/m2 by Hansen et al. (2011) and −1.1 ± 0.4 Watt/m^2 by Murphy et al. (2009).

Measured mean global temperature rise of approximately +0.8 °C since 1800 AD are amplified in polar regions to +4 to 5 °C (NASA/GISS. 2013), representing the effects of rising polar sea water temperatures, related decrease in the effect of ice albedo reflection and increase in open water infrared absorption – namely an albedo-flip feedback process leading to melting of continental ice sheets (Figs. 5.25 and 5.26). The overall increase in radiative forcing in the atmosphere of ~3.17 Watt/m^2 (Fig. 5.15) is near ~50 % that involved in the last glacial termination, where loss of ice cover and vegetation accounted for +3.5 ± 1.0 Watt/m^2 and rise in GHG for +3.0 ± 0.5 Watt/m^2 (Hansen et al. 2008). The rise rates of greenhouse gases and mean global temperatures exceed that of recorded Cenozoic climate shifts by more than an order of magnitude, with the exception of temperature rise rates of the Dansgaard-Oeschger cycles of the last glaciation (Table 2.2).

The atmospheric CO_2 rise from ~280 to 397–400 ppm, with a mean of 0.43 ppm/year and reaching 2.9 ppm/year in 1998 and ~2.89 ppm/year during 2012–2013 (NOAA 2013), exceeds any measured in the geological record, including the PETM hyperthermal methane-release event and the K-T asteroid impact (Zachos et al. 2008; Beerling et al. 2002) (Fig. 5.24). Measured temperature rise rates of ~0.003 °C/year and aerosol-masked temperature rise of 0.008 °C/year since 1750 exceed all previous rates, excepting the Dansgaard-Oeschger (D-O) rates in the range of ~0.2 °C/year (Fig. 5.24). A rise of CO_2-equivalent above 500 ppm and

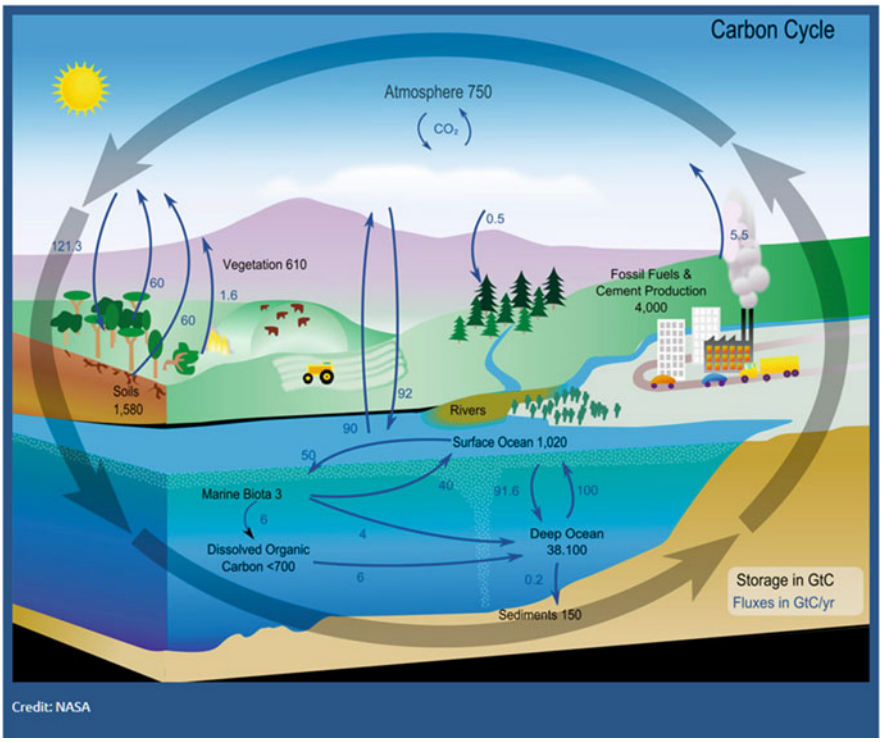

Fig. 5.17 The terrestrial carbon cycle showing the transfer of carbon atoms between various reservoirs in the earth system. The sizes of reservoirs is in billion tons of carbon (GtC). The values for human influences including fossil fuel use and cement production represent the state of the carbon cycle in the mid-1980s. http://scied.ucar.edu/imagecontent/carbon-cycle-diagram-nasa

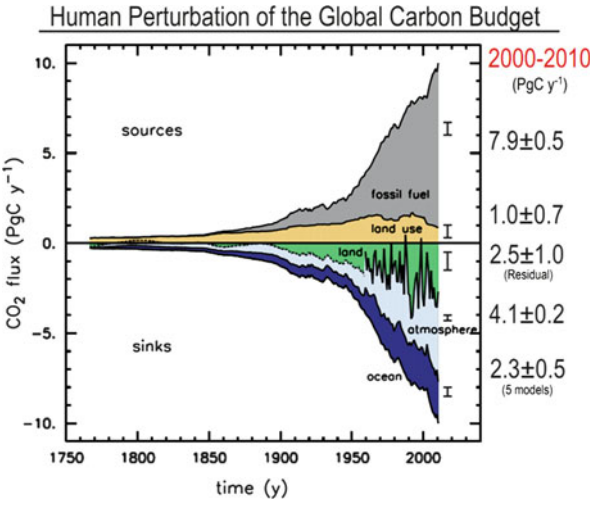

Fig. 5.18 Fractionation of CO_2 emissions (flux GtC/year) from fossil fuels, cement and land use between atmosphere, oceans and land (Le Quéré et al. 2012; Global Carbon Project 2012; Courtesy P. Canadell)

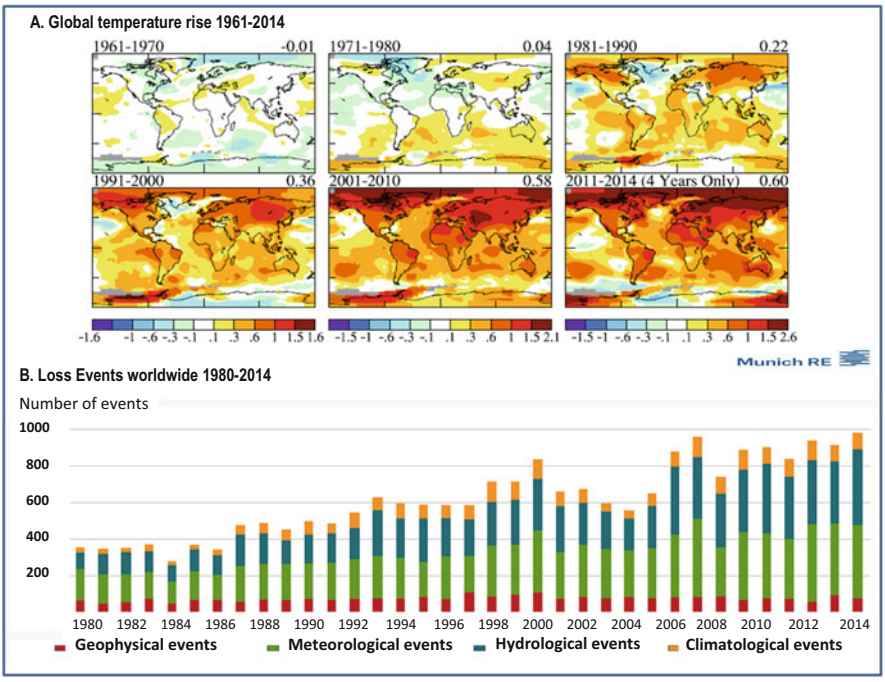

Fig. 5.19 (**A**) Decadal surface temperature anomalies relative to 1951–1980 base period. (http://www.columbia.edu/~jeh1/mailings/2015/20150116_Temperature2014.pdf) climate science, awareness and solutions, earth institute, Columbia University, J. Hansen, by permission; (**B**) Loss events worldwide 1980–2014, Münchener Rückversicherungs-Gesellschaft, NatCatSERVICE, Munich Re-insurance, 2015 (By permission)

mean global temperatures above +4 °C would track toward greenhouse Earth conditions such as existed during the early Eocene some 50 million years-ago (Zachos et al. 2001). Based on paleoclimate studies, the current levels of CO_2 of 397.34 ppm (NOAA 2013 Mouna Loa CO_2) and of CO_2-equivalent of above >455 ppm (IPCC-AR4 2007), a value which includes the equivalent effects of methane and nitrous oxide, commit the atmosphere to a warming trend approaching the upper stability level of the Antarctic ice sheet of 500±50 ppm CO_2.

Based on palaeoclimate studies, using multiple proxies, including soil carbonate $\delta^{13}C$, alkenones, boron/calcium, stomata leaf pores, the current levels of CO_2 of 396–400 ppm and of CO_2-equivalent (a value which includes the equivalent effects of methane and nitrous oxide) of >470 ppm commit the atmosphere to a warming trend tracking toward ice-free Earth conditions.

Global warming is expressed by expansion of the tropics and a shift of mid-latitude high pressure ridges toward the poles, where warming (Fig. 5.22) leads to ice/water albedo-flip inherent in melting of sea ice and ice sheets (Figs. 5.25 and 5.26). The rise in sea water temperature enhances the hydrological cycle, with consequent floods and hurricanes. Current trends are shifting the atmosphere to a state

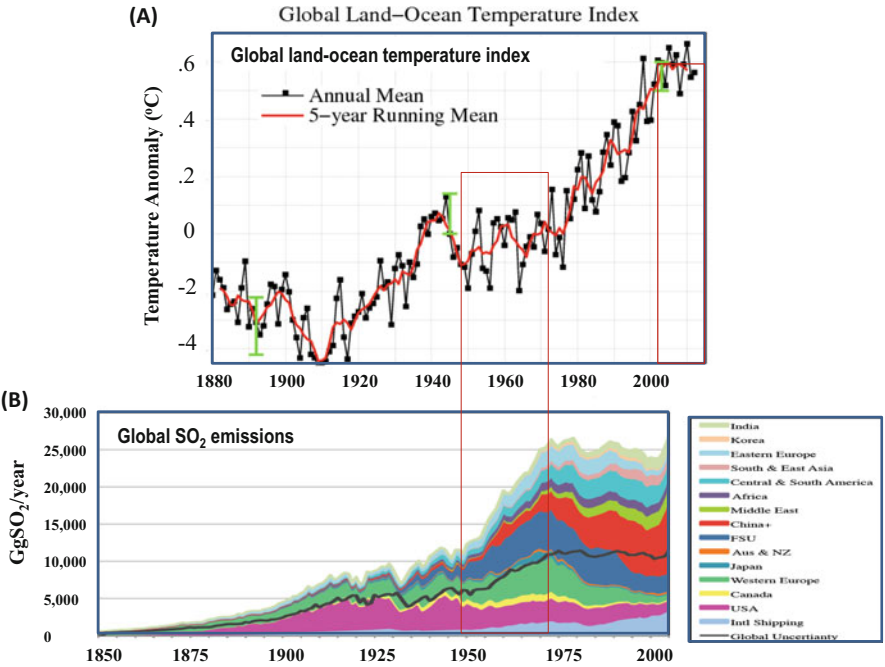

Fig. 5.20 Effects of sulphur emissions on global temperatures. (**A**) Annual mean and 5-years running mean temperatures 1880–2010 (NASA GISS/Temperature. http://data.giss.nasa.gov/gistemp/graphs_v3/; (**B**) Global SO_2 emissions 1850–2005 (Smith et al. 2011). Note the coincidence between increased emission of SO_2 and the slow-down in warming during ~1950–1975 and from about ~2001

analogous to the end-Pliocene, before 2.8 Ma-ago, a period when the bulk of the Greenland and west Antarctic ice sheets melted (PRISM 2012). The Earth's polar ice caps, source of cold air vortices and ocean currents such as the Humboldt and California current, which keep the Earth's overall temperature in balance, are melting at an accelerated rate (Velicogna 2009). Melting of the large ice sheets is doubling every 5–10 years (Figs. 5.25 and 5.26), facilitated by sub-glacial melt flow (Chandler et al. 2013) and exceeding the contribution to sea level rise from thermal expansion and mountain glaciers. In Greenland mass loss increased from 137 GtI/year in 2002–2003 to 286 GtI/year in 2007–2009, i.e., an acceleration of -30 ± 11 Gt/year2 in 2002–2009. In Antarctica mass loss increased from 104 Gt/year in 2002–2006 to 246 Gt/year in 2006–2009, i.e., an acceleration of -26 ± 14 Gt/year^2 in 2002–2009 (Velicogna 2009).

Sea level rise sensitively represents the sum-total of climate change processes, including thermal expansion of water, melting ice sheets and mountain glaciers. The relations between sea levels and mean temperatures during the glacial-interglacial cycles and between temperature rise rate (T°C/year) and sea level rise rate (SL/year) for the twentieth and twenty-first centuries and past glacial terminations (Figs. 5.27 and 5.28) indicate the (SL/T) ratio of glacial terminations (~7–20) exceed those of

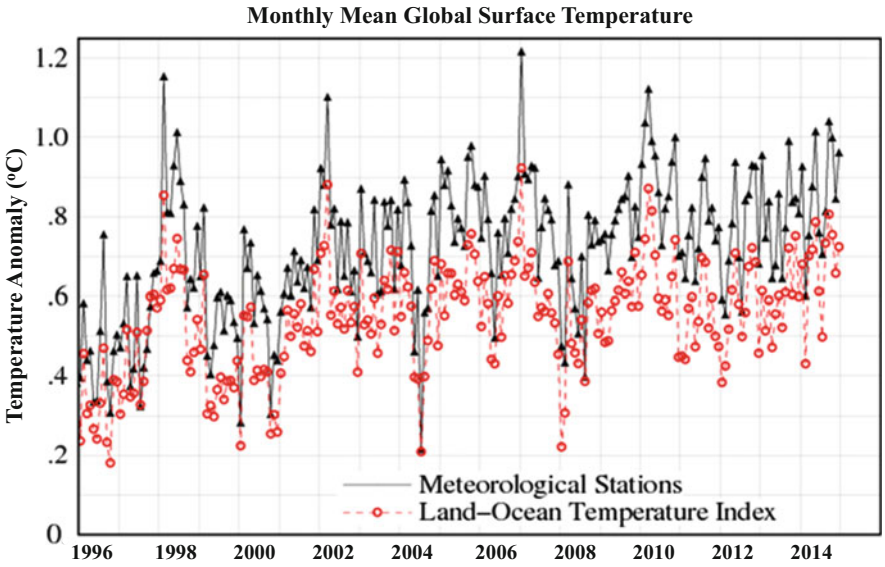

Fig. 5.21 Monthly mean global surface temperatures during 2006–2012 including variations recorded in meteorological stations and from satellite (NASA/GISS Temperatures. http://data.giss.nasa.gov/gistemp/graphs_v3/Fig.C.gif)

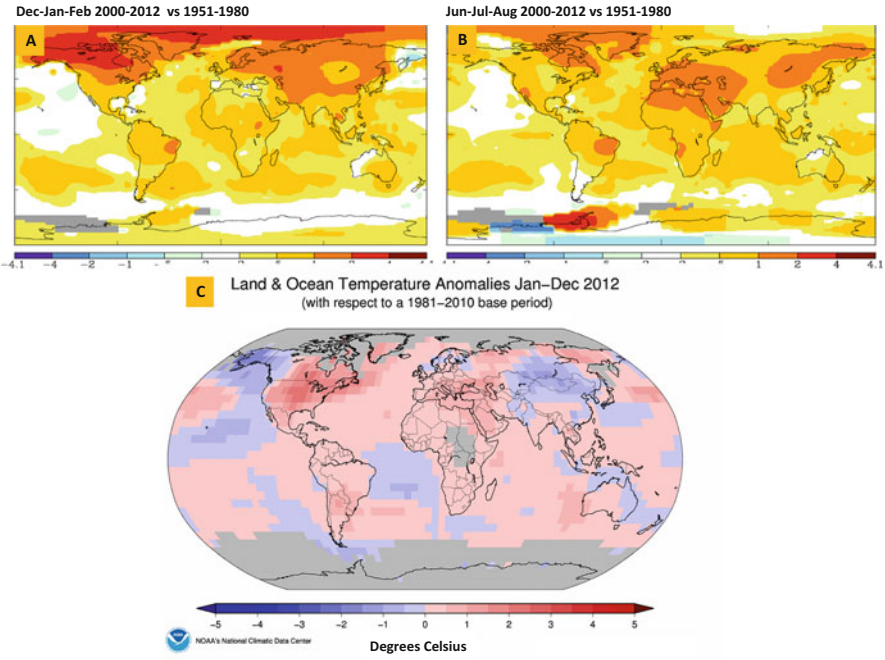

Fig. 5.22 Global warming (**A**) during Dec–Feb 2000–2012 relative to 1951–1980; (**B**) during Jun–August 2000–2012 relative to 1951–1980, and (**C**) Jan–Dec 2012 relative to 1981–2010 (Sources: http://data.giss.nasa.gov/gistemp; http://www.ncdc.noaa.gov/sotc/service/global/map-blended-mntp/201201-201212.gif Note the strong rates of warming in polar regions during winter, related to retention of heat by the higher greenhouse gas levels)

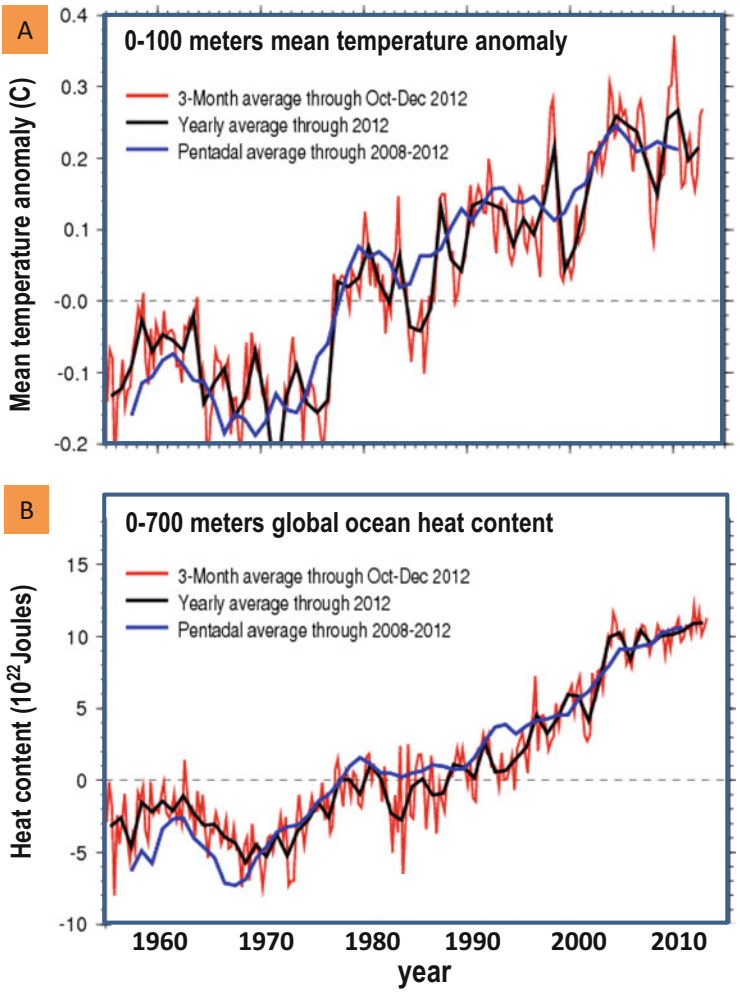

Fig. 5.23 Ocean heat contents: (**A**) 0–100 m depth mean temperature anomaly; (**B**) 0–700 m depth global ocean heat content. http://www.nodc.noaa.gov/OC5/3M_HEAT_CONTENT/ http://www.nodc.noaa.gov/OC5/3M_HEAT_CONTENT/index3.html

twentieth and twenty-first centuries ratios (<<1.0) by one to two orders of magnitude, giving a measure of the lag of sea level rise behind land-sea temperatures. Thus (1) Modern T°C/year (1975–2012 ~ 0.016 °C/year) exceed those of glacial terminations (~0.0001–0.0004 °C/year) by near to one order of magnitude (Diffenbaug and Field 2013) (Fig. 5.28); (2) Modern sea level rise rates (~1–5 mm/year) are similar or somewhat lower than those of glacial terminations (~3–10 mm/year), and both are significantly lower than Dansgaard-Oeschger sea level rise rates (~10–300 mm/year) (Ganopolski and Rahmstorf 2002; Jouzel 2005).

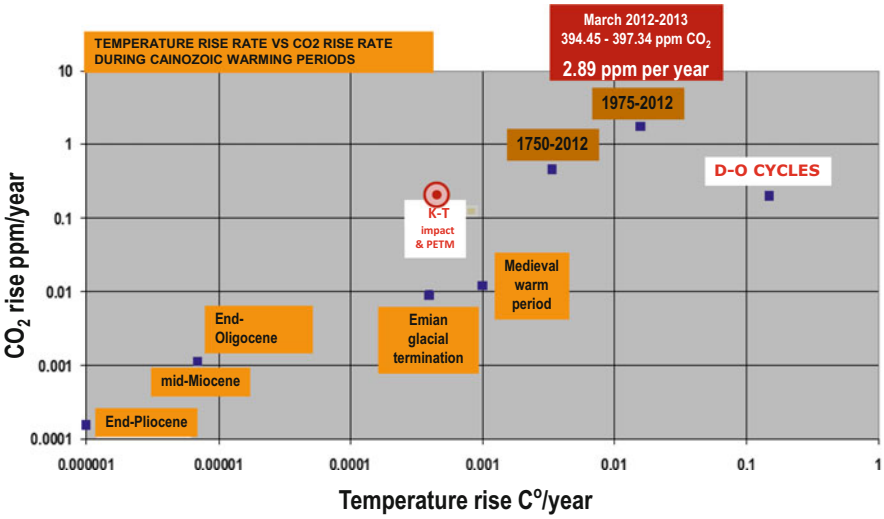

Fig. 5.24 Relations between CO_2 rise rates and mean global temperature rise rates during warming periods, including the Paleocene-Eocene thermal maximum, Oligocene, Miocene, late Pliocene, Eemian (glacial termination), Dansgaard-Oeschger cycles, medieval warming period, 1750–2012 and 1975–2012 periods (Data sources – Table 2.2)

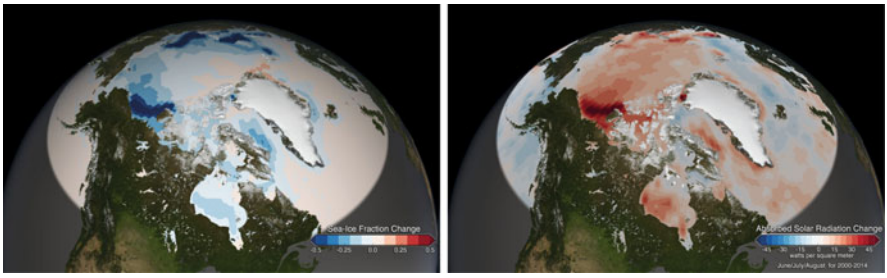

Fig. 5.25 The Arctic Ocean is absorbing more of the sun's energy in recent years as reflective sea ice melts and darker ocean waters are exposed. The increased darker surface area during the Arctic summer is responsible for a 5 % increase in absorbed solar radiation since 2000 (Image credit: NASA Goddard's Scientific Visualization Studio/Lori Perkins. http://svs.gsfc.nasa.gov/cgi-bin/details.cgi?aid=4245)

Kemp et al. (2011) reconstructed sea levels for the past 2100 years from salt-marsh sedimentary sequences from the US Atlantic coast, showing sea level was (1) stable from at least 100 BC until 950 AD; (2) increased from 950 AD for 400 years at a rate of 0.6 mm/year as related to the Medieval Warm Period; (3) was stable or slightly declined until the nineteenth century; (4) since 1865–1892 rose by an average of 2.1 mm/year, consistent with global temperature. Since the early twentieth century, the rate of sea level rise increased from ~1 mm/year to ~3.5 mm/year, the 1993–2009 rate being 3.2±0.4 mm/year, a three to four-fold increase since the onset

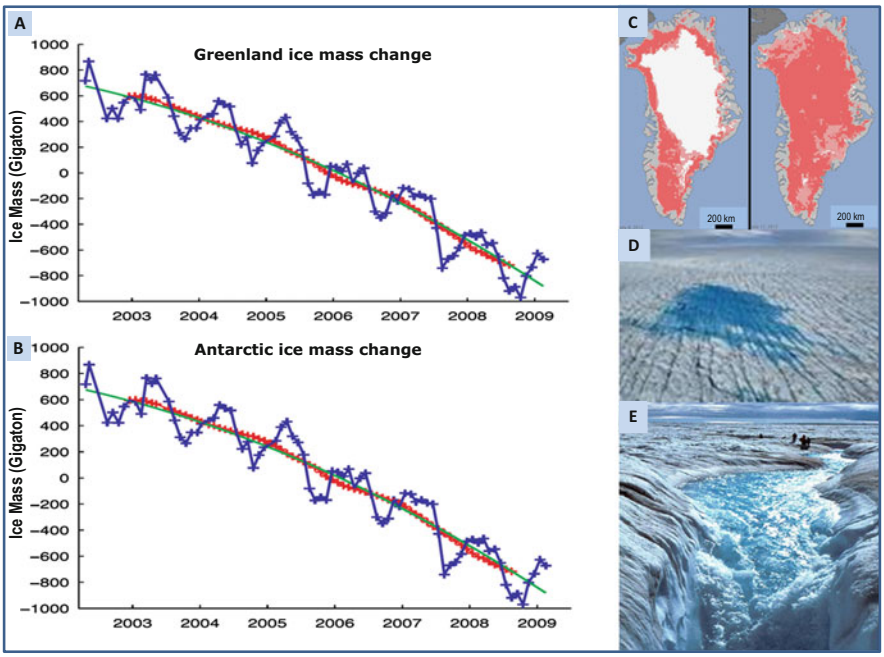

Fig. 5.26 Rates of ice melt in (**A**) Greenland and (**B**) Antarctic (Velicogna 2009). Mass change deduced from gravitational field measurements time series of ice mass changes for the Antarctic ice sheet estimated from GRACE monthly mass solutions for the period from April 2002 to February 2009. Unfiltered data are *blue crosses* (Velicogna 2009; Geophysical Research Letters, with permission); (**C**) Greenland summer ice extent (NASA) http://www.nasa.gov/topics/earth/features/greenland-melt.html; (**D**) Greenland surface ice melt (NASA); (**E**) Moulin drainage conduit, Greenland. Melt water flows into a large moulin in the Greenland ice sheet (Image credit: Roger J. Braithwaite, The University of Manchester, UK. Image Source: http://www.wunderground.com/climate/greenland.asp. (NASA))

of the industrial age (Rahmstorf 2007) (Fig. 5.29). In geological terms human-induced climate change constitutes a global oxygenation event on a scale exceeding any recorded since 55 Ma-ago.

With ensuing desertification of temperate zones, e.g. North Africa, southern Europe, south and southwest Australia and southern Africa, forests become prey to heat waves and firestorms (Hansen et al. 2012). Warming of the oceans leads to a decrease in CO_2 solubility, lowered pH, decrease in biological calcification and of CO_2 sequestration. Increased evaporation in warming oceans leads to an enhanced hydrological cycle, including abrupt precipitation events, floods, and the intensification of cyclones and associated destruction of vegetation (Munich Re-Insurance 2012). Hansen et al. (2011) estimate the current Earth radiative imbalance, namely of heat trapped in the Earth surface and atmosphere, as ~0.6 Watt/m^2. Multiplying this figure by the surface area of Earth (~510×10^6 km^2) indicates an added ~306 megawatt (306 × 10^6 Joules per second). According to Hansen et al. (2012) this equates "*400,000 Hiroshima atomic bombs per day 365 days per year.*"

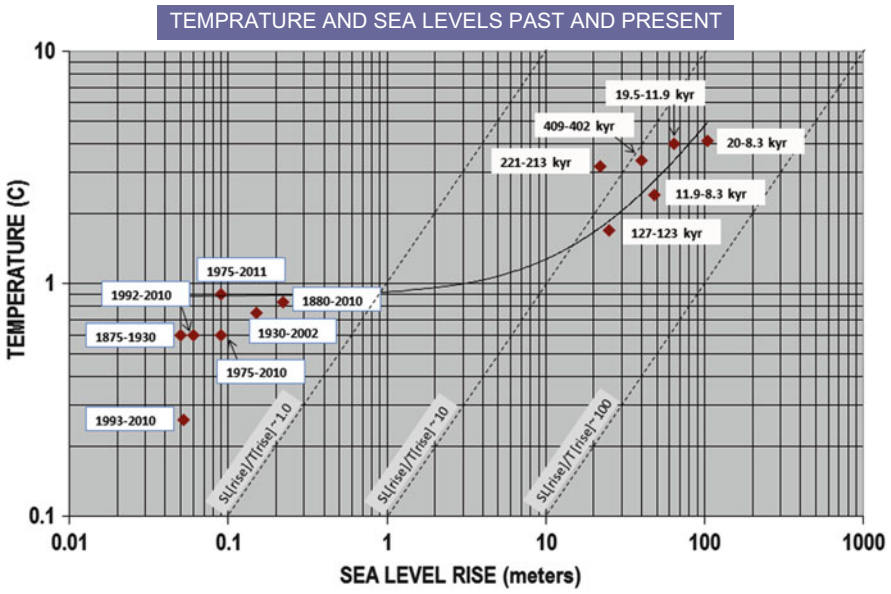

Fig. 5.27 Relations between sea levels (SLm in meters) and temperatures (T°C) during glacial terminations and post-1750 periods. Note the lag by more than an order of magnitude of the ratio of sea level rise to temperature rise (SLm/Tc >10 for glacial terminations and below SLm/Tc <1.0 for post-1750 time intervals) (Data sources: Temperatures – Hansen et al. (2007, 2008); IPCC-AR4 (2007). Sea levels – IPCC-AR4 (2007) and Siddall et al. (2003))

The onset of an irreversible change in global climate from relatively stable state across critical threshold, referred to as tipping point (Lenton et al. 2009), occurs when the climate system transgresses a point beyond which amplifying positive feedbacks drive irreversible changes until negative feedbacks, such as significant decrease in solar insolation or depletion in the source of greenhouse gases, stabilize a new climate state. Such climate shifts may consist of multiple events, including melting and collapse of Greenland and west Antarctic ice sheets, much of the latter being grounded below sea level, melting of permafrost, boreal forest dieback and tundra loss, Indian and west African monsoon shifts, Amazon forest dieback, ozone hole growth and changes to the ENSO circulation and ocean deep water formation patterns (Fig. 5.7). In desert and semi-arid regions global warming leads to heat waves and droughts, which have increased by more than a factor of two since the 1980 (Munich Re-insurance 2012) (Figs. 5.30A, and 5.31) as indicated by the shift in weather profile analyzed by Hansen et al. (2012) (Fig. 5.32). Drying up temperate forests become prey to firestorms, driving loss of CO_2 from desiccated and burnt vegetation and soils.

The rise in temperatures decreases the ocean's ability to sequester CO_2 where the dissolved gas forms bicarbonate and carbonic acid (Fig. 5.33), thereby lowering the water pH. In turn this results in dissolution of biogenic carbonates in plankton and

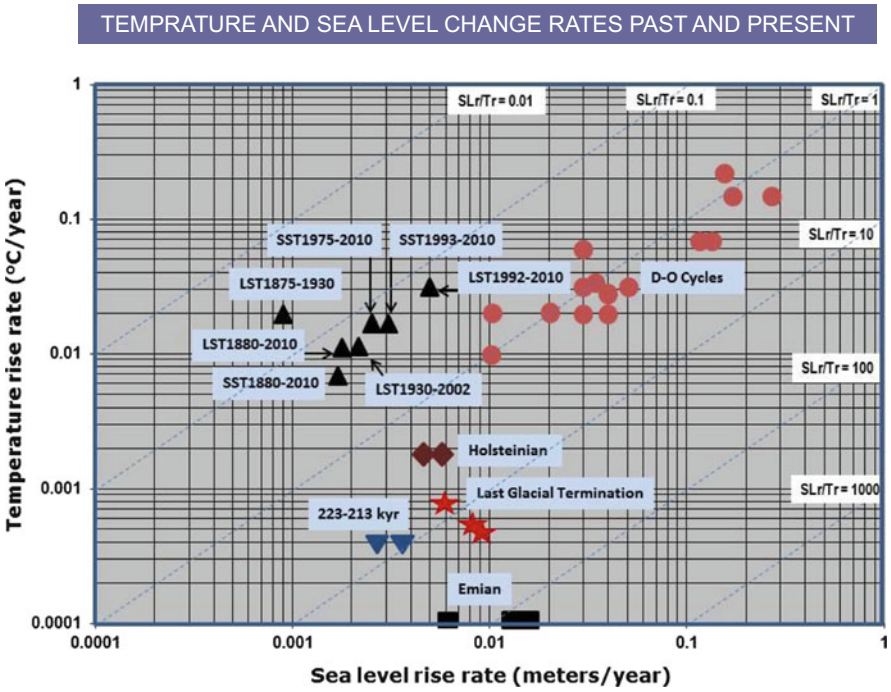

Fig. 5.28 Relations between temperature rise rates (T°C/year) and sea level rise rates (meters/year) during glacial termination intervals, Dansgaard-Oeschger [D-O] cycles and post-1750 periods. Modern temperature rise rate exceed glacial termination rates by about or more than an order of magnitude. D-O temperature and sea level rise rates are higher than those of both glacial terminations and modern rates. Modern sea level rise to temperature rise are the lowest, representing lag effects

corals, retarding CO_2 capture. The deep ocean sink for CO_2 is >39,000 GtC, near to 70 times that of the original CO_2 level of the atmosphere. The oceans absorb nearly 40 % of the anthropogenic CO_2 (Fig. 5.18), leading to an increase in the concentration of carbonic acid (H_2CO_3) and thus an overall increase in acidity (Fig. 5.34), namely reduction in the pH of seawater, with effects on the marine food chain (Fig. 5.35c). As the mixing time between surface and deep ocean waters is in the order of a thousand years, a disequilibrium results between the surface and the deep oceans the likes of which have not been seen for over 55 million years (McCulloch 2008). The carbonate ion CO_3^{-2} concentration of seawater is sensitive to minor changes in pH and a shift from ~8.2 (the current value) to ~8.0 due to doubling of atmospheric CO_2 would reduce CO_3^{-2} by nearly 40 %, with major consequences for calcifying organisms (McCulloch 2008), including coral reefs and plankton. Coral reefs are particularly sensitive – and the large mass extinctions left the Earth without living reefs for at least 4 million years, referred to as “reef gaps” (Veron 2008). Causes of these extinctions include (1) changes independent of the carbon cycle, including direct physical destruction from asteroid impacts, dust clouds, sea-level regressions

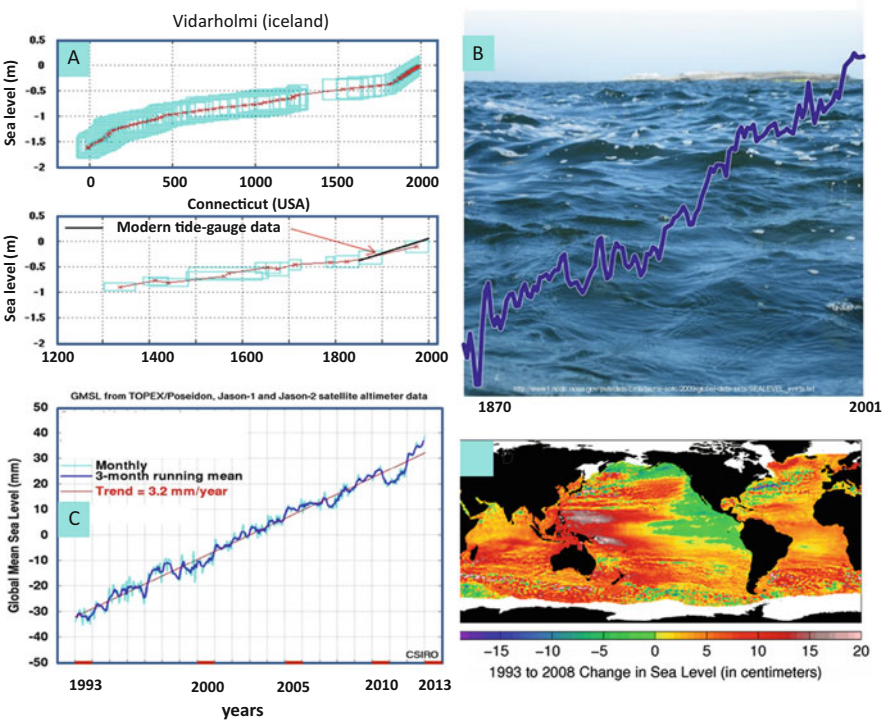

Fig. 5.29 Historic and twentieth to twenty-first centuries sea level rise: (**A**) Historic sea level rises in Vidarholmi, Iceland, and Connecticut; (**B**) 1870–2001 sea level rise (NOAA); (**C**) 1993–2013 sea level change rate; (**D**) 1993–2008 total sea level rise. Note the high sea level rise rates in the west Pacific Ocean, related to the westward flow of warm water driven by La Nina events (CSIRO http://www.cmar.csiro.au/sealevel/index.html, by permission)

during glacial periods, extreme temperature changes, salinity, diseases and toxins; (2) changes linked to the carbon cycle, including acid rain, variations in ocean chemistry, including hydrogen sulphide, anoxia, methane, carbon dioxide and acidity. The prospect of ocean acidification has the potential to trigger a sixth mass extinction event in the oceans (Veron 2008).

In a landmark paper *Extinction Risk from Climate Change* Thomas (2004) review shifts and redistribution of species during the previous 30 years, which form the basis for assessments of future extinction risks for regions covering about 20 % of the land surface. Assuming mid-range climate warming for 2050 some 15–37 % of species in the sample regions are committed to extinction. Minimal climate-warming scenarios result in lower extinctions of about 18 % and maximum-change in ~35 %, namely driving more than one million species to extinction. A comprehensive publication edited by Hannah (2011) '*Saving a million species: Extinction risk from climate change'* includes marine or freshwater environments, explains the science behind the projections, sets forth new risk estimates for future climate change and

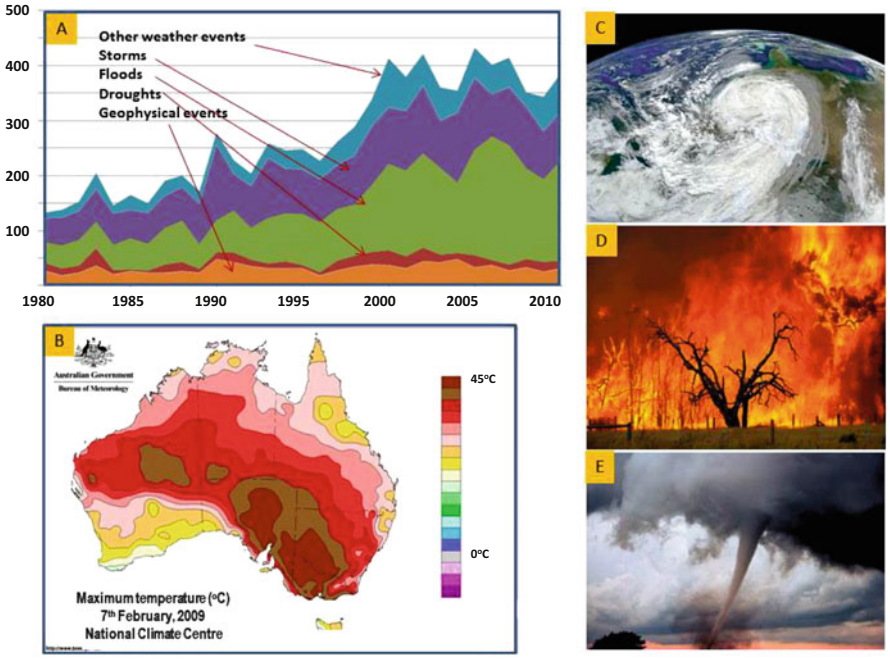

Fig. 5.30 Extreme weather events: (**A**) Number of reported disasters 1980–2010 (http://make-wealthhistory.org/2011/05/30/the-number-of-natural-disasters-is-on-the-rise/) (Courtesy Gifty Dzah, Oxfam GB Policy and Practice Communications Team); (**B**) Maximum temperature 7th February, 2009 (Australian Bureau of Meteorology, by permission); (**C**) Hurricane Katrina (NASA); (**D**) Fire storm – Victoria, 7th February, 2009; (**E**) tornado – A Oklahoma in 1999 (NOAA Photo Library via Creative Commons) http://www.neontommy.com/news/2012/04/tornadoes-storms-predicted-throughout-weekend

considers the conservation and policy implications of the estimates. A review of the book in the British Journal of Entomology states "*it is no longer a question of whether or not we are in the midst of a mass extinction event, we are, the question now is, what can we do about it*?"

In a key paper Hansen et al. (1988) modeled the climate effects of rising GHG for the period 1958–1988. Scenario [A] assumes exponential growth in trace greenhouse gases; Scenario [B] assumes reduced linear growth of trace gases, and scenario [C] a rapid curtailment of trace gas emissions by the year 2000. In all three models peak temperatures reached the previous maximum Holocene levels. For model [A] the authors state "*Our model results suggest that global greenhouse warming will soon rise above the level of natural climate variability*". This observation was reported by James Hansen to the US Congress on 23 June, 1988. By 2012, allowing for the masking effect of sulphur aerosols, the unmasked temperature equivalent of the GHG rise has reached level remarkably close to that of Scenario [A]. Hansen et al. (2008) regard a CO_2 level of ~350 ppm as the maximum allowable before amplified feedbacks lead to climate tipping points beyond human control. Following the 1998 peak El Nino event (Fig. 5.36), mean temperature rise

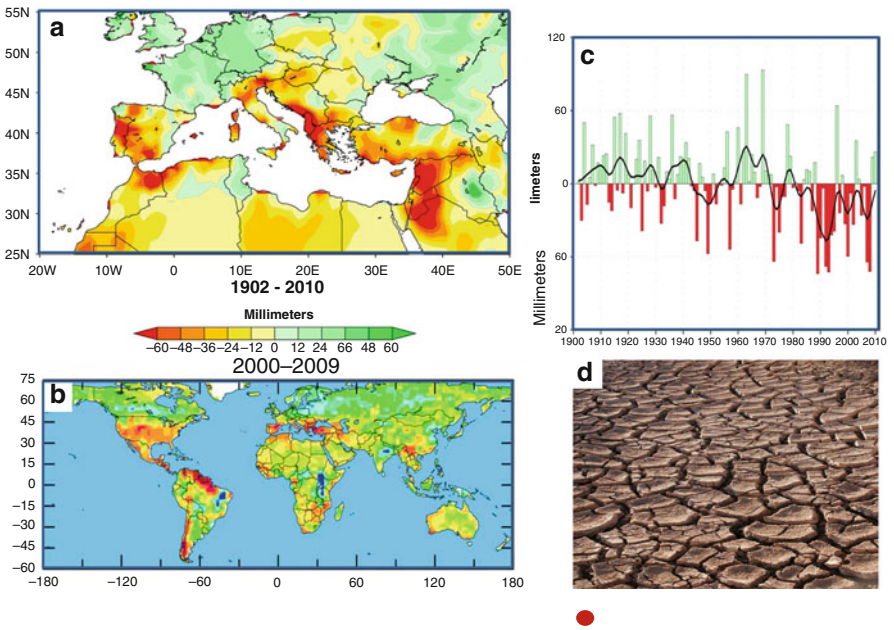

Fig. 5.31 (**a**) Winter precipitation trends in the Mediterranean region for the period 1902–2010; (**b**) 2000–2009 droughts. The map uses a common measure, the Palmer Drought Severity Index, which assigns positive numbers when conditions are unusually wet for a particular region, and negative numbers when conditions are unusually dry. A reading of −4 or below is considered extreme drought. Regions that are *blue* or *green* will likely be at lower risk of drought, while those in the *red* and *purple* spectrum face more unusually extreme drought conditions. (https://www2.ucar.edu/atmosnews/news/2904/climate-change-drought-may-threaten-much-globe-within-decades. Courtesy Ivonne Mondragon, UCAR (University Corporation for Atmospheric Research; (**c**) *Reds* and *oranges* highlight lands around the Mediterranean that experienced significantly drier winters during 1971–2010 than the comparison period of 1902–2010. B and C – Credit NOAA http://www.noaanews.noaa.gov/stories2011/20111027_drought.html; (**d**) drought (http://upload.wikimedia.org/wikipedia/commons/e/e1/Drought.jpg)

rate declined relative to 1975–1998, in part due to a surge in SO_2 emissions effecting higher atmospheric albedo (Fig. 5.15) and to a decline in sunspot activity (Fig. 5.3). A dominance of the La Nina cycles during 2000–2012 (Fig. 5.36) raises the question whether this phase is being enhanced by increasing ice melt driving the relatively cold Humboldt and California currents.

Peak temperatures relative to the 1951–1980 period were reached in 1998, 2002, 2006, 2010 and 2014 (Fig. 5.21) (NASA/GISS 2013). Positive feedbacks to global warming include summer exposure of open water surfaces in Polar Regions, replacing the reflective properties of ice surfaces with absorption by dark water. Hudson (2011) estimates the rise in radiative forcing due to total removal of Arctic summer sea ice as 0.7 Watt/m^2, which is close to the total of methane release since 1750 (~0.5 Watt/m^2), although this amount would be in part offset by increased summer cloudiness. The subsequent increase in evaporation is leading to the advance of cold vapor-laden fronts and to snow storms in the north Atlantic. Further positive feedbacks

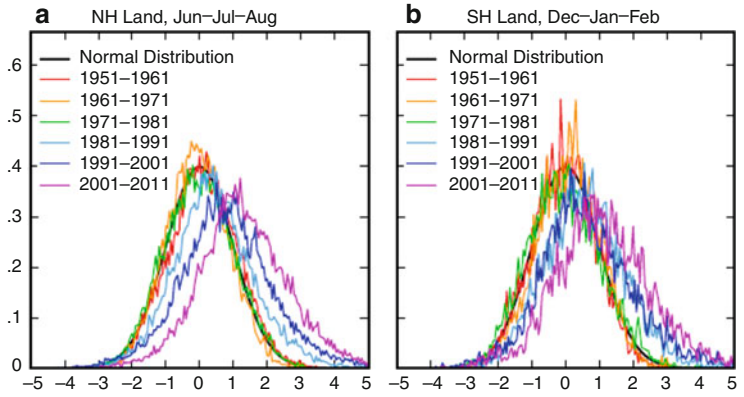

Fig. 5.32 Frequency of occurrence (y-axis) of local temperature anomalies divided by local standard deviation (x-axis) obtained by binning all local results for the indicated region and 11-year period into 0.05 frequency intervals. Area under each curve is unity. Anomalies are relative to 1951–1980 climatology, and standard deviations are for the same 1951–1980 base period (Hansen et al. 2012). (**a**) Northern hemisphere summer; (**b**) Southern hemisphere summer

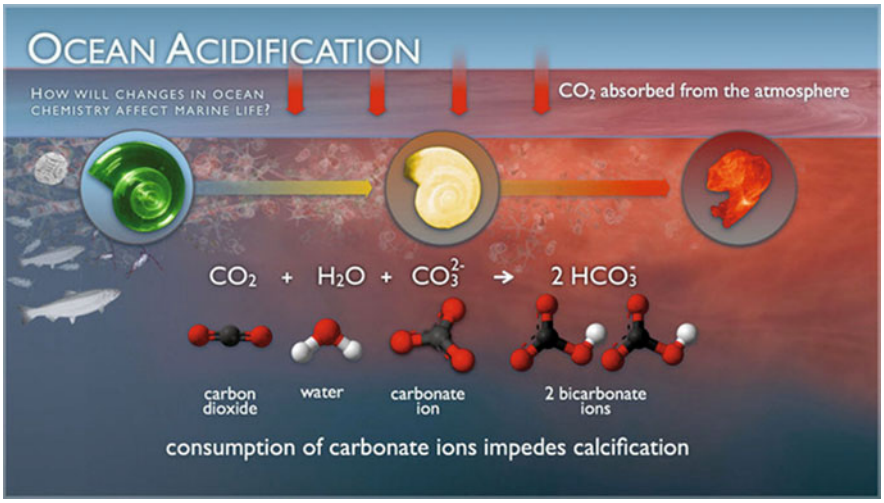

Fig. 5.33 Chemical reaction of CO_2, water and carbonate ion producing bicarbonate ions, impeding calcification (http://www.pmel.noaa.gov/co2/file/Ocean+Acidification+Illustration)

occur due to the release of methane from Arctic permafrost (total estimated as ~900 GtC), high-latitude peat lands (~400 GtC), tropical peat lands (~100 GtC) and vegetation subject to fire and/or deforestation (CSIRO 2009) (Fig. 5.42).

By the onset of the third millennium H. sapiens has released more than 560 GtC from fossil biospheres and land clearing into the atmosphere, and is proceeding at a rate of ~2 ppm CO_2 per year, unprecedented in geological history. Current economic

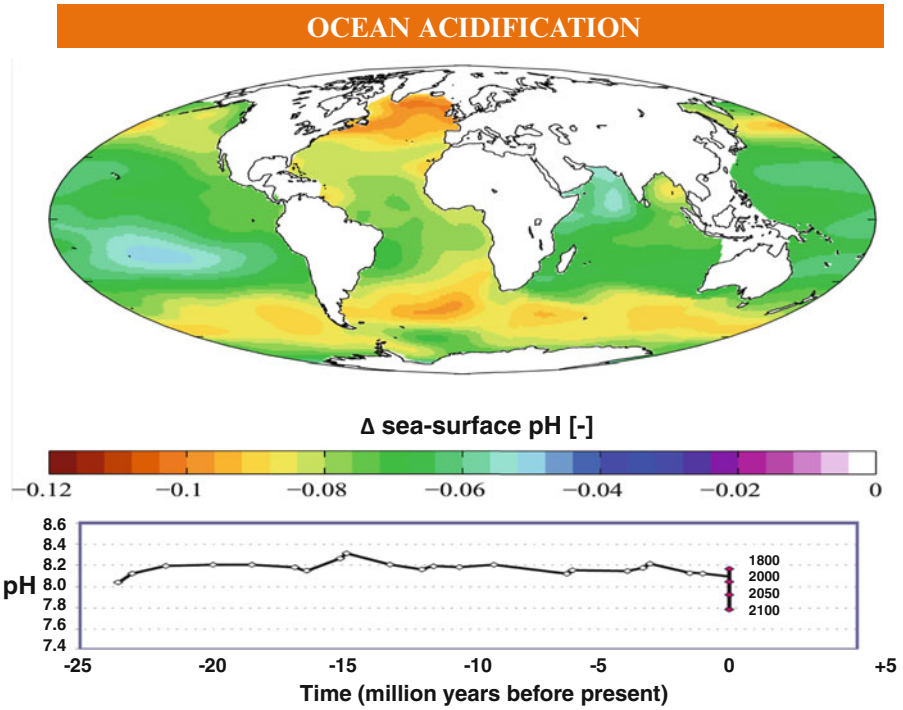

Fig. 5.34 Ocean acidification. The map displays greater decline in pH in the cold sub-polar oceans (0.08–0.1 pH units) relative to tropical and subtropical waters (0.05–0.08 pH units), reflecting the stronger sequestration of atmospheric CO_2 in lower temperature waters (http://upload.wikimedia.org/wikipedia/commons/9/99/AYool_GLODAP_del_pH.png)

reserves include ~900 GtC Coal, ~150 GtC Oil, ~105 GtC Gas, and almost open ended reserves of tar sands oil, oil shale and coal-seam gas (Global Carbon Project 2012). A close parallel is the release to the atmosphere of some ~2000 billion tons carbon at the Paleocene–Eocene boundary ~55 million years-ago (Zachos et al. 2008), estimated to have raised atmospheric CO_2 levels at a rate of about 0.11–0.13 ppm/year (Table 2.2), with attendant extinction of deep sea pelagic foraminifera (Panchuk et al. 2008). Other exceptions are global volcanic eruptions and asteroid impacts which have ignited regional to global wildfires (Durda and Kring 2004) and, in the case of impacts, excavated and vaporized carbon-rich sediments.

By the end of the twentieth century and first decade of the twenty-first century climate change has ceased to be an abstract scientific notion and is manifesting itself through a spate of extreme weather events around the globe (Figs. 5.30, 5.31, and 5.32). The number of reported disasters has increased from ~135 in 1980 to near-400 between 2000 and 2010. According to Williams (2012) "*While the scientific debate spirals on into ever more intransigent spirals of obfuscation, the world continues to change around us. I've written before about the extraordinary number of extreme weather events last year, and the record number of temperature records set. 2011 is no different so far, with serious droughts developing in some parts of the*

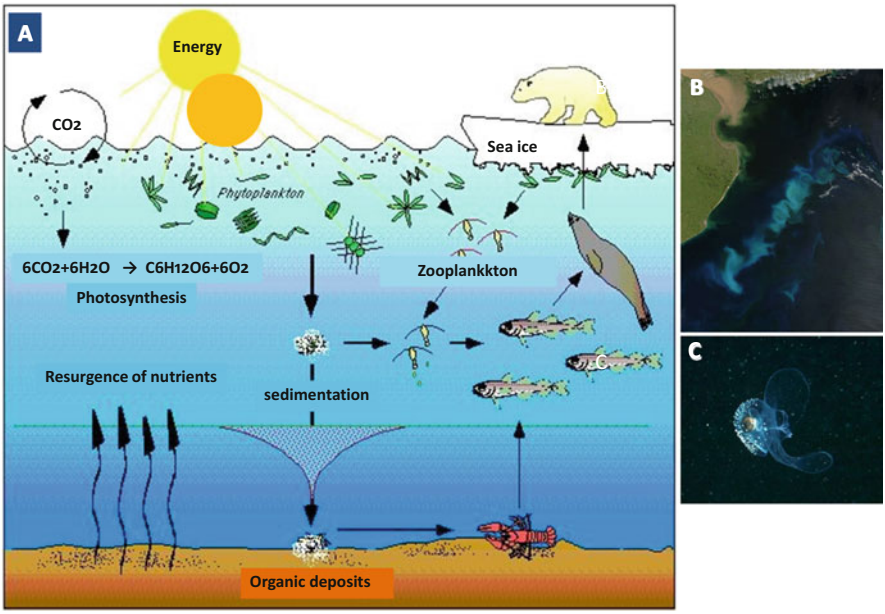

Fig. 5.35 (**A**) The marine food chain http://www.arctic.noaa.gov/images/arctic_marine_food_web.jpg; (**B**) An oceanic phytoplankton bloom in the South Atlantic Ocean, off the coast of Argentina (NASA. http://en.wikipedia.org/wiki/File:Phytoplankton_SoAtlantic_20060215.jpg); (**C**) Pteropods – http://upload.wikimedia.org/wikipedia/commons/a/aa/Sea_butterfly.jpg

world, and the US experiencing a vicious storm season … If it feels like there are far more hurricanes and floods these days, then your instincts are correct. The number of weather related disasters has increased dramatically in the last 30 years." The United States has become a focus of climate change-driven natural disasters, in part a consequence of its becoming an open corridor between the high-temperature Gulf of Mexico and the Arctic. The number of extreme weather events has quadrupled between 1980 and 2012 (Williams 2012).

5.4 The Sixth Mass Extinction of Species

In 2009 Joachim Hans Schellnhuber, Director of the Potsdam Climate Impacts Institute and Climate Advisor to the German Government, stated: "*We're simply talking about the very life support system of this planet*". The consequences for the biosphere of accelerating climate change are discussed by Baronsky et al. (2013) in the following terms: "*Localized ecological systems are known to shift abruptly and irreversibly from one state to another when they are forced across critical thresholds. Here we review evidence that the global ecosystem as a whole can react in the same way and is approaching a planetary-scale critical transition as a result of*

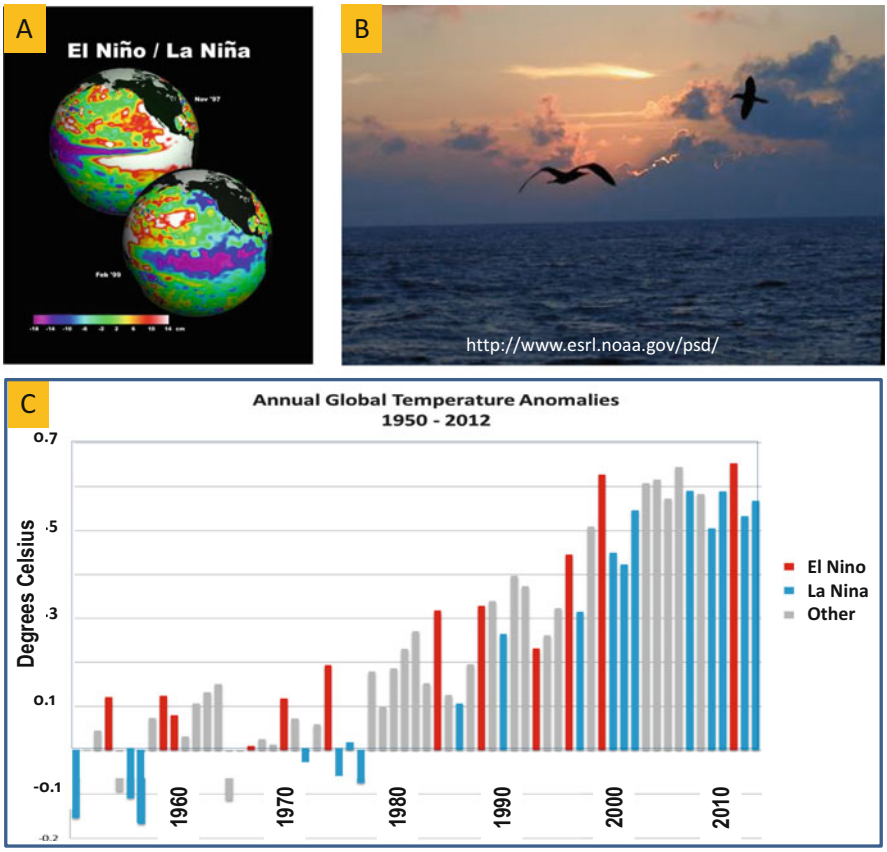

Fig. 5.36 Effects of global warming on the ENSO cycle. (**A**) The El Nino phase (near-uniform temperatures and air-pressure along the equatorial Pacific) with consequent low or negative SOI (Southern Oscillation Index) and La Nina phase (warm water driven westward with consequent high SOI) http://sealevel.jpl.nasa.gov/science/elninopdo/learnmoreninonina; (**B**) The Pacific Ocean http://www.esrl.noaa.gov/psd; (**C**) Annual global temperature anomalies as related to the ENSO cycle http://www.ncdc.noaa.gov/sotc/service/global/enso-global-temp-anom/201213.png; Note the high global temperatures induced by the El Nino phase due to the dispersal Pacific-wide and global-wide warm low-pressure air currents by the latitudinal Walker circulation and the longitudinal Hadley cell

human influence." and "*Climates found at present on 10–48 % of the planet are projected to disappear within a century, and climates that contemporary organisms have never experienced are likely to cover 12–39 % of Earth. The mean global temperature by 2070 (or possibly a few decades earlier) will be higher than it has been since the human species evolved.*"

The devastation of habitats amounting to a crisis in the biosphere is manifest (Vitousek 1994; Casper 2009). A rapid polar-ward shift of climate zones is manifest. According to Xu et al. (2013) and NASA (2013b) vegetation growth at Earth's northern latitudes increasingly resembles lusher latitudes to the south and

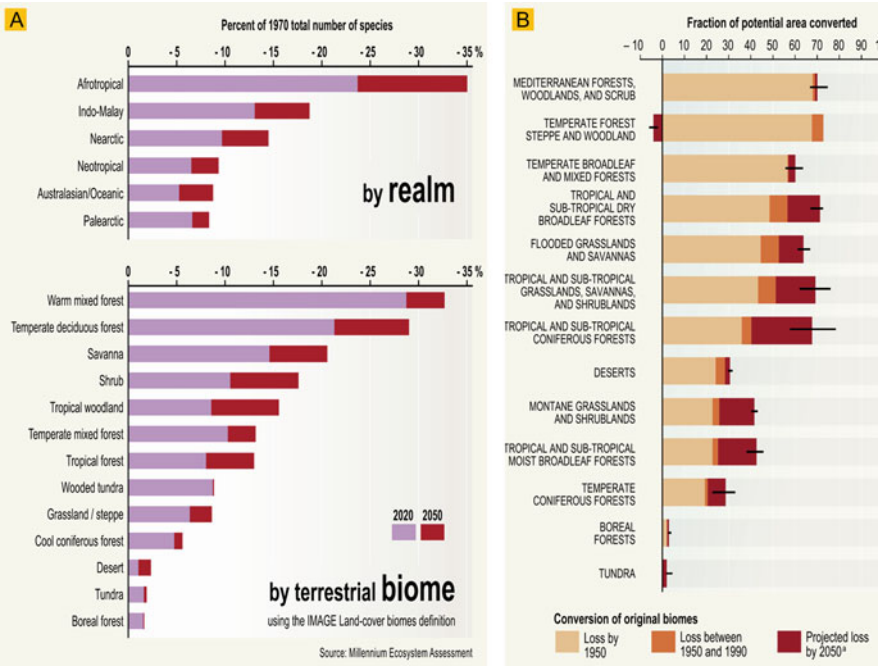

Fig. 5.37 (**A**) Relative loss of biodiversity of vascular plants between 1970 and 2050 as a result of land Use change for different biomes (a biome is a major regional group of distinctive plant and animal communities) and realms. Extinctions will occur between now and sometime after 2050, when populations reach equilibrium with remaining habitat (A biome is a major regional group of distinctive plant and animal communities). (**B**) Conversion of terrestrial biomes: It is not possible to estimate accurately the extent of different biomes prior to significant human impact, but it is possible to determine the "potential" area of biomes based on soil and climatic conditions. This figure shows how much of that potential area is estimated to have been converted by 1950 (medium certainty), how much was converted between 1950 and 1990 (medium certainty), and how much would be converted under the four millennium assessment scenarios (low certainty) between 1990 and 2050. From "ecosystems and human well-being – biodiversity synthesis". Millennium ecosystems assessment. http://www.unep.org/maweb/en/Synthesis.aspx. (World Resources Institute, by permission)

temperature and vegetation growth at northern latitudes now resemble those found 4° to 6° of latitude farther south as recently as 1982. Arctic sea ice and the duration of snow cover are diminishing, the growing season is getting longer and plants are growing to a greater extent. In the Arctic and boreal areas the characteristics of the seasons are changing, leading to great disruptions for plants and related ecosystems. The Arctic's greenness is visible on the ground as an increasing abundance of tall shrubs and trees in locations all over the circumpolar Arctic. Greening in the adjacent boreal areas is more pronounced in Eurasia than in North America, driven by amplified greenhouse effects.

Plants and organisms display remarkable adaptation and regeneration powers where medium to long-term environmental changes occur. However, abrupt transitions

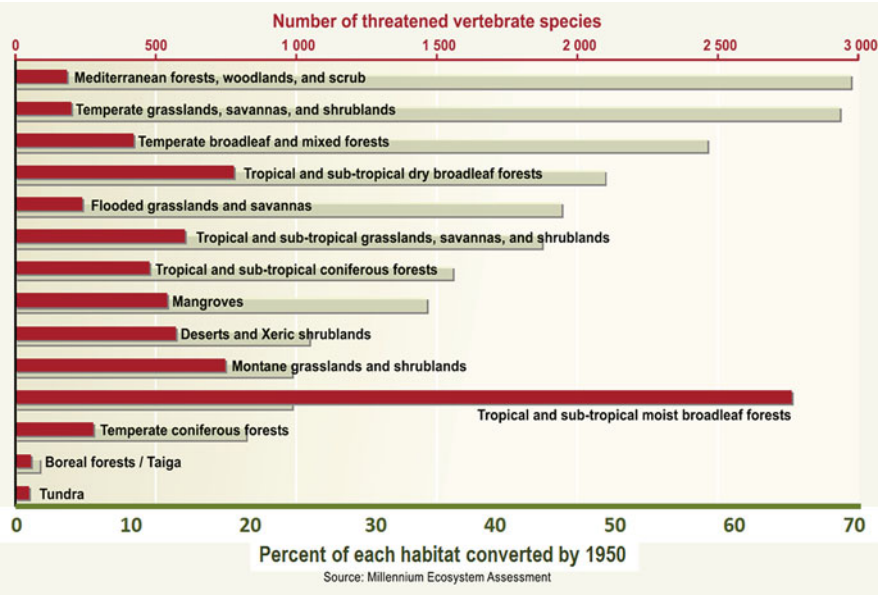

Fig. 5.38 Threatened vertebrates in 14 biomes ranked by the amount of their habitat converted by 1950. Percent of converted habitats – in *green*; Percent of threatened species – in *red*. From "Ecosystems and human well-being – Biodiversity Synthesis". Millennium Ecosystems Assessment. http://www.unep.org/maweb/en/Synthesis.aspx (World Resources Institute, by permission)

and tipping points in the physical environment may exceed the adaptive capacity of some species, resulting in extinction. By 1950 near to 70 % of Mediterranean and temperate forests and near 50 % of tropical and sub-tropical forests were lost (Fig. 5.37). Projected changes in biodiversity need to discriminate between the effects of climate and land-use change effects (de Chazal and Rounsevella 2009). Habitat loss leading to decreased species richness is the most common land-use change. Habitats most affected by climate change factors include grassland, shrubland, boreal forests, cool conifer forests and Tundra, whereas habitats mostly affected by land clearing are tropical forests, warm mixed forests and temperate deciduous forests (Fig. 5.37). Threatened and lost mammal species concomitant with loss of forest habitats, particularly pronounced in tropical and sub-tropical habitats, are documented in reports by the Millennium Ecosystem Assessment program (Fig. 5.38).

In the oceans the marine food chain (Fig. 5.35) may collapse in part under the pressures of decreasing pH and increasing temperatures. According to Veron (2008), "*if CO_2 levels are allowed to increase to 650–700 ppm, as is projected to occur later this century, a return to pre-industrial level will take a period of about 30,000 and 35,000 years. Initially acidification is buffered by bicarbonate–carbonate ion exchange, but once the buffers are overwhelmed the pH changes abruptly. The oceans will remain acidified until neutralized by the dissolving of marine carbonate rocks*

and the weathering of rocks on land, a hugely protracted process. When CO2 levels increase to 560 ppm, the Southern Ocean surface waters will be undersaturated with respect to aragonite, and the pH will be reduced by about 0.24 units—from almost 8.2 today to a little more than 7.9. At the present rate of acidification, all reef waters will have a $\Omega_{aragonite}$ *of 3.5 or less by the middle of this century. Should CO2 levels reach 800 ppm later this century, the decrease will be 0.4 units and dissolved carbonate ion concentration will have decreased by almost 60 %. At that point all the reefs of the world will be eroding relicts. The levels of CO2 and pH predicted by the end of this century may not have occurred since the Middle Eocene, but the all-important rate of change we are currently experiencing has no known precedent. There can be no evolutionary solution for such a rate of change. Ultimately—and here we are looking at centuries rather than millennia—the ocean pH will drop to a point at which a host of other chemical changes, including anoxia, would be expected. If this happens, the state of the oceans at the end of K/T, or something like it, will become a reality and the Earth will enter the sixth mass extinction. Another 1–3 decades like our last will see the Earth committed to a trajectory from which there will be no escape*."

5.5 The Faustian Bargain

By November 2014 atmospheric CO_2 at Mouna Loa, Hawaii, has reached 397.13 ppm, a rise of 2.03 ppm since November 2013, implying a return to Pliocene-like atmospheric radiative forcing at a rate unprecedented in the Cainozoic geological record (Fig. 5.24, 5.27, 5.28) (Diffenbaug and Field 2013), except for instant rises of GHG associated with asteroid impacts. Continuation of carbon emission at rates of near-30 GtC/year or higher implies a rise of atmospheric CO_2 to levels of above 600 ppm (Figs. 5.39 and 5.40), a level unrecorded since the Eocene pre-32 Ma-ago (Zachos et al. 2001). Amplifying feedbacks from vulnerable carbon pools (Fig. 5.42) are capable of raising atmospheric CO_2 to levels which resulted in mass extinction at 55 Ma-ago (Zachos et al. 2008).

A perspective on such development is allowed by the mid-Miocene (~16 Ma) warm period. Only small ice caps existed during this period while sea levels were about 40–50 m higher than at present. However, whereas the transition from end-Miocene conditions to the present took place over some 5.2 million years, the rise of mean global temperature since the eighteenth century would hardly allow many species to adapt. However, whereas species have adapted to shifting states of the climate, the extreme rate at which radiative greenhouse gas forcing is rising – ~3 ppm during 2012–2013 – would not allow many species the time to adapt.

The extent to which global warming and ocean acidification will develop depends on a number of factors, including:

A. Estimated reserves of fossil fuels are large enough for atmospheric CO_2 levels to reach more than 1000 ppm, or higher where unconventional resources such as tar sands, shale gas and coal seam gas are included (Fig. 5.41). The extent to

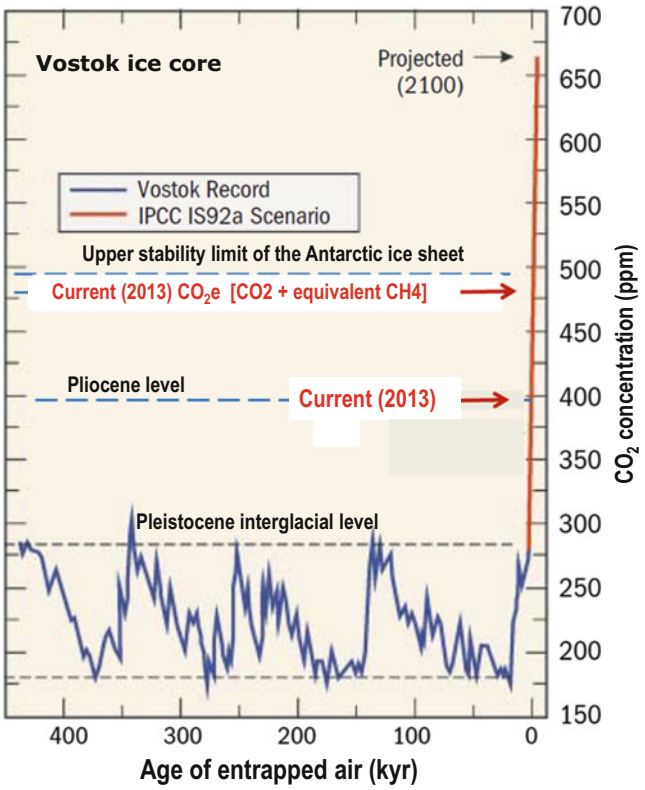

Fig. 5.39 The Vostok ice core record for atmospheric concentration (Petit et al. 1999) and the 'business as usual' prediction used in the IPCC third assessment. The current concentration of atmospheric carbon dioxide (CO_2) is also indicated. The current and Pliocene CO_2 levels, the CO_2-e (total CO_2 + equivalent CH_4) and the stability threshold of the Antarctic ice sheet are indicated (http://www.globalcarbonproject.org/science/index.htm. Courtesy P. Canadell)

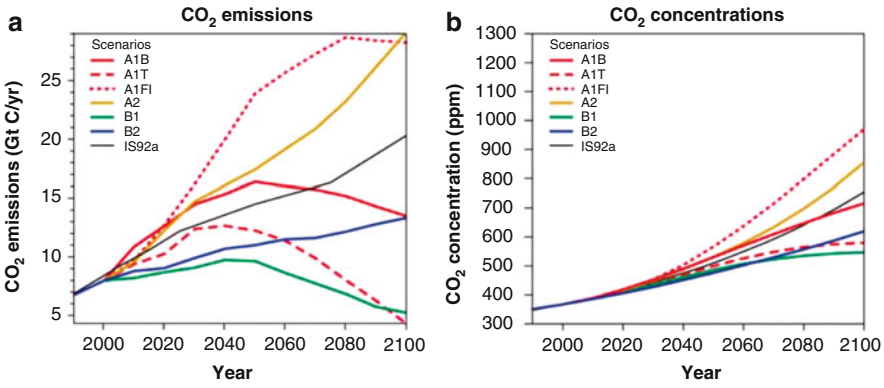

Fig. 5.40 Projections of CO_2 emissions and atmospheric CO_2 concentrations to 2100 AD. (**a**) – CO_2 emissions; (**b**) – atmospheric CO_2 concentrations; Global carbon project (http://www.globalcarbonproject.org/science/index.htm)

which the estimated resources of coal (>10,000 GtC), oil (~700 GtC) and gas (>2000 GtC) would be combusted and released to the atmosphere within the next few decades and centuries depends critically on global economic developments and the effects of extreme weather events on industry and transport systems. A central looming factor arises from increasing droughts in otherwise agriculturally productive parts of the world, including southern Europe, northern India and Australia (Figs. 5.31, 5.47, 5.43, 5.44, and 5.45). Rising temperatures through the twenty-first century (Fig. 5.45) can only enhance this trend, leading to global droughts (Figs. 5.31, 5.45, and 5.47) and food shortages. With this perspective carbon emissions are inherently self-limiting, leading to an inevitable decline of their sources. The extent to which amplifying feedbacks from current and future CO_2 levels would contribute to further rises in atmospheric greenhouse gases, global warming and the crossing of climate tipping points (Fig. 5.48) is difficult to quantify.

B. Vast amount of carbon stored in the Arctic and boreal regions, estimated at over 1.3 trillion tons of frozen carbon, is more than double that previously estimated (Canadell 2009) (Fig. 5.42). Carbon in permafrost is found largely in northern regions including Canada, Greenland, Kazakhstan, Mongolia, Russia, Scandinavia, and USA. Radioactive ^{14}C carbon dating shows that most of the carbon dioxide currently emitted by thawing soils in Alaska is released from carbon frozen thousands of years-ago and decomposes when soils thaw under warmer conditions. The evidence to date shows that carbon in permafrost is likely to play a significant role in the twenty-first century climate given the large carbon deposits, the readiness of organic matter to release greenhouse gases when thawed, and the fact that high latitudes will experience the largest relative

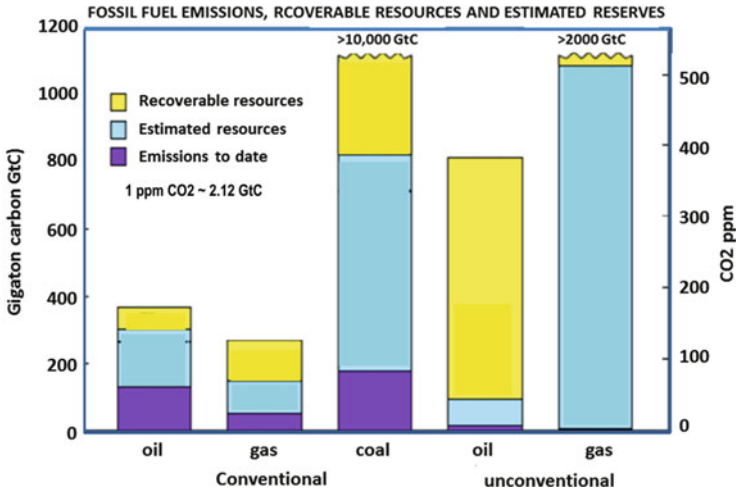

Fig. 5.41 Estimates of fossil fuel resources and equivalent atmospheric CO_2 levels, including (1) emissions to date; (2) estimated reserves, and (3) recoverable resources (1 ppm CO_2 ~ 2.12 GtC) (Hansen et al. 2012); http://www.pnas.org/content/109/37/E2415/1

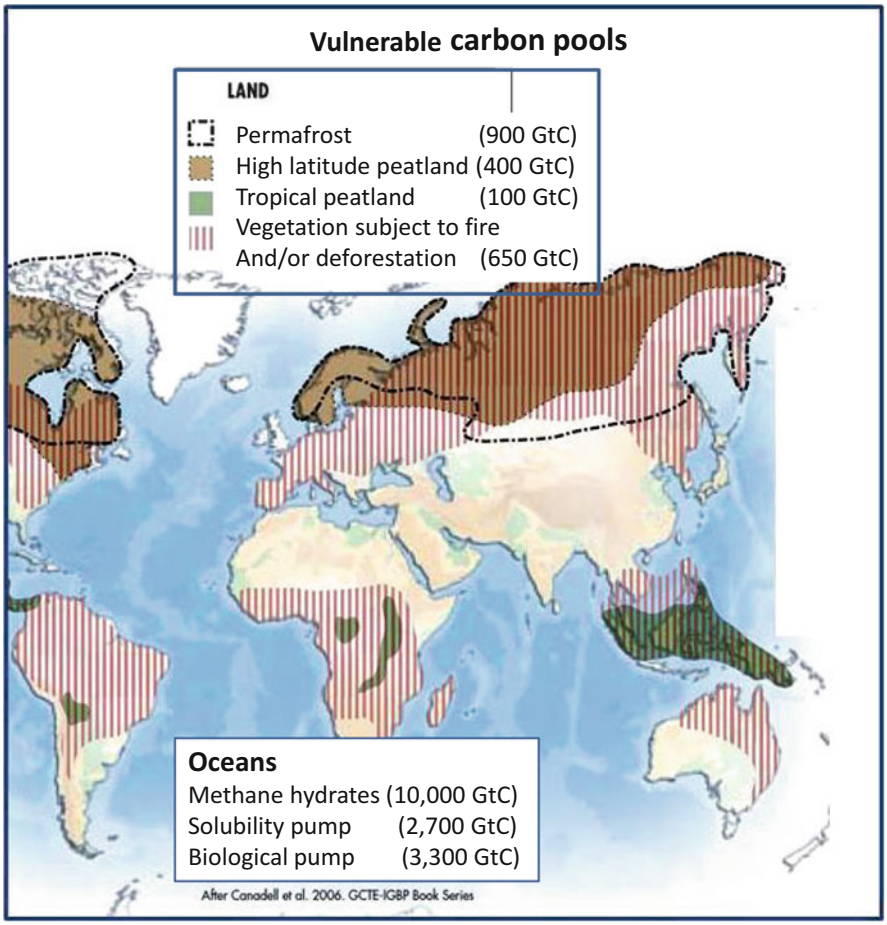

Fig. 5.42 Vulnerable carbon sinks. (**a**) Land: Permafrost – 600 GtC; High-latitude peatlands – 400 GtC; tropical peatlands – 100 GtC; vegetation subject to fire and/or deforestation – 650 GtC; (**b**) Oceans: Methane hydrates – 10,000 GtC; Solubility pump – 2700 GtC; Biological pump – 3300 GtC (After Canadell et al. 2007 GCTE-IGBP Book series; The Global carbon cycle; UNESCO-SCOPE policy briefs; Vol. 2. Courtesy P. Canadell)

increase in air temperature of all regions (Canadell 2009). Oxidation of ~6000 GtC from fossil fuel, vulnerable vegetation and methane pools in permafrost and peat land would consume about 2.10^{13} tons O_2, i.e. about 1 % of the atmospheric inventory of $1.4.10^{15}$ ton O_2. Given oxygen atmospheric residence time of 4500 years and an oxygen cycle in the order of 3.10^{14} ton O_2 per-year for the atmosphere and biosphere, long term decline in photosynthesis would result in several percent decline in atmospheric O_2, similar to developments during geological greenhouse states (Berner et al. 2007). The direct dependence of photosynthesis (Figs. 5.11 and 5.12) on ocean temperature, pH (Figs. 5.33 and 5.34) and O_2

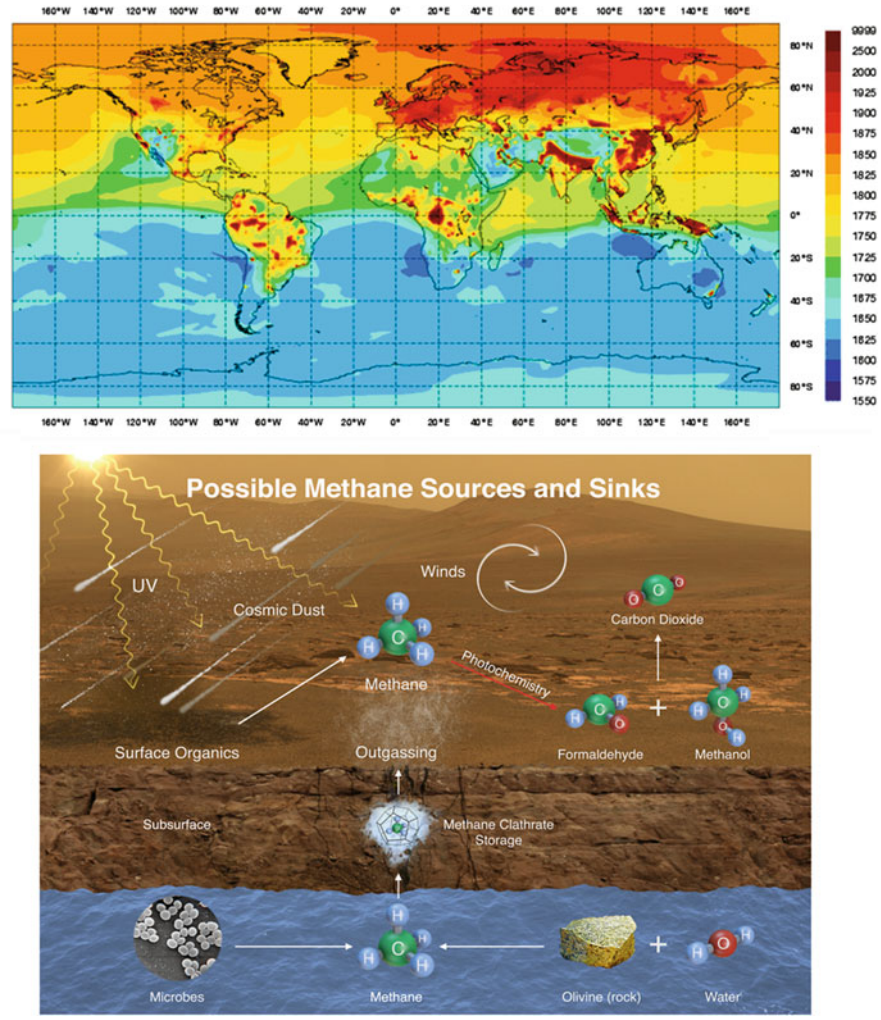

Fig. 5.43 (**a**) Global monthly mean of methane, January 2003. http://www.gmes-atmosphere.eu/d/services/gac/reanalysis/macc/macc_monthly_fields!Methan, by permission, Courtesy Miha Razinger (**b**) Methane sources and sinks. Surface methane mean 1731.73 ppbv, mazimum 4249.85. http://www.nasa.gov/jpl/msl/pia19088/

levels (Fig. 5.13) render the current trend (Fig. 5.34) deleterious to the marine food chain (Fig. 5.35).

C. The dissociation and rate of release of methane deposits from permafrost and frozen Arctic lakes and sediments as a feedback to global warming is critical to near-future greenhouse gas trajectories. The magnitude of methane deposits (Fig. 5.46), gas reservoirs (Fig. 5.47) and coal seam gas reserves and their release,

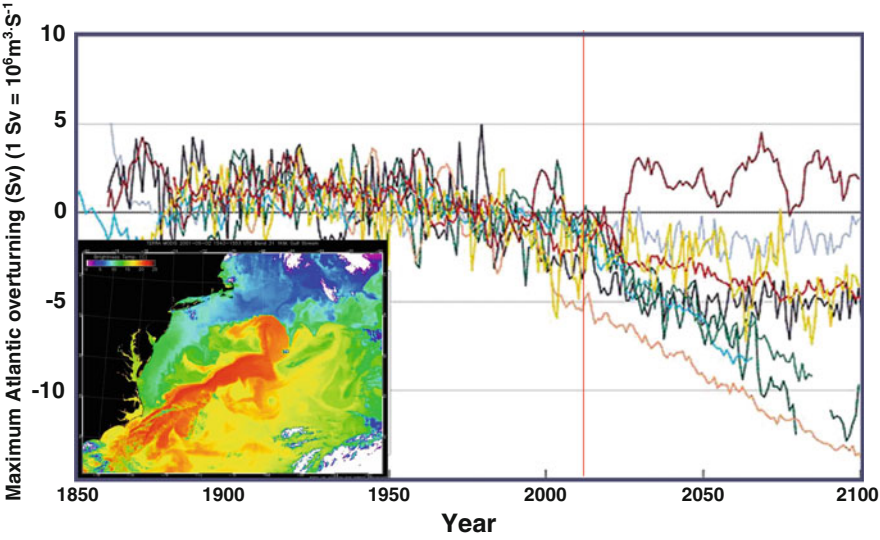

Fig. 5.44 (**a**) Observed and simulated change in ocean circulation strength with time performed by several research institutes using different coupled atmosphere-ocean models and common forcing scenarios (Compiled by Kutzbach and Fischer-Bruns http://www.pnas.org/content/98/19/10529.full.pdf+html; (**b**) Satellite infrared image of the North Atlantic Thermohaline Current (NASA – http://eoimages.gsfc.nasa.gov/images/imagerecords/1000/1393/modis_brighttemp_glfstr_lrg.jpg)

either as feedbacks to global warming or due to human exploitation, constitutes key factors threatening the future of the biosphere.

D. The North Atlantic Thermohaline Current (NATH) overturning and deep water formation has been declining since about 1950 (Fig. 5.48). Estimates vary between 1 and 4 Sverdrup (1 Sv = $10^6 m^3.s^{-1}$).[1] Advanced melting of Greenland ice (Figs. 5.25 and 5.26) and increasing fluxes of cold ice-melt water into the North Atlantic would lead to collapse of the NATH. The timing and synergy of tipping points around the world, including the effects of feedbacks from fire on atmospheric CO_2, outlined by Lenton et al. 2009), include melting of Arctic Sea, Greenland and west Antarctic ice, permafrost and Tundra loss, changes in the ENSO, changes in the West African and Indian monsoon patterns, Boreal forest decline and Amazon dieback (Figs. 5.48).
E. Changes in the ENSO reverse the trend recorded from the Pliocene to the Pleistocene glacial-interglacial cycles, signifying a return to climate conditions of about 3 million years-ago, including drought conditions in the southwest Pacific, storminess in northwest South America and gradual greening of parts of the Sahara (Fig. 5.48).

The consequences of a synergy between the processes outlined above, underpinned by the unprecedented rates at which these processes are taking place

[1] 1 Sverdrup = one million cubic meters of water flow per second.

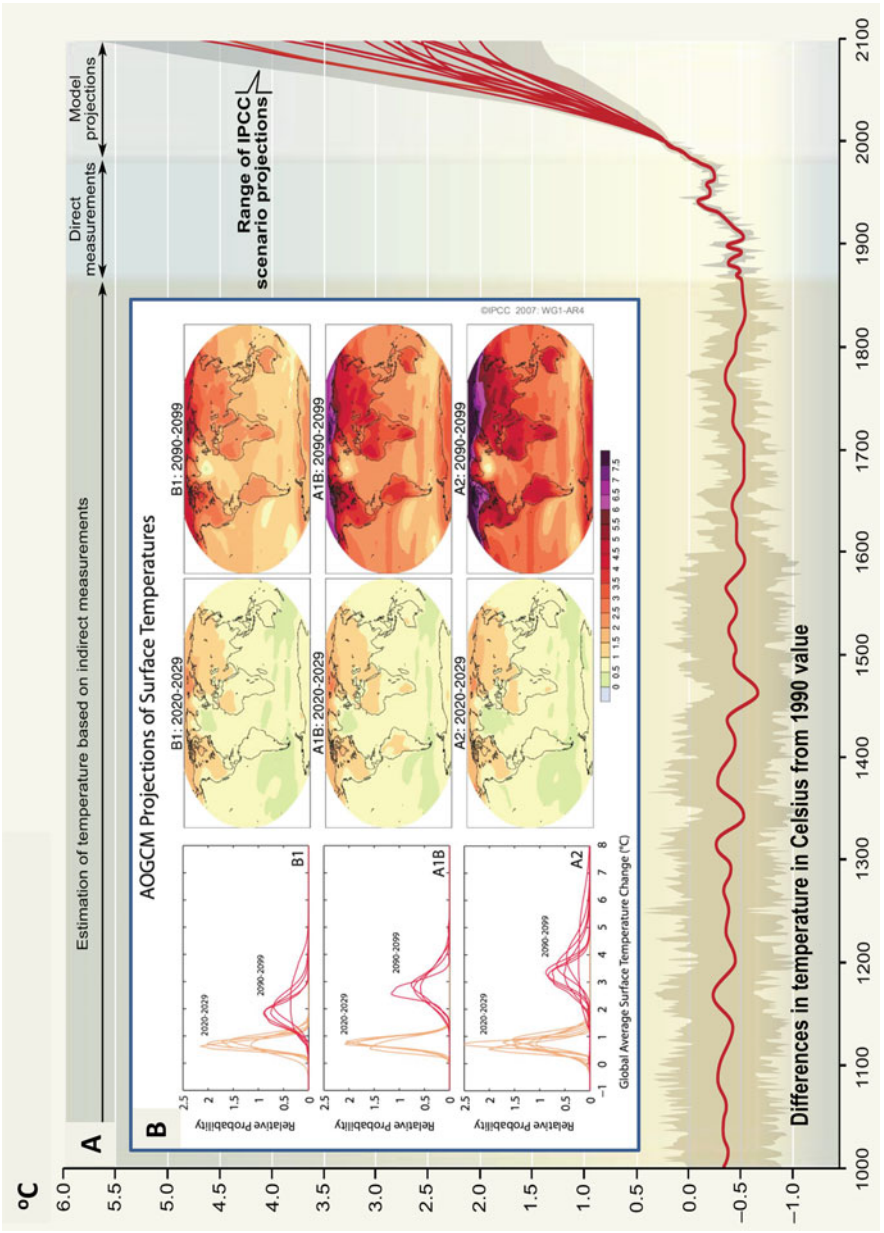
°C
A
B
Estimation of temperature based on indirect measurements
Direct measurements
Model projections
Range of IPCC scenario projections
AOGCM Projections of Surface Temperatures
B1: 2020-2029
B1: 2090-2099
A1B: 2020-2029
A1B: 2090-2099
A2: 2020-2029
A2: 2090-2099
©IPCC 2007: WG1-AR4
Relative Probability
Global Average Surface Temperature Change (°C)
Differences in temperature in Celsius from 1990 value

Fig. 5.45 (**a**) Historical and projected variations in earth's surface temperature. Estimated global temperature averages for the past 1000 years, with projections to 2100 depending on various plausible scenarios for future human behaviour (http://www.unep.org/maweb/en/Synthesis.aspx. World Resources Institute, (by permission); http://www.unep.org/newscentre/default.aspx?DocumentID=2697&ArticleID=9293&l=en); (**b**) Atmosphere–Ocean Global Circulation Model (AOGCM) projections of surface temperatures. Projected surface temperature changes for the early and late twenty-first century relative to the period 1980–1999. The central and right panels show the atmosphere–ocean general circulation multi-model average projections for the B1 (*top*), A1B (*middle*) and A2 (*bottom*) SRES scenarios averaged over decades 2020–2029 (*centre*) and 2090–2099 (*right*). (IPCC-AR4 2007. The physical science basis. Working group I contribution to the fourth assessment report of the intergovernmental panel on climate change. Cambridge University Press. Figure SPM-6. (by permission). http://www.ipcc.ch/publications_and_data/ar4/wg1/en/spmsspm-projections-of.html)

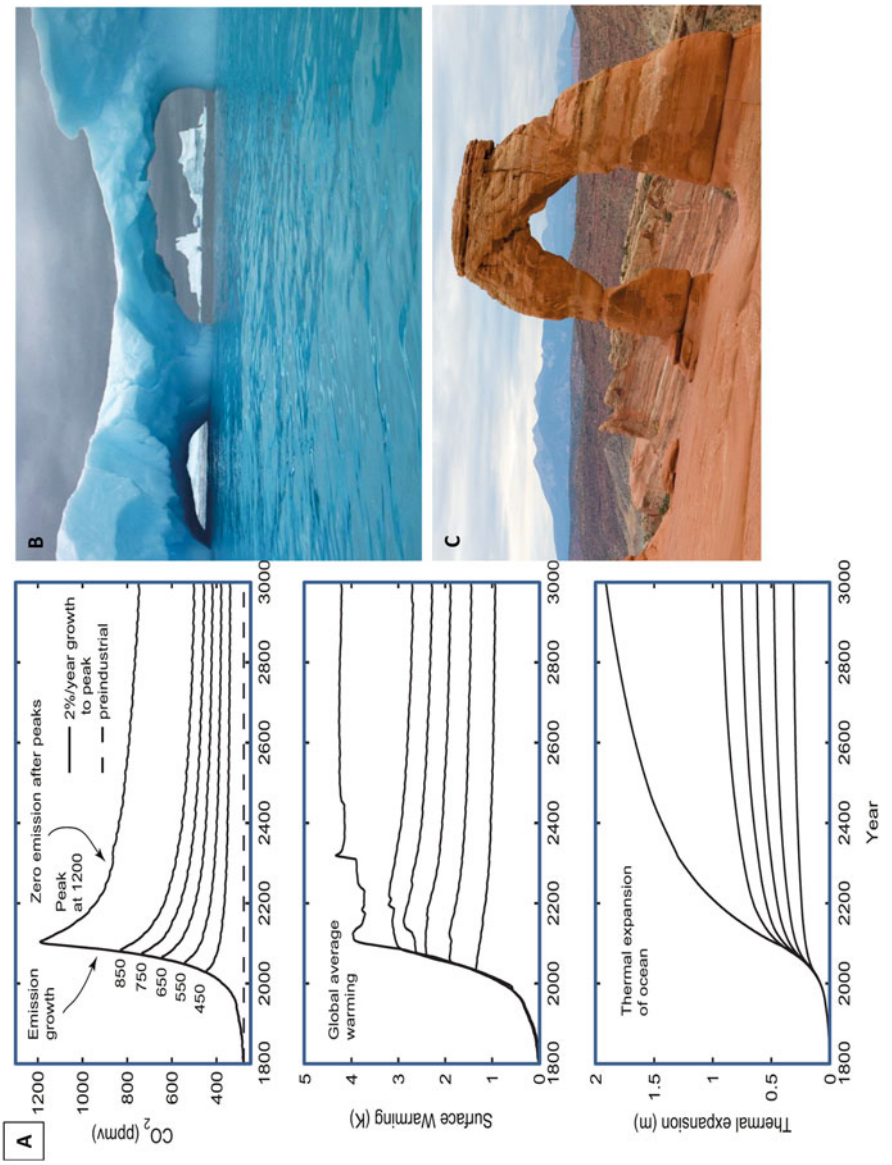
A
B
C
Emission growth
Zero emission after peaks
Peak at 1200
2%/year growth to peak
preindustrial
850
750
650
550
450
CO_2 (ppmv)
Global average warming
Surface Warming (K)
Thermal expansion of ocean
Thermal expansion (m)
Year

Fig. 5.46 (**A**) Carbon dioxide and global mean climate system changes relative to preindustrial conditions in 1765 from illustrative model, the Bern 2.5CC EMIC, whose results are comparable to the suite of assessed EMICs. Climate system responses are shown for a ramp of CO_2 emissions at a rate of 2 %/year to peak CO_2 values of 450, 550, 650, 750, 850, and 1200 ppmv, followed by zero emissions. Results have been smoothed using an 11-year running mean (Solomon et al. 2009); (**B**) Ice Arch. http://icestories.exploratorium.edu/dispatches/big-ideas/ice/ Creative commons. (**C**) Delicate Arch, National Park in Moab, Utah, the LaSalle Mountains are seen in the background. http://commons.wikimedia.org/wiki/File:Delicate_Arch_LaSalle.jpg

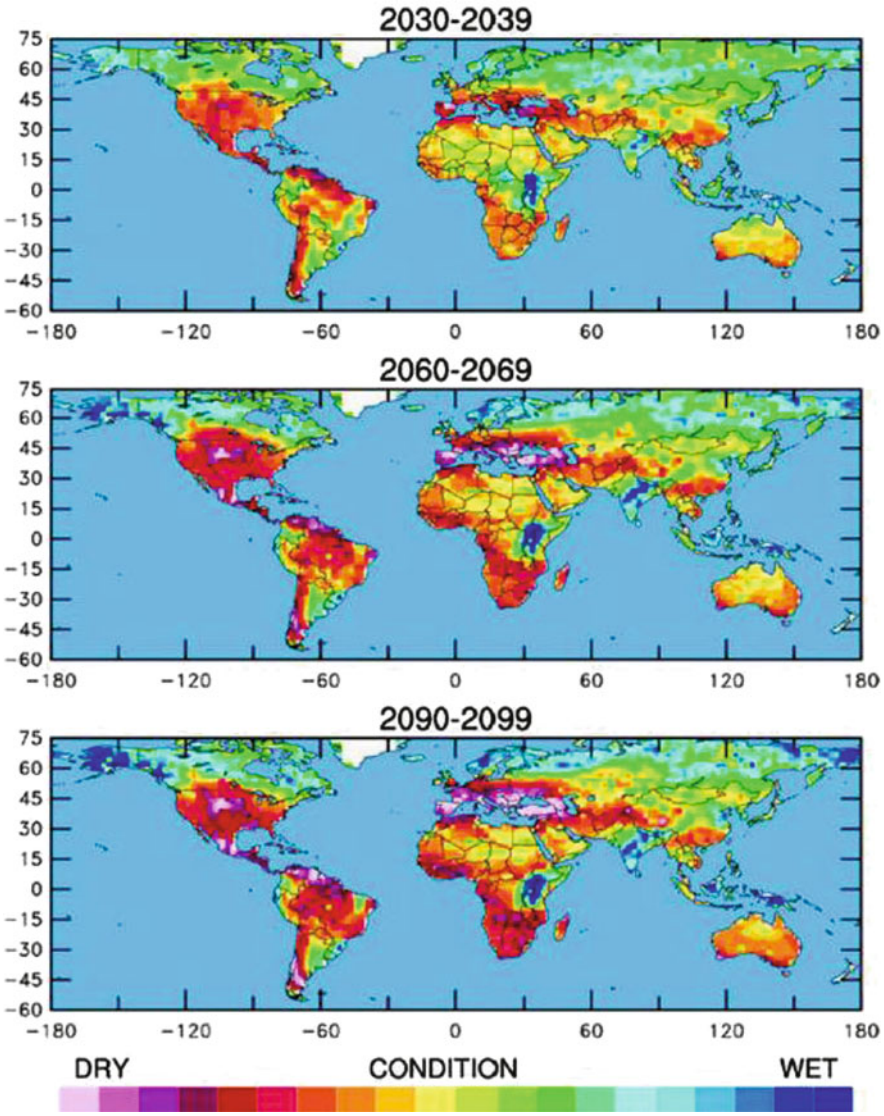

Fig. 5.47 2030–2099 droughts. The map uses a common measure, the Palmer drought severity index, which assigns positive numbers when conditions are unusually wet for a particular region, and negative numbers when conditions are unusually dry. A reading of −4 or below is considered extreme drought. Regions that are blue or green will likely be at lower risk of drought, while those in the *red* and *purple* spectrum face more unusually extreme drought conditions (https://www2.ucar.edu/atmosnews/news/2904/climate-change-drought-may-threaten-much-globe-within-decades. Courtesy Ivonne Mondragon, UCAR (University Corporation for Atmospheric Research)

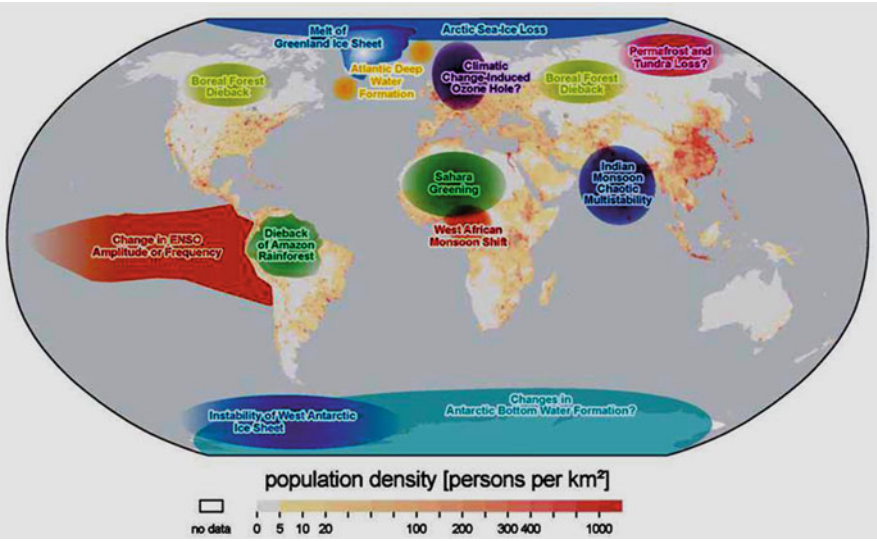

Fig. 5.48 A map of potential policy-relevant tipping elements in the climate system, overlain on global population density. Subsystems indicated could exhibit threshold-type behaviour in response to anthropogenic climate forcing, where a small perturbation at a critical point qualitatively alters the future fate of the system. They could be triggered this century and would undergo a qualitative change within this millennium. Excluded from the map are systems where threshold appears inaccessible this century, e.g., East Antarctic Ice Sheet, or the qualitative change would appear beyond this millennium, e.g. marine methane hydrates. Question marks indicate systems whose status as tipping elements is particularly uncertain (Lenton et al. 2009. Proceedings National Academy of Science USA, by permission)

(Fig. 5.24), can hardly be quantified. Whereas the precise timing of global climate tipping points remains difficult to define, the current intensification of extreme weather events around the globe, expressed by the increased variability of climate events (Rahmstorf and Coumou 2011; Hansen et al. 2012) (Fig. 5.32) may express tipping elements in the climate. A rise of ~0.2–1.0 °C in sea surface temperature during 1800–2011 (NASA/GISS 2013) (Figs. 5.22 and 5.23) has led to enhanced intensity and in some instances frequency of hydrological evaporation/precipitation cycle in several parts of the world, resulting in intensification of cyclones and floods (Fig. 5.30). The rise in land temperatures results in an increased frequency and intensity of heat waves and fires, at a rate about two to three fold during 1980–2012 (Munich Re-Insurance 2012) (Figs. 5.19 and 5.30).

As stated by the IPCC (2012): "*Models project substantial warming in temperature extremes by the end of the 21st century. It is virtually certain that increases in the frequency and magnitude of warm daily temperature extremes and decreases in cold extremes will occur in the 21st century on the global scale. It is very likely that the length, frequency and/or intensity of warm spells, or heat waves, will increase over most land areas. Based on the A1B and A2 emissions scenarios, a 1-in-20 year hottest day is likely to become a 1-in-2 year event by the end of the 21st century in most regions, except in the high latitudes of the Northern Hemisphere, where it is*

likely to become a 1-in-5 year event". Rahmstorf and Coumou (2011) conducted a statistical analysis of the relations between long-term climate trends and the incidence of extreme weather events, finding that the number of record-breaking heat events increases approximately in proportion to the ratio of warming trend to short-term standard deviation, or variability. Short-term variability decreases the number of heat extremes, whereas a longer term climatic warming trend increases it.

Since about 2006 the rate of atmospheric methane rise increased to more than 7 ppb/year (Fig. 5.16). By 2010 reports of advanced release of methane from the East Siberian Arctic Shelf (ESAS) have been communicated by Shakova (2010), Shakova et al. (2010). The summary report reads: "*Remobilization to the atmosphere of only a small fraction of the methane held in East Siberian Arctic Shelf (ESAS) sediments could trigger abrupt climate warming, yet it is believed that sub-sea permafrost acts as a lid to keep this shallow methane reservoir in place. Here, we show that more than 5000 at-sea observations of dissolved methane demonstrates that greater than 80 % of ESAS bottom waters and greater than 50 % of surface waters are supersaturated with methane regarding to the atmosphere. The current atmospheric venting flux, which is composed of a diffusive component and a gradual ebullition component, is on par with previous estimates of methane venting from the entire World Ocean. Leakage of methane through shallow ESAS waters needs to be considered in interactions between the biogeosphere and a warming Arctic climate*." In an interview (Shakova 2010) clarifies that the concentration of atmospheric methane over parts of the East Siberian shelf is 8–10 % higher than global concentration, the highest recorded in the Pleistocene ice cores and that the amount of methane released from the East Siberian shelf is greater than the total released from the world oceans.

Projections of twenty-first century climate trends suggest that, excepting the masking effects by sulphur aerosols, the climate is fast-tracking toward conditions such as existed during the Pliocene (~5.3–2.6 Ma) and the peak Miocene (~16 Ma), when temperatures were ~2 °C to ~4 °C higher than pre-industrial Holocene levels. A development of pre-Oligocene (pre-34 Ma) ice-free conditions, when atmospheric CO_2 levels exceeded ~500 ppm, depends on the growth rate of carbon emission and atmospheric CO_2 and on amplifying feedbacks from the land, permafrost, ice sheets and oceans. According to Hansen et al. (2012) "*Burning all fossil fuels would create a different planet than the one that humanity knows. The palaeoclimate record and ongoing climate change make it clear that the climate system would be pushed beyond tipping points, setting in motion irreversible changes, including ice sheet disintegration with a continually adjusting shoreline, extermination of a substantial fraction of species on the planet, and increasingly devastating regional climate extremes*". However it is unlikely that the world's fossil fuel reserves, estimated as >13,000 GtC (Hansen et al. 2012) (Fig. 5.41) could be combusted as deteriorating global climate, extreme weather events and their consequences for agriculture and industry can only reduce the use of fossil fuels, rendering emissions self-limiting.

Should the global community choose to focus its remaining resources on mitigation of carbon emissions, climate geo-engineering effort (Royal Society 2009) and

Table 5.1 Proposed solar mitigation and atmospheric carbon sequestration methods

Method	Supposed advantages	Problems
SO_2 injections	Cheap and rapid application	Short atmospheric residence time; ocean acidification; retardation of monsoons
Space sunshades	Rapid application; no direct effects on ocean pH	Possibly limited space residence time; uncertain positioning
Iron filing enhancing ocean fertilization	CO_2 sequestration	Decaying phytoplankton release CO2 back to the water and atmosphere
Ocean pipe systems for circulation of cold water and enhanced CO_2 sequestration	CO_2 sequestration	Accelerated warming of deep water; limited depth of penetration of the pipes
Land-based NaOH pipe systems sequestering CO_2 to $NaCO_3$	CO_2 sequestration	The $NaCO_3$ requires processing to separate and bury CO_2 in the ground; the CO_2 needs to be stored underground
Biochar – Soil carbon burial	Effective storage of carbon in soils	Possibly limited scale; requires large international efforts
Serpentine CO_2 sequestration	CO_2 sequestration	Scale unknown

adaptation to the fast deteriorating climate, some of the methods outlined in Table 5.1 may apply. A species which has placed a man on the moon should also be able to develop a range of effective greenhouse gas sequestration methods in order to protect its home planet. Since the onset of sulphur emissions from coal and oil, masking the effects of greenhouse gas radiative forcing by about −1.1–1.5 Watt/m^2 since 1750 (IPCC-AR4 2007; Murphy et al. 2009; Hansen et al. 2011; Hansen 2012a, b), near-to 50 % of global warming has been transiently mitigated, constituting an unintended geo-engineering measure. Regional variations occur, with large concentrations of aerosols over industrial centers in the Northern Hemisphere. With the acceleration of climate change since about 1975 an increase in sulphur emissions is being considered in order to cool the planet, along with a range of other mitigation and CO_2 draw-down methods (Table 5.1).

Principal observations include (Glikson 2012):

1. Stratospheric sulphur injections are both short-lived and destructive in terms of ocean acidification and retardation of the monsoon and of precipitation over large parts of the Earth, including Africa, southern and Southeast Asia.
2. Retardation of solar radiation through space sunshades is of limited residence time and would not prevent ocean acidification from ongoing carbon emission.
3. The dissemination of ocean iron filings and temperature exchange through pipe systems are likely ineffective in transporting CO_2 to safe water depths.
4. CO_2 sequestration using soil carbon, biochar and possible chemical methods such as “sodium trees”, combined with rapid decline in industrial CO_2 emissions, can in principle help slow down, and in future even reverse, the current rise in atmospheric CO_2 toward mean global temperatures above 2°°C.

5. Budgets on a scale of military spending (>$20 trillion since WWII) are required in order to attempt to retard, and in future possibly reverse, current trend toward likely tipping points, including increasing release of methane from permafrost and Arctic sediments.
6. Top priority ought to be given to fast track methods of CO_2 sequestration.

Given the short-lived stratospheric residence time of SO_2 of up to about 2 years, continuous replenishment would be required. Deleterious consequences, including further ocean acidification and retardation of the monsoon over parts of the Earth, including Africa, southern and Southeast Asia, would ensue. Retardation of solar radiation through space sunshades may have longer residence time, but would not, in isolation, prevent further ocean acidification. Dissemination of ocean iron filings and temperature exchange through pipe systems are likely ineffective in transporting sufficient amounts of CO_2 for storage into "safe" water depths. By contrast, global efforts at CO_2 sequestration, using soil carbon, biochar and possible chemical methods such as "sodium trees" and CO_2 absorption by hydrosilicates such as serpentinite, combined with rapid decline in industrial CO_2 emissions, could in principle help slow down, if not reverse, the current rise in greenhouse gases.

Should a global effort at mitigation and adaptation not occur, rapid warming and ocean acidification would affect the base of the food chain (Fig. 5.35) and thereby survival of large mammals and many other species. Warm acid oceans would be severely depleted in corals, phytoplankton, krill and higher marine life. As occurred during the K-T extinction small burrowing mammals could fare better. Many bird species, deprived of many of their migratory routes and nesting homes, would suffer demise. A yet higher scale of Mass Extinction would ensue from a nuclear coup-de-grace, increasingly likely on a planet stressed by environmental crises, compounding a '*greenhouse summer*' with a '*nuclear winter*'. The enhanced hydrological cycle, favoring extensive growth in expanded tropical and subtropical regions, could lead to the opening of new ecological niches and proliferation of resistant life forms such as insect species.

Ultimate consequences of global warming are alluded to in Ward's (2007) '*Under A Green Sky*', portraying three scenarios:

(A) Drastic cut in carbon emissions in an attempt to keep atmospheric CO_2 below 450 ppm;

(B) Atmospheric CO_2 level reaches 700 ppm by the year 2100 while sea level rises on the scale of meters and the North Atlantic conveyer collapses;

(C) by 2100 CO_2 levels reach 1100 ppm and temperatures 10 °C above pre-industrial level, ensue in total melt of polar and glacier ice and in deep ocean anoxia, culminating in the sixth great mass extinction, as has already commenced (Figs. 5.49 and 5.50).

5.6 The Post-anthropocene World

The longevity and potential irreversibility of atmospheric CO_2 modeled by Solomon et al. (2009) and Eby et al. (2009) implies long term tropical conditions (Fig. 5.46, and 5.51) postdating a cessation of emissions by at least 1000 years.

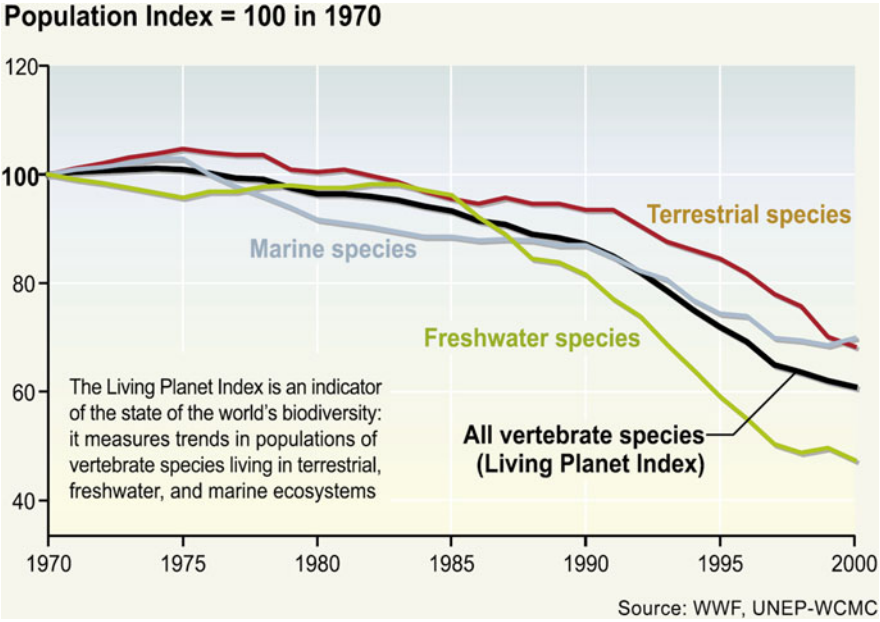

Fig. 5.49 The living planet index 1970–2000. The index currently incorporates data on the abundance of 555 terrestrial species, 323 freshwater species, and 267 marine species around the world. While the index fell by some 40 % between 1970 and 2000, the terrestrial index fell by about 30 %, the freshwater index by about 50 %, and the marine index by around 30 % over the same period. From "Ecosystems and human well-being – Biodiversity Synthesis". Millennium Ecosystems Assessment. http://www.unep.org/maweb/en/Synthesis.aspx (World Resources Institute, by permission)

Following cessation of emissions the rate of temperature transfer to the oceans declines but atmospheric temperatures decline at a slower rate. A rise of atmospheric CO_2 to peak levels of 450–600 ppm would result in dry season reduction in rainfall and continental dust-bowl conditions in several regions and in inexorable sea level rise for peak CO2 concentrations exceeding ~1000 ppm (Solomon et al. 2009). Multi-millennial simulations by Eby et al. (2009) find the period required to absorb anthropogenic CO_2 strongly depends on the total amount of emissions and that for emissions similar to known fossil fuel reserves, the time to absorb 50 % of the CO_2 is more than 2000 years. The long-term climate response appears to be independent of the rate at which CO_2 is emitted over the next few centuries. The lifetime of the surface air temperature anomaly might be as much as 60 % longer than the lifetime of anthropogenic CO_2 and that two-thirds of the maximum temperature anomaly will persist for longer than 10,000 years, suggesting the consequences of anthropogenic CO_2 emissions will persist for many millennia (Eby et al. 2009).

According to Berger and Loutre (2002) current climate change is leading to an exceptionally long interglacial period ahead (Fig. 5.51). These authors state: '*The present day CO_2concentration (397 ppm by 2012) is already well above typical interglacial values of ~290 ppmv. This study models increases to up to 750 ppmv over the next 200 years, returning to natural levels by 1000 years. The results suggest that, under very small insolation variations, there is a threshold value of*

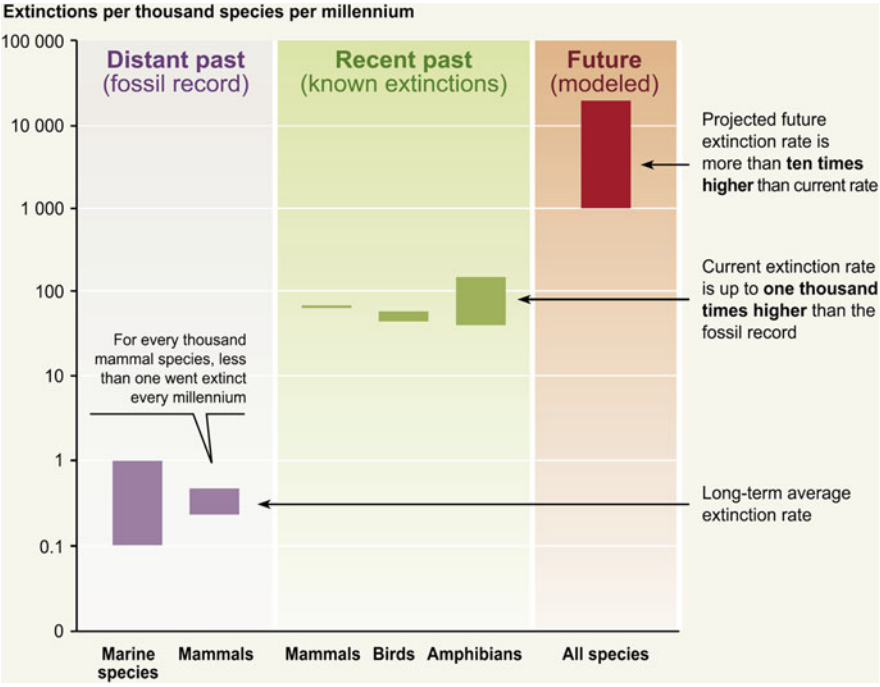

Fig. 5.50 Species extinction rates. "Distant past" refers to average extinction rates as calculated from the fossil record. "Recent past" refers to extinction rates calculated from known extinctions of species (*lower estimate*) or known extinctions plus "possibly extinct" species (*upper bound*). A species is considered to be "possibly extinct" if it is believed to be extinct by experts but extensive surveys have not yet been undertaken to confirm its disappearance. "Future" extinctions are model-derived estimates using a variety of techniques, including species-area models, rates at which species are shifting to increasingly more threatened categories, extinction probabilities associated with the IUCN categories of threat, impacts of projected habitat loss on species currently threatened with habitat loss, and correlation of species loss with energy consumption. The time frame and species groups involved differ among the "future" estimates, but in general refer to either future loss of species based on the level of threat that exists today or current and future loss of species as a result of habitat changes taking place roughly from 1970 to 2050. Estimates based on the fossil record are low certainty. The lower-bound estimates for known extinctions are high certainty, while the upper-bound estimates are medium certainty; lower-bound estimates for modelled extinctions are low certainty, and upper-bound estimates are speculative. From "Ecosystems and human well-being – Biodiversity Synthesis". Millennium Ecosystems Assessment. http://www.unep.org/maweb/en/Synthesis.aspx (World Resources Institute, by permission)

CO_2above which the Greenland ice sheet disappears. The climate system may take 50,000 years to assimilate the impacts of human activities during the early third millennium. In this case an 'irreversible greenhouse effect could become the most likely future climate. If the Greenland and west Antarctic ice sheets disappear completely, then today's 'Anthropocene' may only be a transition between the Quaternary and the next geological period'.

Flooding of low-lying river systems (Ganges, Mekong, Yellow River, Nile, Indus, Tigris/Euphrates, Mississippi, Rhine, Thames), would decimate major agrarian

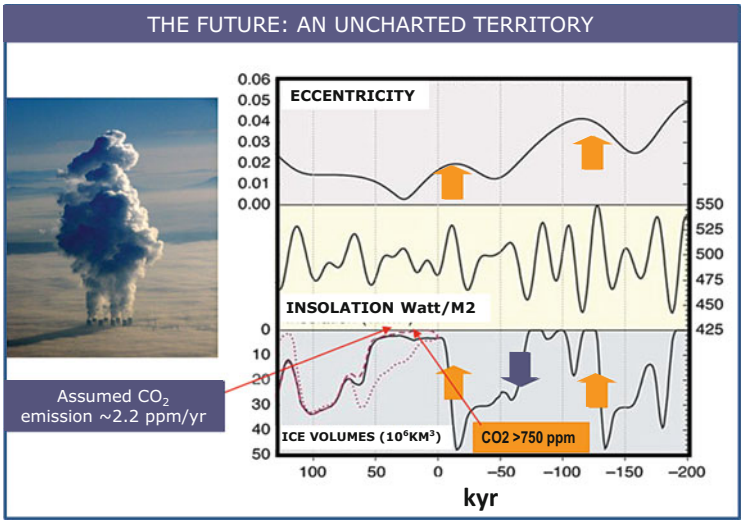

Fig. 5.51 An exceptionally long interglacial ahead? (Berger and Loutre 2002). Long-term variations of eccentricity (*top*), June insolation at 65ºN (*middle*), and simulated Northern Hemisphere ice volume (increasing downward) (*bottom*) for 200,000 years before the present to 130,000 from now. Time is negative in the past and positive in the future. For the future, three CO_2 scenarios were used: last glacial-interglacial values (*solid line*), a human-induced concentration of 750 ppmv (*dashed line*), and a constant concentration of 210 ppmv (*dotted line*) (American Association for the advancement of Science, by permission)

populations and abruptly curtail food supplies to urban centers. Flooding of tropical river valleys (e.g. Amazon and Congo rivers) will destroy vast tracts of rainforest. Depending how far global warming proceeds and the extent to which humanity's nuclear arsenal is released, by accident or design, some members of the species may survive, mostly those genetically adapted to extreme conditions in remote parts of the globe.

Rising Arctic temperatures will still leave the polar regions within human body temperature comfort zones. There, small human clans such as the Inuit may survive, provided ocean acidification and intense radioactivity do not completely destroy the base of the food chain. The intensified hydrological cycle will enhance precipitation in the Siberian Taiga, benefiting Caribou herds and the nomad Laps. People are likely to survive in volcanic ocean islands higher than a few tens of meters high and in sheltered mountain valleys. In the tropics, buffering of rising temperatures by increased clouding and heavier precipitation may allow survival of original tropical humans whose respiratory system has adapted to extreme humidity and heat over thousands of years, for example those who live in the foothills of the Himalayas.

In all these regions, rising temperatures would lead to a rise in the destructive role of bush fires. In temperate climate zones, the site of major urban populations, encroaching desert conditions such as the northward advance of Sahara-like conditions into southern Europe, and the dependence of populations on stressed global networks of food, fuel, technology and medication, could prove calamitous. More confident survivors will include grasses, insects, some bird species and extremo-

phile habitats of abyssal volcanic vents that do not depend on photosynthesis. If surviving birds, descendants of the fated dinosaurs, would eclipse the mammals, whose limited heat tolerance may seal their fate, the circle would be complete. Habitat niches would be created to be filled by surviving species – a new evolutionary cycle would commence.

Despite detailed studies of past climates, paleontology, evolutionary biology and, most particularly, the nature of mass extinctions of species, with few exceptions to date Earth science has been less than inclined to attempt projections of the nature of the forthcoming biological cycle, in the wake of the ongoing sixth mass extinction of species. Perhaps the subject is too scary and ought to be relegated to the unthinkable. Built into science fiction literature is a plethora of imagined *parallel-universe* scenarios, portraying future generations of humans and their robotic offspring on Earth, the planets and space, where they produce synthetic foods, mine asteroids, wage star wars, destroy the locals and disseminate their genome to outer galaxies. But while such futuristic fictions may serve to divert attention from the current plight of *Homo sapiens*, only rarely is it realized that sophisticated *parallel-universe* societies already exist right under our feet and around us in the form of the colonial insects – termite nests and bee hives, and that the proliferation of the arthropods across the wide range of climate zones and their resistance to ionizing radiation would ensure survival of insect species relative to that of mammals and bird species. Based on the brief ~2 million years episode of a species mastering control over fire – a source of energy exceeding its own physiological capabilities by orders of magnitude – future biospheres will be dominated either by survivors of the genus *Homo* or, alternatively, by radiation-resistant arthropods species. Thus where the upper safe radiation limit for humans is about ~70 rads (1 rad = 0.01 Joul/kg) (CDC 2011), according to Bakri et al. (2005) irradiation data generated since the 1950s, covering over 300 arthropod species, indicate the dose needed for sterilization of arthropods varies from less than 500 rad for blaberid cockroaches to 30,000 rad or more for some arctiid and pyralid moths. Having originated about the *Cambrian Explosion* of life, when small bivalve-like shells were dated as 541–539 Ma (Braun et al. 2007) in the classic outcrops of the Burgess Shale (Gould 1990), the highly advanced colonial intelligence of insect colonies is likely to dominate future cycles of the terrestrial biosphere.

Chapter 6
Rare Earth

"For we are the local embodiment of a Cosmos grown to self-awareness. We have begun to contemplate our origins: star-stuff pondering the stars; organised assemblages of ten billion-billion-billion atoms considering the evolution of atoms; tracing the long journey by which, here at least, consciousness arose. Our loyalties are to the species and the planet. WE speak for the Earth. Our obligation to survive is owed not just to ourselves but also to that Cosmos, ancient and vast, from which we spring … We succeeded in taking that picture [from deep space], and, if you look at it, you see a dot. That's here. That's home. That's us. On it everyone you know, everyone you love, everyone you've ever heard of, every human being who ever was, lived out their lives. The aggregate of all our joys and sufferings, thousands of confident religions, ideologies and economic doctrines. Every hunter and forager, every hero and coward, every creator and destroyer of civilizations, every king and peasant, every young couple in love, every hopeful child, every mother and father, every inventor and explorer, every teacher of morals, every corrupt politician, every superstar, every supreme leader, every saint and sinner in the history of our species, lived there – on a mote of dust suspended in a sunbeam. The Earth is a very small stage in a vast cosmic arena. Think of the rivers of blood spilled by all those generals and emperors so that in glory and triumph they could become the momentary masters of a fraction of a dot. Think of the endless cruelties visited by the inhabitants of one corner of the dot on scarcely distinguishable inhabitants of some other corner of the dot. How frequent their misunderstandings, how eager they are to kill one another, how fervent their hatreds. Our posturing, our imagined self-importance, the delusion that we have some privileged position in the universe, are challenged by this point of pale light. Our planet is a lonely speck in the great enveloping cosmic dark. In our obscurity – in all this vastness – there is no hint that help will come from elsewhere to save us from ourselves…"

(Carl Sagan, Cosmos 1980).

A.Y. Glikson, C. Groves, *Climate, Fire and Human Evolution*, Modern Approaches in Solid Earth Sciences 10, DOI 10.1007/978-3-319-22512-8_6

Abstract The emergence of the genus *Homo*, and subsequently of *Homo sapiens*, have led to a unique phenomenon in the history of nature where the advanced technological achievements of the species in mastering fire, combustion, the electromagnetic spectrum and nuclear power have given it the illusion of god-like powers. The arrogance of supremacy is blinding the species to its intrinsic origin from and relation with nature, endangering its survival. However, no biological entity, all the way from the DNA/RNA biomolecules to the human brain, can claim possession of intelligence – a faculty written into the laws of nature. Intelligence is no more a property of any species or individual organism than, for example, are the effects of gravity and electromagnetism to which life is subject. From its faith in omnipotent gods, to a mythological faith in human mastery over nature inherited from the scriptures, to a belief in a purported ability of computer technology to colonize extraterrestrial planets, *Homo sapiens* has become subject to a self-referential anthropocentric delusion (Strongman L (2007) The anthropomorphic bias: how human thinking is prone to be self-referential. Working papers no 4–07. Lower Hutt: The Open Polytechnic of New Zealand. http://hdl.handle.net/123456789/1245). For a species which shares some 98.5 % of its genes with primates,- such fantasies deny its inextricable relationship with the terrestrial biosphere, from which it sprang.

Earth constitutes a unique planet in the Solar system (Fig. 6.1) and likely far beyond (Fig. 6.2). Drake and Dava (1992) estimate the frequency of technical civilizations in the Milky Way galaxy in terms of

$$N = R * fp * ne * fl * fi * fc * L.$$

N = the number of civilizations in our galaxy with which communication might be possible (i.e. which are on our current past light cone); R = the average rate of star formation per year in our galaxy fp = the fraction of those stars that have planets ne = the average number of planets that can potentially support life per star that has planets fl = the fraction of the above that actually go on to develop life at some point fi = the fraction of the above that actually go on to develop intelligent life fc = the fraction of civilizations that develop a technology that releases detectable signs of their existence into space L = the length of time for which such civilizations release detectable signals into space. A critical parameter in this equation is "L", the longevity of technological societies measured from the time radio telescopes are invented in an attempt to communicate with other planets. Estimates of "L" range between a minimum of 70 years and 10,000 years, but even in the more optimistic longevity scenario only 2.31 such planets would exist in the galaxy at the present time. Sagan (1980) estimated L on the scale of only a couple of hundred years from the time a civilization discovers nuclear fission. A similar suggestion can be made regarding the onset of combustion of carbon. It will never be known whether an organism exists, in the Milky Way or other galaxies which has triggered a mass extinction of species.

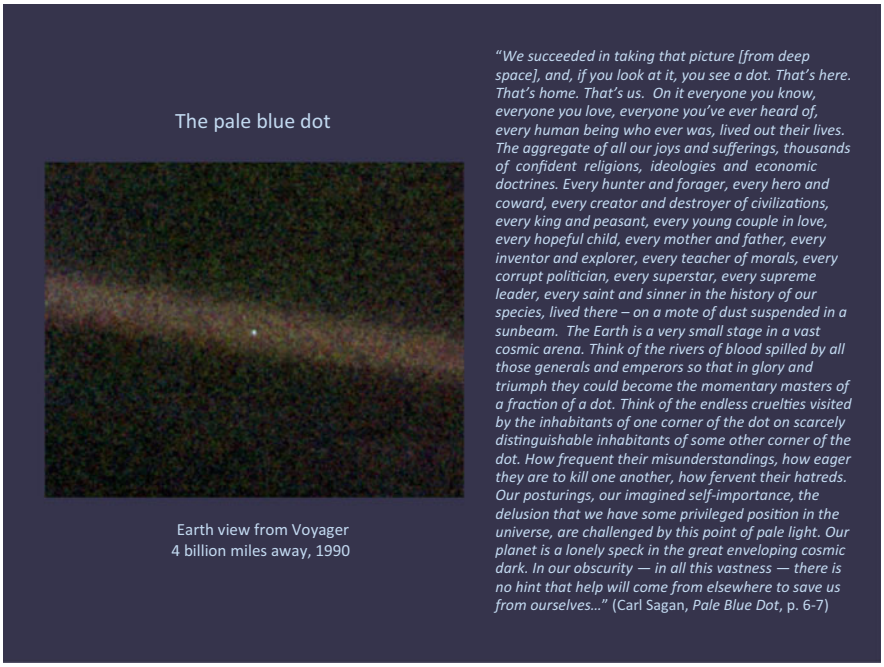

Fig. 6.1 The pale blue dot. Earth viewed by Voyager from a distance of four billion miles (NASA http://thornscompose.com/2009/11/28/advent_part1/)

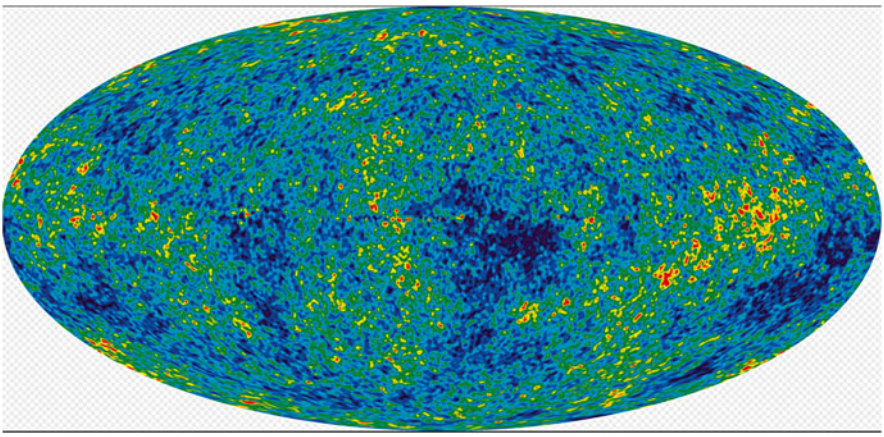

Fig. 6.2 Detailed all-sky picture of the Cosmic Background Radiation (CMB) representing the infant universe, created in 2012 from 9 years of WMAP data. The image reveals 13.77 billion year old temperature fluctuations (shown as colour differences) that correspond to the seeds that grew to become the galaxies. The image shows a temperature range of ±200 micro-Kelvin (Credit: NASA/WMAP (Wilkinson Microwave Anisotropy Probe) Science Team WMAP # 121238 Image. http://map.gsfc.nasa.gov/media/121238/index.html)

Numerous factors have been invoked to suggest the universe can be regarded as 'bio-friendly', hinting at principles written into the laws of nature. An example is the production of the heavy elements on which life depends – carbon, oxygen, sulphur and nitrogen – in the cores of stars allowed by the constants of physics. The emergence of early manifestations of life on Earth as far back as ~3.8 billion years ago (Bolhar et al. 2004), is consistent with the view of a 'bio-friendly' universe (Lineweaver and Davis 2002). According to Davies (2006), whereas no known law of physics contains life as an end state or attractor toward which matter and energy are destined to evolve, the universe contains a number of remarkable necessary features which lead to a habitable nature, including:

A. The Big Bang resulting in dispersal of energy and matter at rates which allow formation of galaxies, stars and consequently habitable planets;
B. The universe expansion rate being relatively smooth, which avoids chaotic disruption and collapse yet containing minor irregularities, as revealed by the satellite WMAP map (Wilkinson Microwave Anisotropy Probe) (Fig. 6.2) and which, with time, coalesced matter into galaxies and stars, the existence of life depending on the primordial density perturbations and fine-tuning of physical constants.
C. The nucleosynthesis of carbon from three nuclei of helium and subsequently synthesis of oxygen and other heavier nuclei as sensitive reactions which depend on the magnitude of the nuclear resonance (Hoyle 1982). The subsequent dissemination of carbon in supernova explosions depending sensitively on the strength of the weak nuclear force.
D. Rees (2001) draws a distinction between universes with physical constants which disallow life, those which allow life and those in which life can flourish. The latter accord with the theory of 'Biological Determinism' where, once conditions exist for life to emerge, the synthesis of bio-molecules and appearance of microbes become inevitable (Shapiro 1986; de Duve 1995).

A prevalent view among cosmologists favors a multiverse where the laws of physics and different energy states and factors such as quantum fluctuations are restricted to particular cosmic regions (Wigner 1961; Rees 1999, 2001; Davies 2004). Davies (2006) draws a distinction between (1) biogenetic principles and processes, and (2) the conditions amenable to emergence of life such as the existence of carbon and of water. Thus, a presence of amino acids does not imply an emergence of life any more than the existence of iron atoms implies an appearance of computers.

The probability of accidental assembly of biomolecules from an aqueous mixture of organic molecules, i.e. the "primordial soup" of Miller (1953), over a period of time **t**, is estimated by Hoyle (1982) as a probability $P_1 = 1/10^{40,000}$. According to Davies (1998) the chance of biomolecule synthesis from amino acids would be in the order of 1/10^120 and this includes environments where favorable conditions for emergence of life exist according to the Drake equation (Drake and Dava 1992). Alternative biogenetic hypotheses include self-organization (Kaufmann 1995), mathematical principles of complexity and information theory, pre-existence of

replicator molecules, such as have not been observed in nature, or 'vacuum fluctuations' inherent in quantum mechanics (Davies 2006). Whether biogenesis has taken place locally and spread through large parts of the universe, according to the theory of Panspermia (Hoyle and Wickramasinghe 1981), remains unknown. Likewise unanswered is the question whether life emerged on Earth at one point of time or a number of times, in particular since biomolecules may have been destroyed during periods of heavy asteroid bombardment (Maher and Stevenson 1988).

In a recent paper Ellis and Silk (2014) raise questions regarding the non-testability of theories such as the multiverse and string theory, stating: "*But conclusions arising logically from mathematics need not apply to the real world. Experiments have proved many beautiful and simple theories wrong, from the steady-state theory of cosmology to the Grand Unified Theory of particle physics, which aimed to unify the electroweak force and the strong force. The idea that preconceived truths about the world can be inferred beyond established facts (inductivism) was overturned by Popper and other twentieth-century philosophers*." And "*Fundamentally, the multiverse explanation relies on string theory, which is as yet unverified, and on speculative mechanisms for realizing different physics in different sister universe*s". Similar reservations can be raised regarding the plethora of untested or untestable hypotheses related to biogenesis and the origin of life.

A number of orbital features have enhanced the evolution of life on Earth, including:

1. The distance of Earth from the Sun intermediary between Venus and Mars, allowing moderate insolation and temperatures and thereby existence of liquid water on the surface.
2. The presence of water in the Earth's mantle and crust, including possible contributions from early comet impacts (Morbidelli et al. 2000). Alternative theory for the origin of water on Earth is suggested in terms of collection of gases (H_2, He, H_2O, and CO) from the solar nebulae (Drake 2005).
3. The retention of water on the Earth's surface, as contrasted with a likely loss of atmosphere from Mars, likely due to the larger dimensions and thus gravity on Earth.
4. The size and location of the planet Jupiter which sweeps a majority of asteroids falling off the asteroid belt between Mars and Jupiter.
5. The effect of the Moon in stabilizing the Earth's axis relative to the Ecliptic plane which, when combined with its orbit around the sun, allows the seasons, with major effects on biological evolution.
6. The early position of the Moon in proximity to Earth which controlled a slow Earth spin rate and major ocean tides, with effects on the evolution of early life forms (Dominei 2009).
7. The homeostatic behaviour of the atmosphere-ocean-biosphere system, with atmospheric greenhouse gas concentrations compensating for the long term increase in solar luminosity (Fig. 1.2). Homeostasis can be disrupted by extreme events, including major volcanic eruptions, asteroid and comet impacts, large-scale release of methane and hydrogen sulphide and anthropogenic emissions which change the composition of the atmosphere (Fig. 6.3).

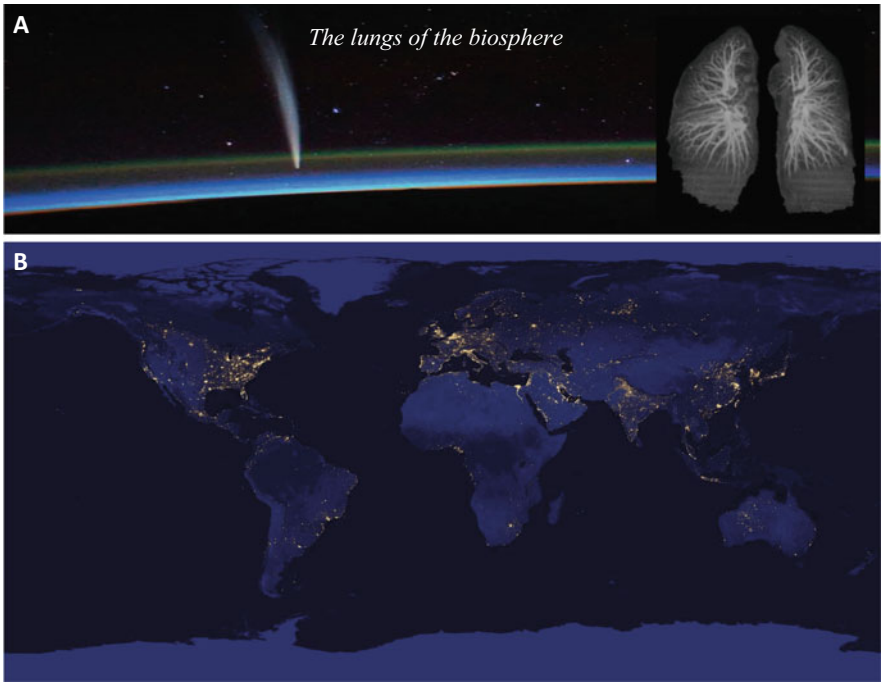

Fig. 6.3 Lungs of the Earth, signifying the juxtaposition of the Earth surface lighted through fossil fuel combustion with the ~10 km-thin atmosphere acting as the Lungs of the biosphere. Images by NASA. http://www.nasa.gov/images/content/712130main_8246931247_e60f3c09fb_o.jpg

The origin and evolution of intelligence on Earth remain unknown. A measure of natural intelligence remains a subject of cosmological theories (Barrow and Tipler 1986; Murphy and Ellis 1995; Rees 1999). The subjective nature of measurements and definitions of intelligence is underpinned by factors such as religion, race, gender, culture, social class and cultural background. The definition of intelligence involves both natural and artificial intelligence, where according to Gregory (1998, cited in Legg and Hutter 2007) "*a fundamental problem in artificial intelligence is that nobody knows what intelligence is*". However, regardless of definitions intelligence is manifest throughout nature in individual and societies, all the way from the DNA-RNA pairs to stromatolite bioherms, the colonial insects, the human brain, cities and empires. Yet perhaps *Homo sapiens*, a *Flatland* inhabitant (Abbott 1884), is far from reaching an understanding of new dimensions of knowledge, such as decrypting the origin of the Big Bang and decoding the origin of natural intelligence and life. Perhaps it is the wilful arrogance and self-destructive nature of the species which prevents it from achieving deeper perceptions?

The polarity between observations of gradual biological evolution versus mass extinction events parallels the polarity of uniformitarian views of terrestrial history

(James Hutton: 1726–1797; Charles Lyell: 1797–1875) versus the notion of catastrophism (Cuvier: 1769–1832). Following initial accretion of asteroid and cometary fragments and dust, including amino acid components (Chyba 1993; Chyba and Sagan 1996; Delsemme 2000), oxygen ($^{18}O/^{16}O$) isotopic evidence from 4.4 Ga zircons suggests that granitic crust formed at that stage was in part cool enough to allow liquid water near the surface (Wilde et al. 2001; Peck et al. 2001; Mojzsis and Harrison 2000). Cometary seeding of planetary atmospheres is capable of contributing extraterrestrial organic components, incinerated upon impact, possibly leading to shock synthesis of new organic molecules (Chyba and Sagan 1996). Cometary components of terrestrial sediments include aminoisobutayric acid (AIB), isovaline (Zhao and Bada 1989; Zahnle and Grinspoon 1990) and noble gases such as ^{3}H (Farley et al. 1998).

The transformation from organic molecules (amino acids, purine, pyrimidine), to complex information-rich biomolecules (peptide, nucleic acid, protein, enzyme) whose genetic information cannot be expressed by mathematical algorithms, has been estimated as a chance probability of $1:10^{120}$ (Davies 1998). Intrinsic to the question of the origin of early biomolecules is the nature of environmental settings of prebiotic molecules and early microorganisms. Earliest replicating cells at submarine hot springs probably required only twenty or so elements available and a similar number of fundamental organic molecular components (Wald 1964; Eck and Dayhoff 1968). Original biomolecules could have been synthesized from amino acid of both terrestrial and cometary derivation. Panspermia theories, rather than offering an explanation for the origin of biomolecules, only defer the question further back in time and space, reflecting popular fads that advocate extraterrestrial origins of life.

Definitions of life in terms such as in the *Encyclopaedia Britannica*: "*matter that includes responsiveness, growth, metabolism, energy transformation, and reproduction*" and distinctions between animate and inanimate matter are complicated by the existence of intermediate entities, including DNA-free viruses and sub-micron nanobes (Uwins et al. 1998) (Fig. 6.6). Views of these entities vary, from "*organisms at the edge of life*" (Rybicki 1990) or fragments of DNA and larger cells. Once primordial biomolecules have formed, natural selection accounts for their evolution trajectories in terms of mutations, adaptations and self-repair, all the way from microbes to brains. According to Ellis (2005) "*Ever higher levels of interaction and causality arose as complexity spontaneously increased in the expanding Universe, allowing life to emerge. Darwinian processes of selection guided the physical development of living systems, including the human brain*". However, properties such as directionality and intentionality inherent in evolutionary chains, and the transfer of intelligence, constitute outstanding issues. The question arises, does intelligence constitute the property of organisms and species or, alternatively, does intelligence reside in unknown laws of nature, manifested by life forms. Such a question would perhaps be analogous, for example, to a question such as "*does gravity constitute an inherent property of organisms or is it a feature inherent in the basic laws of nature*?"

Inherent in the question are little-understood top-to-base causality processes (Ellis 2005), directionality and intentionality. Teilhard de Chardin (1959, p. 111) hinted at the existence of laws of complexity giving rise to awareness and consciousness, stating: "… *the higher the degree of complexity in a living creature, the higher its consciousness, and vice versa. The two properties vary in parallel and simultaneously*". The semi-autonomous existence of different organizational levels within complex systems, including sub-atomic particles, atoms, molecules, biomolecules, nerves and brains, led Ellis (2005) to state: "*although the laws of physics explain much of the world around us, we still do not have a realistic description of causality in truly complex hierarchical structures*"

Prior to the mastery of fire little difference existed between the behaviour of *Hominins* and intelligent primate species. The mastery of fire and the expression by *Homo* through burial, art and eventually science, distinguishing the genus from all other animals, remain to be explained. Acting as a mirror of the world around it, a product of millions of years of evolution, the apparent ability of the human brain to perceive the physical laws and their underlying mathematical logic requires that, embedded in the brain are the very codes it can perceive around it. Where science is based on empirical observations and mathematical calculations, the origin of intuitive and perceptive ideas remains unknown. It may be instructive to examine aspects of human behaviour which appear to correlate with physical wave patterns, even if only as metaphors. In quantum mechanics, whereas the statistical behaviour of collections of particles is defined by thermodynamic laws, it is not possible to predict the behaviour of any single photon or quanta. By analogy, whereas the behaviour of populations may follow statistical patterns, the behaviour of individuals may be less or even unpredictable, giving rise to the concept of "free will". If so, free will may display an analogy to solitons (solitary waves) formed through interference and amplification of wave patterns, propagating a powerful pulse.

The transition from organisms controlled purely by genetic and instinctive factors to organisms which develop thought processes and cultural traits remains little understood. The origin and nature of intelligent coordination of social systems intrinsic to stromatolites, sponges, termite nests, bee hives and modern cities – where biological evolution is supplemented or superseded by cultural evolution – is likewise obscure. Molecular biology and paleontological studies, documenting the physical evolution of species, face difficulty in elucidating the progress of intelligence. The evolution of the basic blocks of living organisms, a hierarchy ranging from atoms (C, O, H, S, N), to nucleic acids (adenine, cytosine, guanine, thymine, uracil), to complex DNA and RNA chains, genes, chromosomes, cell nuclei and multicellular organisms, raises fundamental questions regarding the relation between the biological 'hardware' and the intelligent 'software' of life (Noble 2008). The question of the origin of life may be illustrated by a hypothetical example: A computer is discovered on a beach by an alien. Identifying its building blocks – a motherboard, electronic circuits, transistors, chips, vacuum tubes, gates – the alien is unable to understand the origin of the computer and the mind which has

designed it. Having established anatomical and behavioral Darwinian evolution through mutation, adaptation, and natural selection, to date science has not determined how the initial RNA-DNA biomolecules, and thereby the phenomenon of life, have emerged. Nor does the question whether the evolutionary chain, from DNA and RNA molecules all the way to the brain, suggest progressive evolution of natural intelligence or, alternatively, whether the codes which govern this progression are written into the laws of physics.

Answers to the fundamental questions remain elusive. Has the Big Bang originated by chance or as an expression of unknown pre-universe physical principles? Have the first bio-molecules emerged as a probability or, alternatively, as an inevitable expression of un-decoded laws of organization and complexity? Do viruses and nanobes represent transitions between inanimate matter and life? Interpretations of intelligent behaviour including modification and transfer of genetic codes, chance survival, trial and error, instinctive behaviour and independent cerebral processes give rise to further questions. Observations of the paleontological record and of living organisms suggest the origin and evolution of the communal intelligence of organisms – stromatolite bioherms, sponges, termite colonies, bee hives or human societies – involve a sense of purpose. The highly sophisticated strategies of species in mating, prioritizing survival and growth of their genes and progenies, hunting methods (Fig. 6.4), building sophisticated colony structures (Fig. 6.5), designing traps for potential prey, developing camouflage, misleading competitors and numerous other strategies, speak of advanced intelligence and even thought processes. Navigation and migration patterns of animal and insect species across the globe, guided by weather patterns, magnetic fields, the stars and chemical and electromagnetic signals, remain little explained.

Perhaps it is *Homo sapiens'* anthropocentric illusion that decrees it alone is capable of thought. Whereas as a collective, since about 90,000 years ago, *Homo sapiens* developed unprecedented technology, science and art, it is less clear how the thought processes of pre-sapiens humans and of animals differ (Figs. 6.4 and 6.5).

Fundamental questions remain, foremost of which is the evidence for purpose in the natural world – instinctive, subconscious or conscious purpose**.** Although a sense of purpose may be invoked for the trajectories followed from *Big Bang* through expansion of the universe, formation of galaxies, stars and planets, and for the structural and magmatic evolution of Earth, only the phenomenon of life involves a clear sense of purpose through the reproduction, metabolism, responsiveness, transformation of energy, genetic inheritance and diversification, energy transformation and adaptation of life forms.

Biochemical interpretations of the causation and origin of life are exemplified by those of Cairns-Smith (1978, 1990, 2009), where life evolves through complex self-replication of clay crystals where proto-organic molecules are catalyzed by the surface properties of the silicates. Other theories revolve around questions such as whether metabolic processes preceded reproductive processes, or *vice versa* (Pross 2004). This author suggests that "*a causal connection between replication*

Fig. 6.4 Shared principles of natural intelligence: (**a**) Termite mound, Litchfield National Park, Northern Territory, Australia; http://en.wikipedia.org/wiki/File:Cathedral_Termite_Mound_-_brewbooks.jpg; (**b**) The Empire State Building http://phildesimone.com/empirestate.html and New York crowd http://upload.wikimedia.org/wikipedia/commons/f/f0/G20_crowd.jpg Creative Commons

and metabolism can only be demonstrated if replication would have preceded metabolism" and "*there is no substantive evidence for a 'metabolism first' mechanism for life's emergence, while a coherent case can be made for the 'replication first' group of mechanisms. The analysis reaffirms our conviction that life is an extreme expression of kinetic control, and that the emergence of metabolic pathways can be understood by considering life as a manifestation of 'replicative chemistry'*". These

Fig. 6.5 Shared principles of natural intelligence: (**a**) the Gladiator Spider casting its net, Photo credit: Geoff Gallice, via Wikimedia Commons http://www.iflscience.com/plants-and-animals/ogre-faced-spider-throws-net-over-its-prey-gladiator; (**b**) Fisherman casting his net in a Kiribati lagoon. Creative Commons: Australian Government Department of Foreign Affairs and Trade, 2011. http://tcktcktck.org/2014/03/rising-tides-threaten-island-nation-kiribati/61163

theories invoke spontaneous chemical to biochemical reactions, leaving the question of "purpose" unanswered.

In the absence of an explanation of the origin of the phenomenon of life, poetic metaphors such as a 'life force' (Fig. 6.6) have been invoked, providing no explanation. On the global scale, the Gaia Hypothesis, which views Earth as an organism

Fig. 6.6 Epitaph: The life force is stronger than *H. sapiens*' damaging power. (**a**) Nanobes, found living in deep fractures (Courtesy of P.J.R. Uwins); (**b**) Diatoms seen through a microscope, encased within a silicate cell wall and living between crystals of annual sea ice in McMurdo Sound, Antarctica (NOAA Corps2365 Collection. Author. G. T. Taylor, Stony Brook University http://commons.wikimedia.org/wiki/File:Diatom)

maintaining a homeostatic balance (Lovelock and Margulis 1974), offers an attractive combination of known and unknown elements of the biosphere, but beyond concepts that transcend the boundary between science and philosophy, the human brain remains in a realm of *Flatland* (Abbott 1884), blind to dimensions it is unable to perceive.

We may never know.

Chapter 7
Prometheus: An Epilogue

Superstrings

Tiny wispy strings
Cryptic little things
Shape universes, sing
Oh take me on your wings.
X-apparitions chase
Light speed – a cosmic race
Appears from quantum space
Oblivious to my race.
DNA chains extend
RNA healers bend
Repair a link, append
life's wonder: self-amend.
RNA chains collapse
A lover's final gasp
Queen Cleo's sacrifice
While gods are playing dice.
Unseen hands strum guitar
Bells' echoes reach afar
No strings attached, no bar
Can bind a young blue star.
My thought waves rise and ebb
Brains weave a spider's web
Probe truths or make believe
Loft crests I can't achieve.
Web sites each other find
A net's collective mind
Tripwire humankind
A cyclops stumbling blind.

(By Andrew Glikson)

Abstract Nature covers its deepest secrets, providing only hints into that which, from lack of a better term, may be referred to as universal intelligence. Science mostly explains the *hows*, but not the *whys*: Empirical observations, experiments and mathematical formulations which explain how the atmosphere–ocean-land system has evolved, decoding the DNA and Darwinian evolution of life, have to date been unable to explain the sense of purpose perceived in life. Nor has evolu-

A.Y. Glikson, C. Groves, *Climate, Fire and Human Evolution*, Modern Approaches in Solid Earth Sciences 10, DOI 10.1007/978-3-319-22512-8_7

tionary theory been able to date to decipher whether life is written into the laws of nature or has emerged as a unique improbable accident. Earth, a lonely faint blue dot in the universe, the only home of *Homo sapiens*, bears the genes of cosmic processes from the *Big Bang* to the formation of galaxies and nucleosynthesis in the cores of stars to the origin of planets and habitable planets. We may never know the underlying factor for the *Big Bang*, how the physical laws came into being, what is the raison d'etre of synthesis of carbon, hydrogen, oxygen and nitrogen into self-replicating self-repairing DNA-RNA molecules, and what is the origin and raison d'etre of intelligence. We may never know whether individual and collective intelligence evolves along with physiological evolution or, alternatively, is inherent in natural laws as are gravity and the electromagnetic force. Where science ends unknown, poetry and music are born.

The human quest for an insight into the origin and nature of life, ranging from mythology (Fig. 7.1) to the Gaia metaphor (Lovelock and Margulis 1974) to the space perspective of the faint blue dot (Fig. 6.1) hints at the design of natural systems by repetitive kaleidoscopic patterns on a hierarchy of scales (Ellis 2005). A seamless connectivity between all levels, from galaxies and stars to planetary systems to living organisms to individual minds. Universes are born out of a void through *vacuum fluctuations*; matter and antimatter mutually annihilate, residues of such cosmic orgies of self-destruction expand forming a multi-universe, clouds of hydrogen coalesce into nebulae which collapse gravitationally into stars and galaxies; young blue stars mature into red old giants which explode, shrivel and die. Stars, like life forms, bear genetic codes – chemical elements synthesised in the furnaces of earlier stellar generations. Electrons and positrons collide, obliterating each other. Nuclear fusion that fuels stars bears an uncanny analogy to biological procreation through gravitational attraction, mutual collapse, a rise of temperature and the fusion of two charged protons into helium. Stars mature, their cores shrink,

Fig. 7.1 A black-figure Lakonian kylix, c. 570–560 BCE, depicting the Titans Atlas carrying the world on his shoulders and Prometheus being tormented by an eagle sent by Zeus to eat his liver as punishment for giving mankind the gift of fire, stolen from Hephaistos (Gregoriano Etrusco Museum, Vatican)

outer layers of hydrogen expand and incinerate the surrounding planets, the Titan Cronus devouring his children. Stars about 30–50 times the solar mass collapse into black holes where atoms are smashed in a cosmic holocaust. Prehistoric clans evolve into technological civilisations that harness heavy radioactive elements, explode and die through accidents and war, taking other life forms with them. The meaning of positive–negative dichotomies and of creative-destructive cycles, symbolised in Hindu mythology by Vishnu the creator, Brahma the preserver and Shiva the destroyer, evades the human mind.

The birth of a star propagates planetesimal offspring, stony rings coalesce into planets, collapse, melt, thermally convect, segregate iron cores, differentiate and form solid crusts, continents, oceans and atmospheres. Crustal blocks drift, subduct, deform and melt. Earliest life forms include thermophile bacteria using chemical energy around hot submarine springs. Solar light percolates through dust and clouds, photosynthesising single-celled blue-green algae emerge, bacteria form dome-shaped stromatolite colonies designed to maximise protection from the ultraviolet. The first terrestrial societies emerge. Primitive life forms survive the longest – stromatolites exist to this day in tidal environments like Shark Bay, Western Australia. The release of oxygen by photosynthesis locally and transiently reverses entropy. Released oxygen forms an ozone shield, a haven where life can evolve, allowing the emergence of plant eaters – bacteria, pteropods, insects and animals which oxidize plant matter. Repeatedly life forms burst in huge variety, then become extinct through extreme environmental adversities brought about by volcanic eruptions and asteroid impacts, their disappearance creating living space for new families and genera. The appearance of chromosome-exchanging Eukaryotes results in genetic diversity. Rapid biological proliferation in the oceans, the *Cambrian Explosion,* follows the appearance of multicellular animals. Life, a spontaneous adaptive force, modifies its environment to suit its purposes.

Life is governed by electromagnetic constants that allow a balance of charges of chemical bonds in biomolecules. The emergence of a brain able to decipher physical laws and their mathematical logic suggests that, built into this cerebral organ, are the very codes it is able to unravel through science, music and art. Brains, acting like mirrors of nature, probe and decode the laws which underlie their own constitution. Human mental parameters may emulate wave patterns, where wavelength and amplitude correlate with the frequency and intensity of brain waves and heart beats. Niels Bohr observed it is not possible to regard the world as consisting of separate bits, since even where these bits are separated by light years they constitute components of a single totality, acting in unison, as indicated by experimental evidence for spontaneous links between spatially separated twin photons. A Janus principle holds (Koestler 1986) – the particle/wave duality in physics may be mimicked by Descartes' body/mind dichotomy – *I think therefore I am.*

Quantum mechanics allow predictions of mass effects but not of the behaviour of individual particles. Compare the tension between the mass behaviour of crowds, the Roman 'monster of one thousand heads' with individual '*free will'*, to the extent that it exists. If '*free will'* can be compared to a *soliton*, a powerful wave which forms where wave patterns are amplified, mass behaviour spells determinism. In

terms of the second law of thermodynamics, an increase in organisational complexity in one part of a system can only result in an increase in entropy elsewhere in the system. The emergence of the human brain and its brainchildren – megalopolis criss-crossed with radiating highways that mimic neuron nerve cells – can only lead to an increase in entropy and chaos elsewhere, including loss of biological diversity, degradation of soils, depletion of ozone and radioactive pollution.

Through prehistoric time and over the Millennia humans expressed their wonder and awe in rock carvings, myths and legends conveying the drama of the human condition through the lives of gods and heroes, projecting human meanings on a universe oblivious to aspirations and suffering. At times these myths proved uncanny foresights that heralded later scientific discoveries. A progression from pantheistic reverence, to sun-worshipping, to monotheism and, finally, to the space cult, has shifted the human focus from the Earth to destinies in outer space, Earth remaining but a corridor, that can be abused.

When carbon, hydrogen, oxygen and nitrogen combined into the four DNA species, adenine, cytosine, guanine and thymine (de Silva and Williams 1991), a plan was embarked on a four billion years-long journey, from microbes to the brain, on a planetary surface subject to repeated volcanic eruptions and extra-terrestrial bombardment. For a biological species to develop brain power that allows it to become the intelligent eyes through which the universe explores itself, as represented by the U figure by John Archibald Wheeler, where a human eye explores beginnings of the universe (Fig. 7.2), hints at unknown natural laws. In terms of such laws the origin of life, manifested all the way from self-repairing DNA-RNA biomolecules to the brain's conscious insight, remains little understood (Davies 1998, 2006). It has not been foreknown until recently that the human brain will itself give rise to one of the most severe mass extinction events in planetary history. According to Wallace Broecker (1987) "*The inhabitants of planet Earth are quietly conducting a gigantic experiment. We play Russian roulette with climate and no one knows what lies in the active chamber of the gun*".

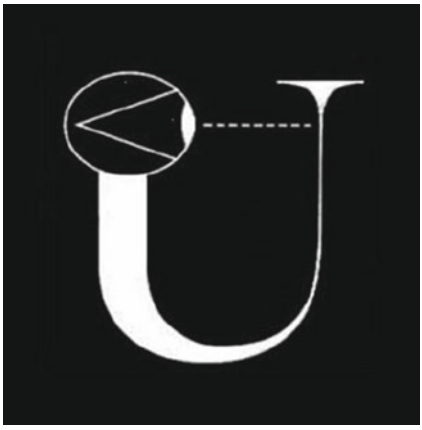

Fig. 7.2 The U symbol, designed by John Wheeler, symbolizing human awareness of the Big Bang

It has been lost on *Homo sapiens* that, by analogy to its own life processes which depend on the oxygen-carbon cycle mediated by the lungs, so does the biosphere depend on the planetary oxygen and carbon cycle (Figs. 1.19, 6.3). The phenomenon of a mammal species perpetrating a mass extinction defies explanation in terms of Darwinian evolution. Having mastered fire *Homo sapiens* began to recruit elements from the periodic table as building blocks for its cultural evolution, including iron, gold and uranium. The discovery of smelting provided the species with tin and lead (>6500 BP), copper and bronze (>5500 BP), iron (>3000 BP) and other metals, allowing production of new tools, ploughs for sowing excess grain, silver and gold for the crafting of ornaments, symbolizing wealth and facilitating trade. Swords and spears elevated homicide to new levels. Subsequent iron-based machines allowed the industrial revolution and vast-scale industrial killings, called "war" (Diamond 2005).

Gold – a soft low-melting (1064 °C) volatile metal, symbolizing the excess resources required for buying power, feeding slaves or sending men to war – manifests mythological aspiration of the human mind. Only limited amounts of loot could be carried across land and sea prior to the rise of mammon but once precious metals assumed token value of wealth and thereby power, they became motivators of wars, destroying civilizations as became the fate of the Aztecs and the Inca of the Americas. A space visitor would watch with disbelief how gold has been mined from 3 km deep beneath the Witwatersrand only to be buried in underground safes at Fort Knox. The traveller would be amazed how communities have been hijacked by the agents of greed and chaos represented by the share market – the lowest common denominator in human affairs.

Societies ruled by tribal shamans, feudal war lords, speculators, thugs and habitual liars have finally opened the Pandora's Box. The mastery of combustion upsetting the carbon-oxygen balance of the atmosphere is culminating in the fission of uranium ^{235}U producing plutonium (^{239}Pu) (half-life 24,360 years), as conveyed by Albert Einstein: "*The splitting of the atom changed everything, save man's mode of thinking; thus we drift towards unparalleled catastrophe*". According to Albert Speer, German physicists, apprising the Nazi government of the possible development of an atom bomb in the spring of 1942, noted a reservation by Werner Heisenberg about a potential conflagration engulfing the atmosphere. The same awesome possibility, fusion of atmospheric nitrogen and oceanic hydrogen turning the planet into a chain-reacting bomb triggered by the explosion of the H-Bomb was considered by Edward Teller, Robert Oppenheimer, Arthur Compton, Hans Bethe and other physicists. Where calculations indicated an atmospheric conflagration was unlikely, a finite possibility remained while the Bikini H-bomb tests went ahead. In the wake of atomic annihilation of the inhabitants of two Japanese cities, global nuclear conflagration becomes a probability resulting from lateral proliferation of nuclear weapons, but becomes a certainty in an environmentally stressed world.

A Damocles sword of Mutual Assured Destruction (MAD) strategy remains. The hapless inhabitants of planet Earth have been given a non-choice between accelerating global heating and a nuclear winter. Experiments with the fate of Earth continue,

and although the Hadron Collider has been deemed safe (Hadron Collider 2008), the consequences of further science fiction-like experiments dreamt by ethic-free people remain unknown.

Once the climate stabilized in the Holocene, allowing production of excess food, a fearful human mind was unleashed, drafting slaves to construct monuments for immortality and soldiers for murderous orgies to appease the gods. Echoing infanticide by rival warlord baboons, the butchering of children on Aztec altars (Clendinnen 1995) and the sacrifice of generations in recurrent wars is symbolized by Saturn devouring its son. The Tower of Babel story tells of humans confused by language that can tell both truths and falsehoods. Nature is full of examples of creatures seducing their prey and destroying their host. Prehistoric and pantheistic humans revered animals, even while hunting and sacrificing them, whereas monotheism is looking to heaven and space for salvation, leaving nature as a corridor to higher realms. Having lost a sense of reverence toward Earth, there is no evidence humans are about to rise above the realm of perceptions, dreams, myths, legends and denial (Koestler 1986).

Planetcide emerges from dark recesses of the prehistoric mind, from the fears of human beings watching the flames around camp fires, yearning for immortality. The transformation of tribal warriors into button-pushing automatons remains shrouded in mystery. Perhaps it is too much to expect any living species to possess the wisdom and responsibility required to control its own inventions. Charity remains, mostly among the wretched of the Earth, where empathy is learnt through suffering. From the Romans to the Third Reich, the rapacious brutality of legions surpasses that of small marauding tribes bound by traditions. Under false flags empires never cease to kill peasants in their rice fields and palm groves. Where the Nazis constructed gas chambers for millions, anthropogenic global heating threatens to turn the entire planet into an open-air inferno on the strength of a Faustian Bargain.

A child of Orwellian Newspeak, planetcide challenges every social system, faith, ideal or philosophy human being ever held. As in the *War of the Worlds* by H.G. Wells, free-thinking cells are destroyed by their parent organism. While the minds of children are poisoned by commercial and political propaganda machines, the ideals of democracy are undermined by the rise of a plutocracy, subterranean drug rings and weapon smuggling networks. Ultimately the rise of Nietzsche's relativistic moral philosophy, justifying the unjustifiable, implies that, without ethics, *Homo sapiens* cannot survive.

What would be the geological legacy of technological civilizations millions of years hence? Erosion, fires and subsequently the next glacial period, albeit delayed, would grind the stone and cement structures of cities into sand and clay. A tell-tale marker horizon of corroded metals, gold, plutonium, precious stones and glass, will accumulate in the abyssal oceans. Already radioactive anomalies have been detected in clay beds and ice varves in several parts of the world (Grossman 2011; Buesseler 1997).

By the end of the first decade of the Second Millennium it was becoming clear *H. sapiens* was not going to undertake a meaningful attempt to slow down, arrest or reverse global warming consequent on the discharge to the atmosphere of some 580

billion tons of carbon from the Earth crust. The bulk of extra-resources continues to be poured into the military, entertainment, sports, gambling, electronic gaming and drugs. With a majority oblivious to the fast changing climate, disinformed by vested interests and their media outlets, betrayed by cowardly leaders and discouraged by the sheer magnitude of the event, beyond human power, few remaining nature lovers and scientists continue to raise the alarm, becoming the subject of witch hunts, while humanity is drifting into unparalleled catastrophes.

The extreme habitability of Earth since at least ~3.8 billion years ago, and the resilience of the biosphere despite massive volcanic eruptions and large asteroid impacts, ensure future life cycles, regardless of the destructive activities of the species *Homo sapiens*.

Existentialist philosophy allows perspectives into, and ways of coping with, what defies rational contemplation. If looking into the sun may result in blindness, according to little-understood poetic aphorism the human insight into nature entails a terrible price. Ethical and cultural assumptions of free will, which may operate to some degree in individual lives, hardly govern the behaviour of societies or nations, let alone a species. However in an existentialist sense hope, essential for survival on the individual scale, is essential for life. Going through the dark night of the soul individuals may experience the emergence of a conscious dignity devoid of illusions, grateful for a fleeting moment of awareness, as in the story of Sisyphus: "*having pushed a boulder up the mountain all day, turning toward the setting sun, we must consider Sisyphus happy*" (Camus 1942; The Myth of Sisyphus).

References

Abbott E (1884) Flatland: a romance of many dimensions. http://en.wikipedia.org/wiki/Flatland

Abu Hamad AMB, Jasper A, Uhl D (2012) The record of Triassic charcoal and other evidence for palaeo-wildfires: signal for atmospheric oxygen levels, taphonomic biases or lack of fuel? Int J Coal Geol 96–97:60–71

Adler J (2013) Why fire makes us Smithsonian Magazine, June 2013

Allwood AC, Walter MR, Burch IW, Kamber BS (2007) 3.43 billion-year-old stromatolite reef from the Pilbara Craton of Western Australia: ecosystem-scale insights to early life on Earth. Precambrian Res 158:198–227

Alvarez W (2003) Comparing the evidence relevant to impacts and flood basalts at times of major mass extinctions. Astrobiology 3:153–161

Alvarez LW, Alvarez W, Asaro F, Michel HV (1980) Extra-terrestrial cause for the cretaceous-tertiary extinction: experimental results and theoretical interpretation. Science 208:1095–1085

Ambrose SH (1998) Late Pleistocene human bottlenecks, volcanic winter, and differentiation of modern humans. J Hum Evol 34:623–651

Bachan A, Van de Schootbrugge B, Fiebig J, McRoberts C, Ciarapica G, Payne J (2012) Carbon cycle dynamics following the end-Triassic mass extinction: constraints from paired δ^{13}Ccarb and δ^{13}Corg. Geochem Geophys Geosyst. doi:10.1029/2012GC004150

Bakri A, Metha K, Lance DR (2005) Sterilizing insects with ionizing radiation. Springer, Dordrecht, pp 233–268

Balter V et al (2008) Record of climate-driven morphological changes in 376 Ma Devonian fossils. Geology 36:907

Barclay RS, McElwain JC, Sageman B (2010) Carbon sequestration activated by a volcanic CO_2 pulse during Ocean Anoxic Event. Nat Geosci 3:205–208

Bard E, Frank M (2006) Climate change and solar variability: what's new under the sun? Earth Planet Sci Lett 248:1–14

Baronsky et al (2013) Approaching a state shift in the Earth's biosphere. Nature 486:52–58. http://www.nature.com/nature/journal/v486/n7401/full/nature11018.html

Barrow J, Tipler F (1986) The anthropic cosmological principle. Oxford University Press, Oxford

Bar-Yosef O (2000) The middle and early upper Paleolithic in Southwest Asia and neighboring regions. In: Bar-Yosef O, Pilbeam D (eds) The geography of Neanderthals and modern humans in Europe and the greater Mediterranean. Peabody Museum Press, Cambridge, MA, pp 107–156

Beerling DJ (2002a) CO_2 and the end-Triassic mass extinction. Nature 415:386–387

A.Y. Glikson, C. Groves, *Climate, Fire and Human Evolution*, Modern Approaches in Solid Earth Sciences 10, DOI 10.1007/978-3-319-22512-8

Beerling DJ (2002b) Low atmospheric CO_2 levels during the Permo- Carboniferous glaciation inferred from fossil lycopsids. Proc Natl Acad Sci U S A 99:12567–12571
Beerling DJ, Berner RA (2000) Impact of a Permo-Carboniferous high O_2 event on the terrestrial carbon cycle. Proc Natl Acad Sci U S A 97:12428–12432
Beerling DJ, Berner RA (2005) Feedbacks and the coevolution of plants and atmospheric CO_2. Proc Natl Acad Sci U S A 102:1302–1305
Beerling DJ, Royer D (2011) Convergent cenozoic CO_2 history. Nat Geosci 4:418–420
Beerling DJ, Osborne CP, Chaloner WG (2001) Evolution of leaf-form in land plants linked to atmospheric CO_2 decline in the Late Palaeozoic era. Nature 410:352–354
Beerling DJ, Lomax BH, Royer DL, Upchurch GR, Kump LR (2002) An atmospheric pCO_2 reconstruction across the cretaceous-tertiary boundary from leaf mega fossils. Proc Natl Acad Sci U S A 99:7836–7840
Bekker A, Kaufman AJ (2007) Oxidative forcing of global climate change: a biogeochemical record across the oldest Paleoproterozoic ice age in North America. Earth Planet Sci Lett 258:486–499
Belcher CN (2009) Re-igniting the cretaceous-paleogene firestorm debate. Geology 37:1147–1148
Belcher CM, Collinson ME, Sweet AR, Hildebrand AR, Scott AC (2003) "Fireball passes and nothing burns"—The role of thermal radiation in the K-T event: evidence from the charcoal record of North America. Geology 31:1061–1064
Belcher CM, Yearsley JM, Hadden RM, McElwain JC, Rein G (2010) Baseline intrinsic flammability of Earth's ecosystems estimated from paleo-atmospheric oxygen over the past 350 million years. Proc Natl Acad Sci U S A. doi:10.1073/pnas.1011974107
Berger WH, Jansen E (1994) Mid-Pleistocene climate shift: the Nansen connection. In: Johannessen O, Muench R, Overland J (eds) The polar oceans and their role in shaping the global environment, Geophys Mono 85. American Geophysical Union, Washington, DC, pp 295–311
Berger A, Loutre MF (2002) An exceptionally long interglacial ahead? Science 297:1287–1288
Berna F, Goldberg P, Horwitz LK, Brink J, Holt S, Bamford M, Chazang M (2012) Microstratigraphic evidence of in situ fire in the Acheulean strata of Wonderwerk Cave, Northern Cape province, South Africa. Proc Natl Acad Sci U S A 109(20):1–6
Berner RA (1999) Atmospheric oxygen over Phanerozoic time. Proc Natl Acad Sci U S A 96:10955–10957
Berner RA (2004) The Phanerozoic carbon cycle: CO_2 and O_2. Oxford University Press, New York
Berner RA (2005) The carbon and sulphur cycles and atmospheric oxygen from middle Permian to middle Triassic. Geochim Cosmochim Acta 69:3211–3217
Berner RA (2006) GEOCARBSULF: a combined model for Phanerozoic atmospheric O_2 and CO_2. Geochim Cosmochim Acta 70:5653–5664
Berner RA (2009) Phanerozoic atmospheric oxygen new results using the GEOCARBSULF model. Am J Sci 309:603–606
Berner RA, Beerling DJ, Dudley R, Robinson JM, Wildman RA (2003) Phanerozoic atmospheric oxygen. Ann Rev Earth Planet Sci 31:105–134
Berner RA, Vanderbrook JM, Ward PD (2007) Oxygen and evolution. Science 316:557–558
Bi SY, Wang J, Guan X, Sheng J, Meng N (2014) Three new Jurassic euharamiyidan species reinforce early divergence of mammals. Nature 514:579–584
Bininda-Emonds ORP, Cardillo M, Jones KE et al (2007) The delayed rise of present-day mammals. Nature 446:507–512
Blake RE, Chang SJ, Lepland A (2010) Phosphate oxygen isotope evidence for a temperate and biologically active Archaean ocean. Nature 464:1029–1033
Blois JL, Hadly EA (2009) Mammalian response to Cenozoic climate change. Annu Rev Earth Planet Sci 37:181–208
Bodiselitsch B, Montanari A, Koeberl C, Coccioni R (2004) Delayed climate cooling in the late Eocene caused by multiple impacts: high-resolution geochemical studies at Massignano, Italy. Earth Planet Sci Lett 223:283–302

Bolhar R, Kamber BS, Moorbath S, Fedo CM, Whitehouse MJ (2004) Characterisation of early Archaean chemical sediments by trace element signatures. Earth Planet Sci Lett 222:43–46
Bond WJ, Keeley JE (2005) Fire as global 'herbivore': the ecology and evolution of flammable ecosystems. Trends Ecol Evol 20:387–394
Bowman DM et al (2009) Fire in the Earth system. Science 324:481–484
Brasier MD, Green OR, Jephcoat AP, Kleppe AK, Van Kranendonk MJ, Lindsay JF, Steele A, Grassineau NV (2002) Questioning the evidence for Earth's oldest fossils. Nature 416:76–81
Braun AJ, Chen J, Waloszek D, Maas M (2007) First early Cambrian Radiolaria. Special publications. Geol Soc London 286:143–149
Breecker DO, Sharp ZD, McFadden LD (2009) Atmospheric CO_2 concentrations during ancient greenhouse climates were similar to those predicted for A.D. 2100. Proc Natl Acad Sci U S A 107:576–580
Brenchley PJ, Carden GA, Hints L, Kaljo D, Marshall JD, Martma T, Meidla T, Nõlvak J (2003) High-resolution isotope stratigraphy of late Ordovician sequences: constraints on the timing of bio-events and environmental changes associated with mass extinction and glaciation. Geol Soc Am Bull 115:89–104
Broecker W (1987) Unpleasant surprises in the greenhouse? Nature 328:123–126
Broecker WS (2000) Abrupt climate change: causal constraints provided by the paleoclimate record. Earth Sci Rev 51:137–154
Broecker WC, Stocker TF (2006) The Holocene CO_2 rise: anthropogenic or natural? Eos 87:27–29
Brown P, Sutikna T, Morwood M et al (2004) A new small-bodied hominin from the late Pleistocene of flores, Indonesia. Nature 431:1055–1061
Brown S, Scott AC, Glasspool IJ, Collinson M (2012) Cretaceous wildfires and their impact on the Earth system. Cretac Res 36:162–190
Browning JV, Miller KG, Pak DK (1996) Global implications of lower to middle Eocene sequence boundaries on the New Jersey coastal plain: the icehouse cometh. Geology 24:639–642
Buckley BM, Anchukaitisa KJ, Penny D, Fletcher R, Cook ER, Sano M, Nam LC, Wichienkeeo A, Minh TT, Mai Hong T (2010) Climate as a contributing factor in the demise of Angkor, Cambodia. Proc Natl Acad Sci U S A 107:6478–6752
Buesseler KO (1997) The isotopic signature of fallout North Pacific Plutonium in the North Pacific. J Environ Radioact 36:69–83
Byerly GR, Lowe DR (1994) Spinels from Archaean impact spherules. Geochim Cosmochim Acta 58:3469–3486
Cairns-Smith AG (1978) Precambrian solution photochemistry, inverse segregation, and banded iron formations. Nature 276:807–808
Cairns-Smith AG (1990) Seven clues to the origin of life. Cambridge University Press, Cambridge. ISBN 9780521398282
Cairns-Smith AG (2009) An approach to a blueprint for a primitive organism. In: Waddington CH (ed) The origin of life: towards a theoretical biology 1, Aldine Transaction, pp 57–66. Edinburgh University Press, Edinburgh
Calver CR (2000) Isotope stratigraphy of the Ediacarian (Neoproterozoic III) of the Adelaide rift complex, South Australia, and the overprint of water column stratification. Precambrian Res 100:121–150
Camus A (1942) The myth of sisyphus. Alfred A Knopf, New York, 120 pp
Canadell P (2009) Super-size deposits of frozen carbon threat to climate change. http://www.eurekalert.org/pub_releases/2009-06/gcp-sdo_1063009.php
Canadell JG et al (2007) Contributions to accelerating atmospheric CO_2 growth from economic activity, carbon intensity and efficiency of natural sinks. Proc Nat Acad Sci 104:18866–18870
Canfield D, Poulton SW, Narbonne GM (2007) Late-Neoproterozoic deep-ocean oxygenation and the rise of animal life. Science 315:92–95
Cartmill M, Smith FH (2009) The human lineage. Wiley-Blackwell, Hoboken
Casper K (2009) Changing ecosystems – effects of global warming. 247 pp. http://books.google.com.au/books?id=ZnU14onKLs8C&printsec=frontcover&source=gbs_ge_summary_r&cad=0#v=onepage&q&f=false

CDC (Centre for Desease Control and Prevension) (2011) http://www.bt.cdc.gov/radiation/arsphysicianfactsheet.asp
Chandler M, Dowsett H, Haywood A (2008) The PRISM model/data cooperative: mid-pliocene data-model comparisons. PAGES News, 16 No 2
Chandler DM et al (2013) Evolution of the subglacial drainage system beneath the Greenland Ice Sheet revealed by tracers. Nat Geosci 6:195–198
Chyba CF (1993) The violent environment of the origin of life: progress and uncertainties. Geochim Cosmochim Acta 57:3351–3358
Chyba CF, Sagan C (1996) Comets as the source of prebiotic organic molecules for the early earth. In: Thomas PJ, Chyba CF, McKay CP (eds) Comets and the origin and evolution of life. Springer, New York, pp 147–174
Claeys P, Kiessling W, Alvarez W (2002) Distribution of Chicxulub ejecta at the cretaceous-tertiary boundary. In: Koeberl C, MacLeod KG (eds) Catastrophic events and mass extinctions: impacts and beyond, vol 356. Geological Society of America, Boulder, pp 55–68
Clendinnen I (1995) Aztecs: an interpretation. Cambridge University Press, Cambridge, 389 pp
Clift PD et al (2007) Holocene erosion of the lesser himalaya triggered by intensified summer monsoon. Geology 36:79–82
Cloud P (1968) Atmospheric and hydrospheric evolution of the primitive. Earth Sci 160:729–738
Cloud P (1973) Paleoecological significance of the banded iron formation. Econ Geol 68:1135–1143
Collinson ME, Steart DC, Scott AC, Glasspool IJ, Hooker JJ (2007) Episodic fire, runoff and deposition at the Palaeocene–Eocene boundary. J Geol Soc 164:87–97
Cortese G, Abelmann A, Gersonde A (2007) The last five glacial-interglacial transitions: a high resolution 450,000-year record from the subantarctic Atlantic. Paleoocean 22:PA4203
Courtillot VE, Rennes PR (2003) On the ages of flood basalt events. Compt Rendus Geosci 335:113–140
Covey C, Morrison D, Toon OB, Turco RP, Zahnle K (1997) Environmental perturbations caused by the impacts of asteroids and comets. Rev Geophys 35:41–78
Crane PR, Lidgard S (1989) Angiosperm diversification and paleolatitude gradients in cretaceous floristic diversity. Science 246(4930):675–678
Crowley JC (1999) Pre-Mesozoic ice ages: their bearing on understanding the climate system. Geological Society of America, Boulder
Crowley TJ, Berner RA (2001) CO_2 and climate change. Science 292:870–872
Crutzen PJ, Stoermer EF (2000) The 'anthropocene'. Glob Change Newsl 41:17–18
CSIRO Report 2009/108. Permafrost melt poses major climate change threat http://www.csiro.au/Portals/Media/Permafrostclimate-change-threat.aspx
Cui Y, Kump LR, Ridgwell AJ, Charles AJ, Junium CK, Diefendorf AF, Freeman KH, Urban NM, Harding IC (2011) Slow release of fossil carbon during the Palaeocene–Eocene thermal maximum. Nat Geosci 4:481–485
Cullen HM, deMenocal PB, Hemming S et al (2000) Climate change and the collapse of the Akkadian empire: evidence from the deep sea. Geology 28:379–382
Curnoe D, Ji X, Herries AIR et al (2012) Human remains from the Pleistocene-Holocene transition of southwest China suggest a complex evolutionary history for East Asians. PLoS One 7(3):e31918. doi:10.1371/journal.pone.0031918
Dakos V, Scheffer M, Van Nes EH, Brovkin V, Petoukhov V, Held H (2008) Slowing down as an early warning signal for abrupt climate change. Proc Natl Acad Sci U S A 105:14308–14312
Darwin C (1859) On the origin of species. John Murray, London
Dauphas N, van Zullen M, Wadhawa M, Davies AM, Marry B, Janney P (2004) Clues from Fe isotope variations on the origin of early Archaean BIFs from Greenland. Science 306:2077–2080
Davies PCW (1998) The fifth miracle. Penguin Books, London
Davies PCW (2004) Multiverse cosmological models. Mod Phys Lett A 19:727–743
Davies P (2006) The search for life in the universe. In: From stars to brains. Manning Clark House, Canberra, 90 pp

Dawkins R (1976) The selfish gene. Oxford University Press, Oxford, 384 pp
de Chazal J, Rounsevella MDA (2009) Land-use and climate change within assessments of biodiversity change: a review. Glob Environ Chang 19:306–315
de Duve C (1995) Vital dust. Basic Books, New York
de Silva JRF, Williams RJP (1991) The biological chemistry of the elements. Clarendon, Oxford
Deino AL, Kingston JD, Glen JM, Edgar RK, Hill A (2006) Precessional forcing of lacustrine sedimentation in the late Cenozoic Chemeron basin, central Kenya rift, and calibration of the Gauss/Matuyama boundary. Earth Planet Sci Lett 247:41–60
Delsemme AH (2000) Cometary origin of the biosphere – 1999 Kuiper prize lecture. Icarus 146:313–325
deMenocal PB (2001) Cultural responses to climate change during the late Holocene. Science 292:667–673
deMenocal PB (2004) African climate change and faunal evolution during the Pliocene-Pleistocene. Earth Planet Sci Lett 220:3–24
Dennell RW, Roebroeks W (2005) Out of Africa: an Asian perspective on early human dispersal from Africa. Nature 438:1099–1104
Diamond J (2005) Collapse: how societies choose to fail or succeed. Viking, New York
Diffenbaug NS, Field CB (2013) Changes in ecologically critical terrestrial climate conditions. Science 341(6145):486. doi:10.1126/science.1237123
DiMaggio EN, Campisano CJ, Rowan J et al (2015) Late Pliocene fossiliferous sedimentary record and the environmental context of early *Homo* from afar. Ethiopia Sciencexpress. doi:10.1126/science.aaa1415
Dominei B (2009) Without the moon, would there be life on earth? Scientific American, Apr 2009. http://www.scientificamerican.com/article/moon-life-tides/
Drake MJ (2005) Origin of water in the terrestrial planets. Meteorit Planet Sci 40:519–527
Drake F, Dava S (1992) Is anyone out there? The scientific search for extraterrestrial intelligence. Delacorte Press, New York, pp 55–62
Duck LJ, Glikson M, Golding SD, Webb R, Riches J, Baiano J, Sly L (2008) Geochemistry and nature of organic matter in 35 Ga rocks from Western Australia. Geochim Cosmochim Acta 70:1457–1470
Dunbar RIM (1992) Neocortex size as a constraint on group size in primates. J Hum Evol 22:469–493
Dunbar RIM (1996) Grooming, gossip and the evolution of language. Faber and Faber, London, 219 pp
Dunlop JSR, Buick R (1981) Archaean epiclastic sediments derived from mafic volcanics, North Pole, Pilbara Block, Western Australia. Geol Soc Aust Sp Pub 7:225–233
Dunlop JSR, Muir MD, Milne VA, Groves DI (1978) A new microfossil assemblage from the Archaean of Western Australia. Nature 274:676–678
Durda DD, Kring DA (2004) Ignition threshold for impact-generated fires. J Geophys Res 109:1–14
Eby N, Zickfeld K, Montenegro A, Archer D (2009) Lifetime of anthropogenic climate change: millennial time scales of potential CO_2 and surface temperature perturbations. J Climate 22:2501–2511
Eck RV, Dayhoff MO (1968) Evolution of the structure of ferredoxin based on living relics of primitive amino acid sequences. Science 152:363–366
Eigenbrode JL, Freeman KH (2006) Late Archaean rise of aerobic microbial ecosystems. Proc Natl Acad Sci U S A 103:15759–15764
Ellis G (2005) Physics, complexity and causality. Nature 435:743
Ellis G, Silk J (2014) Scientific method: defend the integrity of physics. Nature 516:321–323
Endicott P, Ho SYW, Stringer C (2010) Using genetic evidence to evaluate four palaeoanthropological hypotheses for the timing of Neanderthal and modern human origins. J Hum Evol 59:87–95
EPICA Community Members (2004) Eight glacial cycles from an Antarctic ice core. Nature 429:623–628

Erwin DH (1994) The Permo–Triassic extinction. Nature 367:231–236
Erwin DH (2006) Extinction – how life on earth nearly ended 250 million years-ago. Princeton University Press, Princeton/Oxford, 296 pp
Eugster HP (1966) Sodium carbonate-bicarbonate minerals as indicators of PCO_2. J Geophys Res 71:3369–3378
Eyles N (1993) Earth's glacial record and its tectonic setting. Earth Sci Rev 35:1–248
Faith JT, Choiniere JN, Tryon CA, Peppe DJ, Fox DL (2011) Taxonomic status and palaeoecology of Rusingoryx atopocranion (Mammalia, Artiodactyla), an extinct Pleistocene bovid from Rusinga Island, Kenya. Quatern Res 75:697–707
Faith JT, Potts R, Plummer TW, Bishop LC, Marean CW, Tryon CA (2012) New perspectives on middle Pleistocene change in the large mammal faunas of East Africa: Damaliscus hypsodon sp. nov. (Mammalia, Artiodactyla) from Lainyamok, Kenya. Palaeogeogr Palaeoclimatol Palaeoecol 361–362:84–93
Faith JT, Tryon CA, Peppe DJ, Beverly EJ, Blegen N (2014) Biogeographic and the evolutionary implications of an extinct late Pleistocene impala from the Lake Victoria Basin, Kenya. J Mamm Evol 21:213–222
Farley KA, Montanari A, Shoemaker EM, Shoemaker CS (1998) Geochemical evidence for a comet shower in the late Eocene. Science 280:1250–1253
Farquhar J, Bao H, Thiemens M (2000) Atmospheric influence of Earth's earliest sulphur cycle. Science 289:756
Farquhar J, Peters M, Johnston DT, Strauss H, Masterson A, Wiechert U, Kaufman AJ (2007) Isotopic evidence for Mesoarchaean anoxia and changing atmospheric sulphur chemistry. Nature 449:706–709
Feakins SJ, deMenocal PB, Eglinton TI (2005) Biomarker records of late Neogene changes in northeast African vegetation. Geology 33:977–980
Fedorov AV, Dekens PS, McCarthy M, Ravelo AC, deMenocal PB, Barreuri M, Pacanowski RC, Philander SG (2006) The Pliocene Paradox. Science 312:1485–1489
Flannery TF (1994) The future eaters: an ecological history of the Australasian lands and people. Angus & Robertson, Sydney
Frakes LA, Francis JE, Syktus JI (1992) Climate modes of the Phanerozoic. Cambridge University Press, Cambridge
French BM (1998) Traces of catastrophe. Lunar Planetary Institute, Houston, 954, 120 pp
Friend CRL, Bennett VC, Nutman AP, Norman M (2007) Seawater-like trace element signatures (REE+Y) of Eoarchaean chemical sedimentary rocks from southern West Greenland, and their corruption during high-grade metamorphism. Contrib Mineral Petrol 183(4):725–737
Gammage B (2012) The biggest estate on earth: how aborigines made Australia. Allen and Unwin, Crows Nest, 384 pp
Ganopolski A, Rahmstorf S (2002) Abrupt glacial climate changes due to stochastic resonance. Phys Rev Lett 88:3–6
Gardner AF, Gilmour I (2002) An organic geochemical investigation of terrestrial cretaceous–tertiary boundary successions from brownie butte, Montana, and the Raton Basin, New Mexico. In: Koeberl C, MacLeod KG (eds) Catastrophic events and mass extinctions: impacts and beyond, vol 356. Geological Society of America, Boulder, pp 351–362
Garrells RM, Perry EM, MacKenzie FT (1973) Genesis of Precambrian banded iron formations and the development of atmospheric oxygen. Econ Geol 68:1173–1179
Gathorne-Hardy FJ, Harcourt-Smith WEH (2003) The super-eruption of Toba, did it cause a human bottleneck? J Hum Evol 45:227–230
Gentry AW (2010) Bovidae. In: Werdelin L, Sanders WJ (eds) Cenozoic mammals of Africa. University of California Press, Berkeley, pp 741–796
Gibbon E (1788) The decline and fall of the roman empire. http://books.google.com/books?id=f8-2ONV-foQC&pg=PA158
Glasspool IJ, Scott AC (2010) Phanerozoic concentrations of atmospheric oxygen reconstructed from sedimentary charcoal. Nat Geosci 3:627–630

Glikson AY (1972) Early Precambrian evidence of a primitive ocean crust and island nuclei of sodic granite. Geol Soc Am Bull 83:3323–3344
Glikson AY (1980) Uniformitarian assumptions, plate tectonics and the precambrian earth. In: Kroner A (ed) Precambrian plate tectonics. Elsevier, Amsterdam, pp 91–104
Glikson AY (1984) Significance of early Archaean mafic–ultramafic xenolith patterns. In: Kroner A, Goodwin AM, Hanson GN (eds) Archaean geochemistry. Springer, Berlin, pp 263–280
Glikson AY (2001) The astronomical connection of terrestrial evolution crustal effects of post-3.8 Ga mega-impact clusters and evidence for major 3.2 Ga bombardment of the Earth–Moon system. J Geodyn 32:205–229
Glikson AY (2004) Early Precambrian asteroid impact-triggered tsunami: excavated seabed debris flows exotic boulders and turbulence features associated with 3.47–2.47 Ga-old asteroid impact fallout units, Pilbara Craton, Western Australia. Astrobiology 4:1–32
Glikson AY (2005) Asteroid/comet impact clusters, flood basalts and mass extinctions: significance of isotopic age overlaps. Earth Planet Sci Lett 236:933–937
Glikson AY (2006) Asteroid impact ejecta units overlain by iron-rich sediments in 3.5–2.4 Ga terrains, Pilbara and Kaapvaal cratons: accidental or cause–effect relationships? Earth Planet Sci Lett 246:149–160
Glikson AY (2008) Milestones in the evolution of the atmosphere with reference to climate change. Aust J Earth Sci 55:125–139
Glikson AY (2010) Archaean asteroid impacts, banded iron formations and MIF-S anomalies: a discussion. Icarus 207:39–44
Glikson AY (2012) Geoengineering the climate? A southern hemisphere perspective: a symposium, Australian Academy of Science, National Committee for Earth System Science, pp 42–43
Glikson AY (2013) The asteroid impact connection of planetary evolution. Springer Briefs, Dordrecht, 149 pp
Glikson AY (2014) Evolution of the atmosphere, fire and the Anthropocene event horizon. Springer Briefs, Dordrecht, 174 pp
Glikson AY, Vickers J (2006) The 3.26–3.24 Ga Barberton asteroid impact cluster: tests of tectonic and magmatic consequences, Pilbara Craton, Western Australia. Earth Planet Sci Lett 241:11–20
Glikson AY, Vickers J (2007) Asteroid mega-impacts and Precambrian banded iron formations: 2.63 Ga and 2.56 Ga impact ejecta/fallout at the base of BIF/argillite units, Hamersley Basin, Pilbara Craton, Western Australia. Earth Planet Sci Lett 254:214–226
Glikson AY, Allen C, Vickers J (2004) Multiple 3.47-Ga-old asteroid impact fallout units, Pilbara Craton, Western Australia. Earth Planet Sci Lett 221:383–396
Glikson M, Duck LJ, Golding SD, Hofmann A, Bolhar R, Webb R, Baiano JCF, Sly LI (2008) Microbial remains in some earliest Earth rocks: comparison with a potential modern analogue. Precambrian Res 164:187–200
Glikson AY, Jablonski D, Westlake S (2010) Origin of the Mt Ashmore structural dome, west Bonaparte Basin, Timor Sea. Aust J Earth Sci 57:411–430
Glikson AY, Uysal IT, Fitz Gerald JD, Saygin E (2013) Geophysical anomalies and quartz microstructures, Eastern Warburton Basin, North-East South Australia: tectonic or impact shock metamorphic origin? Tectonophysics 589:57–76
Global Carbon Project, Global Carbon Budget (2012) http://www.globalcarbonproject.org/carbonbudget/12/hl-full.htm
Gold T (1999) The deep hot biosphere. Springer, New York, 235 pp
Goldblatt C, Zahnle KJ (2011) Clouds and the faint young sun paradox. Clim Past 7:203–220
Goldblatt C, Claire MW, Lenton TM, Matthews AJ, Watson AJ, Zahnle KJ (2009) Nitrogen-enhanced greenhouse warming on early Earth. Nat Geosci 2:891–896
Goldin TJ, Melosh HJ (2009) Self-shielding of thermal radiation by Chicxulub impact ejecta: firestorm or fizzle? Geology 37:1135–1138
Golding D, Glikson M (2010) Earliest life on Earth: habitats, environments and methods of detection. Springer, Dordrecht, 316 pp

Golding SD, Duck LJ, Young E, Baublys KA, Glikson M (2011) Earliest sea floor hydrothermal systems on earth: comparison with modern analogues. In: Golding S, Glikson MV (eds) Earliest life on earth: habitats, environments and methods of detection. Springer, Dordrecht, pp 1–15

Goodwin AM, Monster J, Thode HG (1976) Carbon and sulphur isotope abundances in Archaean iron-formations and early Precambrian life. Econ Geol 71:870–891

Goren-Inbar N, Alperson N, Kislev ME, Simchoni O, Melamed Y, Ben-Nun A, Werker E (2004) Evidence of Hominin control of fire at Gesher Benot Ya'aqov, Israel. Science 304:725–727

Gostin VA, Zbik M (1999) Petrology and microstructure of distal impact ejecta from the flinders ranges Australia. Metor Planet Sci 34:587–592

Gostin VA, Haines PW, Jenkins RJF, Compston W, Williams IS (1986) Impact ejecta horizon within late Precambrian shale, Adelaide Geosyncline, South Australia. Science 233:198–200

Gould SJ (1990) Wonderful life: the burgess shale and the nature of history. W W Norton & Company, Newport Beach, 347 pages

Gradstein FM, Ogg JG (2004) Geologic time scale 2004—why, how, and where next. Lethaia 37:175–181

Grasby SE, Sanei H, Beauchamp B (2011) Catastrophic dispersion of coal fly ash into oceans during the latest Permian extinction. Nat Geosci 4:104–107

Grey K (2005) Ediacaran Palynology of Australia. Association of the Australasian Palaeontologists Memoir 31, Canberra, 439 pp

Grey K, Walter MR, Calver CR (2003) Neoproterozoic biotic diversification: snowball earth or aftermath of the Acraman impact? Geology 5:459–462

Griffin DR (1992) Animal minds. University of Chicago Press, Chicago

Grossman E (2011) Radioactivity in the ocean: diluted, but far from harmless. Environment 360. http://e360.yale.edu/feature/radioactivity_in_the_ocean_diluted_but_far_from_harmless/2391/

Groves C (1993) Our earliest ancestors. In: Burenhult G (ed) The first humans: human origins and history to 10,000 BC. Harper-Collins Publishers, New York, pp 33–40, 42–45, 47–52

Hadron Collider (2008) LHC switch-on fears are completely unfounded. The Institute of Physics. PR 48 (08)

Hallam A, Wignall PB (1997) Mass extinctions and their aftermath. Oxford University Press, Oxford

Halverson GP, Hoffman PF, Schrag DP, Maloof AC, Adam C, Hugh A, Rice N (2005) Toward a neoproterozoic composite carbon-isotope record. GSA Bull 117:1181–1207

Hames W, McHone JG, Renne P, Ruppel C (2003) The Central Atlantic magmatic province: insights from fragments of Pangea. Geophys Monog Ser 136:267 pp

Hannah L (ed) (2011) Saving a million species: extinction risk from climate change. Island Press, Washington, D.C, 432 pp

Hansen J (2012a) http://www.columbia.edu/~jeh1/mailings/2012/20120330_SlovenianPresident.pdf

Hansen J (2012b) http://www.ted.com/talks/james_hansen_why_i_must_speak_out_about_climate_change.html

Hansen JE, Sato M (2012a) Paleoclimate implications for human-made climate change. Clim Change 2012:21–47

Hansen JE, Sato M, Ruedy R (2012b) Public perception of climate change and the new climate dice. The Environmentalist.org 2012/04

Hansen J, Fung I, Lacis A, Rind R, Lebedeff S, Ruedy R, Russell G, Stone P (1988) Global climate changes as forecast by Goddard Institute for Space Studies 3D model. J Geophys Res 93:9341–9364

Hansen J, Sato M, Kharecha P, Lea DW, Siddall M (2007) Climate change and trace gases. Phil Trans Roy Soc 365A:1925–1954

Hansen J, Sato M, Kharecha P, Beerling D, Masson-Delmotte V, Pagani M, Raymo M, Royer DL, Zachos JC (2008) Target atmospheric CO_2: where should humanity aim? Open Atmos Sci J 2:217–231

Hansen J, Sato M, Kharecha P, von Schuckmann K (2011) Earth's energy imbalance and implications. Atmos Chem Phys 11:13421–13449
Hansen J, Sato M, Ruedy R (2012) Perception of climate change. Proc Nat Acad Sci www.pnas.org/cgi/doi/10.1073/pnas.1205276109 1–9
Harris TM (1958) Forest fires in the Mesozoic. J Ecol 46:447–453
He T, Pausas JG, Belcher CM, Schwilk DW, Lamont BB (2012) Fire-adapted traits of Pinus arose in the fiery cretaceous. New Phytol 194:751–759
Henn BM, Cavalli-Sforza LL, Feldman MW (2012) The great human expansion. Proc Natl Acad Sci U S A 109:17758–17764
Henshilwood CS et al (2011) A 100,000-year-old ochre-processing workshop at Blombos Cave, South Africa. Science 334:219–222
Herring JR (1985) Charcoal flux into sediments of the North pacific ocean: the Cenozoic record of burning. IN: the carbon cycle and atmospheric CO_2: natural variations Archaean to present. Geophy Monogr 32:419–442
Hessler AM (2012) Earth's earliest climate. Nature Educ Knowl 3(10):24. http://www.nature.com/scitable/knowledge/library/earth-s-earliest-climate-24206248
Hessler AM et al (2004) A lower limit for atmospheric carbon dioxide levels 3.2 billion years ago. Nature 428:736–738
Heubeck C (2009) An early ecosystem of Archaean tidal microbial mats (Moodies group, South Africa, ca. 3.2 Ga). Geology 37:931–934
Hildebrand WS, Gilmour I, Anders E (1990) Major fires at the cretaceous-tertiary boundary. Geol Soc Am Spec Paper 247:391–400
Hoetzel S, Dupont L, Schefuß E, Rommerskirchen F, Wefer G (2013) The role of fire in Miocene to Pliocene C4 grassland and ecosystem evolution. Nat Geosci 6:1027–1030
Hoffman PF, Schrag DP (2000) Snowball Earth. Sci Am 282:68–75
Hoffman PF, Schrag DP (2002) The snowball Earth hypothesis: testing the limits of global change. Terra Nova 14:129–155
Hoffman PF, Kaufman AJ, Halverson GP, Schrag DP (1998) A Neoproterozoic snowball Earth. Science 281:1342–1346
Hoffman PF, Halverson GP, Domack JM, Husson JA, Higgins D, Schrag DP (2007) Are basal Ediacaran (635 Ma) post-glacial "cap dolostones" diachronous? Earth Planet Sci Lett 258:114–131
Hoffman HJ, Grey K, Hickman AH, Thorpe RI (1999) Origin of 3.45 Ga coniform stromatolites in the Warrawoona Group, Western Australia. Bull Geol Soc Am 111:1256–1262
Holland HD (2006) The oxygenation of the atmosphere and oceans. Phil Tran Roy Soc B: Biol Sci 361:903–915
Hovers E, Kuhn S (2004) Transitions before the transition: evolution and stability in the middle Palaeolithic and middle Stone Age. Springer, New York, pp 171–188
Hoyle F (1982) The universe: past and present reflections. Annu Rev Astron Astrophys 20:1–35
Hoyle F, Wickramasinghe NC (1981) Evolution from space. Simon & Schuster, NewYork, pp 35–49
Hren MT, Tice MM, Chamberlain CP (2009) Oxygen and hydrogen isotope evidence for a temperate climate 3.42 billion years ago. Nature 205:205–208
Hudson SR (2011) Estimating the global radiative impact of the sea-ice-albedo feedback in the Arctic. J Geophys Res 116, D16102
Hudspith V, Scott AC, Collinson ME, Pronina N, Beeley T (2012) Evaluating the extent to which wildfire history can be interpreted from inertinite distribution in coal pillars: an example from the Late Permian, Kuznetsk Basin, Russia. Int J Coal Geol 89:13–25
IPCC-AR4 (2007) Contriibution of working group I to the fourth assessment report of the intergovernmental panel of climate change. http://www.ipcc.ch/publications_and_data/ar4/wg1/en/contents.html
IPCC (2012) Managing risks of extreme events and disasters in advanced climate change - a special report of working groups I and II of the IPCC. Field CB et al., Cambridge University Press, Cambridge, 582 pp

Isbell JL, Miller MF, Wolfe KL, Lenaker PA (2003) Timing of late Paleozoic glaciation in Gondwana: Was glaciation responsible for the development of northern hemisphere cyclothems? In: Chan MA, Archer AW (eds) Extreme depositional environments: mega end members in geologic time. Geological Society of America, Boulder, pp 5–24

Jablonski NG, Frost S (2010) Cercopithecoidea. In: Werdelin L, Sanders WJ (eds) Cenozoic mammals of Africa. University of California Press, Berkeley, pp 393–428

Ji QZ, Luo C, Yuan JR, Wible J, Zhang JP, Georgi JA (2002) The earliest known eutherian mammal. Nature 416:816–822

Jin C et al (2014) Chronological sequence of the early Pleistocene Gigantopithecus faunas from cave sites in the Chongzuo, Zuojiang River area, South China. Quat Int 354:4–14

Joachimski MM et al (2012) Climate warming in the latest Permian and the Permian–Triassic mass extinction. Geology 40:195–198

Johnson C (2013) Hunting or climate change? Megafauna extinction debate narrows. http://thecon versation.com/hunting-or-climate -change-megafauna-extinction-debate-narrows-10602#comment_156216

Jones PD, Osborn TJ, Briffa KR (2001) The evolution of climate over the last millennium. Science 292:662–667

Jones GS, Gregory JM, Stott PA, Tett SFB, Thorpe RB (2005) An AOGCM simulation of the climate response to a volcanic super-eruption. Climate Dynam 25:725–738

Joordens JCA, Vonhof HB, Feibel CS et al (2011) An astronomically-tuned climate framework for hominins in the Turkana basin. Earth Planet Sci Lett 307:1–8

Joordens JCA, Dupont-Nivet G, Feibel CS et al (2013) Improved age control on early *Homo* fossils from the upper Burgi Member at Koobi Fora, Kenya. J Hum Evol 65:731–745

Joordens JCA et al (2015) *Homo erectus* at trinil on java used shells for tool production and engraving. Nature 518:228–231

Joos F, Gerber S, Prentice IC, Otto-Bliesner BL, Valdes PJ (2004) Transient simulations of Holocene atmospheric carbon dioxide and terrestrial carbon since the last glacial maximum. Global Biogeochem Cycles 18:GB2002

Jourdan F, Marzoli A, Bertrand HS, Cirilli S, Tanner LH, Kontak DJ, McHone G, Renne PR, Bellieni G (2009) 40Ar/39Ar ages of CAMP in North America: implications for the Triassic–Jurassic boundary and the 40 K decay constant bias. Lithos 110:167–180

Jourdan F, Reimold UW, Deutsch A (2012) Dating terrestrial impact structures. Elements 8:49–53

Jouzel J (2005) Stable carbon cycle – climate relationship during the late Pleistocene. Science 310:1313–1317

Jouzel J et al (2007) Orbital and millennial Antarctic climate variability over the past 800,000 years. Science 317:793–796

Kahlke R-D (2014) The origin of Eurasian Mammoth faunas (Mammuthus-Coelodonta faunal complex). Quat Sci Rev 96:32–49

Kaiho KY, Kajiwara K, Tazaki M, Ueshima N, Takeda H, Kawahata T, Arinobu R, Ishiwatari A, Hirai MA (1999) Oceanic primary productivity and dissolved oxygen levels at the Cretaceous/tertiary boundary: their decrease, subsequent warming, and recovery. Paleoceanography 14:511–524

Kamo SL, Czamanske GK, Amelin Y, Fedorenko VA, Davis DW, Trofmov VR (2003) Rapid eruption of Siberian flood-volcanic rocks and evidence for coincidence with the Permian-Triassic boundary and mass extinction at 251 Ma. Earth Planet Sci Lett 214:75–91

Kasting JF (1993) Earth's early atmosphere. Science 259:920–926

Kasting JF, Ono S (2006) Palaeoclimates: the first two billion years. Philos Trans R Soc Biol Sci 361:917–929

Kaufmann S (1995) At home in the universe. Oxford University Press, Oxford

Kay CE (1994) Aboriginal overkill and native burning: implications for modern ecosystem management. West J Appl For 10:121–126

Keller G (1986) Stepwise mass extinctions and impact events; late Eocene to early Oligocene. Mar Micropaleontol 10:267–293

Keller G (2005) Impacts volcanism and mass extinction: random coincidence or cause and effect? Aust J Earth Sci 52:725–757
Keller G (2012) The cretaceous-tertiary mass extinction, chicxulub impact, and deccan volcanism. In: Talent JA (ed) Earth and life. Springer, Berlin, pp 759–793
Kemp AC, Horton BP, Donnelly JP, Mann ME, Vermeere M, Rahmstorf S (2011) Climate related sea-level variations over the past two millennia. Proc Natl Acad Sci www.pnas.org/cgi/doi/10.1073/pnas.1015619108
Kharecha P, Kasting J, Seifert JA (2005) A coupled atmosphere-ecosystem model of the early Archaean earth. Geobiology 3:53–76
Kirschvink JL (1992) Chapter 2.3: Low-latitude Late Proterozoic global glaciation: the snowball earth. In: Schopf JW, Klein C, de Maris (eds) The protoerozoic biosphere. Cambridge University Press, New York, pp 51–52
Kittel C, Kroemer H (1980) Thermal physics, 2nd edn. W.H. Freeman and Company, San Francisco
Klein R (2009) The human career: human biological and cultural origins. University of Chicago Press, Chicago
Klein RG, Edgar B (2002) The dawn of human culture. Wiley and Son, New York, 288 pp
Knauth LP (2005) Temperature and salinity history of the Precambrian ocean: implications for the course of microbial evolution. Palaeogeogr Palaeoclimatol Palaeoecol 219:53–69
Knauth LP, Lowe DR (2003) High Archaean climatic temperature inferred from oxygen isotope geochemistry of cherts in the 3.5 Ga Swaziland Supergroup, South Africa. GSA Bull 115(5):566–580
Knoll AH, Javaux EJ, Hewitt D, Cohen P (2006) Eukaryotic organisms in Proterozoic oceans. Phil Trans R Soc London Part B 361:1023–1038
Koestler A (1986) Janus: a summing up. Picador Books, London
Kohler E et al (2002) Hearing sounds, understanding actions: action representation in mirror neurons. Science 297:846–848
Konhausser K, Hamada T, Raiswell R, Morris R, Ferris F, Southam G, Canfield D (2002) Could bacteria have formed the Precambrian banded iron-formations? Geology 30:1079–1082
Kopp RE, Kirschvink JL, Hilburn IA, Nash CZ (2005) The Paleoproterozoic snowball Earth: a climate disaster triggered by the evolution of oxygenic photosynthesis. Proc Natl Acad Sci U S A 102:11131–11136
Korte C, Kozur HW (2010) Carbon-isotope stratigraphy across the Permian–Triassic boundary: a review. J Asian Earth Sci 39:215–235
Kreidenweis SM, Seinfeld JH (1988) Nucleation of sulphuric acid-water and methanesulphonic acid-water solution particles: implications for the atmospheric chemistry of organosulphur species. Atmos Environ 22:283–296
Kring DA, Durda DD (2002) Trajectories and distribution of material ejected from the chicxulub impact crater: implications for post impact wildfires. J Geophys Res 107:6–22
Kump LR (2009) The rise of atmospheric oxygen. Nature 451:277–278
Kump LR, Arthur MA, Patzkowsky ME, Gibbs MT, Pinkus DS, Sheenan PM (1999) A weathering hypothesis for glaciation at high atmospheric pCO_2 during the late Ordovician. Palaeoclimatol Palaeogeogr Palaeoecol 152:173–187
Kurschner WM et al (2008) The impact of Miocene atmospheric carbon dioxide fluctuations on climate and the evolution of terrestrial ecosystems. Proc Natl Acad Sci U S A 105:449–453
Kutzbach JE, Ruddiman WF, Vavrus SJ, Philippon G (2010) Climate model simulation of anthropogenic influence on greenhouse-induced climate change (early agriculture to modern): the role of ocean feedbacks. Clim Change 99:351–381
Kyte FT, Shukolyukov A, Lugmair GW, Lowe DR, Byerly GR (2003) Early Archaean spherule beds: chromium isotopes confirm origin through multiple impacts of projectiles of carbonaceous chondrite type. Geology 31:283–286
Lameira AR, Hardus ME, Bartlett AM et al (2015) Speech-like rhythm in a voiced and voiceless orangutan call. PLoS One. doi:10.1371/journal.pone.0116136

Laris P (2002) Burning the seasonal mosaic: preventative burning strategies in the wooded savannah of Southern Mali. Hum Ecol 30:155–186
Legg S, Hutter M (2007) Universal intelligence: a definition of machine intelligence. Mines Mach 17:391–444
Lenton TM, Held H, Kriegler E, Hall JW, Lucht W, Rahmstorf S, Schellnhuber HJ (2009) Tipping points in the Earth system. Proc Natl Acad Sci U S A 105:1786–1793
Lepre CJ et al (2011) An earlier origin for the Acheulian. Nature 477:82–85
Le Quere C et al (2014) Global carbon budget 2013. Earth Syst Sci Data 6:235–63
Lewis HT (1985) Why Indians burned: specific versus general reasons. In: Lotan JE et al. Proceedings–symposium and workshop on wilderness fire: Missoula, Montana, 15–18 Nov 1983
Lewis CFM, Miller AAL, Levac E, Piper DJW, Sonnichsen GV (2012) Lake Agassiz outburst age and routing by labrador current and the 8.2 ka cold event. Quat Int 260:83–97
Lineweaver CH, Davis TM (2002) Does the rapid appearance of life on Earth suggest that life is common in the universe? Astrobiology 2:293–304
Lisiecki LE, Raymo ME (2005) A Plio-Pleistocene stack of 57 globally distributed benthic $\delta^{18}O$ records. Paleoceanography 20, PA1003. doi:10.1029/2004PA001071
Liu Z et al (2009) Global cooling during the Eocene-Oligocene climate transition. Science 323:1187–1190
Longdoz B, Francois LM (1997) The faint young sun climatic paradox: influence of the continental configuration and of the seasonal cycle on the climatic stability. Global Planet Change 14:97–112
Lovelock JE, Margulis L (1974) Atmospheric homeostasis by and for the biosphere: the Gaia hypothesis. doi:10.1111/j.2153-3490.1974.tb01946.x
Lowe DR (1980) Stromatolites 3,400-Myr old from the Archaean of Western Australia. Nature 284:441–443
Lowe DR (1983) Restricted shallow water sedimentation of early Archaean stromatolitic and evaporitic strata of the strelley pool chert, Pilbara Block, Western Australia. Precambrian Res 19:239–283
Lowe DR (1994) Abiological origin of described stromatolites older than 3.2 Ga. Geology 22:387–390
Lowe DR, Tice MM (2004) Geologic evidence for Archaean atmosphere and climatic evolution: fluctuating levels of CO_2, CH_4, and O_2 with an overriding tectonic control. Geology 32:493–496
Lowe DR, Byerly GR, Asaro F, Kyte FJ (1989) Geological and geochemical record of 3400 million year old terrestrial meteorite impacts. Science 245:959–962
Lowe DR, Byerly GR, Kyte FT, Shukolyukov A, Asaro F, Krull A (2003) Characteristics, origin, and implications of Archaean impact-produced spherule beds, 3.47–3.22 Ga, in the barberton greenstone belt, South Africa: keys to the role of large impacts on the evolution of the early Earth. Astrobiology 3:7–48
Luo Z (2007) Transformation and diversification in early mammal evolution. Nature 450:1011–1019
Luo Z, Yuan C, Meng Q, Ji Q (2011) A Jurassic eutherian mammal and divergence of marsupials and placentals. Nature 476:442–445
Maher KA, Stevenson DJ (1988) Impact frustration of the origin of life. Nature 331:612–614
Marlon JR et al (2008) Climate and human influences on global biomass burning over the past two millennia. Nat Geosci 1:697–702
Marlon JR et al (2009) Wildfire responses to abrupt climate change in North America. Proc Natl Acad Sci U S A 106:2519–2524
Marshall JD (1992) Climatic and oceanographic isotopic signals from the carbonate rock record and their preservation. Geol Mag 129:143–160
Marshall JD, Brenchley PJ, Mason P, Wolff GA, Astini RA, Hints L, Meidla T (1997) Global carbon isotopic events associated with mass extinction and glaciation in the late Ordovician. Palaeogeogr Palaeoclimatol Palaeoecol 132:195–210

Martin W, Baross J, Kelley D, Russell MJ (2008) Hydrothermal vents and the origin of life. Nat Rev Microbiol 6:805–814
Maruoka T, Koeberl C, Bohor BF (2007) Carbon isotopic compositions of organic matter across continental Cretaceous-tertiary (K-T) boundary sections: implications for paleoenvironment after the K-T impact event. Earth Planet Sci Lett 253:226–238
Maslin MA, Christensen B (2007) Tectonics, orbital forcing, global climate change, and human evolution in Africa: introduction to the African paleoclimate special volume. J Hum Evol 53(5):443–464
Maslin MA, Trauth MH (2006) Plio-Pleistocene East African pulsed climate variability and its influence on early human evolution. In: Grine FE, Fleagle JG, Leakey JG (eds) The first humans – origin and early evolution of the genus Homo. Springer. doi:10.1007/978-1-4020-9980-9
Maslin MA, Trauth MH (2009) Plio-pleistocene East African pulsed climate variability and its influence on early human evolution. In: The first humans – origin and early evolution of the genus *homo*. Verteb Paleobiology Paleoanthropology, Springer Science, Dordrecht, 151–158
Maslin MA, Brierley CM, Milner AM, Shultz S, Trauth MH, Wilson KE (2014) East African climate pulses and early human evolution. Quat Sci Rev 101:1–17
Mather TA, Pyle DM, Allen AG (2004) Volcanic source for fixed nitrogen in the early Earth's atmosphere. Geology 32:905–908
Matsuzawa T (2012) What is uniquely human? A view from comparative cognitive development in humans and chimpanzees. In: De Waal FBM, Ferrari PF (eds) The primate mind, Harvard University Press, Cambridge, pp 288–305
McBrearty S, Brooks AS (2000) The revolution that wasn't: a new interpretation of the origin of modern human behaviour. J Hum Evol 39:453–563
McCollom TM, Seewald JS (2006) Carbon isotope composition of organic compounds produced by abiotic synthesis under hydrothermal conditions. Earth Planet Sci Lett 243:74–84
McCracken MC, Covey C, Thompson SL, Weissman PR (1994) Global climatic effects of atmospheric dust from an asteroid or comet impact on Earth. Glob Planet Change 9:263–273
McCulloch MT (2008) Current state and future of the oceans and marine life in a high CO_2 world. In imagining the real: life on a greenhouse earth. Manning Clark House conference, Canberra, pp 25–27
McCulloch MT, Bennett VC (1994) Progressive growth of the Earth's continental crust and depleted mantle: geochemical constraints. Geochim Cosmochim Acta 58:4717–4738
McElwain JC, Punyasena SW (2007) Mass extinction events and the plant fossil record. Trends Ecol Evol 22:549–557
McElwain JC, Beerling DJ, Woodward FI (1999) Fossil plants and global warming at the Triassic-Jurassic boundary. Science 285:1386–1390
McGhee GR (1996) The late Devonian mass extinction. Columbia University Press, New York
McGlone MS, Wilmshurst J (1999) Dating initial Maori environmental impacts in New Zealand. J Q Sci 59:5–16
McHenry HM (2009) Human Evolution. In: Ruse M, Travis J (eds) Evolution: the first four billion years. The Belknap Press of Harvard University Press, Cambridge, MA, 265 pp
Melosh HJ, Vickery AM (1991) Melt droplet formation in energetic impact events. Nature 350:494–497
Melosh HJ, Schneider NM, Zahnle KJ, Latham D (1990) Ignition of global wild fires at the Cretaceous/tertiary boundary. Nature 343:251–254
Miguel CD, Henneberg M (2001) Variation in hominid brain size: how much is due to method? HOMO – J Comp Hum Biol 52:3–58
Miller S (1953) A production of amino acids under possible primitive Earth conditions. Science 117:528–529
Miller GH (2005) Ecosystem collapse in Pleistocene Australia and a human role in megafauna extinction. Science 309:287–290

Miller KG, Wright JD, Katz ME, Wade BS, Browning JV, Cramer BS, Rosenthal Y (2009) Climate threshold at the Eocene-Oligocene transition: Antarctic ice sheet influence on ocean circulation. In: Koeberl C, Montanari A (eds) The late Eocene earth—Hothouse, Icehouse, and Impacts. Geol Soc Am Sp Pap 452:1–10

Mithen SJ (2003) After the ice: a global human history, 20,000–5000 BC. Harvard University Press, Cambridge, MA, 2004. Weidenfeld & Nicolson, London

Mojzsis SJ (2007) Sulphur on the early Earth. In: Van Kranendonk MJ, Smithies RH, Bennett VC (eds) Earth's oldest rocks, vol 15, Developments in precambrian geology. Elsevier, Amsterdam, pp 923–970

Mojzsis SJ, Harrison TM (2000) "Vestiges of a beginning" clues to the emergent biosphere recorded in the oldest known rocks. GSA Today 10:1–6

Mojzsis SJ, Arrhenius G, McKeegan KD, Harrison TM, Friend CRL (1996) Evidence for life on Earth before 3800 million years ago. Nature 270:43–45

Mojzsis SJ, Harrison TM, Pidgeon RT (2001) Oxygen-isotope evidence from ancient zircons for liquid water at the Earth's surface 4,300 Myr ago. Nature 409:178–181

Monechi S, Buccianti A, Gardin S (2000) Biotic signals from nannoflora across the iridium anomaly in the upper Eocene of the Massignano section: evidence from statistical analysis. Mar Micropaleontol 39:219–237

Mora CI, Driese SG, Colarusso LA (1996) Middle to late Paleozoic atmospheric CO_2 levels from soil carbonate and organic matter. Science 271:1105–1107

Morbidelli A et al (2000) Source regions and timescales for the delivery of water to the Earth. Meteor Planet Sci 35:1309–1329

Morgan TJH, Uomini NT, Rendell LE et al (2015) Experimental evidence for the co-evolution of hominin toolmaking teaching and language. Nat Commun 6:6029. doi:10.1038/ncomms7029

Morris RC (1993) Genetic modeling for banded iron-formation of the Hamersley group, Pilbara Craton, Western Australia. Precambrian Res 60:243–286

Morris I (2011) Why the west rules for now: the patterns of history, and what they reveal about the future. Picador, New York

Munich Re (2012) Cat report underscores extreme weather in U.S.; Sandy Losses http://www.insurancejournal.com/news/international/2013/01/03/275865.htm

Murphy NC, Ellis GFR (1995) On the moral nature of the universe: theology, cosmology, and ethics. Fortress Press, Minneapolis

Murphy DM, Solomon S, Portmann RW, Rosenlof KH, Forster PM, Wong T (2009) An observationally based energy balance for the Earth since 1950. J Geophys Res 114:D17107. doi:10.1029/2009JD012105

Narby J (2005) Intelligence in nature. Penguin, New York

NASA (2013) Amplified greenhouse effect shifts north's growing seasons. http://www.nasa.gov/home/hqnews/2013/mar/HQ_13-069_Northern_Growing_Seasons.html

NASA/GISS (2013) Temperatures. http://data.giss.nasa.gov/gistemp/

Nichols GJ, Jones TP (1992) Fusain in carboniferous shallow marine sediments, Donegal, Ireland: the sedimentological effects of wildfire. Sedimentology 39:487–502

Niklas KJ, Tiffney BH, Knoll AH (1985) Patterns in vesicular plant diversification: an analysis at the species level. In: Valentine J (ed) Phanerozoic diversity patterns: profiles in macroevolution. Princeton Legacy Library, Princeton University Press, Princeton

NOAA (2012) Carbon dioxide levels reach milestone at arctic sites. http://researchmatters.noaa.gov/news/Pages/arcticCO2.aspx

NOAA (2013) Mouna Loa CO_2. http://www.esrl.noaa.gov/gmd/ccgg/trends/

Noble D (2008) The music of life: biology beyond genes. Oxford University Press, Oxford, 153 pp

Noffke N et al (2006) A new window into early Archaean life: microbial mats in earth's oldest siliciclastic tidal deposits (3.2 Ga Moodies Group, South Africa). Geology 34:253–256

Noffke N, Christian D, Wacey D, Hazen RM (2013) Microbially induced sedimentary structures recording an ancient ecosystem in the ca. 3.48 billion-year-old dresser formation, Pilbara, Western Australia. Astrobiology 13(12):1103–1124

Nutman AP, Friend CRL (2006) Re-evaluation of oldest life evidence: infrared absorbance spectroscopy and petrography of apatites in ancient metasediments, Akilia, W. Greenland. Precambrian Res 147:100–106
Nutman AP, Clark Friend RL, Bennett VC, Wright D, Norman MD (2010) 3700 Ma premetamorphic dolomite formed by microbial mediation in the Isua supracrustal belt (W. Greenland): simple evidence for early life? Precambrian Res 183:725–737
O'Leary M, Bloch JI, Flynn JJ et al (2013) The placental mammal ancestor and the post-K-Pg radiation of placentals. Science 339:662–667
Ohmoto H, Watanabe Y, Ikemi H, Poulson SR, Taylor BE (2006) Sulphur isotope evidence for an oxic Archaean atmosphere. Nature 442:908–911
Olsen PE, Sues HD (1986) Correlation of continental late Triassic and early Jurassic sediments and patterns of the Triassic–Jurassic tetrapod transition. In: Padian K (ed) The beginning of the age of dinosaurs. Cambridge University Press, Cambridge, pp 321–351
Oparin AI (1924) The origin of life. Moscow Workers Publisher (in Russian). Translation: The origin of life. Dover, New York, 1952
Overpeck J, Bette T, Otto-Bliesner L, Gifford H, Mille M, Daniel RM, Alley RB, Kiehl JT (2006) Paleoclimatic evidence for future ice-sheet instability and rapid sea-level rise. Science 311:1747–1750
Panchuk K, Ridgwell A, Kump LR (2008) Sedimentary response to Paleocene-Eocene thermal maximum carbon release: a model-data comparison. Geology 36:315–318
Patterson N, Richter DJ, Gnerre S, Lander ES, Reich D (2006) Genetic evidence for complex speciation of humans and chimpanzees. Nature 441:1103–1108
Pavlov AA, Kasting JF (2002) Mass-independent fractionation of sulphur isotopes in Archaean sediments: strong evidence for an anoxic Archaean atmosphere. Astrobiology 2:27–41
Pearson PN, Foster GL, Wade BS (2009) Atmospheric carbon dioxide through the Eocene–Oligocene climate transition. Nature 461:1110–1113
Peck WH, Valley JW, Wilde SA, Graham CM (2001) Oxygen isotope ratios and rare earth elements in 3.3 to 4.4 Ga zircons: ion microprobe evidence for high $\delta^{18}O$ continental crust and oceans in the Early Archaean. Geochim Cosmochim Acta 65:4215–4229
Pekar S, Christie-Blick N (2007) Showing a strong link between climatic and pCO_2 changes: resolving discrepancies between oceanographic and Antarctic climate records for the oligocene and early miocene (34–16 Ma). University of Nebraska Antarctic Drilling Program. http://digitalcommons.unl.edu/andrillaffiliates/17
Perry EC, Ahmed SN (1977) Carbon isotope composition of graphite and carbonate minerals from 3.8-AE metamorphosed sediments, Isukasia, Greenland. Earth Planet Sci Lett 36:280–284
Petit JR et al (1999) 420,000 years of climate and atmospheric history revealed by the Vostok deep Antarctic ice core. Nature 399:429–436
Petraglia M et al (2007) Middle paleolithic assemblages from the Indian subcontinent before and after the Toba super-eruption. Science 317:114–116
Phillips MJ, Bennett TH, Lee MSY (2009) Molecules, morphology, and ecology indicate a recent, amphibious ancestry for echidnas. Proc Natl Acad Sci U S A 106:17089–17094
Pidgeon RT (2014) Zircon radiation damage ages. Chem Geol 367:13–22
Pidgeon RT, Nemchin A, Cliff J (2013) Interaction of weathering solutions with oxygen and U–Pb isotopic systems of radiation-damaged zircon from an Archaean granite, Darling Range Batholith, Western Australia. Contrib Mineral Petrol 166:511–523
Poag CW (1997) Roadblocks on the kill curve: testing the Raup hypothesis. Palaios 12:582–590
Pollard D, DeConto RM (2005) Hysteresis in Cenozoic antarctic ice sheet variations. Glob Planet Chang 45:9–21
Pope KO, Baines KH, Ocampo AC, Ivanov BA (1997) Energy volatile production and climatic effects of the Chicxulub Cretaceous/tertiary impact. J Geophys Res 102:21645–21664
Potts R (1998) Environmental hypothesis of hominin evolution. Yearb Phys Anthrop 41:93–136
Potts R (2012) Environmental and behavioral evidence pertaining to the evolution of early *Homo*. Curr Anthropol 53:S299–S317

Power MJ (2013) A 21,000 history of fire. In: Belch CM (ed) Fire phenomena and the earth system: an interdisciplinary guide to fire science. Willey and Sons, Manchester, pp 207–227
Power MJ, Marlon J, Cannon SH (2008) Changes in fire regimes since the last glacial maximum: an assessment based on global synthesis and analysis of charcoal data. Climate Dynam 30:887–907
Price GD (1999) The evidence and implications of polar ice during the Mesozoic. Earth Sci Rev 48:183–210
PRISM (2012) Global warming analysis, pliocene research, interpretation and synoptic mapping. US Geological Survey. http://geology.er.usgs.gov/eespteam/prism/index.html
Pross A (2004) Causation and the origin of life: metabolism or replication first? Origins Life Evol Bios 34:307–321
Pyne SJ (1982) Fire in America: a cultural history of wild and rural fire. Princeton University Press, Princeton
Pyne SJ (1995) World fire: the culture of fire on earth. Henry Holt and Company, New York
Racki G (2003) End-Permian mass extinction: oceanographic consequences of double catastrophic volcanism. Lethaia 36:171–173
Rahmstorf SR (2007) A semi-empirical approach to projecting future sea level rise. Science 315:368–370
Rahmstorf SR, Coumou D (2011) Increase of extreme events in a warming world. Proc Natl Acad Sci U S A 108:17905–17909
Rahmstorf S, Stocker TF (2004) Thermohaline circulation: past changes and future surprises? Box 5.6 in global change, The IGBP series 2005, pp 240–241. http://www.pik-potsdam.de/~Stefan/Publications/Book_chapters/rahmstorf&stocker_2004.pdf
Ramachandran VS (2000) Mirror neurons and imitation learning as the driving force behind "the great leap forward" in human evolution http://edge.org/3rd_culture/ramachandran/ramachandran_index.html
Rampino MR, Self S (1993) Climate-volcanism feedback and the Toba eruption of ~74,000 years-ago. Quat Res 40:269–280
Rees MJ (1999) Just six numbers: the deep forces that shape the universe. Weidenfeld and Nicholson, London
Rees MJ (2001) Our cosmic habitat. Princeton University Press, Princeton
Renne PR, Zhang Z, Richards MA, Black MT, Basu AR (1995) Synchrony and causal relations between Permian – Triassic boundary crises and Siberian flood volcanism. Science 269:1413–1416
Roberts JA, Bennett PC, González LA, Macpherson GL, Milliken KL (2004) Microbial precipitation of dolomite in methanogenic groundwater. Geology 32:277–280
Roberts P, Delson E et al (2014) Continuity of mammalian fauna over the last 200,000 y in the Indian subcontinent. Proc Natl Acad Sci U S A 111:5848–5853
Robinson JM (1989) Phanerozoic O_2 variation, fire and terrestrial ecology. Palaeogeogr Palaeoclimatol Palaeoecol 75:223–240
Roe G (2006) In defence of Milankovitch. Geophys Res Lett 33:L24703
Roebroeks W, Villa P (2011) On the earliest evidence for habitual use of fire in Europe. Proc Natl Acad Sci U S A 108:5209–5214
Rose NM, Rosing M, Bridgwater D (1996) The origin of metacarbonate rocks in the Archaean Isua supracrustal belt, West Greenland. Am J Sci 296:1004–1044
Rosing MT (1999) 13C-depleted carbon microparticles in >3700-Ma sea-fl oor sedimentary rocks from West Greenland. Science 283:674–676
Rosing MT, Bird DK, Sleep NH, Bjerrum CJ (2010) No climate paradox under the faint early Sun. Nature 464:744–749
Ross CA, Ross RP (1995) Permian sequence stratigraphy. In: Scholle PA et al (eds) The Permian of northern Pangea, vol 1. Springer, Berlin, pp 98–123
Rothwell GW, Scheckler SE, Gillespie WH (1989) Elkinsia gen nov a Late Devonian gymnosperm with cupulate ovules. Bot Gaz 150:170–189

Royal Society (2009) Geo-engineering the climate: science, governance and uncertainty. ISBN 978-0-85403-773-5
Royer DL (2006) CO_2-forced climate thresholds during the Phanerozoic. Geochim Cosmochim Acta 70:5665–5675
Royer DL (2008) Linkages between CO_2, climate, and evolution in deep time. Proc Natl Acad Sci U S A 105:407–408
Royer DL, Berner RA, Beerling DJ (2001) Phanerozoic atmospheric CO change: evaluating geochemical and paleobiological approaches. Earth-Sci Rev 54:349–392
Royer DL, Berner RA, Montañez I, Neil P, Tabor J, Beerling DJ (2004) CO_2 as a primary driver of Phanerozoic climate. GSA Today 14:3
Royer DL, Berner RA, Park J (2007) Climate sensitivity constrained by CO_2 concentrations over the past 420 million years. Nature 446:530–532
Ruddiman WF (1997) Tectonic uplift and climate change. Plenum Press, New York, 535 pp
Ruddiman WF (2003) Orbital insolation, ice volume, and greenhouse gases. Quat Sci Rev 22:1597–1629
Ruddiman WF (2008) Earth's climate, past and future, 2nd edn. WH Freeman, New York. ISBN 978-0-7167-8490-6
Russell EWB (1983) Indian-set fires in the forests of the Northeast United States. Ecology 64:78–88
Russell MJ, Hall AJ (2006) The onset and early evolution of life. Geol Soc Am Mem 198:1–32
Rybicki EP (1990) The classification of organisms at the edge of life, or problems with virus systematics. S Afr J Sci 86:182–186
Ryder G (1991) Accretion and bombardment in the Earth–Moon system: the lunar record. Lunar Planet Sci Instit Contrib 746:42–43
Sagan C (1980) Cosmos. Macdonald Futura Publishers, London, 365 pp
Sagan C, Mullen G (1972) Earth and mars: evolution of atmospheres and surface temperatures. Science 177:52–56
Sanders WJ, Gheerbrant E, Harris JM et al (2010) Chapter 9: Proboscidea. In: Werdelin L, Sanders WJ (eds). Cenozoic mammals of Africa. University of California Press, Berkeley, pp 161–251
Schidlowski M, Appel PWU, Eichmann R, Junge CE (1979) Carbon isotope geochemistry of the 3.7×109-years old Isua sediments, West Greenland: implications for the Archaean carbon and oxygen cycles. Geochim Cosmochim Acta 43:189–199
Schoene B et al (2015) U-Pb geochronology of the Deccan traps and relation to the end-cretaceous mass extinction. Science 347(6218):182–184
Schopf JW, Packer BM (1987) Early Archaean (3.3-billion to 3.5-billion-year-old) microfossils from Warrawoona Group, Australia. Science 237:70–73
Schopf JW, Kudryavtsev AB, Czaja AD, Tripathi AB (2007) Evidence of Archaean life: stromatolites and microfossils. Precambrian Res 158:141–155
Schulte P, Alegret L, Arenillas I, Arz JA, Barton PJ, Bown PR, Bralower TJ, Christeson GL et al (2010) The Chicxulub asteroid impact and mass extinction at the Cretaceous- Paleogene boundary. Science 327(5970):1214–1218
Scott AC, Glasspool IJ (2005) Charcoal reflectance as a proxy for the emplacement temperature of pyroclastic flow deposits. Geology 33:589–592
Scott AC, Glasspool IJ (2006) The diversification of Paleozoic fire systems and fluctuations in atmospheric oxygen concentration. Proc Natl Acad Sci U S A 103:10861–10865
Scott AC, Kenig F, Plotnick RE, Glasspool IJ, Chaloner WG, Eble CF (2010) Evidence of multiple late Bashkirian to early Moscovian (Pennsylvanian) fire events preserved in contemporaneous cave fills. Palaeogeogr Palaeoclimatol Palaeoecol 291:72–84
Scott AC, Bowman DMJS, Bond WJ, Pyne SJ, Alexander ME (2014) Fire on earth: an introduction. Wiley Blackwell, Oxford, 413 pp
Sepkoski JJ (1996) Patterns of Phanerozoic extinction: a perspective from global data bases. In: Walliser OH (ed) Global events and event stratigraphy. Springer, Berlin, pp 35–52

Shakova N (2010) http://hot-topic.co.nz/siberian-seabed-methane-first-numbers/
Shakova N et al (2010) Extensive methane venting to the atmosphere from sediments of the East Siberian Arctic Shelf. Science 327:1246–1250
Shakun JD, Clark PU, He F, Marcott SA, Mix AC, Liu Z, Otto-Bliesner B, Schmittner A, Bard E (2012) Global warming preceded by increasing carbon dioxide concentrations during the last deglaciation. Nature 484:49–55
Shapiro R (1986) Origins. Summit Books, New York
Shen H (2012) Drought-hastened Maya decline: a prolongued dry period contributed to civilization collapse. Nature. http://www.nature.com/news/drought-hastened-maya-decline-1-11780. Accessed 05 Jan 2013
Sheuyangea A, Oba G, Weladji RB (2005) Effects of anthropogenic fire history on savannah vegetation in Northeastern Namibia. J Environ Manag 75:189–198
Shukolyukov A, Kyte FT, Lugmair GW, Lowe DR, Byerly GR (2000) The oldest impact deposits on Earth. In: Koeberl C, Gilmour I (eds) Lecture notes in Earth science 92: impacts and the early Earth. Springer, Berlin, pp 99–116
Siddall M, Rohling EJ, Almogi-Labin A, Hemleben CH, Meischner D, Schmelze I, Smeed DA (2003) Sea-level fluctuations during the last glacial cycle. Nature 423:853–858
Siegenthaler U et al (2005) Stable carbon cycle–climate relationship during the late Pleistocene. Science 310:1313–1317
Simonson BM, Glass BP (2004) Spherule layers – records of ancient impacts. Ann Rev Earth Planet Sci 32:329–361
Simonson BM, Hassler SW (1997) Revised correlations in the early Precambrian Hamersley Basin based on a horizon of re-sedimented impact spherules. Aust J Earth Sci 44:37–48
Simonson BM, Davies D, Hassler SW (2000) Discovery of a layer of probable impact melt spherules in the late Archaean Jeerinah Formation, Fortescue Group, Western Australia. Aust J Earth Sci 47:315–325
Smith SJ, van Aardenn J, Klimont Z, Andres RJ, Volke A, Delgado Arias S (2011) Anthropogenic sulphur dioxide emissions: 1850–2005. Atmos Chem Phys 11:1101–1116
Smithsonian Institute (2012) What does it mean to be human? http://humanorigins.si.edu/research/asian-research/hobbits; http://humanorigins.si.edu/research/asian-research/earliest-humans-china
Solanki SK (2002) Solar variability and climate change: is there a link? A&G (2002) 43(5):5.9–5.13. doi:10.1046/j.1468-4004.2002.43509.xhttp://astrogeo.oxfordjournals.org/content/43/5/5.9.abstract http://astrogeo.oxfordjournals.org/content/43/5/5.9.full.pdf+html
Solomon S, Plattner GK, Knutti R, Friedlingstein P (2009) Irreversible climate change due to carbon dioxide emissions. Proc Natl Acad Sci U S A 106:1704–1709.0812721106 January 28, 2009
Spoor F, Gunz P, Neubauer S, Stelzer S, Scott N, Kwekason A, Dean MC (2015) Reconstructed *Homo habilis* type OH 7 suggests deep-rooted species diversity in early Homo. Nature 519:83–86. doi:10.1038/nature14224
Steffen W, Crutzen PJ, McNeill JR (2007) The Anthropocene: are humans now overwhelming the great forces of nature? Ambio 36:614–621
Steffensen JP et al (2008) High-resolution Greenland ice core data show abrupt climate change happens in few years. Science 321:680–684
Stephens NP, Sumner DY (2002) Late Devonian carbon isotope stratigraphy and sea level fluctuations, Canning Basin, Western Australia. Palaeo 191:203–219
Stephens SL, Martin RE, Clinton NE (2007) Prehistoric fire area and emissions from California's forests, woodlands, shrub lands and grasslands. For Ecol Manag 251:205–216
Stevens JR (1989) Hominid use of fire in the Lower and Middle Pleistocene: a review of the evidence. Curr Anthropol Uni Chicago Press 30:1–26
Stevenson DJ (1987) Origin of the moon-the collision hypothesis. Ann Rev Earth Planet Sci 15:271–315

Stewart JR, Stringer CB (2012) Human evolution out of Africa: the role of Refugia. Clim Change Sci 335:1317–1321
Stocker B, Strassmann K, Joos F (2010) Sensitivity of Holocene atmospheric CO_2 and the modern carbon budget to early human land use: analysis with a process-based model. Biogeosci Discuss 7:921–952
Storey M, Roberts RG, Saidin M (2012) Astronomically calibrated 40Ar/39Ar age for the Toba super-eruption and global synchronization of late quaternary records. Proc Natl Acad Sci 109:18684–18688
Strauss H, Peters-Kottig W (2003) The Paleozoic to Mesozoic carbon cycle revisited: the carbon isotopic composition of terrestrial organic matter. Geochem Geophys Geosyst 4(10):1083
Strik G, de Wit MJ, Langereis CG (2007) Palaeomagnetism of the Neoarchaean Pongola and Ventersdorp Supergroups and an appraisal of the 30–19 Ga apparent polar wander path of the Kaapvaal Craton, Southern Africa. Precambrian Res 153:96–115
Stringer C, Andrews P (2011) The complete world of human evolution (revised edition). Thames & Hudson, London
Strongman L (2007) The anthropomorphic bias: how human thinking is prone to be self-referential. Working papers no 4–07. Lower Hutt: The Open Polytechnic of New Zealand. http://hdl.handle.net/123456789/1245
Su DF, Harrison T (2015) The palaeoecology of the Upper Laetolil Beds, Laetoli Tanzania: a review and synthesis. J African Earth Sci 101:405–419
Suddendorf T (2012) The gap: the science of what separates us from other animals. Basic Books, New York, 352 pp
Sugitania K, Grey K, Nagaokac T, Mimurad K, Walter M (2009) Taxonomy and biogenicity of Archaean spheroidal microfossils (ca 3.0 Ga) from the Mount Goldsworthy–Mount Grant area in the northeastern Pilbara Craton, Western Australia. Precambrian Res 173:50–59
Surovell TA, Grund BS (2012) The associational critique of quaternary overkill and why it is largely irrelevant to the extinction debate. Am Antiq 77(4):672–687
Teaford MF, Ungar PS (2000) Diet and the evolution of the earliest human ancestors. Proc Nat Acad Sci USA 97:13506–13511
Teilhard de Chardin P (1959) The future of man. Random House, San Francisco, 332 pp
Thewissen JGM (2014) The walking whales: from land to water in eight million years. University of California Press, Oakland
Thiemens MH (1999) Atmospheric science – mass-independent isotope effects in planetary atmospheres and the early solar system. Science 283:341–345
Thomas CD (2004) Extinction risk from climate change. Nature 427:145–148
Tice MM, Lowe DR (2006) Hydrogen-based carbon fixation in the earliest known photosynthetic organisms. Geology 34:37–40
Timmreck C et al (2012) Climate response to the Toba super-eruption: regional changes. Quat Int 258:30–44
Tohver E et al (2012) Geochronological constraints on the age of a Permo-Triassic impact event: U-Pb and 40Ar/39Ar results for the 40 km Araguainha structure of central Brazil. Geochim Cosmochim Acta 86:214–227
Tomasello M (1999) The cultural origins of human cognition. Harvard University Press, Cambridge, MA
Trainer MG et al (2006) Organic haze on titan and the early Earth. Proc Natl Acad Sci U S A 103:18035–18042
Trauth MH, Maslin MA, Deino AL, Strecker MR, Bergner AGN, Duhnforth M (2007) High- and low-latitude forcing of Plio-Pleistocene East African climate and human evolution. J Hum Evol 53:475–486
Trauth MH, Maslin MA, Deino AL, Junginger A, Lesoloyia M, Odada EO, Olago DO, Olaka LA, Strecker MR, Tiedemann R (2010) Human evolution in a variable environment: the amplifier lakes of Eastern Africa. Q Sci Rev 29:2981–2988
Trenberth KE, Fasullo JT, Kiehl J (2009) Earth's global energy budget. Am Meteorol Soc 90:311–323

Twitchett RJ, Looy CV, Morante R, Visscher H, Wignall PB (2001) Rapid and synchronous collapse of marine and terrestrial ecosystems during the end-Permian crisis. Geology 29:351–354
Twomey T (2011) Keping fire: the cognitive implications of controlled fire use by middle pleistocene humans. University of Melbourne. http://unimelb.academia.edu/TerrenceTwomey
Uwins PJR et al (1998) Novel nano-organisms from Australian sandstones. Am Mineral 83:1541–1550
Valley JW (2008) The origin of habitats. Geology 36:911–912
Valley JW et al (2002) A cool early earth. Geology 30:351–354
Van Kranendonk MJ, Webb GE, Kamber BS (2003) Geological and trace element evidence for a marine sedimentary environment of deposition and biogenicity of 3.45 Ga stromatolitic carbonates in the Pilbara craton and support for a reducing archaean ocean. Geobiology 1:91–108
Van Kranendonk MJ (2007) Tectonics of the early earth. In: Van Kranendonk MJ, Smithies RH, Bennett VC (eds) Earth's oldest rocks, developments in precambrian geology, vol 15. Elsevier, Amsterdam, pp 1105–1116
Van Zuilen MA, Lepland A, Arrhenius G (2002) Reassessing the evidence for earliest traces of life. Nature 418:627–630
Vasconcelos C, McKenzie JA, Bernasconi S, Grujic D, Tien AJ (1995) Microbial mediation as a possible mechanism for natural dolomite at low temperatures. Nature 377:220–222
Velicogna I (2009) Increasing rates of ice mass loss from the Greenland and Antarctic ice sheets revealed by GRACE. Geophys Res Lett 36(19):L19503
Veron C (2008) Mass extinctions and ocean acidification: biological constraints on geological dilemmas. Coral Reefs 27:459–472
Vitousek PM (1994) Beyond global warming – ecology and global change. Ecology 75:1861–1876
Wacey D (2012) Earliest evidence for life on Earth: an Australian perspective. Aust J Earth Sci 59:153–166
Wagner F, Aaby B, Visscher H (2002) Rapid atmospheric CO_2 changes associated with the 8,200-years-B.P. cooling event. Proc Natl Acad Sci U S A 99:12011–12014
Wald G (1964) The origin of life. Proc Natl Acad Sci U S A 52:595–611
Walsh M (1992) Microfossils and possible microfossils from the early Archaean Onverwacht Group, Barberton Mountain Land, South Africa. Precambrian Res 54:271–293
Walsh M, Lowe DR (1985) Filamentous microfossils from the 3,500 Myr-old Overwacht Group, Barberton Mountain Land, South Africa. Nature 314:530–532
Walter MR, Veevers JJ, Calver CR, Gorjan P, Hill AC (2000) Dating the 840–544 Ma Neoproterozoic interval by isotopes of strontium, carbon, and sulphur in seawater, and some interpretative models. Precambrian Res 100:371–433
Wang Y, Yaoming H, Meng J, Chuankui L, Yuanqing Wang (2001) An ossified Meckel's Cartilage in two Cretaceous mammals and origin of the mammalian middle ear. Science 294:357–361
Wang W, Crompton RH, Carey TS Günther MM Li Y, Savage R, Sellers WI (2004) Comparison of inverse-dynamics musculo-skeletal models of AL 288-1 *Australopithecus afarensis* and KNM-WT 15000 *Homo ergaster* to modern humans, with implications for the evolution of bipedalism. J Hum Evol 47:453–478
Ward PD (2007) Under a green sky: global warming, the mass extinctions of the past, and what they can tell us about our future. Harper Collins, New York, 242 pp
Watson A, Lovelock JE, Margulis L (1978) Methanogenesis, fires and the regulation of atmospheric oxygen. Biosystems 10:293–298
Watson SK, Townsend SW, Schel AM, Wilke C, Wallace EK, Cheng L, West V, Slocombe KE (2015) Vocal learning in the functionally referential food grunts of chimpanzees. Curr Biol 25:1–5
Weiss H et al (1993) The genesis and collapse of third millennium north Mesopotamian civilization. Science 261:995–1004

Weston E, Boisserie J-R (2010) Hippopotamidae. In: Werdelin L, Sanders WJ (eds) Cenozoic mammals of Africa. University of California Press, Berkeley, pp 853–871
Whiteside JH, Olsen PE, Eglinton T, Brookfield ME, Sambrotto RN (2010) Compound-specific carbon isotopes from earth's largest flood basalt eruptions directly linked to the end-Triassic mass extinction. Proc Natl Acad Sci U S A 107(15):6721–6725, pnas.1001706107
Wible JR, Rougier GW, Novacek MJ, Asher RJ (2007) Cretaceous eutherians and laurasian origin for placental mammals. Nature 447 (7147):1003–1006
Wiersma AP, Roche DM, Renssen H (2011) Fingerprinting the 8.2 ka event climate response in a coupled climate model. J Q Sci 26:118–125
Wignall PB (2001) Large igneous provinces and mass extinctions. Earth Sci Rev 53:1–33
Wignall PB, Twitchett RJ (1996) Oceanic anoxia and the end Permian mass extinction. Science 272:1155–1158
Wigner EP (1961) The probability of the existence of a self-reproducing unit. In: Shils E (ed) The logic of personal knowledge. Routledge & Kegan Paul, London, pp 231–238
Wilde SA, Valley JW, Peck WH, Graham CM (2001) Evidence from detrital zircons for the existence of continental crust and oceans on the Earth 4.4 Gyr ago. Nature 409:175–178
Williams J (2012) The number of natural disasters is on the rise. http://makewealthhistory.org/2011/05/30/the-number-of-natural-disasters-is-on-the-rise/
Williams GE, Gostin VA (2005) The Acraman – Bunyeroo impact event (Ediacaran) South Australia and environmental consequences: 25 years on. Aust J Earth Sci 52:607–620
Williams GE, Schmidt PW, Boyd DM (1996) Magnetic signature and morphology of the Acraman impact structure South Australia. Aust Geol Surv Org J Aust Geol Geophys 16:431–442
Wolbach SW, Widicus S, Moecker S (1990) Is the soot layer at the KT boundary really global? Lunar and Planetary Science XXIX 1309
Wood F (2008) China's first emperor and his terracotta warriors. Macmillan Publishing, New York
Wrangham R (2009) Catching fire: how cooking made us human. Basic Books, New York, 320 pp
Xu L et al (2013) Temperature and vegetation seasonality diminishment over northern lands. Nat Clim Change 3(4):581–586
Yokoyama Y, Esat TM (2011) Global climate and sea level: enduring variability and rapid fluctuations over the past 150,000 years. Oceanography 24:54–69
Young GM, von Brunn V, Gold WEL, Minter DJC (1998) Earth's oldest reported glaciation: physical and chemical evidence from the Archaean Mozoan Group (~2.9 Ga). S Africa J Geol 106:523–538
Zachos JC, Breza JR, Wise SW (1992) Early oligocene ice-sheet expansion on Antarctica–stable isotope and sedimentological evidence from Kerguelen Plateau, Southern Indian Ocean. Geology 20:569–573
Zachos J, Pagani M, Sloan L, Thomas E, Billups K (2001) Trends, rhythms, and aberrations in global climate 65 Ma to present. Science 292:686–693
Zachos J, Dickens GR, Zeebe RE (2008) An early Cenozoic perspective on greenhouse warming and carbon-cycle dynamics. Nature 451:279–283
Zahnle KJ (1986) Photochemistry of methane and formation of hydrocyanic acid (HCN) in the Earth's early atmosphere. J Geophys Res 91:2819–2834
Zahnle K, Grinspoon D (1990) Comet dust as a source of amino acids at the Cretaceous/tetiary boundary. Nature 348:157–160
Zahnle K, Sleep NH (1997) Impacts and the early evolution of life. In: Thomas PJ, Chyba CF, McKay CP (eds) Comets and the origin and evolution of life. Springer, New York, pp 175–208
Zeebe RE, Bada JL, Zachos JC, Dickens GR (2009) Carbon dioxide forcing alone insufficient to explain Palaeocene–Eocene thermal maximum warming. Nat Geosci 2:576–580
Zhao M, Bada JL (1989) Extraterrestrial amino acids in cretaceous/tertiary boundary sediments at Stevns Klint, Denmark. Nature 339:443–445
Zimmer C (2005) Smithsonian intimate guide to human origins. Madison Press Books, Totonto, 176 pp

About the Book and the Authors

This book examines milestones in the history of the atmosphere–ocean system – the lungs of the Earth – including the great mass extinction of species, in perspective of the hour of truth Homo sapiens finds itself in. The culmination of the climate change crisis by the twenty-first century, overshadowed by an increasingly probable global nuclear calamity, defines a sixth mass extinction of species as the outcome of the activities of an intelligent but short-sighted species which, alone among all life forms, has mastered fire, enhancing its entropy factor by many orders of magnitude. The effects of fire on the mind and imaginative powers of prehistoric humans are seen as a key for cerebral evolution of Homo sapiens, including the premonition of death, with consequent strive for immortality, omnipotence and omniscience. The book explores some of the deep philosophical issues arising from anthropogenic ecocide, overshadowing every ideal and faith humans held dear over the ages. The question how the Universe reached self-awareness through the eyes of Homo sapiens may remain a mystery for all time. Metaphorically, the sixth mass extinction can be seen as the consequence of the Universe looking at itself through intelligent eyes, in the sense of Carl Sagan.

The Authors

Andrew Y. Glikson, An Earth and paleo-climate scientist, studied geology at the University of Jerusalem and graduated at the University of Western Australia in 1968. He conducted geological surveys of the oldest geological formations in Australia, South Africa, India and Canada; studied large asteroid impacts, including effects on the atmosphere and oceans of mass extinction of species. Since 2005 he studied the relations between climate and human evolution. He

A.Y. Glikson, C. Groves, *Climate, Fire and Human Evolution*, Modern Approaches in Solid Earth Sciences 10, DOI 10.1007/978-3-319-22512-8

was active in communicating nuclear issues and climate change evidence to the public and parliament through papers, lectures, conferences and presentations.

Colin Groves, An anthropologist, primatologist and mammologist at the Australian National University, School of Archaeology and Anthropology, has research interests in human evolution, primates, mammalian taxonomy, skeletal analysis, biological anthropology, ethnobiology and biogeography. Colin Groves conducted extensive fieldwork in Kenya, Tanzania, Rwanda, India, Iran, China, Indonesia, Sri Lanka and the Democratic Republic of Congo. He described Homo ergaster and published *Primate Taxonomy* by the Smithsonian Institution Press (2001) and *Ungulate Taxonomy* (2011).

Index

A
Acraman impact
  and Acritarchs radiation, 61
  stratigraphic distribution, 48
Anthropocene
  Arctic and Antarctic vortices, 128
  climate zones, 125, 131
  cold wind vortexes, 127–128
  decadal surface temperature anomalies, 130, 141
  eastward-directed circum-Antarctic Southern Ocean, 128
  geological era, 86
  global
    annual mean earth's energy budget, 124, 125
    chlorophyll levels, 130, 135
    maps, 130, 134
    photosynthesis levels, 130, 135
    surface temperatures (monthly mean), 130, 143
    warming, 130, 143
  Gulf of Mexico, 127
  layered atmosphere, 124
  moisture-laden air masses, 128
  NASA, 125, 126
  oceans, 125, 129
  poles, 125, 130
  radiant energy, 124–125
  solar radiation, 125
  sulphur emissions, 130, 142
  temperatures, 125
  vertical profile, 124
  weather and climate, 124
  wind patterns, 125, 127, 128
  11-years sun-spot cycle, 124, 126
Archaean atmospheres. *See also* Proterozoic atmospheres
  atmosphere–biosphere system, 7
  BIF, 8, 10, 11
  CO_2 levels, 4
  The faint young sun paradox, 3–4
  gaseous and aerosol composition, 2
  GHG, 3
  Hadean era, 5, 7
  Isua Belt, 10
  liquid water, 2–3
  magnetite (Fe_3O_4), 9
  microbial effects, 2
  MIF-S, 7, 12
  $\delta^{18}O$ ratio and δ, 5–7
  ozone layer, 7, 8
  river cobbles, 9
  Saturn's moon Titan, 9
  UV radiation, 12

B
Banded iron formation (BIF)
  2.48 Ga, 10, 11
  detrital hematite and goethite, 16
  magnetite-quartz banded iron formation, 10, 11
  microbial photoautotrophs, 13
BIF. *See* Banded iron formation (BIF)
Big Bang theory, 180, 182, 185, 190, 192

A.Y. Glikson, C. Groves, *Climate, Fire and Human Evolution*, Modern Approaches in Solid Earth Sciences 10, DOI 10.1007/978-3-319-22512-8

Biosphere
Carboniferous-Permian period, 87
fire-resistant plants, 87
fires, 86
fossil Palaeozoic plants, 86, 87
global fire activity, 88
non-organic combustion processes, 86
oxygenation reactions, 86
photosynthesis, 86

C
Cambrian–Ordovician mass extinction, 62–63
CAMP. *See* Central atlantic magmatic province (CAMP)
Canfield Ocean, 24
Cap carbonate, 23
Carboniferous-Permian glaciation (326–267 Ma), 9, 25, 29, 31, 62
Carbon oxidation
The Arctic Ocean, 139, 145–146
Australian CSIRO, 138
carbonic acid, 148
Cenozoic climate shifts, 139
chemical reaction, 147, 152
climate-warming scenarios, 149
climate zones, 102, 125, 131–133, 175, 176
cold vapor-laden fronts, 151–152
CO_2 rise rates, 139, 145
earth surface and atmosphere, 146
ENSO cycle, 147, 150, 155
Extinction Risk from Climate Change, 149
fossil biospheres, 152
frequency of occurrence, 147, 152
GHG period, 150
global
climate, 147
CO_2 emission, 137
mean positive and negative radiative forcings, 137, 138
temperature, 139, 145
warming, 141, 145
greenhouse gases, 137
Greenland and west Antarctic ice sheets, 142, 147
Holocene levels, 150
ice melt, 141, 146
intransigent spirals, 153
K-T asteroid impact, 139
marine good chain, 148, 154
ocean acidification, 148, 153
ocean's ability, 147
Palaeoclimate studies, 141
Paleocene–Eocene boundary, 153
peak temperatures, 151
policy-relevant tipping elements, 147, 169
reef gaps, 148
sea level rise (twenty-first centuries), 142, 146, 147, 149
semi-arid regions global warming, 147
sub-glacial melt flow, 142
sulphur emissions, 138, 142
temperate zones, 146
temperature rise rates, 142, 148
US Atlantic coast, 145
weather events, 147, 150, 153
winter precipitation, 147, 150, 151, 153
Cenozoic biological evolution
genetic to cultural evolution, 81–84
mammals (*see* Mammals evolution)
primates to humans
australopithecines, 76
cranium studies, 76, 77
fish fossils, 79
Homo ergaster, 78
Homo habilis, 78
Homo rudolfensis, 78
Homo sapiens, 80
Kenyanthropus platyops, 77
"Peking Man", 79
Sahelanthropus tchadensis, 76
Sterkfontein fossils, 77
Cenozoic paleogeography, 35, 36
Central atlantic magmatic province (CAMP), 53
Chimpanzees, comparative study
Citing Life Expectancy, 82
cranial capacity, 76
DNA analysis, 81
mental characteristics, 81
tool-making skills, 81–82
vocal learning, 83
CMB. *See* Cosmic Background Radiation (CMB)
Cosmic Background Radiation (CMB), 178–179
Cretaceous sediments
fern-dominated charcoal, 93
'greenhouse earth' conditions, 91
oxygen levels, 92
plant species, 92
Cretaceous-tertiary boundary (K-T) mass extinction
Chicxulub and Boltysh, 64
Cretaceous mammalian lineages, 67
Deccan volcanism, 66
ejecta and microkrystite spherules, 66

'fire layer', 64, 65
Globotruncana contusa, 64
Cryogenian Snowball Earth (750–635 Ma), 22–23

D
Dansgaard–Oeschger (D–O) events
glaciation, 139, 148
intra-glacial cycle, 40
sea level rise rates, 144
temperature, 42
Devonian mass extinction events
biological activity $\delta^{13}C$ and $\delta^{18}O$, 62
ocean anoxia, 62
Dunbar index, 97

E
Early biospheres
BIF, 13
$\delta^{13}C$ values, 15
DNA/RNA biomolecules, 12
elemental and carbon isotope geochemistry studies, 16
isotopic sulphur $\delta^{33}S$ values, 19
LHB, 14
Miller–Urey experiments, 12
REE+Y patterns, 14
reflectance measurements, 16
stromatolites, 19–21
TEM, 16–19
Early earth systems
Archaean and Proterozoic (*see* Archaean atmospheres)
early biospheres (*see* Early biospheres)
greenhouse states (*see* Glaciations and states, GHG)
Earth
Big Bang, 185
'bio-friendly' factors, 180
biogenetic hypotheses, 180–181
CMB, 178–179
cometary components, 183
information-rich biomolecules, 183
Milky Way, civilizations frequency, 178
multiverse and string theory, 181
orbital features, 181
species
Gaia hypothesis, 187–188
life, definition, 183
molecular biology and paleontological studies, 184
natural and artificial intelligence, 182
natural intelligence, shared principles, 185–187
East Siberian Arctic Shelf (ESAS), 170
EDS. *See* Electron dispersive spectral analysis (EDS)
Electron dispersive spectral analysis (EDS), 16, 17
El Nino Southern Oscillation (ENSO) cycles, 128, 129
cooling and evolution, 37
deep water formation, 147
The El Nino phase, 129
global warming, 155
La Nina phase, 36
The La Nina phase, 129
ocean deep water formation, 147
Pacific and Atlantic Ocean basins separation, 35
End-eocene freeze
biotic transformations, 67
isotopic $\delta^{13}C$ and $\delta^{18}O$, 67
methane hydrates, 67
End-Triassic mass extinction, 55, 63–64
ESAS. *See* East Siberian Arctic Shelf (ESAS)

F
The Faint young sun paradox, 3, 4
The Faustian Bargain, 194
Arctic and boreal regions, 160
CO_2 emissions, 158, 159
CO_2 rise rates and global temperature, 145, 158
2030–2099 droughts, 160, 168
fossil fuel resources, 158, 160
global
effort, 172
photosynthesis, 135, 161
scale, 169
warming, 172
greenhouse gas sequestration methods, 171
historical and projected variations, 160, 164–165
land temperatures, 169
looming factors, 160
marine good chain, 154, 172
methane, 160, 162
mitigation
and adaptation, 172
and CO_2, 171
ocean circulation, 160, 163
oxygen atmospheric residence, 161

The Faustian Bargain (*cont.*)
Pleistocene glacial-interglacial cycles, 163
policy-relevant tipping elements, 163, 169
pre-industrial Holocene levels, 170
record-breaking heat events, 170
sea levels relations, 147, 158
solar mitigation, 171
stratospheric residence, 172
Vostok ice core record, 158, 159
winter precipitation, 151, 160
Fire. *See also* Pre-historic fires
charcoal
charcoal-bearing shales, 89
charcoal-rich units, 89
Triassic-Jurassic boundary, 90, 91
history
charcoal, 89, 90
Devonian plants, 89
Eocene, 94
fire-adapted plants, 88, 89
inertinite, 90
K-T boundary impact, 92, 93
oxygen concentration, Paleozoic, 91
PAH, 92
PETM, 32, 33
Phanerozoic geochemical models, 25
Pliocene and Pleistocene, 43
snowball Earth, 22–23
thermal blanketing effect, 34
Global warming
Arctic lakes, 162
ENSO cycle, 155
human exploitation, 163
and Neolithic burning (*see* Neolithic Burning)
in Polar Regions, 151
semi-arid regions, 147
Globotruncana contusa, 64
Greenhouse gas (GHG)
atmosphere-ocean-biosphere system, 181
CO_2–CH_4 greenhouse atmosphere, 9
gas sequestration methods, 171
glacial periods, 2
Holocene, 136
infrared radiation, 9–10
nitrous oxide and methane, 46
solar luminosity, 4
thermal blanketing effect, 34
Gulf of Mexico, 64, 127, 154

G
Gaia hypothesis, 187–188
Genetic to cultural evolution
comparative study, chimpanzees (*see* Chimpanzees, comparative study)
human ontogeny
aesthetic activities, 83
fire traces, 84
language, 82–83
social learning, 82
GEOCARBSULF model, 30
GHG. *See* Greenhouse gas (GHG)
Glaciations and states, GHG
Antarctic ice sheet, 33
biological evolution, 27, 30–31
cainozoic CO_2 and temperature, 25, 28
Cambrian arthropods, 24–25
"Canfield Ocean", 24
carbon cycle, 26, 28
climate shifts (abrupt), 35, 40
Ediacara fossils, 24
end-Eocene freeze, 33, 34
ENSO, 36, 37
ephemeral lakes, 42
ice ages, 25, 26
Miocene (9.3–8.4 Ma) sediments, 35, 39
Olduvan stone tools, 43

H
Hadean zircons, 7
High resolution TEM (HRTEM), 16, 17
Holocene
burning and land clearing, 133
CO_2 and methane, 112
high temperatures, 111
and Pliocene, 38
pre-industrial temperature, 100
rock painting, 115
in South Africa, 74
surface temperatures, 3
Holocene climates, 38
HRTEM. *See* High resolution TEM (HRTEM)

I
Intertropical Convergence Zone (ITCZ), 42
Isua Belt, 9, 10
ITCZ. *See* Intertropical Congence Zone (ITCZ)

J
Jurassic-Cretaceous extinction, 56, 64

L
Last glacial termination (LGT), 94, 105, 113
Late and end-devonian mass extinctions. *See* Devonian mass extinction events
Late heavy bombardment (LHB), 5, 14
Late permian. *See* Permian-triassic mass extinctions
LGT. *See* Last glacial termination (LGT)
LHB. *See* Late heavy bombardment (LHB)
Little Ice Age (LIA), 60, 94, 129–130

M
Magnetite (Fe_3O_4), 9, 11
Mammal-like reptiles, 70
Mammals evolution
  character definition, 70
  Cretaceous mammals, 69
  extinctions, pattern, 74
  hippopotamus lineage, fossil record, 73
  hypotheses
    explosive, 71
    long fuse, 71
    short fuse, 71, 72
  "mammal-like reptiles", 70
  Meckel's Cartilage, 70
  ontogeny recapitulates phylogeny, 70
  Palaeocene fossil placentals, 72
  Prototheria, 70–71
  Theria, 71
Mass-independent fractionation of sulphur isotopes (MIF-S)
  vs. age, 7, 8
  ($\delta^{33}S$) anomalies, 7
  oxygen levels, 12
Maya civilization
  incipient collapse, 116, 119
Meckel's Cartilage, 70
Medieval Warm Period (MWP), 117
Megafauna, 75
MIF-S. *See* Mass-independent fractionation of sulphur isotopes (MIF-S)
Milankovic cycles, 34–36, 98
Millennium Ecosystem Assessment program, 157
Miller–Urey experiments, 12
Mutual Assured Destruction (MAD), 193

N
NATH. *See* North Atlantic Thermohaline Current (NATH)
Neolithic burning
  agricultural civilizations, 134
  charcoal deposits, 133
  circum-Mediterranean forests, 134
  and civilizations
    anthropocene hypothesis, 117
    climate events (abrupt), 113
    CO_2, CH_4 and N_2O concentration, 116
    global temperature and climate forcings, 112
    Holocene Optimum, 112
    medieval drought, Southeast Asia, 117, 120
    MWP, 117
    Nile River history, 113–114
    radiative forcings, 117, 121
    river civilizations, 118
  fire-stick farming, 133
  Holocene temperature variations, 136
  human-dominated Anthropocene, 136
  human-triggered fires, 136
  North American fire regimes, 133–134
  seasonal/periodic burnings, 133
The North Atlantic Thermohaline Current (NATH), 42, 163
Northern Hemisphere climate
  ice sheets, 29
  surface air temperatures, 38

O
Olduvan stone tools, 42, 43, 77
Organic petrology, 16, 17
Ozone layer
  isotopic fractionation, 8
  oxygen-poor Archaean atmosphere, 7, 8
  radioactive pollution, 192
  UV radiation, 10

P
PAH. *See* Polycyclic aromatic hydrocarbons (PAH)
Paleocene-Eocene thermal maximum (PETM), 32, 33, 67, 93, 145
Peking Man, 79
Permian-Triassic mass extinctions
  251 Ma End-Permian Changhsingian Stage, 63
  260 Ma Late Permian Maokouan Stage, 63
  isotopic δ^{13} C and δ^{34} S mass, 63
  sulphur-reducing microbes, 63

PETM. *See* Paleocene-Eocene thermal maximum (PETM)
Phanerozoic mass extinctions
  biotic effects, 50, 51
  carbon and oxygen isotopic anomalies, 48, 52
  $\delta^{13}C$ curves, 50
  Devonian isotopic excursions, 50
  earthquakes and tsunami, 46
  environmental effects, 46
  greenhouse
    Carboniferous-Permian glaciation (326–267 Ma), 31
    early Jurassic to Cretaceous cool phases (184–66.5 Ma), 32
    late Devonian-early Carboniferous glaciations (371–349 Ma), 31
    late Ordovician glaciation (445.6–443.7 Ma), 31
  marine invertebrates, 46, 47
  δ^{18} O and δ^{13} Ccarb, 47, 48
  Ordovician, 48, 49
  Palaeo-atmospheric CO_2, 53, 55
  Permian–Triassic transition, 50, 53
  volcanic/asteroid events, 57–61
  volcanism, 46, 47
Photosynthesis
  autotrophs, 2
  bacterial activity, 14
  CO_2 and O_2 cycles, 2
  glaciation, 23
  nitrogen, 10
  oxygen, 7
  single-celled blue-green algae, 191
  vegetation, 130
Pleistocene
  glacial-interglacial cycles, 46
  Holocene boundary, 74
  Milankovic cycles, 35
  Savannah environments, Africa, 43
Pliocene
  CO_2 levels, 159
  Holocene climates (late), 38
  modern vegetation albedo distribution, 38
  Northern Hemisphere
    Holocene climates, 38
    vegetation albedo distribution, 38
  orbital forcing cycles, 36
  Pleistocene glacial-interglacial cycles, 163
Polycyclic aromatic hydrocarbons (PAH), 92
Post-anthropocene World
  Arctic temperatures, 175
  biological cycle, 176
  cessation, 172–173
  flooding, 174–175
  interglacial period, 173, 175
  long-term climate response, 173
  radiation-resistant arthropods species, 176
  species extinction rates, 174
  surface air temperature, 173
  temperate climate zones, 175
Pre-historic fires
  apes, neuron patterns, 111
  biomass, reconstructions, 94, 95
  bipolarity, neocortex and mammalian brain, 106
  bootstrap resampling, 96
  burning strategies, 105
  campfires, 106
  charcoal fragments and pollen, 94
  cooking, 104, 105
  East African rift valley, 98
  fossil bovids, 97
  Homo pekinensis lighting fire, 98, 101
  human brain
    body mass ratio, 96
    evolution, 99
  LGT, 94, 105
  Maya war, 107, 108
  mean group size and neocortex ratio, brain, 97
  mtDNA haplogroups, 102, 104
  paleo-climate
    and hominin evolution, 98
    indicators, 94
  sites evidence, fire usages, 101, 103
  Toba super-eruption, 109
  tools, 95, 96
  Wonderwerk cave studies, 101, 102
Prometheus
  blue-green algae, 191
  carbon-oxygen balance, 193
  chromosome-exchanging Eukaryotes, 191
  climate stabilized, Holocene, 194
  electromagnetic constants, 191
  ethical and cultural assumptions, 195
  extra-terrestrial bombardment, 192
  geological legacy, 194
  gold, 193
  Greek mythology, 83
  habitability, 195
  oxygen-carbon cycle, 193
  planetcide, 194
  planetesimal offspring, 191
  prehistoric time, 192

quantum mechanics, 191
technological civilisations, 191
U symbol, 192
vacuum fluctuations, 190
Proterozoic atmospheres. *See also* Archaean atmospheres
Cryogenian glaciations, 23
glaciations, 12
Huronian glaciation, 23
oxygen-poor composition, 23

S
Sixth mass extinction of species
acidification, 158
Arctic and boreal areas, 155
Arctic's greenness, 155
biodiversity, 156, 157
devastation, habitats, 155
ecological systems, 154
marine good chain, 154, 157
Millennium Ecosystem Assessment program, 157
planetary-scale critical transition, 154–155
Solar insolation
glacial terminations, 129
greenhouse gases, 147
magnetic storms, 129–130
orbital forcing, 129
terrestrial climates, 2
Sterkfontein fossils, 77
Stromatolites, 19–21
Sulphur emissions, 130, 138, 142, 171
Sun-spot cycle, 124, 126

T
TEM. *See* Transmission Electron Microscopy (TEM)
Toba volcanic eruption, 109, 110
Transmission Electron Microscopy (TEM)
carbonaceous matter *(cm),* 16, 17
filamentous, 19
3.24 Ga sulphur, 16, 18
tubular bundle, 16, 18, 19

W
Wonderwerk cave studies, 84, 101–103